

**CONFOCAL MICROSCOPY ANALYSIS OF THE ROLES OF
INTRACELLULAR pH IN THE REGULATION OF
POLARISED GROWTH OF *Dryopteris* PROTONEMATA**

Richard M. Parton

**Doctor of Philosophy
University of Edinburgh
1996**



This thesis is dedicated to my Parents and to all those fern gametophytes who selflessly gave up their lives for Science.

"The researches of many commentators have already thrown much darkness on this subject, and it is probable that, if they continue, we shall soon know nothing at all about it"

Mark Twain

"Once you have eliminated the impossible, what ever is left, however improbable, must be correct."

Captain Spock,
(Star Trek VI)

VOLUME-1 CONTENTS

PAGES

Declaration	<i>i</i>
Acknowledgements	<i>ii</i>
Abstract	<i>iii</i>
Abbreviations	<i>iv</i>

Chapter 1 - Introduction and literature review

1.1 Polarity and plant morphogenesis	1
1.2 The study of polarity at the single cell level	1
1.3 Cellular polarity	5
1.4 Apical growth - as an expression of polarity	6
1.5 Mechanics of apical growth: cytology and ultrastructure of tip-growing cells	8
1.6 Regulation of apical growth: general signal perception and transduction	11
1.7 The involvement of ions and ion movements in apical growth	14
1.8 The involvement of Ca ²⁺ ions in the determination and maintenance of polarity in apical growth	15
1.9 Evidence for the involvement of H ⁺ ions in apical growth	18
1.10 Methods for the analysis of intracellular free-ion concentrations <i>in vivo</i>	23
1.11 Imaging of intracellular ion-sensitive dyes	25
1.12 Fern gametophytes as an experimental system	27
1.13 Apical growth of fern gametophytes	29
1.14 Aims	32
Table 1.1 - Simple "model systems" used in the study of polarity and tip growth	2/3
Table 1.2 - Methods used to analyse intracellular Ca ²⁺ and H ⁺ ion concentrations	24

Chapter 2 - Materials and Methods

2.1 Materials and equipment	35
2.2 Culture and handling of plant material	37
2.3 Dye loading methods	42
2.4 Preparation of samples for microscopy	46
2.5 Assessment of viability	46
2.6 Confocal microscopy and imaging	46
2.7 Image processing	50
2.8 Calibration of the dye response	51
2.9 Preparation of diagrams and figures	52
2.10 Statistical analysis	52
Table 2.1 - Gametophyte culture media	38
Table 2.2 - Dyes and loading procedures attempted on <i>D. affinis</i> protonemata	43/44
Table 2.3 - Filter sets for the CLSM	47
Table 2.4 - CLSM imaging parameters	48
Table 2.5 - The effects of altering the objective lens and gain settings on fluorescence and ratio values	49

Chapter 3 - The fern gametophyte as an experimental system for the investigation of tip growth.

3.1 Introduction	53
3.2 Choice of species	53
3.3 Developmental stages of <i>Dryopteris affinis</i> gametophytes	54
3.4 Examination of the apical chlorocytes of protonemata	56
3.5 Light-induced apical "swelling"	59
3.6 Phototropic reorientation of chlorocyte tip growth	61
3.7 Rhizoids	62
3.8 Induction of secondary rhizoids	64
3.9 Indicators of cell stress	64
3.10 Further analysis of gametophyte cytology with fluorescent stains	65
3.11 Discussion	68
Table 3.1 - Positive and negative aspects of the different fern species examined	55
Table 3.2 - Relative proportions of apical chlorocyte "tip forms"	58
Table 3.3 - Rates of extension of protonemata and rhizoids	59
Table 3.4 - Tropic reorientation of apical growth of protonemata - tip forms	62
Table 3.5 - Physical expressions of stress in <i>Dryopteris</i> protonemata	65
Table 3.6 - The growth rates of some commonly studied apically extending cell types	72

Chapter 4 - Assessment of loading methods for pH and calcium sensitive dyes

4.1 Introduction	74
4.2 Microinjection	74
4.3 Acid-loading	76
4.4 Ester-loading	76
4.5 cSNARF-1 AM ester-loading results	78
4.6 Loading pre-treatments	82
4.7 Different fern species	81
4.8 Practical considerations for dye imaging	83
4.9 Discussion	84
Table 4.1 - Methods for loading ion-sensitive dyes into cells	77
Table 4.2 - Chlorocyte viability after cSNARF-1 AM ester-loading	80
Table 4.3 - Individual rhizoid cell viability after cSNARF-1 AM ester-loading and confocal imaging	81
Table 4.4 - Loading pre-treatments	83

VOLUME-1 CONTENTS

PAGES

Chapter 5 - Confocal ratio-imaging of cSNARF-1: assessment of the imaging method

5.1 Introduction	88
5.2 Limitations of the dye	88
5.3 Changes in cSNARF-1 performance due to environmental conditions	90
5.4 Intracellular dye response and calibration	91
5.5 Discussion: the pH response of cSNARF-1 - assessment of the calibration data	93
5.6 Quantitative analysis of images	94
5.7 Application of analysis methods to physiological imaging	100
5.8 Optical artefacts	103
5.9 "Biological" artefacts	105
5.10 Discussion: image quality and data extraction	105
Table 5.1 - Physical and chemical properties of cSNARF-1	89
Table 5.2 - Summary of the weak acid/weak base <i>in situ</i> calibration results	93
Table 5.3 - Comparison of mean ratio values determined from mean fluorescence intensities and directly from ratio images	97
Table 5.4 - Spatial resolution and precision of pH measurement for cSNARF-1 ratio imaging	100

Chapter 6 - Examination of the role of pH in growing rhizoids of *Dryopteris affinis* protonemata

6.1 Introduction	108
6.2 Examination of intracellular pH	108
6.3 Intracellular pH and growth	110
6.4 Extracellular pH and tip growth	111
6.5 Effects of extracellular pH manipulation on intracellular pH	113
6.6 Extracellular pH profiles around cells	114
6.7 Discussion	115
Table 6.1 - Average cytoplasmic pH	109
Table 6.2 - Z-series cytoplasmic pH analysis	110
Table 6.3 - Extracellular pH manipulation media	112

Chapter 7 - Summary

Chapter 8 - Further work

8.1 introduction	122
8.2 Technical improvements	122
8.3 Further work on the role of pH in tip growth	124
8.4 Areas of further interest	125
Table 8.1 - Technical improvements	123

References

VOLUME-2 FIGURES

Chapter 1 Figures

- Fig. 1 - Components of polarity and polarised growth
- Fig. 2 - Generalised signal transduction pathway components
- Fig. 3 - Proton movements around growing tips
- Fig. 4 - Fluorescent dyes used for intracellular ion concentration measurement
- Fig. 5 - The fern life cycle
- Fig. 6 - Developmental stages of a typical fern gametophyte

Chapter 2 Figures

- Fig. 7 - Gametophyte culture treatments
- Fig. 8 - Perfused thin-layer chamber
- Fig. 9 - Handling of liquid-cultured protonemata
- Fig. 10 - Ester-loading of cells with dye
- Fig. 11 - Microinjection of protonemal filaments
- Fig. 12 - Procedure for ionophoretic microinjection of fern protonemata
- Fig. 13 - Scanhead layout and light-path of the Bio-Rad MRC-600 CLSM
- Fig. 14 - Layout of the CLSM
- Fig. 15 - CLSM settings for physiological imaging
- Fig. 16 - Ratio processing procedure
- Fig. 17 - Calibrated pseudocolour look-up table (LUT) for ratio images.

Chapter 3 Figures

- Fig. 18 - Developmental stages of *Dryopteris affinis* gametophytes
- Fig. 19 - Time-course of gametophyte development
- Fig. 20 - Typical protonemal apical-cell structure
- Fig. 21 - Protonemal apical cell tip forms
- Fig. 22 - Apical cell "swelling" response
- Fig. 23 - Phototropic reorientation of apical growth
- Fig. 24 - Typical rhizoid apical structure
- Fig. 25 - Rhizoid tip forms
- Fig. 26 - Apical extension of rhizoids
- Fig. 27 - Secondary rhizoid
- Fig. 28 - Stressed cells
- Fig. 29 - Recovery of rhizoids after stress
- Fig. 30 - Staining of apical structures with fluorescent dyes
- Fig. 31 - Distribution of endoplasmic reticulum in chlorocyte cells
- Fig. 32 - Distribution of mitochondria in apical chlorocytes
- Fig. 33 - Distribution of mitochondria in a rhizoid

Chapter 4 Figures

- Fig. 34 - Microinjection of fern protonemata with fluorescent dyes
- Fig. 35 - Low pH loading of fern protonemata with cSNARF-1 free-acid
- Fig. 36 - Ester-loading of fern protonemata with cSNARF-1 AM
- Fig. 37 - cSNARF-1 imaging and chloroplast autofluorescence
- Fig. 38 - Ester-loading of rhizoids with cSNARF-1 AM
- Fig. 39 - Subcellular localisation of cSNARF-1 in rhizoids after AM ester-loading
- Fig. 40 - Rhizoid viability after cSNARF-1 AM ester-loading and confocal imaging
- Fig. 41 - Confocal optical sectioning

VOLUME-2 FIGURES

Chapter 5 Figures

- Fig. 42 - pH response curve of cSNARF-1 free-acid *in vitro*
- Fig. 43 - Calibration curves for the pH response of cSNARF-1 free-acid *in vitro*
- Fig. 44 - Effects of environmental conditions on the pH response of cSNARF-1 free-acid tested *in vitro*
- Fig. 45 - Calibration of the pH response of cSNARF-1 free-acid *in situ*
- Fig. 46 - Random "noise" levels in confocal fluorescence and ratio images
- Fig. 47 - The influence of fluorescence image pixel intensity on observed ratio value
- Fig. 48 - Estimation of the spatial resolution and precision of pH measurement for cSNARF-1 ratio images
- Fig. 49 - Dissection of physiological cSNARF-1 fluorescence confocal images and their corresponding ratios
- Fig. 50 - Methods of extraction of numerical data from physiological images
- Fig. 51 - Sampling cSNARF-1 confocal ratio images with a linear median transect
- Fig. 52 - Image thresholding to eliminate low signal and vacuolar signal contributions from ratio images
- Fig. 53 - Ratio image of a vegetative hypha of *Neurospora crassa* loaded with cSNARF-1 10 kDa dextran-conjugate
- Fig. 54 - cSNARF-1 dual emission ratio image misalignment artefact
- Fig. 55 - Confocal and non-confocal imaging of cSNARF-1 in a rhizoid of *D. affinis*
- Fig. 56 - cSNARF-1 confocal ratio imaging at different depths within a rhizoid

Chapter 6 Figures

- Fig. 57 - Typical cSNARF-1 confocal ratio images of growing *D. affinis* rhizoids
- Fig. 58 - Cytoplasmic pH in fern gametophyte rhizoids
- Fig. 59 - recovery of rhizoids after intracellular pH manipulation using cell permeant weak acids and bases
- Fig. 60 - Effects of extracellular buffering at pH 5.6 and 6.0 on *D. affinis* rhizoids
- Fig. 61 - Effects of extracellular buffering at pH 7.0 on *D. affinis* rhizoids
- Fig. 62 - Effects of extracellular buffering at pH 8.0 on *D. affinis* rhizoids
- Fig. 63 - Possible positions of pH gradients in a tip-growing cell

DECLARATION

This thesis has been composed by myself and the work of which it is a record has been carried out by myself. All sources of information have been specifically acknowledged by means of reference.

ACKNOWLEDGEMENTS

I would like to express my thanks to all the people who have helped me during the course of this study. In particular I would like to thank the following:

My Supervisors:

Prof. Antony J. Trewavas - for character building.

Dr. Nick Read - for letting me play with his CLSM.

Dr. Adrian F. Dyer - for things “ferny”.

My Parents - for their patience and understanding, for letting me cover the house with references and for proof-reading.

Till C. Jelitto - for being Till.

Sabine Fischer - for showing me that there is life after thesis (just wait until it's her turn to write up!).

I am also grateful to the following for technical assistance:

Dr. Tony C. Collins - how to deal with those horrible computer things!

Dr. Till C. Jelitto - how to deal with those horrible computer things!

(soon to be Dr.) **Sabine Fischer** - how to deal with those horrible computer things!

(You might guess I had a great deal of trouble with computers!)

The people at **Bio-Rad** - for keeping the CLSM alive!

Dr. Mark D. Fricker and Dr. Nick S. White - when the people at Bio-Rad could not help!

Dr. Jim Deacon - for trying to explain statistics to me.

The following people also deserve a mention for their help and friend ship: Dr. H. Knight; Dr. R. Malhó; Dr. P. S. Shacklock; Dr. K. Fallon; Dr. B. Sinclair; Dr. A. Allen; Dr. J. Love; Helen A. Page; Dr. A. J. Collis; Babs & Rita - The autoclave technicians (who had to put up with my constant demands for autoclaved medium and clean glassware); feel free to add your name if you feel neglected:

ABSTRACT

The suitability of *Dryopteris affinis* protonemata, for the study of the roles of pH and $[Ca^{2+}]$ in the maintenance and regulation of polarity in tip growth, was examined with respect to other commonly studied cell types exhibiting polarised growth. Initially, physiological and cytological aspects of tip growth in apical chlorocytes and rhizoid cells were analysed. Secondly, the suitability of different methods of introducing ion-sensitive dyes into cells were assessed. Calcium-sensitive dyes failed to load by any method except microinjection, which could not be used routinely because of the poor recovery of cells after injection and rapid vacuolar internalisation of injected dye free-acids. This prevented analysis of the roles of $[Ca^{2+}]$ in tip growth. Possible ways of overcoming the problems encountered are discussed. The pH sensitive dyes BCECF and carboxySNARF-1 could both be loaded into cells as their cell permeant AM esters without detrimental effects on cell health. However, sequestration within organelles, particularly the vacuole, proved to be a significant limitation. The problems of dye localisation were compensated for to a certain degree by the use of confocal microscopy and ratiometric analysis. Finally, cytoplasmic pH was examined in growing rhizoids by confocal ratio imaging of AM ester-loaded cSNARF-1. The limits of spatial resolution and precision of pH measurement by this method were estimated at between 0.5 and 2.0 μm^2 and ± 0.05 pH unit, respectively (over the pH range 6.9 to 7.3). For rhizoids, average cytoplasmic pH was estimated at 7.1 - 7.3, based on *in vitro* calibration. No significant cytoplasmic pH gradient (ΔpH of >0.1 unit) was found within 40-50 μm of the cell apex in actively growing rhizoids. Internal pH manipulation, using permeant weak acids and bases, reversibly disrupted tip structure and inhibited growth. Buffering external pH over the range 5.6 - 8.0 temporarily halted but did not ultimately inhibit tip growth. These findings suggest that, while maintenance of intracellular pH is essential to apical growth, it is not a fundamental regulator of polarity. Based on the findings of this study, further work required to extend the knowledge of the roles of intracellular [ion] in tip growth is discussed.

Abbreviations

General:

DIC	differential interference contrast (microscopy)
ER	endoplasmic reticulum
EM	electron microscopy
h	hour(s)
kDa	kilodalton
λ	wavelength
MF	actin microfilaments
min.	minute(s)
MT	microtubules
n	number (of samples or replicates)
PC	personal computer
pH _c	cytoplasmic pH (cytosolic pH specified separately)
pH _i	internal pH
pH _o	external pH
pKa	pH at which an acid is present in its protonated and unprotonated forms in equal concentrations
sec.	second(s)
s.d.	standard deviation
s.e.m	standard error
TLC	thin-layer chamber
UV	ultra-violet
VDU	video display unit
V/V	volume by volume
W/V	weight by volume

Continued over

Abbreviations

Chemicals:

-AM	acetoxymethyl (ester group)
BCECF	2',7'-bis-(2-carboxyethyl)-5- (and-6)- carbxyfluorescein
cAMP	cyclic adenosine monophosphate
DiOC ₆	3,3'-dihexyloxacarbocyanine iodide
DiOC ₇	3,3'-diheptyloxacarbocyanine iodide
DMSO	dimethylsulphoxide
CFDA	5-(and-6)-carboxyfluorescein diacetate
DNP	2,4-dinitrophenol
EtOH	ethanol
Fluo-3	1-(2-amino-5-(2,7-dichloro-6-hydroxy-3-oxo-3H-xanthen-9-yl)-2-(2'-amino-5'-methylphenoxy)-ethane-N,N,N',N'-tetraacetic acid.
Fura-2	1-[2-(5-carboxyoxazol-2-yl)-6-aminobenzofuran-5-oxy]-2-(2'-amino-5'-methylphenoxy)-ethane-N,N,N',N'-tetraacetic acid.
HEPES	N-(2-hydroxyethyl)- piperazine-N'-2-ethanesulphonic acid
Indo-1	1-[2-amino-5-(6-carboxyindol-2-yl-phenoxy)]-2-(2'-amino-5'-methylphenoxy)-ethane-N,N,N',N'-tetraacetic acid.
IP ₃	phosphatidylinositoltrisphosphate
LYCH	Lucifer Yellow CH, [6-amino-2,3-dihydro-1,3-dioxo-2 hydrazinocarboxylamino-1H-benz [d,e] isoquinoline-5,8-disulfonic acid]
MES	2-(N-morpholino) ethanesulphonic acid
NMR	nuclear magnetic resonance
Rhod-123	rhodamine 123
SDS	sodium dodecyl sulfate
cSNARF-1	5-(and-6)-carboxy-seminaphthorhodafluor-1
TRIS	2-Amino-2-hydroxymethyl-1,3-propanediol

Continued over

Abbreviations

Imaging Terminology:

Acc	accumulation filter
BL	black level
CA	confocal aperture
CCD	charge-coupled device
COMOS	confocal mouse operated software
K	Kalman filtering
CLSM	laser scanning confocal microscope
LUT	look-up table
MPL	Command line software
ND	neutral density filter
PMT	photomultiplier tube
SOM	keyboard operated confocal software
TCSM	Time-course and ratiometric software
WORM	write-once-read-many

Figure labelling:

Ac	apical cell
AC	apical cytoplasm
Bc	basal cell
Ch	chloroplast
CW	cell wall
C	cytoplasm
ER	endoplasmic reticulum
M	mitochondrion
N	nucleus
P	plastid
PM	plasma-membrane
T	vacuole membrane or tonoplast
V	vacuole

Chapter 1

Chapter 1 - Introduction and Literature Review

POLARITY AND TIP GROWTH IN PLANTS AND FUNGI

1.1 Polarity and plant morphogenesis

Plant organs, tissues and often but not exclusively (Cooke & Lu, 1992) the cells of which they are comprised, are not homogenous but exhibit a specific orientation (polarity) in structure or activity (Schnepf, 1986). The timing of cell division (cell-cycle regulation); its orientation and positioning; the rate, degree and orientation of cell expansion all appear to be highly co-ordinated and precisely regulated during normal development (Francis & Halford, 1995; Pritchard, 1994; Abeysekera & McCully, 1993). These processes, which are themselves inherently polarised either in time or space (Schnepf, 1986), have emerged as the key elements in determining morphology both at the single cell and multicellular levels and so contribute to cell and organ polarity.

Plants are able to alter their development in response to environmental conditions (e.g. light, temperature, gravity, wind, water availability or nutrients), through regulation of the processes described above (Duckett & Gray, 1995; Haley *et al.*, 1995; Bowles, 1995; Bowler & Chua, 1994; Trewavas & Gilroy, 1991). Polarity must, therefore, be carefully controlled and regulated with mechanisms linked to the detection of external stimuli.

Specific examples of polarised events are found at many important stages of plant morphogenesis from the initial fertilisation events (e.g. Brownlee, 1994); early asymmetric embryogenic divisions (e.g. Gilissen *et al.*, 1994; Goodner & Quatrano, 1993); elongation of cells behind the root and shoot apices (e.g. Pritchard, 1994); the development of specialised cells (such as gametes and root hairs by asymmetric division - e.g. Sodmergen *et al.*, 1995; Aeschbacher *et al.*, 1994) to the apical growth of pollen tubes and root hairs (e.g. Schiefelbein *et al.*, 1993; Steer & Steer, 1989).

We still do not fully understand the processes by which cells are organised and cellular development determined in order to produce complex multicellular tissues and organs in relation to the prevailing environmental conditions. Understanding the role that polarised events play, the mechanisms by which such polarity arises and its regulation in response to "developmental" and environmental signals, both at the cellular and multicellular levels, are clearly of major importance. The investigation of such questions is the fundamental aim of much of the recent and on-going plant research (Francis & Halford, 1995; Duckett & Gray, 1995; Haley *et al.*, 1995; Bowles, 1995; Bowler & Chua, 1994; Pritchard, 1994; Abeysekera & McCully, 1993; Benfey *et al.*, 1993; Lloyd, 1991; Sachs, 1991).

1.2 The study of polarity at the single cell level

The importance of polarity in plant morphogenesis, particularly as expressed by individual cells, has been outlined in the previous section. It is the examination of cellular polarity, the mechanisms of its

operation and in particular its regulation, which will be discussed in detail below and was explored during the course of the research described in this thesis.

There are many instances of polarised events expressed at the single cell level within multicellular tissues during cellular differentiation or organ and tissue morphogenesis (see section 1.1). The ability to study such events, however, is generally hampered by difficulties in handling and examining multicellular material. Owing to this and in order also to examine events at the single cell level, and the subcellular mechanisms by which they are brought about and regulated, many researchers have sought simple multicellular or unicellular experimental systems which express cellular polarity. A review of the organisms commonly studied in relation to cellular polarity is given in Table 1.1.

Fern protonemata were used for the experimental investigation of tip growth and polarity described in subsequent chapters (refer to Sections 1.7 and 1.8).

Table: 1.1 Simple model systems used in the study of polarity and tip growth

Experimental System	Processes Examined	Aspects of polarity demonstrated †	References ‡
Higher plants			
Protoplasts	Asymmetric division	a,b	1,2,3
Tissue culture/embryos	Cell/tissue polarity		4,5,31
Root hairs	Tip growth	a,b,c,d,	6,7,8
Pollen tubes			9,10,11,12
Ferns, liverworts and mosses			
Spores	Asymmetric division	a,b	13
Protonemata	Tip growth	a,b,c,d	14,15,16,17,18,19,20,22,23
Rhizoids			23,24,25
Prothalli	Cell/tissue polarity	a,b	26,27,28,29,30

‡ **References:** 1) Kranz *et al.*, 1995; 2) Kuss-Wymer & Cyr, 1992; 3) Kiss *et al.*, 1991; 4) Thorn, 1993; 5) Knox, 1992; 6) Schiefelbein *et al.*, 1993; 7) Schiefelbein *et al.*, 1992; 8) Herrmann & Felle, 1995; 9) Malhó *et al.*, 1994; 10) Pierson *et al.*, 1994; 11) Sodmergen *et al.*, 1995; 12) Steer & Steer, 1989; 13) Miller & Bassel, 1980; 14) Kiss *et al.*, 1995; 15) Cove *et al.*, 1995; 16) Wacker & Schnepf, 1990; 17) Quader & Schnepf, 1989; 18) Schmiedel & Schnepf, 1980; 19) Doonan *et al.*, 1988; 20) Kadota & Wada, 1992a & b; 21) Schmuchow *et al.*, 1990; 22) Racusen *et al.*, 1988; 23) Clark *et al.*, 1995; 24) Alfano *et al.*, 1993; 25) Felle, 1988; 26) Cooke *et al.*, 1995; 27) Cooke & Lu, 1992; 28) Tilney *et al.*, 1990; 29) De Boer & De Does, 1990; 30) Reynolds & Corson, 1979; 31) Verbelen *et al.*, 1995; continued overleaf (refs. 32—62)

† **Aspects of polarity which have been demonstrated to occur and are examined in the references given (see also Section 1.3.1): (a) Initiation; (b) Fixation; (c) Maintenance; (d) Reorientation.**

(Table 1.1: continued over the page)

Table: 1.1 Continued

Experimental System	Processes Examined	Aspects of polarity demonstrated †	References ‡
Fucoid algae			
Eggs	Asymmetric division	a,b,c,d	62
Zygotes	Cell/tissue polarity		32,33,34,35,61,62
Rhizoids	Tip growth	b,c	33,34,36
Filamentous algae			
Filament cells	Tip growth	a,b,c,d	37, 39,40,41,42
Rhizoids			38
Water molds: chytridiomycete and oomycete fungi			
Hyphae	Tip growth	c,d	43,44,45,
Rhizoids			49,60
Filamentous fungi			
Vegetative hyphae	Tip growth	a,b,c,d	46,47,48,49,50,51, 58,59
Yeasts			
Budding yeasts	Tip growth	a,b,c	55
Fission yeasts	Asymmetric division		52,56
Hyphal growth			53,57

‡ **References continued:** 32) Goodner & Quatrano, 1993; 33) Kropf, 1992; 1994; 34) Berger & Brownlee, 1993; 1995a & b; 35) Kropf *et al.*, 1993; 36) Gibbon & Kropf, 1994; 1991; 37) Menzel, 1995; 1994; 38) Leitz *et al.*, 1995; 39) Rusig *et al.*, 1994; 40) Hodick, 1994; 41) Kataoka & Weisenseel, 1988; 42) Galway & Hardham, 1986; 43) Hyde & Heath, 1995; 44) Money & Harold, 1993; 45) Garril *et al.*, 1992; 1993; 46) Levina *et al.*, 1995; 47) Hosking *et al.*, 1995; 48) Lopez-Franco *et al.*, 1994; 49) Gow, 1994; 1989; 50) Jackson & Heath, 1993; 51) Dicker & Turian, 1990; 52) Snell & Nurse, 1993; 53) Chen-Wu *et al.*, 1992; 54) Gabriel & Kopecka, 1995; 55) Sanders & Field, 1995; 56) Verde *et al.*, 1993 and references therein; 57) Akashi *et al.*, 1994; 58) Bartnicki-Garcia *et al.*, 1995; 59) Gow *et al.*, 1993; 60) Kaminskyj *et al.*, 1992; 61) Quatrano *et al.*, 1993; 1995a & b; 62) Brownlee, 1994

† **Aspects of polarity which have been demonstrated to occur and are examined in the references given (see also Section 1.3.1): (a) Initiation; (b) Fixation; (c) Maintenance; (d) Reorientation.**

1.2.1 Experimental systems for the investigation of polarity

Experimental systems may be "Intact organisms" which exist in a simple multicellular or unicellular state such as fern or moss protonemata (see Cooke *et al.*, 1995; Raghavan, 1990) algae and algal zygotes (Goodner & Quatrano, 1993) or fungi (Snell & Nurse, 1993; Jackson & Heath, 1993). Cells derived directly from higher plant tissues are also used, including: isolated and regenerating protoplasts (e.g. Shacklock *et al.*, 1992); tissue-cultured suspension cells (e.g. Roos, 1992); culture tissue undergoing differentiation and somatic embryogenesis (e.g. Gilissen *et al.*, 1994; Pichon &

Desbiez, 1994); even specialised cells such as pollen and root hairs (e.g. Schiefelbein *et al.*, 1993; Steer & Steer, 1989).

The type of experimental material may be further classified as "model" systems and systems with "direct application". For example, fern gametophytes, which are considered of little economic value in their own right, may be thought of as "model" systems. Ferns are studied because they represent a more amenable experimental material (Cooke *et al.*, 1995; Hickok *et al.*, 1995). The study of pollen tubes, however, has direct application in the understanding of mechanisms such as self-incompatibility in agriculturally important species (Franklin-Tong *et al.*, 1995; Dickinson, 1994). Even so, certain "model" pollen species, such as *Lilium* and *Agapanthus* are examined because of convenience (e.g. Pierson *et al.*, 1995). A similar case may be made for fungi with the study of serious plant pathogens such as *Magnaporthe grisea* (rice-blast fungus) (Jelitto *et al.*, 1994) and of "models" such as *N. crassa*, which is favoured for its ease of genetic and experimental manipulation (Levina *et al.*, 1995; Dicker & Turian, 1990).

1.2.2 Perils of the "model" system

The major limitation with all simplified experimental systems comes with attempting to make generalised statements from the findings or when attempting to apply the findings to more complex systems - such as the multicellular tissues and organs of higher plants. In the latter case, the use of cells isolated from multicellular higher plant tissues may prove to be better than, say, the zygote of a marine alga or a moss protonemata if results are to be extrapolated to specific situations in higher plants.

Cell-cell interactions, cell positional information and long-range intercellular signalling, which appear to be so important in higher plant morphogenesis (Aeschbacher *et al.*, 1994; Pontlezica *et al.*, 1993), are particularly difficult to relate to the simpler models. Tissue culture undergoing somatic embryogenesis, multicellular fern gametophytes or moss protonemata (which have been demonstrated to show cell-cell interactions and apical dominance (Reynolds & Corson, 1979; Ootaki & Furuya, 1969)) and early embryos of marine algae (in which the cell wall appears to influence the developmental fate of cells (Berger & Brownlee, 1995a & b; Berger *et al.*, 1994; Kropf *et al.*, 1988; 1993)) may, however, provide useful experimental models.

There are further complications such as evolutionary differences. For example, phytochrome (the photoreceptor sensitive to red and far-red light in plants) shows both structural and functional differences between plants at different evolutionary levels. In the mosses it appears to act directly as a kinase (Algarra *et al.*, 1993). In higher plants, however, it acts, via G-protein interaction, through Ca^{2+} and calmodulin (Bowler & Chua, 1994; Bialy, 1992). Complications also result from the specialisation of cell types. *Fucus* zygotes, during embryogenesis, (Kropf, 1992) and cells of higher plant shoots or roots, during development (Francis & Halford, 1995), both undergo asymmetric divisions. However, a comparison between *Fucus* and the early embryonic divisions of a higher plant

zygote may be more appropriate (Brownlee, 1994). A further instance is that of the polarised cell elongation characteristic of certain cells during root and shoot development (Pritchard, 1994; Benfey *et al.*, 1993) and how this relates to the polarisation that can be induced in cultured cells (and protoplasts) under certain conditions (Verbelen *et al.*, 1995; Kuss-Wymer & Cyr, 1992) and the apical growth exhibited by, for example, pollen tubes (Steer & Steer, 1989).

Despite its complications the use of model systems is highly valuable. Work, which may proceed easily and rapidly in a suitable "simple" system, subsequently directs the lines of questioning and experimentation on more complex systems. Comparison of the two is essential because study of simple systems alone could never provide satisfying or conclusive answers.

1.3 Cellular polarity

It should be appreciated that cellular polarity is a very broad term encompassing a range of physiological events and processes (Nick & Furuya, 1992; Sachs, 1991; Schnepf, 1986). Examples of polarised cellular events include: asymmetric cell division (Kropf, 1992); unequal expansion of cells (Pritchard, 1994); and apical growth (Heath, 1990).

Cellular polarity is also expressed at the subcellular level with the polarised organisation of cellular structures such as organelles, and the distribution of cytoplasmic components, molecules and ions which underlie polarised cellular events and morphology (for example, in *Fucus* embryos: Kropf, 1994; 1992; Goodner & Quatrano, 1993). Many cellular molecules themselves have inherent polarity - particularly important are actin and tubulins which form the "oriented" microfilaments and microtubules of the cytoskeleton (see Heath, 1990; Schnepf, 1986).

1.3.1 Components of cellular polarity

Polarised cellular events may be arbitrarily divided into three or four components (Goodner & Quatrano, 1993; Kropf, 1992; Nick & Furuya, 1992):

1) *Induction* (initiation). The determination and establishment (the latter involving amplification of the initial determinant signal) of a new axis of polarity. This may occur in response to environmental stimuli such as light or gravity (e.g. Goodner & Quatrano, 1993) or more subtle developmental cues such as position relative to other cells (Aeschbacher *et al.*, 1994). There are also "inherited" determinants passed on from the maternal cell, for example: polarity in fission yeasts (Snell & Nurse, 1993); and the polarity of fern spores (Miller *et al.*, 1983; Miller & Bassel, 1980; Miller & Greany, 1976)).

2) *Fixation*. Fixation may be considered at two levels: (A) in the initial polarisation of fucoid zygotes transition from a labile polar axis, which may be re-oriented by subsequent polarising stimuli, to a "permanent" polarity or "memory" which is not further influenced by polarising stimuli, precedes the morphological expression of rhizoid outgrowth (Kropf, 1992); (B) expression of polarity as a

permanent structural feature such as cell wall deposition or polarised outgrowth may be considered to "fix" a certain polar orientation (Kropf *et al.*, 1992; Herth *et al.*, 1990).

3) *Maintenance*. Some forms of expression of polarity, in particular polarised growth, involve active polarised processes which may require to be actively maintained (or orientated) - such as polarised cytological organisation, localised transport, metabolic activity and deposition (Steer & Steer, 1989). However, it is possible that maintenance represents a "default, steady-state" expression of polarity (i.e. once initiated the processes are "self" maintaining).

4) *Re-orientation*. Re-orientation of a labile polar axis before fixation, as discussed above for fucoid rhizoids, is one expression of re-orientation (Kropf, 1992). Additionally, re-orientation can occur after an initial polar axis has been fixed. For example, in the case of polarised growth exhibited by tip-growing cells, orientation may be continually directed or specifically re-directed in response to environmental signals (Gow, 1994; Malhó *et al.*, 1994). Alternatively, re-orientation may involve a certain degree of "depolarisation" followed by establishment of a new polar axis (Kataoka, 1981).

Figure 1 summarises the above concepts and how they may be interrelated. There is significant evidence for the sequence of "events" shown, although, this information comes mainly from studies of *Fucus* embryos (Kropf, 1994; 1992; Goodner & Quatrano, 1993) and pollen tube growth (Steer & Steer, 1989). The model subsequently reflects a significant bias towards tip growth-associated polarity. This model, therefore, may not have a wide biological basis; even so, the concepts provide a useful stance from which to examine other polarised biological events. A detailed comparison of events during *Fucus* embryogenesis, where tip out-growth precedes asymmetric division (Kropf, 1992), and fern spore germination, where asymmetric division occurs before rhizoid out-growth (see Raghavan, 1990), could be useful.

A complete synthesis of the information relating to possible biological mechanisms involved (noted briefly in Fig. 1) in the different "events" of polarisation is not possible in the space available; references for different "events" are given in Table 1.1. Deciphering the biological mechanisms involved is likely to be complicated by: differences dependent upon the nature of the final polar response; with different environmental circumstances triggering a particular response; and specific mechanisms of different cell types or developmental stages. A more detailed discussion of events is given for fern gametophytes in Section 1.7 and apical growth in Section 1.4.

1.4 Apical growth as an expression of polarity

Apical growth in plant (and fungal) cells involves cellular extension as a result of highly localised events, including: restricted wall loosening; polarised transport; and local deposition of new wall and membrane materials (Heath, 1990). Such growth is expressed in a range of cell types (Table 1.1).

Apical growth is generally considered to be an extreme form of the expression of cellular polarity (Schnepf, 1986). This has made it an attractive experimental system for aspects of cell polarity. On the basis of work with fucoid embryos, initiation of tip growth has been demonstrated not to be

equivalent to initiation of polarity but the expression of an established polar axis (Kropf, 1994; 1992). Hyphal branch initiation and maintenance of extension have been shown to be separately regulated in *Fusarium graminearum* (Wiebe *et al.*, 1992). Further, maintenance of pollen tube tip growth has been uncoupled from re-orientation by external stimuli (Malhó *et al.*, 1994). In *Adiantum* fern protonemata, a continual red light (or far-red) stimulus is required for continued apical growth; in darkness growth eventually slows and stops (Kadota & Furuya, 1981; 1977). Again in *Adiantum*, phototropic "bending" is preceded by cytoskeletal dissociation (microfilament and microtubule depolymerisation); these structures are re-established, with new orientation, before re-oriented growth resumes (Kadota & Wada, 1992a). Gravitropic re-orientation of *Chara* rhizoids, however, involves displacement of an apical vesicle-organising-centre and interruption of vesicle flow which is sufficient to re-orientate growth (Leitz *et al.*, 1995, and references cited therein). These are key details in understanding the relationship between cell polarity (see Fig. 1) and tip growth.

1.4.1 Apical growth, polarised cell expansion and polarity

It is likely that tip growth of different cell types, while sharing some similarities in mechanisms (Heath, 1994; Schiefelbein *et al.*, 1993; Kropf, 1992; Heath, 1990), also displays specific differences. It has been suggested that tip growth has evolved independently on several occasions (Derksen & Emons, 1990). Tip growth may serve different purposes; cells are also likely to exhibit specialisations to environmental conditions. Tip growth in many cell types (for example pollen tubes, fungal hyphae and fern protonemata) may be considered to be the "plant" equivalent of animal motility. However, in cells such as fission yeasts it merely allows the attainment of an elongate cell shape (Snell & Nurse, 1993; Heath, 1990). Some tip growth involves penetration of "solid media" (fungi, pollen tubes, rhizoids of fern protonemata) while in other cases passage through liquid (oomycete fungi, algae) and air (fern and moss protonemata) is important. Fern and moss protonemata (Schmiedel & Schnepf, 1980; Dyer, 1979) and fucoid rhizoids (Kropf, 1994) are relatively slow growing while pollen tubes, such as those of *Lilium*, and fungal hyphae, such as those of *Neurospora*, exhibit very high extension rates (Pierson *et al.*, 1995; Lopez-Franco *et al.*, 1994; Steer & Steer, 1989). Such differences should be remembered when attempting to correlate findings from different cell types.

How well information gained from the study of tip growth can be related to other forms of polarity and in particular general polarised cell expansion (for example, expansion of cells in root meristems - Baluska *et al.*, 1995; Pritchard, 1994), is still open to question. Some researchers, such as Steer (1990), view tip growth as a highly specialised event - more akin to amoeboid motion in its cytoskeletal involvement. However, similar cytoskeletal activity to this is involved in cytoplasmic streaming, organelle movement and general elongation in plant cells (Thimann *et al.*, 1992; Heath, 1990; Steer & Steer, 1989). Additionally, fundamental similarities between animals and plants are being recognised in both signal transduction mechanisms (Bowles, 1995; Drobak, 1991; 1992;

Roberts & Harmon, 1992) and determination of polarity and developmental fate by cytoskeleton-membrane-cell wall (equivalent to animal extracellular matrix) interactions (Heath, 1994; Kropf *et al.*, 1993; Nick & Furuya, 1992; Kagawa *et al.*, 1992).

In addition to the study of polarity there is much to be gained from an understanding of apical growth in its own right, particularly when considering its role in angiosperm fertilisation (Franklin, 1995; Chasen, 1994; Heslop-Harrison, 1987) and in the often pathogenic activities of fungi (Gow, 1994; Kwon & Hoch, 1991; Magalhães *et al.*, 1991).

1.5 Mechanics of apical growth: cytology and ultrastructure of tip-growing cells

The cytology and ultrastructure of tip growth has been studied in detail in several cell types, including: pollen tubes (Lancelle & Hepler, 1992; Pierson & Cresti, 1992); fungal hyphae (Vargas *et al.*, 1993; Grove, 1978); furoid rhizoids (Brownlee & Pulsford, 1988; Brawley *et al.*, 1976); and additionally to a lesser extent in fern and moss protonemata (Kiss *et al.*, 1995; Raghavan, 1990; Schmiedel & Schnepf, 1980); root hairs (Lloyd & Wells, 1985) and rhizoids of lower plants (Leitz *et al.*, 1995; Bartnik & Sievers, 1988; Dyer & Cran, 1976). Investigations have covered organelle distribution, cytoskeletal distribution, wall architecture and how these interact with each other and components of the plasma membrane.

1.5.1 Cytology of apical growth

Organelle distribution is highly polarised in all tip-growing systems, although this is more defined in the faster growing cell types; in fungi and pollen tubes distinct "zones" may be identified (Vargas *et al.*, 1993; Grove, 1978). Localisation and orientation of Golgi dictyosomes, endoplasmic reticulum (ER), secretory vesicles and mitochondria, as well as the nucleus in some cases, reflects the polar distribution of synthesis, secretion and metabolic activity required for localised growth (discussed in Steer & Steer, 1989). In several systems nuclear positioning has a significant influence on polarised outgrowth (Steer & Steer, 1989; Mineyuki & Furuya, 1985). A particularly important feature common to several tip-growing systems is an organised collection of vesicles at the apex: the Spitzenkörper in fungal hyphae (Vargas *et al.*, 1993; Smith *et al.*, 1978); "clear zone" in pollen tubes (Lancelle & Hepler, 1992; Pierson *et al.*, 1990; Steer & Steer, 1989); and the vesicle organising centre of *Chara* rhizoids and protonemata (Hodick, 1994; Sievers *et al.*, 1991) and moss caulonemata - but not chloronemata (Schmiedel & Schnepf, 1980; but see also Quader & Schnepf, 1989). These may be either homologous or, more likely, analogous structures.

1.5.2 Cytoskeletal components in tip-growing cells

Cytoskeletal involvement in tip growth has been extensively studied. The important cytoskeletal components which have been recognised and investigated in plants and fungi are: actin (G-actin monomers and F-actin microfilaments (MFs)); tubulin (tubulin monomers and microtubules (MTs));

and the array of associated proteins involved in regulation, motile activities and interactions with other cellular components (for a review of actin and tubulin structure and assembly, see Heath, 1990). Only very recently has it been appreciated that *in vivo*; dynamic assembly and disassembly, rapid redistribution, and close interactions of actin and tubulin, all occur (Mineyuki *et al.*, 1995; Hush, 1994; Hepler *et al.*, 1993; Wasteneys *et al.*, 1993; Zandomeni & Schopfer, 1993; Kuss-Wymer & Cyr, 1992; Kadota & Wada, 1992; Lloyd, 1991) and are critical in understanding their modes of action. Intermediate filaments (Stein & Bronner, 1989) have also been identified in some plants and fungi but experimental work is in its infancy and will not be discussed further here (Heath, 1994).

These cytoskeletal components have been found in all tip-growing cells. However, there is neither complete agreement in their distributions nor their proposed activities (e.g. see Joos *et al.*, 1994, for a discussion of the problem in pollen tubes; Heath, 1994, for fungi). This has made generalisation very difficult. The following discussion has consequently been limited to "cytoskeletal activity" rather than highlighting specific activities attributed to individual components. However, at present it appears that actin is most functionally active in apical organisation and vesicle activities, based on its considerable presence in the apex and the effects of MF disorganising agents on tip growth (Heath, 1990 & 1994; Quader & Schnepf, 1989; Steer & Steer, 1989). Microtubules have been suggested to have a role in the re-enforcement of polarity (Joos *et al.*, 1994; Cyr, 1994; 1995; Mizuta, 1994; Doonan *et al.*, 1988). The situation has become increasingly complex, however, as, with the aid of better techniques, co-localisation, interaction and co-operative activities have been observed or implicated for MFs and MTs and a clearer view of *in vivo* distributions and dynamic activity is emerging (Yuan *et al.*, 1994; Hepler *et al.*, 1993; Vargas *et al.*, 1993; Zandomeni & Schopfer, 1993; Kuss-Wymer & Cyr, 1992; Lancelle & Hepler, 1992; Kadota & Wada, 1992 and references therein; Steer & Steer, 1989; Doonan *et al.*, 1988).

1.5.3 Role of the cytoskeleton in polarity and tip growth

Cytoskeletal activity is implicated in both the early stages of establishment and fixation of polarity (e.g. Bouget *et al.*, 1995; Kropf, 1994; Levina *et al.*, 1994; Goodner & Quatrano, 1993; Kropf, 1992; Tanaka & Wakabayashi, 1992; Quader & Schnepf, 1989; Galway & Hardham, 1986) and during final morphological expression (for general reviews see: Heath 1994; Pritchard, 1994; Kropf, 1992; Lloyd, 1991; Derksen & Emons, 1990). Functional cytoskeleton appears to be an essential component of tip growth and the evidence from direct observations of cytoskeletal distribution and inhibitor studies suggests involvement at several levels.

Cytoskeletal activity functions in organising the distribution, shape and movement of organelles (for example: vacuoles - Joos *et al.*, 1994; Shepherd *et al.*, 1993; ER - McCauley & Hepler, 1992; nuclei, plastids and vesicles - Heath, 1990; 1994; Kadota & Wada 1992a; Steer & Steer, 1989). The cytoskeleton is probably involved in the organisation of vesicles in the apex (the Spitzenkörper and other vesicle organising centres) and the regulation of vesicle fusion (exocytosis) at the tip (Heath,

1994; Vargas *et al.*, 1993; Steer & Steer, 1989) and also recycling (exocytosis) of excess membrane delivered to the tip (e.g. Steer & Steer, 1989).

There is evidence that the cytoskeleton is able to alter the distribution of membrane proteins, either through localised insertion of vesicles or more directly through direct interaction with membrane proteins (Clark *et al.*, 1995; Levina *et al.*, 1994; Heath, 1994, Kropf, 1992; Steer and Steer, 1989). This has important implications in the establishment of localised ion fluxes and intracellular ion gradients associated with polarity and tip growth.

Interaction of cytoskeletal elements may not simply provide transport activity towards the tip but could actually drive and direct forward extension, as in ameoboid motion (Money & Harold, 1993; Steer, 1990). In most plants the main driving force is believed to be turgor pressure (see below). However, the oomycete fungi *Achlya* and *Saprolegnia* were able to continue tip growth at low and effectively zero turgor, respectively (Money and Harold, 1993; Money and Harold, 1992).

The cytoskeleton also has a more direct structural role providing mechanical strength and imposing shape on the nascent tip both directly and through interactions with the cell wall (Kropf, 1994; Heath, 1994; Kadota & Wada, 1992a; Kagawa *et al.*, 1992). The cell wall is itself a dynamic structure with specific control of plasticity and rigidity corresponding to differences in local composition and enzyme activities (Gooday, 1995; Gow, 1994; Taiz, 1994; Fry, 1994; Carpita & Gibeaut, 1993; Money & Harold, 1993; Chen-Wu *et al.*, 1992; Zhu & Boyer, 1992; Steer & Steer, 1989; Murata & Wada, 1989b & c; Heslop-Harrison, 1987; Taiz, 1984, Wada & Staehelin, 1981). Cytoskeletal support is believed to compensate for the necessary weakness (or weakening) of the apical cell wall, the visco-elastic properties of the cytoskeleton allowing controlled apical expansion (Kadota & Wada, 1992a; Kropf, 1992; Steer & Steer, 1989). This is critical where turgor pressure is believed to act in deforming the locally weaker wall of the apex. There is evidence to suggest that cytoskeletal activity, both indirectly, through directing exocytosis of wall materials and enzymes (for example in pollen tubes - Steer & Steer, 1989), and directly, through orientation of cellulose or chitin microfibril deposition (Mizuta, 1994; Lloyd, 1991; Green, 1984), influences cell wall rigidity, plasticity and favoured orientation of expansion. Directed microfibril orientation, however, appears to be a feature associated with more general elongation of cells (Baluska *et al.*, 1995; Pritchard, 1994; Kuss-Wymer & Cyr, 1992; Galway & Hardham, 1986; Green, 1984). Although directed microfibril orientation generally does not occur in pollen tubes, fern rhizoids or tip-growing fungal hyphae it is displayed by tip-growing fern protonemata (Kadota & Wada, 1992a).

The interplay between wall plasticity, turgor pressure, cytoskeletal support and its control of vesicle delivery to the tip, is thought to be critical in tip growth (Lopez-Franco, 1994; Money & Harold, 1993; Kropf, 1992; Zhu & Boyer, 1992; Steer & Steer, 1989). It is important to understand how these complex expressions of polarity and polarised activities are co-ordinated, maintained and directed. The dependence of tip growth upon cytoskeletal activity suggest it as a major target for regulation and hence of significant importance when considering the mechanisms of control.

1.6 Regulation of apical growth: general signal perception and transduction

Plants need to respond both rapidly and specifically to environmental and developmental stimuli and translate these cues (which may be directional or require quantitative as well as qualitative interpretation) into appropriate physiological and developmental events (Section 1.1). This includes the initial establishment and subsequent regulation of cellular polarity. The mechanisms by which this is carried out have been termed signal transduction. A general review of known transduction mechanisms is appropriate here because these are likely to be the same as or related to those involved in the regulation of polarity and tip growth. Additionally, tip growth is regulated in response to a variety of stimuli for which the transduction pathways to other cellular responses have been thoroughly investigated (for example photomorphogenic responses involving phytochrome: Bowler & Chua, 1994; Algarra *et al.*, 1993; Bialy, 1992).

1.6.1 Components of signal transduction

Signal transduction has been well characterised in animal cells and a few essential concepts have emerged which appear to be generally applicable to both animal and plant cells (Fig. 2; also refer to: Poovaiah & Reddy, 1988; Randall & Blevins, 1990; Morré, 1990).

Transduction pathways consist of: a receptor which detects the stimulus and relays it as a cellular event; a signal amplification "cascade" which increases the sensitivity of detection and relays the message throughout the cell; and finally, effectors (protein activities) which perform cellular functions and bring about the response.

Inherent in transduction pathways are both activation and deactivation (down-regulation or desensitisation) mechanisms which allows responses to be limited, which is essential for the correct co-ordination, appropriate quantitative level and appropriate duration of a response (Bowler & Chua, 1994).

Despite the many emerging similarities between signal transduction in animals and plants there exist fundamental differences. The most important of these differences appears to be the relative complexity of plant signal transduction with multiple, different transduction pathways regulating a single physiological response (Bowler & Chua, 1994). Stomatal closure is a good example of this (Blatt & Thiel, 1994; Gautier *et al.*, 1992; Irving *et al.*, 1992; Blatt, 1992; McAinsh *et al.*, 1992; Gilroy *et al.*, 1991). It is likely that this complexity of transduction networking in plants is an adaptation to their sessile lifestyle, reflecting the difference in the way animals and plants deal with their environment.

1.6.2 Second messengers

Second messengers are an important feature of transduction chains. Second messengers are small diffusible "elements" which function in the amplification "cascade". The most common and

ubiquitous such "element" appears to be Ca^{2+} (Hepler & Wayne, 1985). cAMP is important in fungi (Gadd, 1994), although whether cyclic nucleotides have a role in plants is not yet clear (Assmann, 1995). Both IP_3 and H^+ appear to have second messenger roles in plants and fungi (Hosking *et al.*, 1995; Mathieu *et al.*, 1994; Horn *et al.*, 1992; Drobak, 1991; 1992; Xu *et al.*, 1992; Guern *et al.*, 1991; Kurkdjian & Guern, 1989; Morse, 1987).

1.6.3 Calcium-based signal transduction

Calcium-based transduction mechanisms occur throughout eukaryotes (Brownlee, 1994; Roberts *et al.*, 1994; Gilroy *et al.*, 1993; Trewavas & Gilroy, 1991; Tsien & Tsien, 1990; Poovaiah & Reddy, 1988; Hepler & Wayne, 1985; Roux *et al.*, 1986) and many of their molecular components appear to be either conserved between animals and plants or at least have functional equivalents. This includes: calmodulin; Ca^{2+} channels and pumps; Ca^{2+} dependent enzymes (including protein kinases; G-proteins; IP_3 and IP_3 sensitive Ca^{2+} stores; phospholipase-C and also cytoskeletal activities (Grabski *et al.*, 1994; Gilroy *et al.*, 1993; Kikuyama *et al.*, 1993; Roberts & Harman, 1992; Drobak, 1991; 1992; Harmon & McCurdy, 1990; Hedrich & Schroeder, 1989; Blum *et al.*, 1988; Hepler & Wayne, 1985; Klee *et al.*, 1980). Interestingly, no direct equivalent of the animal protein kinase C occurs in plants, although kinases with some similarities have been identified (Roberts & Harman, 1992).

The involvement of controlled changes in intracellular Ca^{2+} levels (preceding response) or components of Ca^{2+} -mediated transduction chains has been demonstrated in many plant responses to important environmental stimuli, including: light (in particular red light), plant hormones, gravity, wind or touch, wounding or pathogens and chemicals (Johnson *et al.*, 1995; Haley *et al.*, 1995; Messiaen *et al.*, 1993; Gilroy *et al.*, 1993; Trewavas & Gilroy, 1991; Zhang *et al.*, 1990).

1.6.4 Protons as second messengers

Proton concentration (alternatively, pH) has received far less attention as a second messenger than Ca^{2+} ions. Nevertheless a variety of cellular responses involve changes in proton movements across the plasma membrane and shifts in cytoplasmic pH (pH_c).

According to measurements performed on a variety of cell types, cytoplasmic pH appears to be maintained within narrow limits at a value slightly above neutral (Guern *et al.*, 1991). Sudden changes in extracellular pH have been found to influence pH_c , although the effect is generally transient (Guern, 1991) as cells re-establish their normal pH_c level. Simple plant and fungal systems are able to regulate their internal pH to tolerate a range of external pH conditions (Harold, 1986).

Regulation of pH_c is intimately associated with activity and regulation of metabolic activities (for example: glycolysis, oxidative respiration, anaerobic respiration, photosynthesis, protein and DNA synthesis) (Takeshige *et al.*, 1992; Guern *et al.*, 1991; Busa & Nuccitelli, 1984). These activities, in association with proton movements across the organelle and plasma membranes, maintain pH_c (Guern *et al.*, 1991; Kurkdjian & Guern, 1989; Busa & Nuccitelli, 1984; Sanders & Slayman, 1982).

The sensitivity to pH of the enzyme activities involved in metabolism and the finding that changes in pH_c do occur (for example in response to increased chloroplast activity upon illumination, Siebke *et al.*, 1992; Takeshige *et al.*, 1992; Guern *et al.*, 1991), suggest that pH_c may act as a second messenger regulating and integrating different metabolic processes. Other cellular events may be co-ordinated with metabolic activity through modifications to pH_c .

Regulation of the cell cycle has been linked to changes in pH_c in animal cells (Grandin & Charbonneau, 1991 and references therein) and a similar involvement may exist in plants (Pichon & Desbiez, 1994). Changes in pH_c are thought to constitute part of the "master oscillator" of the cell cycle and although they occur subsequently to a series of phosphorylation/dephosphorylation events, they are thought to influence subsequent changes in $[\text{Ca}^{2+}]_c$ (Grandin & Charbonneau, 1991).

pH may also function in cell differentiation; differences in pH_c are associated with, and imposed changes influence, the developmental fates of cells of *Dictyostelium* (Inouye, 1985).

Proton movements and changes in pH_c appear to act as signal transducers (i.e. early in the sequence of events after stimulation) for a variety of stimuli, including response to auxin; elicitors of cellular defence response, and blue light-triggered events, in a range of cell types including higher plants, lower plants and fungi (Bowles, 1995; Asard, 1995; Blatt & Thiel, 1994; Blatt & Armstrong, 1993; Blatt, 1992; Weiss & Weisenseel, 1990; Wada & Kadota, 1989; Racusen *et al.*, 1988; Blatt *et al.*, 1981). The exact link between stimulus and proton movement is often unclear with the activity of plasma-membrane redox chains, proton ATP-ases, H^+ exchangers and metabolic activity all being suggested or implicated as possibilities (Hager & Brich, 1993; Gautier *et al.*, 1992; Takeshige *et al.*, 1992; Weiss & Weisenseel, 1990; Sussman *et al.*, 1990; Morr , 1990; Racusen *et al.*, 1988). Equally unclear is the principal role of proton movements, whether pH_c (e.g. Gresik *et al.*, 1991), pH_o (e.g. Kutschera, 1994; Peters & Felle, 1991; Johri & D'souza, 1988) or membrane potential (e.g. Gresik *et al.*, 1991) are important, and whether they are a cause or consequence of cellular response.

Little is understood of the transduction mechanisms of protons. In addition to influencing enzyme activities, pH_c also has an effect on the cytoskeleton (Edmonds *et al.*, 1995; Grabski *et al.*, 1994; Blatt *et al.*, 1981) and membrane activities (Blatt & Armstrong, 1993; Blatt, 1992). Membrane potential, effected by proton movements, also has an effect on membrane protein activities (Hedrich & Schroeder, 1989). Interaction between pH_c and the Ca^{2+} -mediated transduction pathways through both $[\text{Ca}^{2+}]_c$ and calmodulin activity has been discovered (Herrmann & Felle, 1995; Schumaker & Sze, 1990; Felle, 1988; Busa & Nuccitelli, 1984). Changes in pH_c have been linked with phosphorylation events although the relationship between the two is unclear (Hager & Brich, 1993; Sussman *et al.*, 1990; Tognoli & Basso, 1987).

1.6.5 The determination and control of polarity and apical growth

Regulation of polarity must be considered at the different levels described in Section 1.3.1. This includes: regulation of the site and timing of the initiation of polarity; mechanisms by which cellular

components are organised to establish and subsequently maintain polarity; control and maintenance of polarised activities which, in the case of tip growth, means parameters such as the growth rate, apical diameter and growth orientation.

Cytoskeletal activity offers a key point of control as both an effector and regulator of polarity and tip growth (discussed in Sections 1.5.2 - 1.5.3). Cytoskeletal activity is, however, one of many processes directly or indirectly involved in polarity and tip growth (Sections 1.3 - 1.5.3). All cellular activities require to be co-ordinated through an integrated network of control linked additionally to environmental cues.

Current evidence suggests that localised ion movements and distributions, especially calcium ions and related signal transduction components, are fundamental to polarity and tip growth (Heath, 1990). The roles of ion movements and specific ions in tip growth are examined below.

1.7 The involvement of ions and ion movements in apical growth

It is now well established that many (possibly all) eukaryote cells, and especially those exhibiting polarised growth, drive electric currents through themselves (Gow, 1989; 1994; Harold & Caldwell, 1990; Nuccitelli, 1984; Jaffe *et al.*, 1974). The formation of such a current depends upon the spatial segregation of transport activities resulting in differences in the net movements of charge between different parts of the cell with ion passage through the medium completing the "circuit" (Harold & Caldwell, 1990).

1.7.1 Ion movements and electric fields

There is an overwhelming correlation between cellular polarity, in particular tip growth, and the occurrence of electric currents (in pollen tubes: Weisenseel & Jaffe, 1976; fucoid zygotes: Kropf, 1992; 1994; Goodner & Quatrano, 1993; root hairs: Herrmann & Felle, 1995; Miller *et al.*, 1986; fern gametophytes: Racusen *et al.*, 1988; Cooke *et al.*, 1983; Racusen & Cooke, 1982; fungi: Gow, 1989; 1994; De Silva *et al.*, 1992). Despite this, the evidence from the cell types examined does not support the idea that a causal relationship exists between currents and polarity, and in some cases provides positive evidence against it which suggests currents are a consequence of polarity (see Harold & Caldwell (1990) for a discussion of this point).

Three lines of evidence argue strongly against a causal role for electrical fields in polarity. Firstly, to establish an electric field requires a polarised distribution of membrane activities - making it a consequence rather than a cause (Harold & Caldwell, 1990). Secondly, there is no direct correlation between orientation of polarity or growth rate and either magnitude or direction of the electrical field - this is particularly obvious amongst fungal hyphae (and rhizoids) of different species (Gow, 1989; 1994; De Silva, 1992) and in the opposite orientations of current in, for example, pollen tubes and fern protonemata (Weisenseel & Jaffe, 1976; Racusen *et al.*, 1988). Finally, whilst polarity of various cell types may be orientated by applied electrical fields the features of this phenomenon are not

consistent with observations of endogenous electrical fields (particularly the field strengths required) and their proposed modes of action (Malhó *et al.*, 1994; 1995; Gow, 1989; 1994; Harold & Caldwell, 1990).

While there is apparently no absolute requirement for electric fields for the establishment or maintenance of polarised growth, there is too much evidence to discount them having any physiologically relevant role. Several mechanisms have been proposed for the possible action of electrical fields in tip growth, a few of which have been backed up by experimental evidence: electrophoretic localisation of membrane proteins (Kropf, 1992; Jaffe & Nuccitelli, 1977); polarised translocation of charged secretory vesicles (Kropf, 1992); control of localised membrane channel activities through differences in membrane potential (Gow, 1994). Currently a possible role of electric fields in root associations with bacteria and mycorrhizal fungi is being investigated (Berbara *et al.*, 1995; Miller *et al.*, 1986).

1.7.2 The importance of particular ionic species

The present belief is that electric fields are a consequence of tip growth and that ion movements are involved predominantly in growth-related processes such as: localised nutrient uptake; regulation of ionic composition and maintenance of turgor; "acid-induced wall loosening"; regulation of membrane potential; and the establishment and maintenance of intracellular ion (Ca^{2+} and H^+) gradients (Bisson *et al.* 1995; Herrmann & Felle, 1995; Kropf, 1994; 1992; Gow, 1989; 1994; Kutschera, 1994; De Silva *et al.*, 1992; Nawata, 1992; Steer & Steer, 1989; Racusen *et al.*, 1988; Weisenseel & Jaffe, 1976)

Attention has subsequently shifted to the roles of specific ionic species and the existence of gradients in intracellular ion (Ca^{2+} and H^+) concentrations (Steer & Steer, 1989). It now seems likely that gradients in intracellular Ca^{2+} ions (and possibly pH) regulate the maintenance of polarised growth and that asymmetries in local Ca^{2+} ion concentration contribute to the initiation and establishment of polarity, at least under some circumstances (Levina *et al.*, 1995; Herrmann & Felle, 1995; Gibbon & Kropf, 1994; Gow, 1994; Kropf, 1994; 1992; Malhó *et al.*, 1994; Pierson *et al.*, 1994; Berger & Brownlee, 1993; Jackson & Heath, 1993; Miller *et al.*, 1992; Rathore *et al.*, 1991; Heath, 1990; Steer & Steer, 1989). The involvement of Ca^{2+} and H^+ is discussed further below.

1.8 The involvement of Ca^{2+} ions in the determination and maintenance of polarity in apical growth

It is universally agreed that the concentration of cytosolic free calcium ions ($[\text{Ca}^{2+}]_c$) is of major importance in the regulatory activities of cells (Hepler & Wayne, 1985). This value determines the extent to which Ca^{2+} binds to "regulatory sites"; Ca^{2+} fixed to cellular components and sequestered within organelles is not able to contribute to this equilibrium. Localised transient increases in $[\text{Ca}^{2+}]_c$ are a common feature of signalling (Johnson *et al.*, 1995; Friesen *et al.*, 1993; Thorn *et al.*,

1993; Hahn *et al.*, 1992; Berridge, 1991). However, a different expression - that of the "standing" $[Ca^{2+}]_c$ gradient (see Heath, 1990) - appears to be important in tip growth and is discussed below. The "standing" $[Ca^{2+}]_c$ gradient is considered to be a consequence of polarity (Levina *et al.*, 1995; Kropf, 1992) so its role is likely to be one of maintenance in tip growth. Most of the experimental evidence available relates to the steady-state maintenance of tip growth and factors influencing the steady-state; information on the early events of polarisation is weaker. An additional role in tip growth for wall bound Ca^{2+} has been considered but its involvement has never been rigorously investigated (Steer & Steer, 1989).

1.8.1 Evidence of the importance of $[Ca^{2+}]_c$

To demonstrate a causal relationship between $[Ca^{2+}]_c$ (specifically a $[Ca^{2+}]_c$ gradient) and tip growth several criteria must be satisfied:

- 1) Dependence of growth upon Ca^{2+} and/or the existence of a "standing" $[Ca^{2+}]_c$ gradient in growing cells must be demonstrated.
- 2) The pattern of a gradient should correlate with growth orientation.
- 3) Inhibition of the gradient should inhibit growth.
- 4) Manipulations of the gradient should alter growth.
- 5) Establishment of a gradient should precede polarised out-growth

If the involvement of the $[Ca^{2+}]_c$ gradient is fundamental to tip growth then -

- 6) These features should be consistent for different tip-growing organisms.

Research in this area has predominantly been concerned with pollen tubes and fucoid zygotes (Kropf, 1994; 1992; Malhó *et al.*, 1994; Pierson *et al.*, 1994; Berger & Brownlee, 1993; Miller *et al.*, 1992; Rathore *et al.*, 1991; Heath, 1990; Steer & Steer, 1989), but more recently other systems such as root hairs (Herrmann & Felle, 1995) and fungal hyphae (Levina *et al.*, 1995; Gow, 1994; Jackson & Heath, 1993), have been investigated.

Inhibitor studies have been used to block the action of $[Ca^{2+}]_c$ and functionally related molecules, such as calmodulin and IP_3 , so demonstrating participation of $[Ca^{2+}]_c$ in tip growth (e.g. Hosking *et al.*, 1995; Hidaka & Ishikawa, 1992; Corzo & Sanders, 1992; Saunders & Hepler, 1983). The mechanisms of forming a $[Ca^{2+}]_c$ gradient have been investigated and the effects of inhibition of these processes assessed, linking the ability to set up and maintain a gradient with growth (e.g. Herrmann & Felle, 1995; Wacker & Schnepf, 1990; Saunders & Hepler, 1983).

As genetic and molecular biology techniques have improved they too have been used to investigate the mechanisms and regulation of polarity (Gow, 1994; Taylor *et al.*, 1994; Jackson & Heath, 1993; Dicker & Turian, 1990; Jenkins & Cove, 1983).

Initial work on the roles of ions and ion movements was restricted to external measurements (e.g. Kochian *et al.*, 1992; Harold & Caldwell, 1990) and examination of ion movements across

membranes by patch "clamping" (e.g. Levina *et al.*, 1995; Hedrich & Schroeder, 1989). These techniques provided only a limited view of intracellular events.

Attempts at directly measuring $[Ca^{2+}]_c$ followed on from earlier work and, despite failings in the initial methods used (Jackson & Heath, 1993; Heath, 1990; Steer & Steer, 1989), more recent procedures (see Section 1.10) have provided evidence demonstrating the existence of $[Ca^{2+}]_c$ gradients (Kropf, 1994; 1992; Pierson *et al.*, 1994; Berger & Brownlee, 1993; Miller *et al.*, 1992; Rathore *et al.*, 1991). Subsequently, the effects of manipulations of growth on $[Ca^{2+}]_c$ have been monitored directly. Complementary to this, the effects of experimentally applied and observed manipulations of $[Ca^{2+}]_c$ on growth have been studied (for example Malhó *et al.*, 1994). These latter experiments have provided some of the most convincing evidence favouring a causal role for the $[Ca^{2+}]_c$ gradient in the regulation of tip growth.

The volume of data now available is too great to describe in detail here. However, it is clear (based on the criteria above) that the maintenance of tip growth is dependent upon the presence and location of a $[Ca^{2+}]_c$ gradient in all the cell types which have been fully investigated (Levina *et al.*, 1995; Herrmann & Felle, 1995; Berger & Brownlee, 1993; Jackson & Heath, 1993). However, the mechanisms by which such a gradient is set up and maintained, the exact nature (spread, slope and absolute $[Ca^{2+}]_c$ involved), and the proposed activities of the gradient differ widely (see references cited at the end of Section 1.7.2). This is likely to be a reflection of both genuine and experimental differences.

1.8.2 The role of $[Ca^{2+}]_c$ in polarity and tip growth

While it is almost certain that $[Ca^{2+}]_c$ gradients are involved in tip growth, the mechanism of action is largely unknown. Several plausible models have been proposed based on the known important events and mechanics of tip growth (see sections 1.4-1.5.3) for pollen tubes (Steer & Steer, 1989), fucoid zygotes (Kropf, 1992; 1994) and fungal hyphae (Jackson & Heath, 1993). There are several differences between these models. There are also certain common essential concepts. The regulation of cytoskeletal activity by Ca^{2+} (and Ca^{2+} -regulated protein activities), which has been observed under a variety of circumstances, is central to all models. This reflects the known importance of the cytoskeleton in polarity and tip growth (see section 1.5.3). The maintenance of high apical Ca^{2+} yet low subapical levels has been correlated with cytoskeletal structure and transport activities (Steer & Steer, 1989). Another important concept - based on observations from secretory cells - is the control of vesicle fusion at membranes by Ca^{2+} (Steer & Steer, 1989). The localised high concentration at the tip apex is thought to correspond to such activity. In some cell types a $[Ca^{2+}]_c$ gradient is required to maintain polarised organelle distribution (Steer & Steer, 1989); although, this is apparently not the case for moss protonemata (Wacker & Schnepf, 1990). In general, the active processes of tip growth (vesicle movements, tip shape and cell wall deposition) are more sensitive to disruption of $[Ca^{2+}]_c$

than general organisation of the tip. Calcium has also been implicated in turgor regulation (Bisson *et al.*, 1995).

Generally, Ca^{2+} is believed to act directly or through interaction with regulatory proteins such as calmodulin and the various cytoskeleton-associated proteins (Roberts & Harmon, 1992; Harmon & McCurdy, 1990; Klee *et al.*, 1980). An alternative possibility is that the distribution of charge resulting from a "standing" $[\text{Ca}^{2+}]_c$ gradient generates an electrical field (Donnan potential) which has physiological significance (refer to discussion in Section 1.7.1).

The evidence for a role of $[\text{Ca}^{2+}]_c$ in the initiation and early development of polarity is not so definite but involvement is still strongly implicated in the development of fucoid zygotes (Berger & Brownlee, 1993; Kropf, 1992), germination of pollen grains (Heslop-Harrison, 1987), bud formation in mosses (Saunders & Hepler, 1983) and branching in fungi (Dicker & Turian, 1990; Harold & Caldwell, 1990). Whether the latter constitutes an initiation of polarity *de novo* is open to question. It is not clear whether Ca^{2+} is a primary trigger in initiating polarity or is involved in subsequent steps reinforcing the establishment and fixation of a polar axis - discussed in Kropf (1992).

Theories about how a $[\text{Ca}^{2+}]_c$ gradient is initially established are based on mechanisms for localised activation or recruitment of Ca^{2+} channels (e.g. by stretch or voltage activation, local anchoring by the cytoskeleton or local incorporation of channels into the plasma membrane from vesicle secretion (Malhó *et al.*, 1995; Levina *et al.*, 1995; 1994; Kropf, 1992)). Involvement of Ca^{2+} release from internal stores has been suggested as an early amplification step or alternatively as the main source of Ca^{2+} where establishment of the gradient appears to be independent of movement across the membrane (Kropf, 1992).

From the early observations of Ca^{2+} fluxes across the plasma membrane of polarised cells (Harold & Caldwell, 1990), on the basis of which the initial concept of the existence of $[\text{Ca}^{2+}]_c$ gradients was formulated, subsequent work has shown the important contributions of Ca^{2+} fluxes into and out of intracellular Ca^{2+} stores (ER (Gilroy *et al.*, 1993); mitochondria, (Steer & Steer, 1989); vacuoles and vesicles (Gelli & Blumwald, 1993; Zocchi & Rabotti, 1993; Randall, 1992); cytoplasmic calcium buffering proteins (Harold & Caldwell, 1990)) to both the maintenance and regulation of Ca^{2+} gradients.

1.9 Evidence for the involvement of H^+ ions in apical growth

As with Ca^{2+} , the initial association of H^+ ions with tip growth was through the contribution of H^+ to the growth currents of various tip-growing cell types (Fig. 3; Gow, 1994; Harold & Caldwell, 1990; Gow, 1989). The best examples of association between proton movements and tip growth are found amongst the fungi. For example, with both *Neurospora* (Gow, 1989) and *Achlya* (Harold & Caldwell in Heath, 1990; Gow, 1989; Gow *et al.*, 1984) a strong correlation between growth and localised proton entry at the tip was found. The direction of growth of *Achlya* hyphae could be oriented by

protonophores (Gow, 1989) and branch outgrowth is preceded by proton influx and may be induced by protonophores (Harold & Caldwell, 1990).

There is, however, no consistent pattern of proton movements (or local "pH profiles") around the apices of different tip-growing cell types (see Fig. 3). The oomycete fungus *Allomyces macrogynus* has both tip growing rhizoids (specialised for nutrient uptake) and hyphae; contrary to *Neurospora* and *Achlya*, protons in *Allomyces* are extruded from the hyphal apex. However, protons enter at the apices of the tip-growing rhizoids of this fungus (De Silva *et al.*, 1992). Fern and moss protonemata also exhibit proton extrusion at their tips (Bittisnich & Williamson, 1989; Racusen *et al.*, 1988). However, the photosynthetic tip-growing marine alga *Vaucheria* (Kataoka & Weisenseel, 1988; Kataoka, 1981) exhibits localised proton entry at the filament tips while pollen tubes show proton extrusion behind their tips (Obermeyer *et al.*, 1992; Weisenseel & Jaffe, 1976). The situation is even more complex with fucoid embryos where the mechanisms of generating the "acid base and alkali tip" external "pH profile" associated with growth of the rhizoid, are not understood (Gibbon & Kropf, 1991; 1994).

The different organisms also show variation in the importance to growth of extracellular pH (and the maintenance of the extracellular "pH profiles" they generate - see Fig. 3). For fucoid rhizoids, strong buffering of the external medium eliminates the external pH profile but does not reduce tip growth (Gibbon & Kropf, 1991). The site of rhizoid outgrowth can, however, be directed by gradients in external pH (Harold & Caldwell, 1990; Gow, 1989). The growth of *Achlya* is more pH sensitive; a rise in external pH of 2.0 units significantly reduced growth (Gow, 1989). This is thought to be linked to nutrient uptake (De Silva *et al.*, 1992; Gow, 1989). *Neurospora* vegetative hyphae are also affected with changes in growth rate and pattern and shifts in cytoplasmic pH (Parton *et al.*, 1996). The response of root hairs is again different; large, sudden changes in external pH (2 - 3 units up or down from pH 7) cause a transient reduction in growth rate linked to transient displacement of pH_c (Herrmann & Felle, 1995). Such differences are not easily interpreted in terms of a common role for pH (or H^+ ions) in tip growth.

Results from the few measurements of intracellular pH distribution in tip-growing cells which have been performed are equally contradictory, with gradients in pH_c being absent or present in different orientations (fucoid rhizoids - Gibbon & Kropf (1994); fungal hyphae - Roncal *et al.* (1993); Jackson & Heath (1993); root hairs - Herrmann & Felle (1995). Even for the same cell type (*Neurospora*) gradients of pH_c of different orientations have been claimed (Prebble *et al.*, 1994; Gow, 1989). This again argues against a fundamental primary role for pH in regulating tip growth although it may simply reflect problems with methodology (see Section 1.10 and Chapter 5).

1.9.1 The role of protons in apical growth

The question of the role of H^+ ions in tip growth has proven to be more intractable even than experimentally demonstrating a role for Ca^{2+} in this process. The "conflicting" evidence with different

cell types suggests that internal pH and H⁺ ion movements probably do not perform a fundamental "organisational role" in tip growth, as proposed for the steady state [Ca²⁺]_c gradient. Interpretation of the situation with H⁺ is further complicated relative to that of Ca²⁺ in two ways. Firstly, the role of H⁺ ions as second messengers is not as well defined as for Ca²⁺. The second complication is the intimate association of H⁺ ions (pH) with the processes as well as the regulation of metabolic activity and trans-membrane transport processes - both of which are likely to be crucially yet indirectly involved in tip growth (Bush, 1993; Busa & Nuccitelli, 1984). The possible contributions of H⁺ ions (pH) are discussed below.

1.9.2 Protons and transport activities

Protons have been found to be the principal ions coupling metabolic energy to the uptake of solutes across membranes in plants and fungi (Downey & Gideon, 1992; 1994; Bush, 1993; De Silva *et al.*, 1992; Gow, 1990; Hedrich & Schroeder, 1989; Spanswick, 1981). In the fungi *Achlya*, *Neurospora* and *Allomyces*, influx of protons either at the hyphal or rhizoid apex correlates well with nutrient uptake (Gow, 1994; De Silva *et al.*, 1992). While nutrient uptake will directly affect tip growth, it is possible that, linked to this, pH or ion movements at the growing apices function in a chemotropic mechanism directly influencing tip growth (Gow, 1994). The H⁺ movements of pollen tubes are thought to be important in the regulation of turgor pressure (also important in tip growth) through the accumulation of K⁺ (Steer & Steer, 1989; Weisenseel & Jaffe, 1976).

1.9.3 The "acid growth hypothesis"

Why nutrient uptake and turgor regulation require the degree of spatial segregation and localisation of transport activities observed is not clear. In other examples of localised proton movements a direct relationship between the localisation and polarisation of growth is more easily envisaged.

In moss and fern protonemata, which exhibit localised proton efflux from their growing apices, H^+ ions are proposed to contribute directly to the mechanism of apical extension through "acid wall loosening" (Bittisnich & Williamson, 1989; Racusen *et al.*, 1988; Taiz, 1984). While the mechanism of auxin-induced growth by "acid wall loosening" has come under question recently (Kutschera, 1994; Peters & Felle, 1991), the effect of acid (pH 2.5 - 3) on wall extensibility is still valid (Kutschera, 1994). Whether this is the case for protonemata requires further investigation. In this respect it is interesting that in the blue light-induced "apical swelling" of fern protonemata the extrusion of protons is delocalised over a greater region of the apex corresponding to the increased lateral expansion (see Section 1.7). That wall acidification is not similarly required for walled, tip-growing pollen tubes (Steer & Steer, 1989; Weisenseel & Jaffe, 1976), root hairs (Herrmann & Felle, 1995), algae (Kropf, 1991; Kataoka & Weisenseel, 1988) and fungi such as *Neurospora* and *Achlya* (Harold & Caldwell, 1990; Gow, 1989) - all of which actually alkalise their tips - suggests the mechanism may be specific for protonemata or that proton extrusion has an alternative function.

1.9.4 Gradients in cytosolic pH

As has been found for Ca^{2+} , localised ion movements may underlie intracellular ion gradients. Whether a cytosolic gradient is possible is dependent upon three main factors: the cytoplasmic buffer capacity; the rates of proton flux across plasma and organelle membranes; and the relative locations of proton sources and sinks. Several studies suggest that the existence of cytosolic pH domains and gradients is not completely inconceivable (Al-Baldawi & Abercrombie, 1992; Roos, 1992; Kurkdijan & Guern, 1989). Movement of H^+ ions through the cytosol is not as rapid as for other small ions (K^+ , Cl^- , Na^+) due to buffering by fixed or slow diffusing compounds (proteins) (Al-Baldawi & Abercrombie, 1992; Harold & Caldwell, 1990). Cytosolic buffering and rates of proton flux are also amenable to the formation of cytosolic pH domains and gradients under certain circumstances - Al-Baldawi & Abercrombie, (1992) proposed, on the basis of values of proton flux determined for known proton transport activities (500 pmol/cm²s proton equivalents); current estimates of buffer capacities (10 mM/pH unit); and approximations of proton diffusion coefficient of the cytoplasm (10⁻⁶ cm²/s), that a ΔpH_c of the order of 0.1 unit could be set up over 25 μm in an acid transporting epithelial cell. Localised sources and sinks for protons (e.g. involving localised pump and channel activities at the plasma membrane, ER membranes, mitochondria and chloroplasts; discussed in Roos (1992)) and uneven distributions of "buffers" (for example "fixed" cytoskeletal and associated proteins; Al-Baldawi & Abercrombie (1992)) could contribute to the ability of cells to form cytosolic pH domains. Convincing direct evidence (measurement or visualisation) of pH domains is extremely

scarce (Roos (1992) - although possible artefacts affecting this data are discussed in Chapter 5). This may reflect the magnitude of physiologically relevant pH differences. "Relevant" changes which have been measured are between 0.05 and ~ 0.1 pH unit - the lower limit corresponds to the absolute limit of resolution of measurement techniques (Herrmann & Felle, 1995; Busa & Nuccitelli, 1984). Another possible problem is localisation of pH differences to within only a few micrometres of organelle and plasma membranes (Roos, 1992) - a spatial resolution not easily achieved with current techniques (Kurkdjian & Guern, 1989). Some direct evidence for the occurrence of tip growth-associated gradients in pH_c exists, the most convincing example being that of *Pelvetia* rhizoids (Gibbon & Kropf, 1994) which is discussed in more detail in Chapter 6; Section 6.7.

A pH gradient (or plasma-membrane localised pH domains) could provide organisational information in much the same way as suggested for Ca^{2+} (see Section 1.8.2) through its influence on relevant processes. Importantly, pH has been shown to influence the cytoskeleton (Edmonds *et al.*, 1995; Grabski *et al.*, 1994; Tiwari *et al.*, 1994; Kropf, 1994; Lamb *et al.*, 1993; Blatt *et al.*, 1981) and could influence the cortical cytoskeletal organisation of tip-growing cells. There is also evidence that pH could directly interact with Ca^{2+} -related transduction mechanisms (see Section 1.6.4; Lamb *et al.* (1993)). In animal cells endocytosis and exocytosis at the plasma membrane is influenced by local pH (Guern *et al.*, 1991). The pH of compartments involved in the endocytotic and exocytotic pathways is important in vesicle organisation and targeting (Seksek *et al.*, 1995; Rost *et al.*, 1995; Butor *et al.*, 1995). A gradient in the pH of these organelles along the tip could be functionally significant and may interact with pH_c .

The failure to detect a pH gradient in root hairs (Herrmann & Felle, 1995) weakens the case for the general occurrence of a tip growth associated pH gradient. However, this does not rule out the possibility of physiologically relevant, yet highly localised, pH_c differences, possibly within a few micrometres of membranes (Roos, 1992). It is interesting that in both fucoid rhizoids (Gibbon & Kropf, 1994) and root hairs (Herrmann & Felle, 1995) where a pH "gradient" was detected and not detected, respectively, experimental changes in intracellular pH away from normal levels inhibited tip growth.

1.9.5 Second messenger activity of pH or proton movements

Whether or not a functionally important gradient in pH_c exists, it is possible that pH or proton movements could directly influence tip growth as a second messenger. Regulation of pH_c is intimately associated with metabolic activities and their regulation (see Section 1.4.2); pH_c may, therefore, act as an indicator of metabolic state by integrating metabolic activity with other cellular functions (Busa & Nuccitelli, 1984). Changes in pH_c due to changes in metabolism could act to modify tip growth (see Herrmann & Felle (1995 - small shifts in pH_c affect tip growth).

Changes in H^+ flux and or pH_c have also been implicated in signalling roles linked to external stimuli. Localised H^+ entry at the apex of fungal hyphae may contribute to a chemotropic mechanism

(Gow, 1994; Harold & Caldwell, 1990). Proton movements (linked to the activities of the proton ATPase or plasma-membrane redox chain activity) have been recorded in a variety of blue light-mediated responses involving the regulation of tip growth (Weiss & Weisenseel, 1990; Racusen *et al.*, 1988; Kataoka & Weisenseel, 1988; Cooke *et al.*, 1983; Cooke & Racusen, 1982; Kataoka, 1981).

The role of pH and H⁺ flux in tip growth is as yet unclear and while a fundamental organisational role in the maintenance of the steady state, as with [Ca²⁺]_c (Section 1.8), seems unlikely, it cannot yet be dismissed. Maintenance of pH_c is clearly important for cells (Herrmann & Felle, 1995; Guern *et al.*, 1986; Mathieu *et al.*, 1986) although subtle global changes and local domains of different values occur (e.g. Roos, 1992; Gresik *et al.*, 1991; Guern *et al.*, 1991; Kurkdjian & Guern, 1989). Additionally, pH has been shown to influence cellular processes and interact with Ca²⁺ regulatory mechanisms (see previous discussion). There is clearly a case for pH and proton movements acting in a regulatory capacity in tip growth by overlaying or integrating with the organisational information of [Ca²⁺]_c in steady state growth.

1.10 Methods for the analysis of intracellular free-ion concentrations *in vivo*

The need for measurements of intracellular distribution and concentration of particular ion species in order to fully understand their role in determining and maintaining cellular polarity was pointed out in Sections 1.8 & 1.9.

A summary of the principal techniques for intracellular ion measurement (principally Ca²⁺ and H⁺) is given in Table 1.2. The list has been restricted to only those methods which allow *in vivo* measurement. X-ray microanalysis, for example, is used to map intracellular ion distributions within tissues and cells. However, as dead, fixed and sectioned material is used, analysis of transient or dynamic events is not possible.

Table 1.2: Methods for intracellular ion measurement

Methods and application		Localisation of cellular measurement	Estimated limits of precision	spatial resolution	Refs †
Ca²⁺ & H⁺					
Ca ²⁺ & H ⁺ microelectrodes		local cytoplasmic or vacuolar	Ca ²⁺ ±1 nM pH ±0.1*	point measurement	a,b,c, d
pH/ Ca ²⁺ sensitive dyes #	Photometry	average cytoplasmic/vacuolar	Ca ²⁺ ±25-50 nM* pH < ± 0.5*	whole/part cell	e,j
	Imaging	local cytoplasmic/vacuolar		subcellular	e,g,k
	Confocal	local cytoplasmic ^{and/or} vacuolar		subcellular (µm ³ volumes)	b,f,h,i
Ca²⁺ only					
Ca ²⁺ sensitive photoproteins	Photon counting	average cytoplasmic or organellar (nucleus etc.) ‡	not applied (qualitative)	cell population or cell	l,m,n, o
H⁺ only					
³¹ P NMR		average cytoplasmic and vacuolar	pH ±0.1*	cell population	p,q,r
weak acid/base distribution		average cellular pH	qualitative	cell population	s

† **References:** a) Herrmann & Felle, 1995; b) Gibbon & Kropf, 1995; c) Felle; 1993; 1989; 1988 d) Reid & Smith, 1988; e) Rost *et al.*, 1995; f) Levina *et al.*, 1995; g) Pierson *et al.*, 1994; h) Berger & Brownlee, 1993; i) Roos, 1992; j) McAinsh *et al.*, 1992; 1990; k) Inouye, 1985 l) Haley *et al.*, 1995; m) Knight *et al.*, 1993b; n) Kikuyama *et al.*, 1993; o) Futsaelter *et al.*, 1992; p) Guern *et al.*, 1986; q) Mathieu *et al.*, 1986; r) Mimura & Kirino, 1984; s) Gresik *et al.*, 1991.

* Precision of [ion] measurement appears to be seldom quoted in the literature. It is possible that it has been assumed that variation between cells is always greater than the precision limit of the techniques used. The values cited here are based on the standard deviations reported for measurements of the resting state [ion]_i in living cells (50 - 200 nM Ca²⁺ and pH ~7.2). In many cases the techniques are used qualitatively to follow the occurrence rather than the absolute magnitude of changes, this is particularly true of work with Ca²⁺ sensitive photoproteins. For general references see: Pawley (1995); Nuccitelli (1994); Fricker *et al.* (1994); Read *et al.* (1993); Gilroy *et al.* (1993); Guern *et al.* (1991); McCormack & Cobbold (1991); Busa & Nuccitelli (1984).

Does not include CTC or the use of lipophilic [ion] reporters.

‡ Depending upon targeting of photoprotein expression to within intracellular organelles, for example: the nucleus, chloroplasts; or the general cytosol.

The main requirements of a method suitable for investigating the secondary messenger role of ions are:

- A) Non-invasive. The method should not interfere with normal physiological activity or cellular response.
- B) Ion specificity and accurate quantification. Even very small differences in [ion] (< µM) may be biologically relevant. Methods should be precise enough to measure such small differences in the ionic species of interest.

C) Spatial and temporal resolution. Spatial and temporal aspects of [ion] differences and changes are emerging as one of the ways in which information is encoded by these second messengers (e.g. Johnson *et al.*, 1995; Read *et al.*, 1992). It is, therefore, critical that measurements are made with the highest possible resolution (over $< \mu\text{m}$ distances in the ms range).

At present the two most promising methods for the type of investigation described here are ion-selective microelectrodes and imaging of fluorescent ion-sensitive dyes (see Table 1.2 for references). Of these, it is the latter which has provided the clearest picture of dynamic signalling events within living cells in real time. The two methods are often combined (e.g. Kropf, 1994). Photoprotein (aequorin and luciferase)-based methods are not advanced enough to allow routine imaging of intracellular $[\text{Ca}^{2+}]$, but there is growing interest in this area (Haley *et al.*, 1995; Johnson *et al.*, 1995; Mayerhofer *et al.*, 1995; Trewavas & Knight, 1994; Knight *et al.*, 1993b)

1.11 Imaging of intracellular ion-sensitive dyes

The use of ion-sensitive fluorescent dyes in conjunction with fluorescence imaging technology has proved to be one of the more important advances in the study of the second messenger roles of ions (Fricker *et al.*, 1994; Graziana *et al.*, 1993; Read *et al.*, 1992; Thomas & Delaville, 1991; Tsien & Poenie, 1986; Grzynekiewicz *et al.*, 1985; Tsien, 1980). The way in which these dyes work is shown in Fig. 4. Dye molecules reversibly bind to specific ions by ionic interactions at their ion binding site, the structure of which is important to their specificity for particular ionic species. Binding to the specific ion causes conformational changes in the dye molecule which in turn influences its fluorescence excitation and emission properties (Tsien, 1980).

Two major classes of ion sensitive dyes exist: the single wavelength dyes and the dual wavelength or ratio dyes (Tsien & Poenie, 1986; see also Haugland, 1992). For single wavelength dyes, the intensity of fluorescence emission at a particular wavelength increases in proportion to the free [ion]. The problem with this is that it is difficult to distinguish the effects of different dye concentration from [ion] differences. This makes absolute calibration of images difficult (e.g. see Malhó *et al.*, 1994; Shacklock *et al.*, 1992; Read *et al.*, 1992). Ratio dyes provide a solution to the problem of dye concentration and so allow better calibration (Read *et al.*, 1992; Tsien & Poenie, 1986). Two fluorescence measurements are made in ratio imaging, the subsequent ratio of those values is independent of dye concentration while remaining proportional to the free [ion]. Ca^{2+} and pH dyes are the most commonly used and a range of each is available covering a variety of excitation and imaging wavelengths, different ion affinities for use over different ranges of [ion] and with different loading properties and intracellular behaviour (Haugland, 1992). Dyes sensitive to Na^+ , Mg^{2+} , Cl^- and also membrane potential are available (Das *et al.*, 1993; Haugland, 1992; Verkman, 1990; Smith *et al.*, 1988). Dyes and their use are discussed more fully in Chapters 2, 4 and 5.

1.11.1 Methods of examining fluorescence emissions

Once a dye has been introduced into the intracellular environment it has the potential to report intracellular free [ion] accurately, with high spatial and temporal resolution in a relatively non-invasive way. Modern dyes, such as Fura-2, are not expected to have significant buffering effects on intracellular [ion] because they can be used at low concentrations - in the tens of μM - (Thomas & Delaville, 1991) they should not alter intracellular ion concentrations or interfere with the ability of cells to set up gradients. Therefore, the extent to which the potential of dyes is realised depends largely upon the method used to detect the fluorescence emissions of the dye.

There are three main ways of analysing intracellular dye which differ in the cost and complexity of equipment required, the effect on living material and the quality of data which may be obtained. Photometry (e.g. McAinsh *et al.*, 1992; Gilroy *et al.*, 1991; 1990; McAinsh *et al.*, 1990) is the most crude method in which average fluorescence from the specimen is detected by a photomultiplier (or photomultipliers for emission "ratioing"). The fluorescence may be recorded as a voltage output, photon counts or processed directly to a ratio trace. This method is useful for detecting large or global changes in response to stimuli and may be coupled to electrophysiological measurements (Dr. Rui Malhó, personal communication).

The simplest true imaging method is accomplished with a charge coupled device (CCD, for example an extended ISIS intensified CCD camera - Gilroy *et al.* (1991). Fluorescence images are generally captured and stored as digital images using the appropriate computer technology. Stored images can subsequently be processed and analysed. Ratioing may be achieved through digital processing or video signal merging methods (Gustafson & Magnusson, 1992; Gilroy *et al.*, 1991). Even with the use of ratioing such imaging of biological material suffers from various artefacts: fluorescence signal fall off across the uneven thickness of cells; saturation of fluorescence detection in parts of an image; incorrect background subtraction; and the problem of signal averaging across a significant volume of a cell potentially containing dye located within different organelles each with their own specific ionic compositions (Silver *et al.*, 1992; Bolsover & Silver, 1991). More complex imaging processing - such as the use of algorithms designed to reduce out-of-focus blur (deconvolution) - is often used to improve image quality (Keating & Cork, 1994). However, the value of this approach in quantitative ion imaging is questionable because of the mathematical transformations of the image data involved.

Laser scanning confocal microscopy is the method able to provide (directly) the most detailed fluorescence images (for review see Pawley, 1995). Such image quality, however, comes at a cost, both in terms of the complex equipment required, the potentially damaging effects of irradiating specimens with an intense laser beam and the high level of fluorescence required to obtain reasonable image quality. The great advantage of confocal microscopy is its ability to produce optically thin sections from within thick biological specimens (Laurent *et al.*, 1992; 1994; Shotton & White, 1989). In effect, fluorescence information is gathered from a narrow optical plane within a specimen and out-of-focus information (from background fluorescence, non specific staining and scattered light) above

and below that plane is excluded. As a result this form of microscopy improves resolution in the XZ plane (Fricker *et al.*, 1994 and references therein; Goldstein, 1992). This improved resolution in the XZ plane provides increased contrast, relative to conventional fluorescence techniques, when imaging brightly stained structures against a general non-specific background fluorescence. When this is combined with the ability to merge optical sections taken at different depths complex subcellular detail within cells can be visualised.

When applied to quantitative fluorescent ion sensitive dye imaging, confocal microscopy reduces the problems resulting from dye sequestration within organelles (which can be more easily identified and the associated "domains" of different [ion] better interpreted), uneven dye distribution and uneven specimen thickness which can be significant in conventional fluorescence microscopy where the signal detected is averaged over a much greater depth of the cell (see Chapters 4 and 5). The spatial resolution of confocal microscopy coupled with the digital image capture and processing employed by the laser scanning type of confocal microscopes make this approach particularly useful for quantitative fluorescence imaging work even when using non-ratioable dyes.

1.12 Fern gametophytes as an experimental system

The most commonly used systems for the study of cellular polarity have been mentioned in Section 1.2.1. Owing to the inherent problems of using "model" systems, with evolutionary differences and specialisation of function, there is an obvious benefit to be gained from studying and comparing a variety of different systems exhibiting similar phenomena such as polarised growth. Fern gametophytes are a potentially useful experimental system and as yet have not been widely exploited with the latest techniques available for investigating polarity and tip growth.

Fern gametophytes, despite a loss of favour as experimental systems after a peak of interest around the middle of this century (Miller, 1968; Laetsch, 1967), do have many useful attributes and are beginning to feature more regularly again in the literature (e.g. Wada *et al.*, 1995; Kiss *et al.*, 1995; Cooke *et al.*, 1995; Hickok *et al.*, 1995; Clark *et al.*, 1995; Wada *et al.*, 1995; Raghavan, 1992; 1993; Scheuerlein *et al.*, unpublished manuscript 1992).

1.12.1 The fern gametophyte

The position of the gametophyte in the fern life-cycle and the developmental stages of a typical gametophyte are shown in Figs. 5 and 6. While ferns (sporophyte stage) have vascular tissue and should be considered as higher plants, the gametophyte is non-vascular and more closely resembles lower plants such as mosses and liverworts. Gametophytes are, therefore, widely considered as lower plants (Wada & Kadota, 1989). Even so, their higher evolutionary status should be remembered.

Two publications provide an extensive review of all aspects of the biology of fern gametophytes. Dyer (1979) deals with the older literature, covering early work on structural analysis in detail, while

Raghavan (1990) gives a more up to date view of the work on ferns yet still includes a great deal of the older background material.

1.12.2 Investigations of polarity and polarised growth in the fern gametophyte

There are three key developmental steps in the early development of fern gametophytes which provide good opportunities to study polarity and polarised growth in morphogenesis:

A) Spore germination. Three main aspects of spore germination have attracted interest: 1) induction of germination (Raghavan, 1993; Scheuerlein *et al.*, 1991; Lino *et al.*, 1989; Cooke *et al.*, 1987; Miller & Wagner, 1987; Wayne *et al.*, 1986; Wayne & Hepler, 1984; 1985; Edwards & Miller, 1972); 2) the initial asymmetric division of the spore cell, characteristic of early germination in nearly all species (Gantt & Arnott, 1965); 3) the different developmental fates of the unequally sized cells resulting from asymmetric division (Miller & Bassel, 1980; Miller & Greany, 1976; Fraser & Smith, 1974).

B) Apical growth. Apical growth occurs in the protonemal initial and, subsequently, in the apical chlorocyte during the protonemal (or "first filament") stage of development (Kiss *et al.*, 1995; Kadota & Wada, 1989a). The filamentous protonemal stage appears to be common to most homosporous ferns, although the number of cells and length of the filament before transition to planar growth occurs (prothallus formation) depends strongly upon the conditions of growth. The species *Schizaea pusilla* is unusual in that it remains in the protonemal form throughout the gametophyte stage. Apical growth is also exhibited by the elongating rhizoid cells (Miller *et al.*, 1983; Gantt & Arnott, 1965). These two cell types provide a useful comparison of tip growth as cells of diverse function from the same organism, this comparison is even more interesting (from a developmental point of view) in that both cell types can have arisen from one asymmetric division of a unicellular spore (Miller & Bassel, 1980).

The tropic growth responses of both cell types provide the opportunity for the mechanisms of re-orientation of polarity to be investigated (Kadota & Wada, 1992a & b; Dr. A.F. Dyer, personal communication). The roles of cell : cell signalling, plant "hormones" and "age" or increasing development of individual cells along a filament have been studied in relation to their involvement in apical dominance and maintenance of polarity along the length of a protonemal filament (Tilney *et al.*, 1990; Smith, 1979; Reynolds & Corson, 1979).

C) Transition. Transition is the change from the early protonemal stage (first filament) to the prothallial stage (flat plate). This photomorphogenetic phenomenon, which has been used as a model for understanding the mechanisms of determination of shape and form in plants, can be broken up roughly into three events (Raghavan, 1990; Howland & Edwards, 1979):

1) The change from apical extension to isodiametric expansion at the tip (i.e. a change in growth polarisation). A characteristic increase in cell diameter and reduction in cell elongation is the earliest morphological expression of changing illumination from red (or darkness) to blue light.

- 2) The change in the regulation of the cell cycle to increase the rate of cell division (Davis, 1971). However, under conditions of red and blue light illumination where cell division rates were the same while cell expansion alone differed, isodiametric cells still formed in blue light, but not in red.
- 3) the change in the orientation of the plane of cell division from transverse in the protonema to longitudinal (considered to be the decisive event of transition).

Additional events that have been studied include polarised organelle movements, in particular the nucleus during tip growth and the cell cycle (Mineyuki & Furuya, 1985; Wada *et al.*, 1980; Ito, 1969) and chloroplasts, which move in response to illumination conditions (Yatsuhashi & Wada, 1990). The triggering of further asymmetric divisions of subapical protonemal cells by blue light to produce secondary rhizoids (which proceeds in a similar way to the initial asymmetric division of the spore) has also received attention (Dyer & King, 1979).

1.13 Apical growth of fern gametophytes

The apical chlorocyte, during conditions of filamentous growth, and the rhizoid both show elongation by apical extension. Growth has been demonstrated both in rhizoids (Takahashi, 1961) and elongating apical chlorocytes (Davis *et al.*, 1974; Stockwell & Miller, 1994) to be restricted to a narrow region of the apex. In protonemata this location also corresponds to the site of new cellulose microfibril deposition (Wada & Stachelin, 1981).

1.13.1 Tip growth of the apical chlorocyte

In most gametophyte species growth of the apical chlorocyte by apical extension occurs under conditions of darkness, low light intensity, red light or far-red light (Furuya, 1978, Davis *et al.*, 1974). The involvement of phytochrome has been shown in the regulation of the occurrence (Kadota & Furuya, 1981) and rate (Cooke & Paolillo, 1979) of apical extension. The response to light is both qualitative and quantitative (Cooke & Paolillo, 1979). Depending upon the exact illumination conditions, the rate of tip extension and the cell diameter are variable and inversely proportional, while the change in cell volume is the same (Cooke & Paolillo, 1979; Miller & Stephani, 1971). Under higher light intensity or blue light, apical extension is inhibited and isodiametric cell expansion occurs. These photomorphogenic responses have been particularly well studied in relation to the nature and location of the photoreceptors involved (Wada & Kadota, 1989 and references therein; Furuya, 1978 and references therein), namely: phytochrome; an, as yet, uncharacterised blue light receptor; and putative receptor, P580 (Miller & Miller, 1967).

1.13.2 Tip growth of the rhizoid

Rhizoids only grow by apical extension (Takahashi, 1961). Work on rhizoid elongation has largely been concerned with nutrient requirement (rhizoids are non-photosynthetic and so are dependent upon the chlorocyte cells) and, in particular, the absolute requirement of rhizoids for Ca^{2+} (or Mg^{2+} or

Mn²⁺) ions for elongation (Miller *et al.*, 1983). Additionally, rhizoid cells are incapable of division while protonemal apical cells divide to produce a single file of cells during filamentous growth (Dyer, 1979).

1.13.3 Cytology and tip growth

Cytology and ultrastructure has been examined in both protonemata and rhizoids (see Chapter 3), although good data is somewhat limited (Kiss *et al.*, 1995). In general, structural features are as would be expected from examination of other tip-growing cell types (see Section 1.5). Polarisation is more distinct in rhizoids than protonemal apical cells - which have some similarity to moss protonemal apical cells - and are not significantly different in their overall organelle content from subapical protonemal cells (Schmiedel & Schnepf, 1980; Cran, 1979). The apical cell of *Schizaea pusilla* protonemata, which remains filamentous throughout the gametophyte phase, shows a greater degree of polarisation than other ferns such as *Adiantum* (Kiss *et al.*, 1995; Wada & O'Brian 1975).

Positioning of the nucleus close to the apical dome (the region of expansion) appears to be important to apical extension in protonemal apical cells. Displacement of the nucleus from the tip of an apical chlorocyte stops growth, subsequently lateral out-growth occurs opposite to the new nuclear position (Mineyuki & Furuya, 1985; Wada *et al.*, 1980; Ito, 1969). This is in contrast to other tip-growing cell types including rhizoids where the nucleus lies well behind the growing point, although in both fern cell types, nuclear migration keeps pace with apical extension (Steer & Steer, 1989; Dyer & Cran, 1976).

1.13.4 Mechanisms regulating apical growth and transition

As with other tip-growing cell types, the mechanisms involved in determining and regulating tip growth have attracted interest. For fern protonemata, one of the key questions investigated has been how is filament diameter regulated and how are filament diameter and apical extension rate related (Cooke & Paolillo, 1979; Miller & Stephani, 1971)? This question relates to the variable elongation rates and apical diameters during filamentous growth; induction, by red light, of apical extension in non-growing dark-treated protonemata; and most specifically to the control of transition from elongation to isodiametric cell expansion mediated by blue light.

1.13.5 Role of the cytoskeleton in tip growth and transition

Several investigations (see Cooke & Racusen, 1982 for discussion) found that neither measurements of extension rate nor total growth rate fitted in with the expected behaviour of factors under direct photocontrol. It was finally proposed that, in fact, the cross-section area of a protonemal filament was the aspect of tip growth directly regulated (Mohr, 1980; Cooke & Paolillo, 1979).

This proposal was further investigated to determine a possible biological mechanism. Microtubule disorganising drugs, such as colchicine, were found to cause increased diameter in chlorocyte cells

(Murata & Wada, 1989a, Miller & Stephani, 1971). Based on this finding, the knowledge that microtubules (MT) in some way act to orient cellulose microfibril deposition and the proposed role of cellulose microfibril orientation in "restricting" cell expansion to a particular direction, a mechanism was postulated to account for the regulation of apical chlorocyte diameter (see Section 1.5.3; Cooke & Racusen, 1982; Cooke & Paolillo, 1979; Davis *et al.*, 1974). Microtubules were proposed to orient cellulose microfibrils such that lateral expansion was restricted.

This hypothesis has been, to some extent, supported by the findings in subsequent studies. Detailed examination of the microtubule cytoskeleton (Murata & Wada, 1989a & b; Murata *et al.*, 1987) revealed a circular arrangement of cortical MTs immediately behind the apex in tip-growing - but not blue light treated isodiametrically expanding - apical cells. In further agreement, cellulose microfibril orientation was found to reflect MT orientation - both in the circular subapical orientation during tip growth and random arrangement after blue light irradiation (Murata & Wada, 1989b). These data support a role for microtubules, possibly through ordered cellulose microfibril deposition, in restricting lateral cell expansion at the critical site just behind the extreme apex and so regulating filament diameter. The effects of blue light - causing disruption of this arrangement with subsequent increase in cell diameter are consistent with this role.

There is, however, further evidence which suggests that the situation is, in fact, more complex. Similarly oriented actin microfilaments (MFs) have been localised with the circular band of cortical MTs, occupying a narrower region towards the apical dome (Kadota & Wada, 1992a & b; 1989a). MFs have been implicated in tip growth in the other tip-growing systems studied and roles in structural organisation and vesicle transport have been suggested (see Sections 1.5.2-1.5.3). This MF arrangement has been shown to undergo similar alteration to the MTs in response to blue light (Kadota & Wada, 1992a). In a further complication, MT disrupting drugs (which induced swelling) caused a loss of the MT organisation but not the arrangement of cellulose microfibril deposition or the arrangement of MFs (Kadota & Wada, 1992a & b). On the other hand, the MF disorganising drug cytochalasin B disrupted both MF and MT arrangement and inhibited tip growth (Kadota & Wada, 1992b).

The exact role which these cytoskeletal elements play in regulating tip growth in fern apical chlorocytes, how they interact and how their activity is regulated, are not yet understood. It is also not clear what other controls are exerted on tip growth (but see Racusen *et al.*, 1988 and section 1.13.6), such as direct control of apical extension, regulation of the zone of cell wall loosening or active control of the localisation of new wall deposition - all of which have been suggested for other systems (Sections 1.6.5-1.9.5).

The circular arrangement of MT and MF found behind the apical dome of tip-growing apical chlorocytes is not shared by rhizoids (Murata *et al.*, 1987) nor any of the other commonly studied tip-growing cell types (Kadota & Wada, 1992a). In all such cells, actin MF's appear to be the important cytoskeletal elements at the apex (e.g. Jackson & Heath, 1990; Steer & Steer, 1989). In the fern

rhizoid, dense arrays of MF's are located in the cortex and the endoplasm, and further cortical arrays fan out behind the apex (Kadota & Wada, 1989a). MT's are found behind the apex running roughly parallel to the growth axis (Murata *et al.*, 1987).

The involvement of MT in the regulation of filament diameter during apical chlorocyte elongation suggests a similarity to polarised cell expansion in higher plants (Baluska *et al.*, 1995; Zandomeni & Schopfer, 1993; Kuss-Wymer & Cyr, 1992). This apparent difference in the mechanism of tip growth regulation in ferns from other tip-growing cell types makes them an interesting comparison for further investigation.

1.13.6 The roles of ion movements, Ca^{2+} and H^+

The electrical properties and ion transport activities of gametophytes have also been examined in relation to tip growth (Racusen *et al.*, 1988 and references therein). The major findings of these studies were: 1) That net Ca^{2+} influx at the apex was associated with apical extension; 2) That an "electrical dipole" was associated with tip growth but was eliminated by blue light treatment and was not associated with isodiametric expansion induced by blue light; 3) Localised apical extrusion of protons occurred during tip growth but was reduced and delocalised laterally round the apex upon blue light treatment - preceding transition to isodiametric expansion. Possible interpretations for all of these findings in relation to mechanisms of regulating tip growth and polarity have been previously discussed both for ferns and other cell types (Sections 1.6-1.9.5). There is no significant work extending these findings in ferns, although the investigation of the roles of Ca^{2+} mediated signal transduction has been taken further in the related moss protonemata (Hahm & Saunders, 1991; Herth *et al.*, 1990; Wacker & Schnepf, 1990; Saunders & Hepler, 1983; Schmiedel & Schnepf, 1990).

1.14 AIMS

As discussed in the introduction, polarity and tip growth are a topic of keen interest. Recently the intracellular [ion] in regulating tip growth has become more clearly understood with the discovery of tip-focused [ion] gradients associated with apical growth in certain cell types. However, this discovery is still relatively new and many questions remain unanswered. The research of this thesis was intended to focus on two key questions:

- 1) How widespread is the phenomenon of tip-focused [ion] gradients associated with apical growth?
- 2) How do signals from physiological stimuli interact with the maintenance of steady-state growth to determine its initiation and termination, rate and direction?

In order to contribute to the first question it was decided not to work on one of the more commonly researched tip-growing cell types (pollen tubes or fungal hyphae for example), but to use a cell type which had not previously been examined with respect to the role of intracellular [ion] gradients in regulating tip growth. The fern gametophyte fitted this description and additionally, had several other features which made it attractive:

1) There is a long history of work on tip growth and its regulation in fern gametophytes. Whilst the role of intracellular [ion] gradients had not been tackled directly, several previous studies in ferns provided a basis for the work to be performed in the present study (see Section 1.12.2 of the Introduction and Racusen *et al.*, (1988) and references cited therein).

2) The fern gametophyte conveniently provides the opportunity to work on two different tip-growing cell types: the apical chlorocyte and the rhizoid. Both cell types may be present on an organism consisting of only two cells. The genetic origin and previous history of both cell types can, therefore, be easily established which allows much more meaningful comparisons to be made.

3) Unlike some of the other cell types used as models for examining tip growth, the gametophyte apical chlorocyte has many features common to higher plant cells, for example: chloroplasts; the ability to divide; photomorphogenic responses and a low level of specialisation. However, the fern rhizoid is much more specialised yet has the same genetic basis. This provides an interesting contrast.

4) The control of polarity and tip growth of the apical chlorocyte of gametophytes by light is a well characterised phenomenon. This provides a useful tool for investigating the regulation of polarity and tip growth. This is relevant to the second question considered.

The overall aim of the work carried out in this study was, therefore, to investigate the involvement of intracellular Ca^{2+} ions and H^{+} ions in the regulation and maintenance of polarised growth in cells of fern protonemata.

Dye-based imaging methods were chosen as the means of examining intracellular [ion] in living gametophyte cells. The arguments in favour of this choice are given in Sections 1.10 and 1.11 of the introduction. Although this technology is now relatively well established in animal cell research it is still novel in its application to plant cells. An example of successful application of these techniques to fern gametophytes could not be found, although it has been used in fern spores (Scheuerlein *et al.*, 1991) and in the related moss protonemata (Demkiv *et al.*, 1994; Hahm & Saunders, 1991). The potential for dye-based imaging applied to the study of fern gametophytes may, therefore, be considered to be untested. For this reason it was necessary to re-evaluate the fern gametophyte as an experimental system with respect to the use of dye-based imaging technology.

1.14.1 Specific aims

During the development of the research described in this thesis specific aims were set. The aims have been grouped into three sets which correspond to Chapter 3; Chapters 4 and 5; and Chapter 6, respectively.

The first set of aims were to assess the suitability of fern protonemata as an experimental system for the study of polarity and tip growth at the single cell level. This involved:

- 1) Choosing the most appropriate species of fern gametophyte.
- 2) Devising suitable methods for the culture and handling of individual protonema so that imaging could be performed while cells remained viable.

3) Examining the structure and behaviour of protonemata under examination conditions to demonstrate that normal development occurred and additionally, to select the most useful developmental stages and events for examination.

The second set of aims were related to the application of dye based imaging technology in order to study intracellular [ion]:

1) Loading of cells with ion sensitive dyes and determining the best procedures for quantitative imaging while retaining cell viability, normal response and development. Although a range of loading methods exist there is almost no information on their application to protonemal cells. A range of methods and dyes, therefore, had to be tested empirically.

2) Evaluating the different techniques (discussed in Section 1.11) for examining the fluorescence emissions of ion sensitive dyes. In particular, non confocal and confocal imaging methods and ratiometric image analysis were considered.

3) Assessing the validity of the imaging method: analysis of errors, artefacts and limits to resolution. One of the problems discovered with the application of imaging-based technology during the course of the research was the inherent difficulty in interpreting images and obtaining rigorously quantitative data. This necessitated a careful examination of the imaging method itself.

The third set of aims were based on the application of imaging techniques to investigate specific biological questions related to polarity and tip growth:

1) To investigate the existence in gametophyte cells of gradients in intracellular [ion] associated with the maintenance of polarised growth.

2) To investigate the degree of association between intracellular [ion] and growth by manipulations of each.

The extent of the research carried out was limited at several critical stages. The choice of dye was limited to the pH sensitive dye cSNARF-1, the only dye which could be reliably introduced into cells. This limited the area of research to the role of intracellular proton concentration in tip growth, discussed in Section 1.9 of the introduction. Initially, difficulties with chlorocyte cells and the subsequent lack of time lead to the research concentrating on the rhizoid and specifically on steady-state tip growth.

Based on the research carried out a range of possible improvements to techniques and an outline of the most profitable areas of future research using the fern gametophyte as an experimental system have been proposed.

Chapter 2

Chapter 2 - Materials and Methods

2.1 Materials and equipment

2.1.1 Chemicals

In general, chemicals were obtained from either Sigma Chemical Co. (Poole, Dorset, UK), BDH Chemical Co. (Poole, Dorset, UK), or Aldrich Chemical Co. (Gillingham, Dorset, UK).

Calcium Green-1 (free-acid and AM ester), Fluo-3 (free-acid and AM-ester), Indo-1 (free-acid and AM ester), Fura-2 (free-acid and AM-ester), BCECF free-acid, cSNARF-1 (free-acid, AM ester and dextran-10 kDa), cSNARF-6 and Pluronic F-127 were obtained from Molecular Probes Inc. (Eugene, Oregon, USA).

2.1.2 Culture and handling apparatus

This includes the components from which improvised apparatus was assembled (see Figs. 8 and 9).

Nylon mesh - Lockertex, Locker Wire Weavers Ltd. (Warrington, UK).

Sylgard - 184 silicone elastomer, Dow Corning. Obtained through BDH Chemical Co. (Poole, Dorset, UK)

Silicone grease - M494, ICI. Obtained through Ambersil Ltd. (Bridgewater, UK).

Plastic Petri dishes (55 mm) - PDS-160-011B, Fisons Scientific Equipment Ltd. (Loughborough, Leicestershire, UK).

Falcon tubes - 15 ml polypropylene. Obtained through A and J. Beveridge Ltd. (Edinburgh, UK).

Humbrol spray gun, Humbrol Ltd. (Hull, UK).

Cellophane - 525 pu cellulose (uncoated Rayophane), A.A. Packaging (Walmer Bridge, Lancs., UK).

Parafilm - PM 992, American National Can Co. Obtained through Sigma Chemical Co. (Poole, Dorset, UK).

Centrifuge - Gallenkamp Junior, Gallenkamp, (UK).

UV source for sterilisation - NIS G15T8 (15W) Germicidal, (Japan).

Illumination filters - Rosco Supergel: Red #26 (12 % Transmission, peak 600-740 nm); Blue #74 (4 % transmission, peak 480 ± 20 nm), Rosco (Sydenham, London, UK).

2.1.3 Bright-field, DIC and fluorescence microscopy

Glass coverslips - No. 1.5, 22x50 mm and 22x26 mm, Chance Proper Ltd. (Smethwick, Warley, UK).

General light microscope - Reichert-Jung Polyvar, Leica UK Ltd. (Milton Keynes, UK).

Injecting and fluorescence microscope - Nikon Diaphot TMD inverted microscope, Nikon UK Ltd. (Kingston, Surrey, UK).

Newport Vibration isolated workstation - V W series, Newport Corporation (Irvine, California, USA).

2.1.4 Confocal microscopy and associated equipment (Fig. 14)

Confocal Microscope - Bio-Rad MRC 600 laser scanning confocal microscope (CLSM) built around a Nikon Diaphot TMD inverted microscope with excitation provided from a 25 mW Argon ion laser (lines at 488 and 514 nm), Bio-Rad Microscience (Hemel Hempstead, Herts., UK).

Microcomputer for image capture and processing - RM Nimbus 486sx (fitted with a Synergy framestore and scan card), supplied by Bio-Rad Microscience (Hemel Hempstead, Herts., UK).

Data storage devices - Panasonic 940 MB WORM optical disc drive, Phoenix computers Ltd. (Brackmills, Northants, UK) and - Fujitsu 128 MB 3.5 inch rewritable optical drive, Fujitsu Europe Ltd. (Uxbridge, Middlesex, UK).

Hard copy devices - Mitsubishi CP200B colour and CP68B monochrome copy processors, Mitsubishi Electric Corporation, Japan. Obtained through Optivision (Ossett, West Yorks, UK). - Polaroid VI 350 Quick-Print video printer, Polaroid Corporation (Cambridge, MA, USA).

2.1.5 Photomicrography

Photographic Films - Kodak T-MAX 100 and 400 black and white film, Kodak Ltd., (UK) and - Fujichrome Velvia 50 colour slide film, Fuji Photo Film Co. Ltd. (Tokyo, Japan).

2.1.6 Microinjection

Capillary glass - GC 150F and GC 120F Borosilicate glass, Clark Electromedical Instruments (Pangbourne, Reading, UK).

Micro-electrode puller - Narishige PB 7, obtained through Nikon UK.

Micromanipulators - Narishige N-88, obtained through Nikon UK.

Needle holder - EH-3MS 120W, Clark Electromedical Instruments (Pangbourne, Reading, UK).

Pressure Probe (For Pressure microinjection) - See Oparka et al., (1991b).

2.2 Culture and handling of plant material

2.2.1 Spore collection and storage

Mature, fertile fronds of *Dryopteris affinis* were gathered from a plant within the University grounds between September and October, during dry weather. Fronds were immediately placed between sheets of grease-proof paper and left for 24 h to allow spore release. The resulting combination of spores, sporangia and other debris was filtered through three layers of lens tissue to isolate the spores. The procedure was speeded up considerably by using a whirlimixer to provide vigorous agitation.

Isolated dry spores were sealed into vials and stored at 4 °C in the dark. In this state spores were expected to remain viable for up to 10 years (Dr. A.F. Dyer - personal communication). To protect the bulk stock, 2 – 3 mg of spores were regularly removed, divided into 0.2 mg aliquots and sealed in Eppendorf pots. This substock was stored at 4 °C in the presence of silica gel to prevent hydration.

2.2.2 General culture conditions

Growth room conditions were as described for *Dryopteris affinis* culture in Dyer, 1979. Temperature was maintained at between 19°C and 21°C and care was taken to avoid localised overheating as a result of illumination. Illumination was provided by a combination of tungsten (40 watt, Thorn EMI) and fluorescent (65/80 Watt, OSRAM Lite Guard) sources. Different illumination qualities were produced by using celluloid filters: Rosco supergel no. # 26 for red light; and Rosco supergel no. # 74 for blue light. Gametophytes were cultured in Petri dishes placed inside a foil-lined cardboard box with the illumination filter built into the lid and black plastic covering the inside base.

2.2.3 Media

As material was only cultured for relatively short periods, a minimal medium of inorganic salts was found to be sufficient. Media (listed in Table 2.1) were modifications of a standard medium described in Dyer, 1979 (see also Murashige & Skoog, 1962; Mohr, 1956).

Media components were stored at 14°C as 10x strength stock solutions; all media were made up with double distilled water. The pH of media was adjusted with fresh 2 M KOH. In the case of standard culture medium the pH was set to 5.6 before autoclaving.

Table 2.1: Gametophyte Culture Media

Medium	Composition		Buffering	Notes
Dyer, 1979	Ca(NO ₃) ₂ MgSO ₄ KNO ₃ FeCl ₃ KH ₂ PO ₄ K ₂ HPO ₄ Agar	6.1 mM 2.0 mM 1.2 mM 0.06 mM ↓ ↓ 1.8 mM 0.7–2.0% w/v	Phosphate pH 4.9–5.6	Culture of gametophytes on solid medium
Standard liquid medium	as above – KH ₂ PO ₄ – K ₂ HPO ₄ – FeCl ₃ + 0–0.1% (v/v) Tween-20		none pH 5.6 (KOH)	Culture of rhizoids and 1–4 cell protonemata
Buffered liquid medium	as standard liquid medium + MES 5–20 mM + HEPES 5–20 mM + KOH / KCL as required		MES/HEPES pH 5.6–8.0 (KOH)	Culture at defined pH
Marashige & Skoog medium	see Kadota & Furuya, 1977		Phosphate pH 5.6	<i>A. capillus-veneris</i> culture

Medium for liquid culture differed from the standard agar-medium by the omission of H₂NaPO₄ and FeCl₃ which appeared to precipitate and affect gametophyte growth. Tween-20 detergent was included in culture media at between 0.010 and 0.005% (v/v), its function was to act as a "wetting" agent to aid even distribution of spores, prevent clumping of gametophytes during culture and to prevent adhesion to surfaces during isolation. Solid medium was produced by adding 1 – 2% (w/v) Bactoagar (Difco Laboratories, Detroit, Michigan, US) to liquid medium before autoclaving.

2.2.4 Spore washing and pre-treatment

2.2.4.1 Aseptic technique

In order to reduce contamination of cultures all glassware and autoclavable materials were autoclaved at 121°C for 15 min.; media were similarly treated for 30 min. as 500 ml volumes. Non-

autoclavable materials were surface sterilised with 70% (v/v) ethanol or UV light. Manipulations of culture material were, as far as possible, carried out inside a laminar flow hood.

2.2.4.2 Washing and sterilisation

The spore washing and sterilisation methods used were modifications of those described in Dyer, (1979). The washing procedure involved centrifugation to pellet the suspended spores followed by removal of the supernatant by suction (Fig. 7). Washing comprised two stages; wash-1 was made with 0.0075% (v/v) Triton X-100 detergent and wash-2 with 0.0080 % (v/v) Tween-20 detergent. The latter proved to be less harmful to the spores over long periods. For rhizoid culture wash-2 was often omitted. The use of detergents allowed isolation of spores by centrifugation by preventing them from floating.

A two day incubation period in darkness was included to allow germination of fungal and bacterial spores; washing was then repeated with the contaminants in this more vulnerable state. Where spores were intended for culture on agar, a further more stringent sterilisation with hypochlorite was required (see Lino *et al.*, 1989; Dyer, 1979; Gantt & Arnott, 1965). The procedure for sterilisation was as follows: 0.2 mg of spores were suspended in 5 ml of 0.05 % (v/v) hypochlorite, agitated for 15 sec., diluted to 10 ml, then centrifuged and the supernatant removed. Hypochlorite residue was removed by repeating wash-2 so that the total time in the presence of hypochlorite was kept below 3 min. This was found to reduce contamination considerably without noticeably reducing spore germination.

2.2.4.3 Synchronisation

A germination synchronisation scheme devised by A.F. Dyer and described in Dyer, (1979) was used in some cases to obtain even development, however, as this was also found to increase levels of contamination its use was limited.

2.2.5 Spore sowing

Spores for culture in liquid media were sown as a well "wetted" evenly distributed suspension of 0.2 mg spores in 50 ml of medium (+0.005% (v/v) Tween-20). Spore suspensions were sown onto solidified media with an aerosol spray gun; the concentration of spores was adjusted to reduce the volume delivered and prevent the medium surface from becoming flooded. The spray gun was cleaned before and after use by washing through with hypochlorite solution followed by sterile medium.

2.2.6 Cell Culture

2.2.6.1 General precautions

Fern gametophytes were found to be extremely sensitive to chemical contaminants, therefore, a set of glassware, which was kept separate from general usage, was used for their culture. "Fern culture" glassware was cleaned by machine wash - which included an acetic acid rinse.

Further problems were encountered with the use of plastic Petri dishes. It was suspected that chemicals (plasticizers), in certain types of dishes and under certain circumstances, caused disruption of normal growth and resulted in the build up of high levels of fungal and bacterial contaminants. These problems were avoided by using glassware as far as possible. Plastic Petri dishes used to make chambers (Fig. 8) were treated with ethanol to aid removal of chemical contaminants. High temperatures, long UV exposure or high intensity white light were all suspected of encouraging the release of chemicals from plastics and were avoided.

2.2.6.2 Liquid culture

Liquid-cultured protonemal filaments were grown under continuous red light ($2.0 - 5.0 \mu\text{m}^{-2} \text{s}^{-1}$) in 55 mm glass Petri dishes covered with plastic Petri dish lids and sealed with Parafilm. After spore germination cultures were disturbed as little as possible to ensure straight even growth of protonemal filaments. In addition, continuous illumination was provided and maintained at the same level and orientation.

2.2.6.3 Culture on solidified (agar) medium

Growth on agar medium was carried out under conditions as described above using 90 mm glass dishes. Plates used to grow gametophytes for microinjection were set up with a 10 mm layer of 1% (w/v) agar medium, overlaid with a sheet of sterile wetted cellophane, itself covered with a 500 – 1000 μm layer of 2% (w/v) agar medium. Plates were mounted on a perspex rack orientated at 80° to the light source. This provided protonemal filaments lying almost parallel to the medium surface.

2.2.6.4 Rhizoid culture

Spores for rhizoid production were cultured first under continuous white light ($50 \mu\text{m}^{-2} \text{s}^{-1}$) in 15 ml of medium sealed in 100 ml conical flasks. Once the first signs of rhizoid emergence were seen (after ~4 days) the germinated spores were transferred to thin layer chambers (Fig. 8) for a further 12 – 72 h period. After transfer to the chambers physical disturbance was kept to a minimum, movement of chambers caused both clumping and physical damage of rhizoid tips if not performed with extreme care.

2.2.7 Handling of experimental material

2.2.7.1 Handling of liquid cultured protonemal filaments (Fig. 9)

Liquid-cultured protonemal filaments at the 2 – 3 cell stage were isolated from the culture plates by collection on a wet nylon mesh (Lockertex no. N80, 20 µm weave) "scoop". Even in the presence of detergent it was found that a large proportion of filaments in undisturbed culture had risen to the surface film. This population proved to be the most convenient to isolate from the bulk medium which was usually contaminated with fungal and bacterial colonies. Protonemata collected from the medium surface were immediately transferred to fresh, sterile, liquid medium (containing 0.004% (v/v) Tween-20) and agitated gently to give a suspension.

The filament suspension was handled using modified (5 mm tip diameter) glass Pasteur pipettes. Exchange of media, concentration of the suspension and washing were carried out using a "filter-tube". "Filter-tubes" consisted of 30 mm sections cut from a 15 ml polypropylene Falcon tube with nylon mesh fixed to one end. This type of tube gave the least problems with adherence of filaments to the plastic surface. The "filter-tube" was placed in a 55 mm glass Petri dish containing medium and filled with filament suspension. Subsequent exchange of medium was made by addition to and removal from the Petri dish (see Fig. 9). To reduce physical damage to gametophytes the liquid level in the filter-tube was not allowed to fall below 5 mm.

2.2.7.2 Handling of rhizoids

Rhizoid tips were found to be intolerant of the handling procedures as described above - Fig. 28 G-J illustrates some of the effects of such mechanical stress on rhizoids. Rhizoids were, therefore, cultured in the chambers which would later be used for examination and experimentation (Fig. 8). When necessary, sunken rhizoids could be transferred using a modified glass pipette (described above: Section 2.2.7.1). A period of 6 – 12 h was allowed after transfer to identify those cells damaged during the procedure.

2.2.7.3 Handling of gametophytes for microinjection

Agar-grown protonemal filaments for microinjection were isolated attached to 10 mm² sections of the upper thin layer of 2% (w/v) agar. Sections were mounted on slides and flooded with medium. Filaments remained anchored to the agar by their rhizoids. Similar procedures were used by Racusen *et al.*, (1988) for impalement of gametophytes with microelectrodes. Rhizoids were prepared for microinjection by mixing germinated liquid-cultured spores with an equal volume of 1% (w/v) ultra low-temperature setting agar (at about 25 - 30 °C). The resulting suspension was spread thinly over glass coverslips and set for 5 min. at 4 °C. Slides were incubated in a humid chamber at standard temperature and illumination for 36 - 48 h to allow rhizoid elongation.

2.3 Dye loading methods

2.3.1 Methods for cell permeant dyes

Most of the organelle specific vital stains used were readily cell permeable and rapidly accumulated within cells (Table 2.2). The ion-sensitive dyes in their free acid state were, however, notable for being cell impermeant. Several of these dyes are also available in a cell permeant ester form, although many of those tested failed to accumulate within cells (see Table 2.2 and Fig. 10). Cell permeant dyes were added directly to gametophyte suspensions to give the correct loading concentration. In all cases the concentrations of solvents (DMSO, EtOH and acetone) were kept as low as possible, generally <1% (v/v) (Oparka & Read, 1994; Murata & Wada, 1989a). The degree of loading was assessed by fluorescence microscopy.

Three general loading protocols were used: the *load and wash out*, the *load and dilute*, and the *continuous loading*. In the first method cells were loaded to the desired level before all free dye was washed out using the "filter-tube" previously described (section 2.2.3). In the second method dye concentration was reduced by dilution so that loading continued at a very reduced rate. The third method was employed in cases where loading was very variable within a population or the best loading level was difficult to find. Dye fluorescence in selected cells was examined continuously during continuous loading and, once suitably loaded, cells were quickly examined and discarded. The latter two methods were made possible by the optical sectioning ability of confocal microscopy (Pawley, 1995) and the use of the non-fluorescent ester forms of dyes (see Haugland, 1992). Artefacts as a result of overloading cells with dye were assessed by comparing low loading levels, which gave poor image quality, with higher loadings giving good images (see also McCauley & Hepler, 1990).

2.3.2 Low pH loading of the free acids of dyes

The method of low pH or "acid" loading, as described in Read *et al.* (1992) (and references therein), was attempted with a range of ion-sensitive dyes (Table 2.2). Highly fluorescent dye free-acid was added to suspensions of cells in medium at pH 5.0 – 4.5. Incubation periods of between 30 min. and 6 h were used before the free dye was washed out.

Table 2.2: Dyes and loading procedures attempted on *D. affinis* protonemata

† Dyes and applications	Loading Method	‡ Reference examples	Cell Type	Dye μM	# Loading Time	Observations	*Imaging
Ca²⁺ Sensitive Dyes							
Calcium Green-acid	Microinjection	Hodick <i>et al.</i> , 1991 Read <i>et al.</i> , 1992	Chlorocyte	100	Pulsed loading over 2-3 min.	Sequestered within the vacuole over time	CLSM-1
Calcium Green-AM	Ester-loading	R.E. Cleland-personal communication	Chlorocyte	50-100	up to 24 h	Slowly accumulate weak vacuolar loading	CLSM-1
			Rhizoid	20-50	30-120 min.		
Fluo-3-AM	Ester-loading	Irving <i>et al.</i> , 1992	Chlorocyte	50-100	up to 6 h	weak vacuolar loading	CLSM-1
Fura-2-AM	Ester-loading	Brownlee <i>et al.</i> , 1987	Chlorocyte	50	up to 5 h	no loading	NC
Fura-2-acid	Low pH loading	Kiss <i>et al.</i> , 1991	Chlorocyte	50-100	up to 5 h	no loading	NC
Indo-1-AM	Ester-loading	Hahm & Saunders, 1991	Chlorocyte	50	up to 5 h	weak vacuolar loading	NC
Indo-1-acid	Low pH loading	Hahm & Saunders, 1991 Kiss <i>et al.</i> , 1991 Grolig & Wagner, 1991	Chlorocyte	50	up to 5 h	weak vacuolar loading	NC
pH Sensitive Dyes							
BCECF-AM	Ester-loading	Irving <i>et al.</i> , 1992 Slayman <i>et al.</i> , 1994 Davies <i>et al.</i> , 1990	Chlorocyte	10-30	10-60 min.	Strong cytoplasmic loading but deteriorates with time. Up to 20 μM /20 min survival is good	CLSM-1
cSNARF-1-AM	Ester-loading	Slayman <i>et al.</i> , 1994	Chlorocyte	5-40	15-60 min.	As for BCECF Up to 5 μM /20 min. survival is good	CLSM-2
			Rhizoid	2-5	10-30 min.		
cSNARF-1-acid	Low pH loading	Levina <i>et al.</i> , 1995	Chlorocyte	40-100	up to 24 h	Wall binding Little dye entry	CLSM-3

Table 2.2: Continued, Dyes and loading procedures attempted on *D. affinis* protonemata

†Dyes	Application	‡ Reference	Cell Type	Dye µg/ml	# Loading Time	Observations	*Imaging
Organelle Specific Dyes							
Nile Red	Lipids/ membranes	Greenspan <i>et al.</i> , 1985 Yuan & Heath, 1991	Chlorocyte	1-4	15-60 min.	Tends to precipitate	CLSM-4
Calcofluor	Cellulose (cell wall)	Kadota & Wada, 1989a	Rhizoid	< 0.5	examined during loading	Very light loadings required	CLSM-4
Rhodamine-123	Mitochondria		Chlorocyte and Rhizoid	50	10-20 min.	Tends to precipitate	NC
DiOC ₆	Mitochondria	Matzke & Matzke, 1986	Chlorocyte	2-6	30-60 min.	Mitochondria distorted with higher conc ⁿ . and loading times	CLSM-1
DiOC ₆	ER	McCauley & Hepler, 1990; 1992	Rhizoid	1	35-55 min.	Examined during loading	CLSM-1
Acridine Orange (in pH 7.0 medium)	Vacuole	Gilroy <i>et al.</i> , 1990	Chlorocyte	10-15	up to 20 min.	Cells look very healthy	CLSM-1
LYCH	Vacuole	Wright & Oparka, 1994	Chlorocyte	10-20	20-60 min.	Examined during loading Problems with toxicity	CLSM-1
CFDA	Cytoplasm (‘live stain’)	Oparka & Read, 1994	Chlorocyte Rhizoid	0.2-15	5-20 min.	General staining Stressful	CLSM-1
			Chlorocyte Rhizoid	1	1-24 h	Wall binding No uptake	CLSM-1
			Rhizoid	2-4	10-30 min.	Similar to BCECF	CLSM-1

† See Abbreviations section for the full names of dyes.

‡ References apply to the use of dyes and loading methods in other plant cells.

* CLSM = confocal examination (see Chapter 2, Table 2.3 for CLSM filter sets: 1-4), NC = not examined with the CLSM.

loading terminated by washing out excess dye or by dilution.

2.3.3 Microinjection

2.3.3.1 Ionophoretic microinjection

Microinjection delivers dye directly into individual cells through a fine glass needle. In ionophoretic microinjection a current is applied between the injecting needle and the medium which drives the negatively charged dye free-acid into the impaled cell (for example see Knight *et al.* (1993a)).

Needles for ionophoretic microinjection were pulled from filamented borosilicate glass tubes (GC 120F, Clark Electromedical Instruments) using a Narishige PB-7 single stage electrode puller. Various settings of heat and tension (applied by weights) were tried to determine the best needle type. Needle quality was found to be very variable from day to day so settings were regularly modified. The best needle type was found to be one of moderate taper length and even taper with a fine tip (<1 μm by examination under the microscope); needles had to be sturdy enough not to bend against the cell wall but fine enough to penetrate easily. Needles were back-filled from a modified plastic syringe with 2 – 5 μl of 100 μM dye free-acid (usually Calcium Green-1) followed by 1 M KCl to fill the needle.

Protonemal filaments were prepared for microinjection as described in Sections 2.2.6.3 and 2.2.7.3. A 10 – 20 μm tip diameter suction pipette filled with silicone fluid (Dow Corning, 200/100 CS) was used to stabilise cells for microinjection. A low angle of needle approach, perpendicular to the cell wall, was used (see Fig. 11). The site of injection was usually opposite the holding pipette at the centre of the cell.

Needle blockage upon cell penetration, as a result of cytoplasm being forced up the needle by the cell's turgor pressure, was found to be a problem during microinjection. To overcome this the turgor pressure of cells was reduced by including 125 mM sorbitol in the bathing medium. Alternatively, turgor pressure was opposed by using a needle holder (EH-3MS 120W, Clark Electromedical Instruments) filled with solution to prevent any backflow. While the former method proved more successful, however, the latter was thought to be less disruptive to the cell.

Immediately after needle penetration of the cell current was applied at 3.0-4.5 nA (as described in Knight *et al.*, 1993a) for 2 – 3 sec. and repeated in pulses as necessary. Success of microinjection was determined from the quantity of dye introduced and its distribution within the cell, examined by fluorescence microscopy (see Chapter 4). After delivering dye the needle was withdrawn by applying backwards tension over the next 3 – 10 min. (Hepler *et al.*, 1993); removal too quickly caused cells to collapse. The procedure followed for ionophoretic microinjection is shown in Fig. 12.

2.3.3.2 Pressure microinjection

Pressure microinjection was performed in a similar manner to the above except that the pressure probe technique (Oparka *et al.*, 1991b) was used to drive a volume of dye solution into cells. The needles used were pulled from borosilicate glass (GC 150F, Clark Electromedical Instruments) to

produce a wider tip diameter (still $<1 \mu\text{m}$) and shorter taper than for iontophoresis (see Corrêa & Hoch, 1993; Oparka *et al.*, 1991). Cells were injected under liquid medium or embedded in agarose. Pressure was kept at zero in the system until the needle had been located at the cell wall. Just prior to penetration of the cell the pressure in the probe was increased to $\sim 0.2 \text{ MPa}$ to counteract cell turgor. Pressure was increased further after penetration to force dye into the cell (up to 0.4 MPa). Before removing the needle the pressure in the system was slowly reduced to zero.

2.4 Preparation of samples for microscopy

As gametophytes were generally examined from below using an inverted microscope slides were prepared with the experimental material sandwiched between two coverslips (a $22 \times 50 \text{ mm}$ no. 1.5 coverslip as a base and a similar $22 \times 26 \text{ mm}$ coverslip as a cover). The covering glass was always supported either by a ring of silicone grease (M 494, ICI) or a $1 - 1.5 \text{ mm}$ thick Sylgard gasket (184 silicone elastomer, Dow Corning) see Davis *et al.*, (1974). Where continued access to gametophytes or maintenance of growth conditions over extended periods was required a thin-layer chamber was used.

Movement of individual cells during examination on the microscope stage presented a serious limitation during experiments. In an attempt to "anchor" gametophytes in place the base coverslip was coated with poly-lysine (Kadota & Wada, 1992a) applied as a one in one hundred dilution of the 1% (w/v) stock solution for 30 sec. then washed off for 5 min. in running water. This practice was subsequently abandoned when damage to cells was suspected. Sealing gametophytes between coverslips or within a thin-layer chamber and the use of a vibration-isolated workstation were found to reduce the problems of vibration and movement considerably.

2.5 Assessment of viability

Viability was assessed on two levels; firstly, the appearance of cells under the microscope and secondly, continued growth and development. The first level was most commonly used with protonemal filaments due to their lack of cytoplasmic streaming and slow growth rate (McCauley & Hepler, 1990). Rhizoids were more commonly assessed on the basis of continued growth as well as appearance. This is discussed further in Chapter 3. The effects of handling procedures and loading and imaging of ion-sensitive dyes were assessed by following development over extended periods (up to 96 h for chlorocyte cells).

2.6 Confocal microscopy and imaging

Confocal fluorescence imaging was carried out with the Bio-Rad MRC-600 CLSM (Figs. 13 and 14) controlled from the SOM (version 4.62(a)), COMOS (version 6.05-4) and TCSM (version 1.0 rev 1.19d) software. (The older versions of software were later replaced with COMOS, TCSM and MPL version 7.)

2.6.1 CLSM Set-up procedure

Set-up procedures were followed as described in the Bio-Rad CLSM operations manual. Briefly, after insertion of the correct filter set for the dye being examined (see Fig. 13 and Table 2.3), both the excitation laser beam and then the emission signal beams were aligned. Next the required imaging-variables (settings of the various functions are described in Table 2.4) were set. Settings of imaging variables which gave the best images, with the least stress to the biological sample (Table 2.4), were determined on the basis of factors described in Fig. 15 and by trial and error with individual dyes and loading protocols.

Table 2.3: Filter sets for the CLSM

Filter set	Excitation (laser)	Dichroic mirror-1	Emission-1 (PMT-1)	Dichroic mirror-2	Emission-2 (PMT-2)	Example of dye imaged
1	488 nm	510 LP	515 LP	/	/	Calcium Green-1
2	514 nm	550 LP	640±20*	610 LP	580±10*	cSNARF-1
3	488 nm	550 LP	640±20*	610 LP	580±15*	cSNARF-1
4	488 nm	527 LP	600 LP	565 LP	540±15*	Nile red

LP = long pass filter: allows wavelengths above the stated value to pass through and reflects the rest.

***** = bandwidth filter: allows wavelengths within the given range to pass through and reflects the rest.

2.6.2 Image collection

The basic process of image generation is described in Fig. 14. Collection of sequential optical sections in the z-plane was made with the COMOS *z-series* command using the focus motor to step the focus up through the specimen. Time series over 1 – 2 min. were collected with the COMOS *time-series* command. However, due to changes in specimen focus position and orientation, longer time series were collected manually. Bright-field images were collected via a transmission detector which gathered transmitted laser light behind the microscope condenser and delivered it, via a fibre-optic cable, direct to PMT-2 (Fig. 13).

Table 2.4: CLSM imaging parameters

Variable	Description	Settings used‡	Significance
laser power	25 mW Argon ion laser	ND allowing 1%-3% transmission	Optimisation of signal detection
scan speed	pixel dwell time and number of lines scanned	1-3 s per frame (512 lines)	
low signal enhance†	signal integrated over full pixel dwell-time	on/off	
photomultiplier gains	photomultiplier sensitivity	1 to 8	
black-level setting	light level detected as "0" signal	dark signal pixel intensity set at ~ 10	
accumulate filter*	addition of successive images	n = 2-5	Improvement in the signal to noise ratio
Kalman filter*	averaging of successive images	n = 2-10	
objective	x40, x60 dry (NA 0.95) and x60 oil (NA 1.4)		Determines optical resolution and pixel size
confocal apertures	controls optical sectioning	4-5 (~ 30% open)	
electronic zoom	image size / area scanned	3-4	

‡ Settings refer to the Bio-Rad MRC-600 confocal microscope (see Pawley, 1995 for a more detailed explanation of settings).

† Only available in slow scan mode.

* Alternative collection filters.

2.6.3 Simultaneous dual-emission ratio imaging

Simultaneous dual-emission ratio imaging was performed by simultaneous collection of two fluorescence images, at different wavelengths, with the two photomultipliers. To get the best alignment of the two images for ratioing the initial emission signal beam alignment was critical. It was also important to use the correct coverslip thickness setting on objectives and have the same confocal aperture setting for both channels.

cSNARF-1 was imaged with laser-excitation at 514 nm. A neutral density filter of 2 or 1.5 was used to reduce excitation intensity to 1 or 3% laser power, respectively. Emissions were collected simultaneously at 580 ± 15 nm (CH-2) and 640 ± 20 nm (CH-1). "Pinhole" apertures (Fig. 13) were generally set at 4 – 5 units (recommended in Fricker *et al.* (1994); see also Pawley (1995)). The following objectives were used throughout: Nikon x40 or x60 plan apo dry objective, numerical aperture (NA) = 0.95; x60 plan apo oil immersion NA = 1.40. Optical section thickness achieved with the x40 dry and x60 oil objectives (CA = 5) was estimated in terms of the distance, down the length of an XZ image of a 200 nm fluorescent bead, between the fluorescence values of half the maximum fluorescence intensity - the FWHM value - as described in Pawley, (1995). For excitation at 514 nm and emission at 640 nm optical section thickness was estimated as 1.3 μ m for the x40 dry objective and 0.8 μ m for the x60 oil objective.

Table 2.5A shows the difference in fluorescence signal collection for different objectives (at confocal aperture (CA) =4). Differences in fluorescence are due to differences in the numerical aperture and in the optical section thickness sampled by different objectives at the selected CA. For the different types of objectives tested (plan apo dry and oil and plan objectives), not only did the absolute fluorescence intensity collected with the same [dye] and gain settings vary, but ratios varied, showing that light collected at the Ch-1 and Ch-2 wavelengths were unequally affected. However, different magnifications of the same type of objective (e.g. x40 and x60 plan apo dry) did not differ significantly and could probably be used interchangeably.

Table 2.5: The effects of altering the objective lens (A) and gain settings (B) on fluorescence emissions and ratio values for cSNARF-1 imaging (excitation 514 nm)

A) The effects of using different objectives on dual channel fluorescence ratio imaging of cSNARF-1 free-acid (150 μ M) at pH 7.0 (confocal aperture = 4)

Objective	NA	Ch-1 fluo†	*relative fluo (%)	Ch-2 fluo†	*relative fluo (%)	Ratio (absolute fluo Ch-2/Ch-1)
x40 plan apo dry	0.95	131.06	= 100%	150.46	= 100%	1.15
x60 plan apo dry	0.95	63.30	= 48.3%	72.82	= 48.4%	1.15
x60 plan apo oil	1.40	78.37	= 59.8%	94.64	= 62.9%	1.21
x100 plan apo oil	1.40	39.58	= 30.2%	47.41	= 31.5%	1.2
x60 plan	0.85	40.37	= 30.8%	71.02	= 47.2%	1.76

* absolute fluorescence scaled relative to that of the x40 plan apo dry objective = 100% (gain constant).

† Fluorescence emission intensity, 0-255 grey level scale (Ch-1 = 640 nm and Ch-2 = 580 nm emission).

B) The effects of slight non-linearity in gain increase on dual channel fluorescence ratio imaging of cSNARF-1 free-acid (150 μ M) at pH 7.0 (x40 dry NA 0.95 objective; confocal aperture = 4)

*Ch-1 % gain	*Ch-2 % gain	gain ratio Ch-1/Ch-2	Ch-1 fluo† (Em 640 nm)	Ch-2 fluo† (Em 580 nm)	Ratio (absolute fluo Ch-2/Ch-1)
55.0	65.9	1:1.198	65.2	74.3	1.16
55.0	65.9	1:1.198	130.6‡	148.9‡	1.14‡
58.4	70.0	1:1.1986	94.2	101.1	1.08
62.6	75.0	1:1.198	128.9	132.8	1.04
66.8	80.0	1:1.1976	169.7	166.6	0.99

* Gain setting range from 0-10.

† Fluorescence emission intensity, 0-255 grey level scale.

‡ Two image accumulation.

Scan speeds of F-1 or F-2 were used for image capture with either direct scanning, Kalman n = 2 or Accumulate n = 2 – 3, depending upon signal strength. Both channels were used in "low signal" mode. Gain settings were kept standard to allow better comparison of ratio images. However, as can be seen in Table 2.5B the increase in sensitivity was not linear with a linear increase in gain setting over the full range of settings - between 50 and 80% gain setting linearity was lost. This non-linearity in gain control resulted in slight differences in the ratio when different gain settings were used,

despite ensuring a constant ratio in gain setting for the two channels. This meant that even with systematic gain settings only calibrated images could be directly compared and gains could not be altered during an imaging session without re-calibration. Blacklevels were always set to give an average "dark" current (pixel value) signal of roughly 10 (on a pixel greyscale 0 - 255) over a single image frame.

Gain and pinhole aperture settings were not altered during experiments because of their effect on ratio values. However, the scan speed, scanning mode, ND and blacklevels were changed freely according to circumstances. Images were usually maintained at an average pixel intensity of between 75 and 200 for regions of cell cytoplasm. Saturation (pixel intensities of 255) was avoided, as were regions of pixel intensity below ~ 50 (see Chapter 5). The zoom used was kept below 4.0 (See the discussion of optical resolution and pixel size in Chapter 5).

2.6.4 Imaging of structural features

Imaging of structural features was usually done by collection of the fluorescence image with one channel and simultaneous bright-field (transmitted light image) collection with the other. Due to the high spatial resolution required, often with weak dye fluorescence, high gain settings (up to 8.0) and F-2 scan speed with Kalman filtering of 5 – 20 were used. ND filters of 1.5 – 2 were used to avoid radiation damage to cells, especially when using the stronger 488 laser excitation. Z-series were collected with steps of 0.5 to 2.0 μm .

2.7 Image processing

2.7.1 "Visual enhancement" processing

Processing images containing structural detail was of an empirical nature with the aim of "visual enhancement". Processing was kept to a minimum with continual reference to the original to avoid the creation of artefacts. Sharpening of structural detail was achieved using the COMOS *edge enhancement* and *local contrast enhance* commands. The COMOS *contrast stretch* and the *greyscale "ramp"* adjustment were used in conjunction with COMOS *contrast fix* to reduce background fluorescence, pick out weak signal and enhance particular structural details.

2.7.2 General numerical processing

Length measurements were made with the COMOS *length* command. Measurement of individual growth rates was performed by overlaying consecutively collected images (using the *merge* command) and measuring the difference in length directly. The average pixel intensity in areas of ratio images was determined with the COMOS *histogram* command either within boxes or user-defined areas. Pixel intensities along a user-defined line were measured with the MPL *length n* command (where n was the width in pixels averaged across each pixel on the line). See the detailed

discussion in Chapter 5; Sections 5.6 and 5.7. The only enhancement used on images from which pixel intensity data was to be extracted was the median 3x3 filter (see Section 2.7.3).

2.7.3 Ratio processing

Ratio processing of cSNARF-1 dual emission fluorescence images was performed by the TCSM software following the protocol described in Fig. 16. As a first step photomultiplier dark signal "noise" was removed by a "dark image" subtraction. "Dark images" were collected just after fluorescent images, on the same gain and blacklevel settings, by blocking the laser illumination path. Secondly, residual noise and low signal was removed by thresholding (generally at between 5 and 20 on the 255 grey scale) After thresholding the two images the ratio image was formed by a pixel by pixel division of the CH-2 image by the CH-1 image. Any image misregistration was corrected by using the COMOS *image edit* command to reposition the CH-2 image relative to CH-1. A 3x3 median filter was generally applied as a final step to reduce the level of random pixel variation. The median filter "corrects" each pixel in a ratio image by first ordering the 9 grey scale values of a 3x3 pixel square (centred on the pixel to be corrected) according to increasing value. The middle value becomes the corrected value of the central pixel. This process is repeated over the whole image.

2.8 Calibration of the dye response

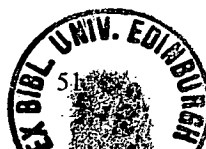
2.8.1 *In vitro* calibration of the pH response of cSNARF-1

In vitro calibration for the pH response of cSNARF-1 free-acid was performed by imaging dye fluorescence from 5 μ l drops of the appropriate dye-buffer mixtures over the pH range 6.0 to 8.0. Image collection and processing were as previously described (Sections 2.6.3 and 2.7.3). The pH of buffer solutions was measured by pH meter - accurate to ± 0.005 pH unit.

Different buffer compositions were compared: simple MES/HEPES buffer, a "pseudocytosol" medium (Fricker *et al.*, 1994), and the weak acid and base buffers used for *in situ* calibrations (see later, also Guern *et al.* (1991)). In order to achieve good comparison between calibrations the dye concentration used in each of the different buffer types was adjusted to give fluorescent image intensities of about 100 in both channels at pH 7.0.

2.8.2 *In situ* calibration of the pH response of cSNARF-1

In situ calibrations were carried out on cSNARF-1 AM ester-loaded gametophyte cells in thin-layer chambers. Intracellular pH equilibration with external media was attempted by several different methods: 1) ionophores - amphotericine, nigericin, and gramicidin at 10 - 100 μ M (T. Jelitto, 1995; O'Brodovich *et al.*, 1993; Dr. M.D. Fricker, personal communication; Davis *et al.*, 1990); 2) the protonophore DNP at 1 mM; and 3) cell-permeant weak acids and bases - propionic acid, NH₃ and trimethylamine at 30-50 mM (Guern *et al.*, 1991).



In cells made permeable to H⁺ by ionophores or DNP an attempt was made to clamp internal pH over the range 6 – 8 with 50 mM MES/HEPES buffered medium (containing 100 mM K⁺ as KOH or KCl and the relevant ionophore or DNP). Images of intracellular cSNARF-1 fluorescence were collected for up to 60 min. after exposure of cells to the "clamping" medium.

The weak acids and weak bases were applied to cells as buffered solutions: propionic acid at pH 6.0, 6.5, and 7.0; NH₃ at 7.0, 7.5; and trimethylamine at 7.5 and 8.0. Buffers were prepared by adjusting 30-50 mM solutions of sodium propionate, NH₄Cl or sodium trimethylamine (made up in basic culture medium) to the desired pH with the corresponding weak acid or base. This concentration of permeant buffer was required to overcome the buffer capacity of cells (estimated at 30 mM/pH unit at physiological pH (7.2) in *Neurospora* (Sanders & Slayman, 1982)). A 50 mM solution of MES/HEPES, already set to the required pH, was then added to give a final MES/HEPES concentration of 5 mM and finally the pH was rechecked. The pH was followed by ratio imaging cSNARF-1 and the "clamped" pH value was recorded between 3 and 10 min. after buffer application.

2.9 Preparation of diagrams and figures

All diagrams were drawn using Harvard Graphics version 3.0. Where diagrams were incorporated into figures containing images they were imported through Microsoft Powerpoint version 4.0. Photographic images were digitised using a Hewlett Packard Scan Jet IICx run from an IBM (120 MHz pentium) PC and stored as TIF files. Digitised photographic images and digitised images recorded on the CLSM (converted from PIC format to TIF format using Confocal Assistant version 3.1) were manipulated in Paint Shop Pro version 3.1.2 and imported into Microsoft Powerpoint version 4.0 for annotation. Graphs were drawn using Biosoft Fig P version 2.7 and imported directly into Microsoft Powerpoint version 4.0. Figures were printed using either a Hewlett Packard Desk Jet 850 colour printer or using a Mitsubishi S3600 colour dye sublimation printer. Output from the Hewlett Packard Desk Jet 850 colour printer was not waterproof and had to be colour photocopied.

2.10 Statistical analysis

Where comparisons between individual experimental values and population means were intended standard deviations (s.d.) about the sample mean (of n individuals) were quoted as the measure of population dispersion. In general, interest was in the behaviour of experimental material at the individual organism level and the techniques of examination and manipulation dealt with single individuals. For comparison between sample populations the standard error on the mean (s.e.m.) was quoted.

Statistical analysis of data derived from ratio images (pH determination - see Sections 2.7.3 and 2.8 above) was complicated by the effects of ratio processing on the variation in the individual fluorescence image pixel values - this is discussed further in Chapter 5; Section 5.6.

Chapter 3

THE FERN GAMETOPHYTE AS AN EXPERIMENTAL SYSTEM FOR THE INVESTIGATION OF TIP GROWTH

3.1 Introduction

In the past the fern gametophyte was commonly used as a model system for the study of polarity, polarised growth and the regulation of these by illumination conditions (see Chapter 1; Section 1.12). However, the roles of intracellular ions in regulating these processes have been largely neglected in ferns. An important aim of the present study was to determine whether these aspects could be further investigated in ferns with the aid of modern techniques. The method of choice for such a study was considered to be imaging of intracellular ion sensitive dyes (see Chapter 1; Sections 1.10 -1.11).

To be useful as a model system for the investigation of polarity and tip growth at the intracellular level two requirements must be met: firstly, cells must exhibit polarity and polarised growth under conditions which allow for observation and experimental manipulation; and secondly, growth and polarity should be experimentally manipulable, preferably by physiological stimuli as well as non-physiological treatments. An additional requirement of the proposed method of investigation, using dye-based imaging techniques, is that cells must be amenable to the application of dye-based imaging technologies (see Chapter 4).

The aim of the work described in this chapter was to examine the development of gametophytes in order to: a) determine which aspects of growth and development may be best exploited for the further study of tip growth and polarity; b) produce suitable experimental material; c) devise suitable procedures for the culture and handling of gametophytes to allow normal development under experimental conditions; d) examine the structure and physiology of gametophyte cells in relation to polarity and tip growth under the experimental growth conditions (defined during steps a-c).

3.2 Choice of species

Whilst much of the earlier work on fern gametophytes has been on *Adiantum* and *Onoclea* species many other species have been used as experimental material (for an overview refer to Dyer, 1979 and Raghavan, 1990). Here, three species of ferns were initially obtained and their suitability for further study assessed: *Dryopteris affinis*, *Pteridium aquilinum* and *Adiantum capillus-veneris*. Suitability was determined on the basis of three main considerations (Table 3.1):

1) **Cell size and structure.** This is important for ease of handling, imaging and microinjection. Larger sized cells were favoured.

2) **Rates of growth and morphological expression.** Faster growing species allow viability to be checked more easily and additionally exhibit a shorter "lag" period between a stimulus and the corresponding morphological response.

3) **Availability of experimental material.** Availability was a significant and limiting factor as relatively large numbers of spores were required to maintain a reliable stock of material.

D. affinis was finally selected as the major test species (Table 3.1). Spores were obtained exclusively from a single source plant which had been previously classified as *Dryopteris affinis* morphotype *affinis / borneri* (Newman) (Dyer & Cran, 1976). This plant has been shown to be triploid and apogamous (A.F. Dyer; personal communication): gametophytes, therefore, show a low degree of genetic variation.

3.3 Developmental stages of *D. affinis* gametophytes

The nature of fern gametophytes and their developmental plasticity was discussed in Chapter 1 (see Figs. 5 and 6). The developmental stages of *D. affinis* gametophytes cultured under red light (see Chapter 2; Section 2.2 for culture conditions) are shown in Figs. 18 and 19. These observations agree with the findings of Dyer (1979).

Two developmental stages were selected for experimental purposes: the 200 - 300 μm long early elongation stage of the primary rhizoid (Fig. 18D) and dim red light-grown protonemata at the two cell stage (Fig. 18I). Both of these stages exhibited active apical growth. These particular stages were selected for their ease of culture and manipulation and suitability for imaging (see later). Earlier stages of both rhizoids and protonemata generally had poorly developed apical structures while older stages were more difficult to culture and more easily damaged during manipulations.

Spore cells were not considered for use as experimental material as their spore-coat and high lipid droplet content complicate the use of imaging technology (see Scheuerlein *et al.*, 1991; Raghavan, 1990 - pp 59-60).

Gametophytes grown in white light, unlike those grown under dim red illumination, did not exhibit polarised apical growth and, as an experimental subject, suffered from intense chloroplast auto-fluorescence (see Chapter 4).

Growth conditions were subsequently optimised for the selected stages (see Chapter 2, Section 2.2). Minimum physical disturbance of cultures and maintenance of constant conditions (illumination and temperature) were found to be essential to provide evenly shaped, rapidly growing cells such as those shown in Figs. 20 and 24.

Table 3.1: Positive and negative aspects of the different fern species examined

Species	* Size	* Rates of growth and development	Supply	Other comments	References
<i>Adiantum capillus-veneris</i>	small diameter: protonemata - < 25 µm rhizoids - < 10 µm	rapid: Elongated protonemata within 6 days. Measurable photomorphogenic response within 3 h.	poor (ready supply not available in Scotland)	+ Significant numbers of relevant publications. + Protonemal cell division arrested in red light. - Chloroplast filled apical protonemal cell.	Murata & Wada, 1989a, b & c Kadota & Wada, 1992a & b
<i>Pteridium aquilinum</i>	small diameter: protonemata - < 25 µm rhizoids - < 10 µm	fairly rapid: Elongated protonemata within 7 days. Measurable photomorphogenic response 4-8 h.	good (freely available)	- Spores very small and difficult to handle. - Chloroplast filled apical protonemal cell	Davis <i>et al.</i> , 1974
<i>Dryopteris affinis</i>	large diameter: protonemata - < 35 µm rhizoids - 12-16 µm	slow: Germination within 5 days; elongated protonemata 8-11 days. Measurable photomorphogenic response 6-12 h.	good (freely available)	+ Previously examined in detail (see Dyer, 1979). + Chloroplast “free” apical zone. - Complex cell-cycle related cytological changes	Dyer & Cran, 1976 Dyer, 1979

* refers to typical red light-grown protonemal filaments cultured in liquid medium.

3.4 Examination of the apical chlorocytes of protonemata

The structure of apical chlorocytes was examined under the light microscope (using DIC optics) for randomly selected samples from cultures grown as described in Chapter 2. Examples of the most commonly observed features are recorded in Figs. 20 and 21. Previous examinations of gametophytes (Kiss *et al.*, 1995; Wada *et al.*, 1980; Schmiedel & Schnepf, 1980; Dyer, 1979; Dyer & Cran, 1976; Wada & O'Brien, 1975; Fraser & Smith, 1974) suggest differences occur between different species of ferns and between ferns and mosses. This increased the need to exactly define the "normal" cytological features of the species of interest before proceeding to experimental investigation and manipulation.

3.4.1 Structural features associated with tip growth

The "typical" *D. affinis* apical chlorocyte cell (Fig. 20) could be characterised into regions along its length. A hemispherical "chloroplast free zone" was the predominant feature at the apex. This zone comprised an apical cytoplasmic accumulation and a significant subapical vacuolated region. The region of cytoplasmic thickening corresponded well with the "growing zone" found in other species - within about 20 μm of the tip in *Dryopteris filix-mas* (Mohr, 1956) and similarly in *P. aquilinum* (Davis *et al.*, 1974; Takahashi, 1961). However, in those species, and also in *Adiantum*, chloroplasts occur throughout the apical region. Electron microscope (EM) examination of *Adiantum* (Wada & O'Brien, 1975) showed apical vacuolation is significantly less than in *D. affinis*. In another species, *Schizaea pusilla*, apical chlorocytes have a similar apical structure to *D. affinis* but with a less well defined chloroplast free zone and less apical vacuolation (Kiss *et al.*, 1995).

The nucleus, which always lay behind the apical vacuole, was associated with a second cytoplasmic accumulation and cluster of chloroplasts and lipid droplets. This structure comprised the "nuclear zone". The nuclear associated cytoplasm was generally connected to the apical cytoplasmic accumulation by large cytoplasmic strands or, in some cells, a peripheral cytoplasmic "network" which occasionally could be seen to extend into the centre of the apex. Cytoplasmic strands radiating from the nucleus have been suggested to function as transport pathways and in organelle movement (Mineyuki & Furuya, 1985; Wada *et al.*, 1982). In *D. affinis* apical chlorocytes, chloroplasts were seen to migrate slowly from the nuclear cluster along such strands. No cytoplasmic streaming was observed in *D. affinis* cells, although it has been recorded in *Adiantum* (Wada *et al.*, 1982). The clustering of chloroplasts may be important in their "transport" in the growing tip, towards better conditions of illumination. Upon white light exposure chloroplasts dissociated from the cluster and migrated round the cell (see Section 3.4.1).

The "subapical vacuolated zone" (the remainder of the cell behind the "nuclear zone") consisted of a large central vacuole surrounded by a thin cytoplasmic "sheath". Thicker cytoplasmic strands often ran the length of this subapical region and were "beaded" with chloroplasts.

Within a population several variations of the standard apical structure already described were observed - see below.

3.4.2 Tip forms

The different tip forms encountered for red light cultured protonemal filaments are shown in Fig. 21 and their occurrence within a typical population is given in Table 3.2. Four basic forms were identified on the basis of chloroplast and cytoplasmic distribution, and position of the nucleus:

1) Vacuolated (Fig. 21A). This form was associated with undisturbed, low intensity ($< 5 \mu\text{Em}^{-2}\text{s}^{-1}$) red light culture conditions in which protonemata displayed relatively rapid apical extension and narrow apical diameter. This form predominated in populations of early protonemal stages (< 5 celled filaments). The vacuolated form was lost following exposure to white light or after gametophyte isolation. However, following such disturbances, if cells were returned to dim red light or darkness and left undisturbed the vacuolated form was regenerated after 30-60 h and again predominated.

2) Tubule (or vesicle) filled (Fig. 21B). This form was similar to the above in the conditions under which it occurred although it was generally a smaller component in populations (Table 3.2). Varying degrees of "filling" of the apical zone were observed. It is possible that this form was an intermediate in the interconversion of tip forms. Often cells which exhibited this tip form had very elongated apical cells indicating either that they were very rapidly elongating or that a significant length of time had passed since the last cell division (and that another round of cell division might be due). This suggests such a tip form may be associated either with rapid tip growth or the onset of cell division.

3) Chloroplast filled (Fig. 21C and D). In the tip forms above chloroplasts were clearly excluded from the extreme apical hemisphere, mainly clustering around the nucleus. Two distinct types of apical distribution of chloroplasts were recognised, in which either the nucleus and associated chloroplasts (Fig. 21C) or individual chloroplasts (Fig. 21D) were located at the apex. The first type was associated with reorientation of polarity (see Section 3.5) or after exposure to white light (see Section 3.4). The latter type occurred at increasing frequency in populations of older filaments (> 5 cells) with narrowing apical diameter. An example of an *Adiantum* apical chlorocyte, with its typical apical distribution of chloroplasts, is shown for comparison (Fig. 21G). *Pteridium aquilinum* protonemata had a similar appearance.

4) Thinning apical cytoplasm (Fig. 21E and F). This form was generally, but not exclusively, associated with the presence of two very recently divided nuclei. Few examples were seen although this could reflect the low occurrence of cell division. Cells of this type which were examined over a period of time always failed to develop further; it is, therefore, possible that this was a very sensitive stage. Alternatively, the morphology may be the result of damage rather than a "normal" tip form.

All the forms (except 4) were demonstrated to undergo both phototropic reorientation and white light induced photomorphogenesis. On the basis of work performed on *Adiantum* (Wada *et al.*, 1980) it is likely that the occurrence of the tip forms (1,2 and 4) is related to the cell cycle. In continuous

red light-illumination cell division in *Adiantum* is completely inhibited and tip structure is fairly constant. However, cycles of red light and darkness induce changes in tip structure which are linked with cell cycle events (Wada *et al.*, 1980). In *D. affinis*, unlike *Adiantum*, cell division proceeded, although at a very low rate, even in continuous red light (see Fig. 19). However, as individual cells were not continuously observed throughout a complete cell division cycle, conclusive association of any of the observed forms with stages of the cell-cycle could not be claimed. The predominant "vacuolated apical zone" form was favoured as the standard form for experimentation.

In addition to the "normal" tip forms, evacuated tips were also found after gametophyte isolation. These failed to develop further from the original apex; such "stress forms" are discussed in Section 3.9 (Fig. 28A-D).

Table 3.2: Relative proportions of apical chlorocyte tip forms

Protonemata population	Isolation treatment †	Tip Forms * (relative percentage)				Total (n)
		⁽¹⁾ Vacuolated	⁽²⁾ Tubule filled	⁽³⁾ Chloro-filled	⁽⁴⁾ Evacuated	
1-2 cell 10 day culture	minimal stress	84.0%	1.6%	14.4%	0.0%	243
	washed	65.5%	6.5%	26.1%	1.8%	1256
2 cell 11 day culture	minimal stress	72.2%	6.7%	21.2%	0.0%	582
	washed	69.4%	10.8%	18.1%	1.45%	815
2-3 cell 12 day culture	minimal stress	83.2%	0.4%	16.4%	0.0%	250
2-4 cell 15 day culture	minimal stress	50.6%	14.7%	34.5%	0.2%	632
	washed	49.4%	3.8%	43.4%	0.4%	1098

* Averages of two independent repeat experiments (no statistical analysis was performed).

† Minimal stress = protonemata lifted from the medium surface and counted. Washed = washing treatment applied as described in Chapter 2; Fig. 9.

(1)-(4) correspond to the tip forms described in the main text. The "evacuated" category here includes both damaged individuals (Fig. 28 B) and the "thinning apical cytoplasm" category (Fig. 21 E and F).

3.4.3 Growth rate

Exact rates for extension of the *D. affinis* apical chlorocyte proved to be difficult to measure for individual cells due to problems with cell division; phototropic, geotropic and photomorphogenic events; and the relatively slow growth rate. Average growth rates were, therefore, determined for cell populations over a period of linear apical extension between the one and two, and two and three

celled growth stages (Table 3.3). This gave values of 6.5 - 7.5 $\mu\text{m}/\text{h}$, older filaments gave slower average growth rates. Rates of extension were very dependent upon culture conditions (particularly illumination) although overall growth (cell volume) was less variable. This has been examined previously by Cooke & Paolillo, (1979; 1980) and Miller, (1980).

Table 3.3: Rates of extension of protonemata and rhizoids

	Treatment	Average growth rate / s.d.		n
Protonemal growth				
Population average (light microscope)	Liquid culture in glassware (floating protonemata) 1-2 cell	7.5 $\mu\text{m}/\text{h}$	†	50
	As above 2-3 cell	6.6 $\mu\text{m}/\text{h}$	†	25
Individual apical chlorocytes (laser scanned*)	Thin-layer chamber (submerged protonemata)	3.59 $\mu\text{m}/\text{h}$	± 0.32	3
Rhizoid growth				
Population average (CCD camera)	Liquid medium sealed under coverslips	5.7 $\mu\text{m}/\text{h}$	± 0.83	14
	Thin-layer chambers (submerged rhizoids)	12.0 $\mu\text{m}/\text{h}$	± 2.31	20
Individual rhizoid average (laser scanned*)	Thin-layer chambers (submerged rhizoids)	13.8 $\mu\text{m}/\text{h}$	± 1.91	7

* CLSM imaging using: Kalman $n = 2$; ND = 3; F2; x40 objective; zoom 4.0. (See Chapter 2).

† A valid s.d. could not be calculated because the degree of co-variance between the two sets of length measurements, at time 1 and 2, used to calculate the growth rate could not be adequately taken into account.

3.5 Light-induced apical "swelling"

The light-induced transition from apical growth to isodiametric expansion in fern protonemata is a well studied example of photomorphogenesis (see Chapter 1). The increase in apical diameter and reduction in polarised extension is commonly known as "swelling" although, strictly, it involves the synthesis and deposition of new wall rather than simply stretching of the existing tip (see Murata & Wada, 1989b & c). This light-induced shift in the polarisation of growth is of particular interest as regards the work here. As an initial step the structural features and sequence of events of this response were examined in *D. affinis* during illumination with white light at 50 - 75 $\mu\text{Em}^{-2}\text{s}^{-1}$. This allowed conditions for observation of the response to be optimised and an estimate to be made of the time-scale over which early events, underlying the more obvious morphological expression, occurred.

3.5.1 The sequence of events in light-induced apical "swelling"

Fig. 22 outlines the sequence of events in the "tip-swelling" response under ideal conditions and their approximate timing after initial white light exposure. Although within an individual population individual protonema showed very close agreement the exact timing of events and the degree of apical "swelling" were noted to be variable for different populations (from different sowings) of

protonemata and depending upon the age of protonemata their general health and any variation in temperature and light intensity during culture. A more systematic analysis of this variation was not possible in the time available. The key stages which were recognised are described below.

Chloroplast redistribution (Fig. 22B) was the earliest recognised event and occurred within the first three hours of white light exposure. This may not be directly involved in the "swelling" response. Chloroplasts dissociated from the "nuclear zone" and distributed throughout the apical cytoplasm as well as migrating in a subapical direction. At the same time the apical cytoplasm thinned and redistributed. Under examination conditions chloroplast reorientation was sometimes restricted, this may have been a stress response due to the high intensity illumination used (Yatsunami & Wada, 1990). Early differentiation between the "tip-swelling" and phototropic responses (see later; Section 3.6) was hampered by similarities in the initial morphological expression. However, by using high intensity illumination apical extension and hence phototropic reorientation was effectively halted.

Measurable swelling response (Fig. 22A and C-E) followed the redistribution of chloroplasts. The occurrence of swelling was defined by measurement of filament diameter at the centre of the apical dome (D_1) and at a second point roughly 100 μm behind the tip (D_2) and calculating the ratio D_1/D_2 . This method has previously been described by Davis, (1969). Initial swelling (values slightly greater than 1) was measured as early as three hours after white light exposure, although the proportion of swollen individuals only became significant after 6 - 10 h (Fig. 22A). After 20 h the average ratio D_1/D_2 was 1.35 (47.0 $\mu\text{m}/34.8 \mu\text{m}$), this often increased to above 2 after 30-60 h. Increase in volume was predominantly through increase in vacuolation.

Apical cell division (Fig. 22Civ and Div) generally followed initial swelling under the optimal conditions used. Nuclear division was visible from 6-9 h after exposure and dividing walls were seen after 9 h. After division swelling continued in the apical cell and to a lesser extent the subapical cell. Further apical divisions occurred between 30 and 60 h to produce two or three isodiametric cells.

Results of similar studies performed with *Adiantum* (Wada *et al.*, 1978) differ mainly in the time-scale of events and the occurrence of apical vacuolation in the cytoplasm filled tip of *Adiantum* which precedes "swelling". It should be noted that parallel populations of protonemata, maintained in red light but sampled at times corresponding to 6 h white light-treatment, gave the same distribution of tip forms as the zero-time control. Events were, therefore, a direct response to the white light exposure and not related to culture-time. Although a relatively slow growing species, the "tip-swelling" of *D. affinis* under optimised conditions compared favourably with that seen in *Adiantum* (measurable swelling recorded from 2 - 3 h; Murata & Wada (1989c) and *Pteridium* (initial apical swelling between 4-8 h; Davis *et al.*, (1974)).

3.6 Phototropic reorientation of chlorocyte tip growth

Gametophytes generally exhibit highly positive phototropic growth under red light illumination conditions (Kadota & Wada, 1992a; Mohr, 1956) and also weak blue light (Hayami, Kadota & Wada, 1992a). This involves a reorientation of polarity or shift in the site of apical extension. This is not the same as phototropic bending in oat coleoptiles which occurs subapically through differential expansion of cells on the light and dark sides (Davis, 1975; Kutschera, 1994 and references cited).

Phototropic reorientation was induced in isolated red light grown *D. affinis* protonemata by illumination with red light ($2-4 \mu\text{Em}^{-2}\text{s}^{-1}$) at 90° to the original growth axis. Tip forms were examined for filament populations over the subsequent 60 h (Fig. 23 and Table 3.4).

Chloroplast redistribution and movement of the nucleus into the extreme tip were observed between 6 - 30 h (Table 3.4 - "green tips"). A close relationship between the position of the nucleus and the polarity of growth has previously been reported in ferns (Mineyuki & Furuya, 1985; Ito, 1969). The first sign of reoriented growth was a characteristic lopsided apical swelling at around 20 h (Fig. 23A). By 60 h there was clear apical extension in the new growth orientation with significant regeneration of the vacuole filled tip form (Table 3.4; Fig. 23B).

The response of isolated gametophytes in darkness after undergoing a reorientation of 90° to the previous growth direction was also examined (Table 3.4). Similar changes in tip forms as occurred with phototropic reorientation were observed. However, growth reorientation was less severe and more variable within the population. The cause of reorientation in darkness appeared to be negative geotropism, although "memory" of the last observed light orientation during the isolation procedure cannot be ruled out.

Phototropic reorientation in the horizontal plane was attempted on the microscope stage using lateral red light illumination of isolated *Adiantum* protonemata. After 9 h the protonemata, which were initially oriented at up to 110° to the illumination source, had exhibited reorientation and significant apical growth towards the light (Fig. 23C). Filaments at between 110° - 150° had partially reoriented, while filaments between 150° - 180° showed no reorientation. Maximum "initial" reorientation was less than 90° , for reorientation angles beyond this there appeared to be an increase by gradual increments (this is shown in Fig. 23D). In the presence of lateral illumination there was no sign of a negative gravitropic response as occurs in darkness (see Table 3.4). Phototropism appeared to override gravitropism. However, these initial observations require further study to clarify the situation.

Table 3.4: Tropic reorientation of apical growth of protonemata - tip forms

Tip forms (see Table 3.2 and Sections 3.4.2; 3.5 and 3.6)							
Swollen	Re-oriented	Chloro-filled	Tubule-filled	Vacuolate	Evacuated	n*	
As isolated	0.4%	/	14.4%	41.6%	84.0%	0.0%	243
0-time control							
+ve Phototropic reorientation (unilateral red light - 2.5 $\mu\text{Em}^{-2}\text{s}^{-1}$)							
6 h Red light	0.0%	10.7%	78.3%	0.3%	21.0%	0.3%	336
20h Red light	1.7%	52.5%	82.3%	0.3%	10.4%	5.3%	356
30h Red light	1.0%	72.7%	79.5%	0.0%	7.1%	12.3%	381
60h Red light	0.2%	81.2%	44.0%	0.8%	44.0%	11%	659
-ve Gravitropic reorientation							
6h Darkness	1.8%	0.0%	84.8%	0.0%	13.4%	0.0%	551
20h Darkness	1.7%	22.3%	69.1%	0.2%	4.3%	2.4%	421
30h Darkness	0.6%	27.2%	59.1%	0.2%	6.5%	6.3%	536
60h Darkness	0.0%	35.5%	34.6%	1.9%	24.7%	3.2%	462

* Results were obtained from a single experiment and the values from three replicates were pooled.

3.7 Rhizoids

Rhizoids represent a much simpler study system than the apical chlorocyte, they are more specialised for tip growth and lack the complications of cell division and chloroplasts (Dyer & Cran, 1976). With their distinct structural and functional features the rhizoid and apical chlorocyte provide an interesting comparison of different tip-growing cell types from a single plant.

The extent of rhizoid elongation was observed to be inversely proportional to the ease of penetration of the medium. Rhizoids penetrated agar at concentrations up to 2% (w/v) unless excess surface liquid was present. Poor rhizoid growth was seen with agar concentrations above 1% (w/v) and cellophane-overlaid agar inhibited rhizoid elongation completely. The best growth was seen in liquid media. For examination and experimentation all rhizoids were liquid cultured.

Obtaining healthy rhizoid tips for examination proved to be difficult, this was mainly due to the intolerance of rhizoids to mechanical and chemical stress. The main indication of such stress was deterioration of the tip structure (see Fig. 28E-J). As a result, pre-grown rhizoids could not be harvested in the same way as protonemata. To overcome this rhizoids were grown under examination conditions (see Chapter 2) and actively growing tips considered to represent the normal tip structure (Fig. 26).

3.7.1 Rhizoid structure

Structure was examined by light-microscopy in both actively growing tips in culture chambers and in carefully isolated "healthy" tips (Figs. 24-27).

A thickened region of apical cytoplasm was clearly visible in all growing tips. Immediately behind this was what appeared to be a network of cytoplasmic strands (Fig. 24). This network gave way to a subapical cytoplasmic "sheath". The region of transition between these structures was seen as a characteristic "V" shape when focusing into the cell, with the main central vacuole appearing to extend into the tip (see Fig. 24). Complementary to the cytoplasmic network, a network of irregular tubules and vesicles could be seen, most likely of vacuolar origin (see later, Section 3.10). Similar structures were observed in *Adiantum* rhizoids. In general these findings agree with structural analysis by Cran (1970), on *D. affinis* rhizoids in which the presence of vacuolar system within the extreme apex was noted with progressive enlargement and fusion of small vesicles at increasing distance from the apex. Fraser & Smith (1974) also suggested a central vacuole subdivided by tonoplast membranes with small vacuoles in the peripheral cytoplasm. These researchers also acknowledge the difficulties of preparing rhizoids for structural analysis. It is likely that the true organisation of the subapical network cannot be appreciated from electron micrographs. The putative network of cytoplasmic strands and vacuolar tubules suggested by DIC images at different focal depths is further supported by the later examination, by confocal microscopy of fluorescent dyes (Section 3.10 and Chapter 4). The effects of stress on the subapical network - where the putative vacuolar tubules could be seen to enlarge and merge to form a large subapical vacuole which became continuous with the main vacuole - argues against the possibility that the strands seen behind the apex were mitochondria.

From the growth sequence in Fig. 26 the movement of the nucleus and plastids can be seen to keep pace with apical extension. This feature is in common with apical chlorocytes, although the nucleus in rhizoids resided at greater distance from the tip. Other features shared with apical chlorocytes include the apical cytoplasmic thickening and, to a lesser extent, the cytoplasmic network behind the extreme apex with strands connecting to the nucleus. Increase in length, as with apical chlorocytes, was predominantly through increased vacuole size with synthesis of new wall material at the tip. Confinement of rhizoid extension to within 1 μm of the extreme tip has been shown by Takahashi (1961).

3.7.2 Differences in rhizoid structure with age

Some variation in tip structure was observed under the defined culture conditions. These different forms represented different stages in rhizoid growth and are shown in Fig. 25. In addition, some of the "stress response" tip forms which resulted from damage to rhizoids are shown in Section 3.9.

The tip structure of newly elongating rhizoids was very simple (Fig. 25A). An apical cytoplasmic thickening was linked by cytoplasmic strands to the nucleus, which was located at the base of the cell

and a large single vacuole filled the intervening space. In more developed rhizoids the network-like distribution of apical cytoplasmic strands, discussed above, had begun to form (Fig. 25B and C). Liquid cultured rhizoids which had achieved the full extent of their growth, attaining lengths in excess of 2000 μm , had distorted, evacuated tips with little cytoplasm (Fig. 25E and F). This agrees, in general, with the structural analyses of different developmental stages by: Gantt & Arnott (1965); Fraser & Smith (1974); and Dyer & Cran (1976).

3.7.3 Growth rate

Growth rates for rhizoids were measured directly for individual cells from time-sequences of images (Fig. 26). Growth rates are shown in Table 3.3 (Section 3.4.3). Measured rates were variable depending upon culture conditions, imaging conditions (see Chapter 4) and the age of rhizoids.

3.8 Induction of secondary rhizoids

In culture under white light illumination secondary rhizoids formed from the basal cell soon after the primary rhizoid had fully developed (~ 10 days after sowing spores - Fig. 18E). However, under red light-illumination there was generally no secondary basal rhizoid. This was also noted by Dyer & Cran, (1976). Secondary rhizoids could be induced on red light-grown filaments by transferring them into white light. The first secondary rhizoid usually emerged 3 - 4 days later, at a point adjacent to the previous position of the apical cell nucleus at the time when white light was initially applied (Fig. 27B). The first detectable sign of the site of rhizoid emergence was found to be the staining of a region of the chlorocyte cell wall by Calcofluor. Association of the position of the nucleus adjacent to the new site of polarised growth was particularly interesting. Whether nuclear division, to form the rhizoid nucleus, preceded the determination of the site of rhizoid emergence still needs to be determined.

3.9 Indicators of cell stress

Morphological indicators of cell viability were of particular importance here with such slow growing cells. Morphology provided a means of immediate assessment. A catalogue of stress features was built up by careful observation (see Table 3.5 and Fig. 28). Many of the stress features recorded here resemble observations made in other studies on the effect of a variety of chemical treatments on protonemal cells and rhizoids (Alfano *et al.*, 1993; Wacker & Schnepf, 1990; Murata & Wada, 1989b; Doonan *et al.*, 1988; Miller *et al.*, 1983; Miller & Bassel, 1980; Schmiedel & Schnepf, 1980; Miller & Greany, 1976). The effects of treatments interacting with the cytoskeleton appear to be similar.

Table 3.5: Physical expressions of stress in *Dryopteris* protonemata

Stress feature	Cell types	Observed Occurrence	Example
Plasmolysis	Chlorocytes & rhizoids	Mechanical damage. Severe chemical damage*.	Fig. 28D
Tip vacuolation, cytoplasmic redistribution, withdrawal of the nucleus	Apical chlorocytes & rhizoids	Mechanical damage Prolonged high illumination under the microscope. Slight chemical stress*.	Fig. 28B, E, G-I
Apical rupture	Apical chlorocytes & rhizoids	Mechanical damage. Severe chemical damage*	Fig. 28J
Branching	Apical chlorocytes & rhizoids	Chemical stress*.	not shown
	Basal chlorocytes	High temperature (>25°C).	not shown
Chloroplast shape/distribution	Chlorocytes	Mechanical damage. Chemical damage*.	Fig. 28B-D
Browning (often associated with extrusion of cytoplasm from the tip)	Apical chlorocytes	Chemical damage*.	not shown
Subapical swelling	Apical chlorocytes	Mechanical damage Prolonged high illumination under the microscope.	not shown
Stunted or swollen rhizoids	rhizoids	Solid media. Cellophane. Chemical stress*.	Fig. 28F

* Chemical agents include: plastisizers, strong detergents (SDS, Triton X-100), hypochlorite, some dyes such as Acridine Orange and DiOC₆, high [K⁺] i.e. >2 mM, (also unidentified chemical contaminants on glassware).

Plastisizers used in the manufacture of certain types of Petri-dishes were discovered to pose a significant threat to rhizoid health, as did chemical residues on glassware, for example, detergents and hypochlorite. The apex of tip-growing cells was the most sensitive region and rhizoids were more sensitive than chlorocytes. The extremely sensitive rhizoid appeared to be "disposable"; chlorocyte growth could continue even after rhizoid destruction and new rhizoids were generated with time. Moderately damaged rhizoids were capable of regeneration (Fig. 29).

3.10 Further analysis of gametophyte cytology with fluorescent stains

Simple bright-field and DIC microscopy were found to provide sufficient cytological information to be useful in the indication of cell health and in the recognition of the expression of photomorphogenic responses. Such direct observation did, however, have limitations and in certain cases was ambiguous. Confocal imaging of organelle specific dyes (see Chapter 2, Table 2.2) was employed to provide more conclusive information and to visualise organelles not easily seen directly.

3.10.1 Apical structure

In order to investigate the nature of the tip cytology in both rhizoids and apical chlorocytes and, in particular, to visualise the distributions of the vacuole and cytoplasm, several dyes were applied.

Acridine Orange has been used in the past as a marker for acidic organelles, particularly plant cell vacuoles (Gilroy *et al.*, 1990). However, in fern gametophytes Acridine Orange proved to be both non-specific and disruptive to cell structure, even at low concentration.

LYCH, shown to be taken up into some plant cell vacuoles (Wright & Oparka, 1994), also proved unsuccessful, staining only the outer cell walls and cross walls (Fig. 30C and D). This is in keeping with its alternative use as an apoplastic tracer (Oparka & Read, 1994). Vacuolar uptake of ester loaded CFDA has been used to examine vacuoles in fungi (Shepherd *et al.*, 1993). This was found to be too non-specific in gametophytes.

More success was achieved with Nile Red, a general lipid and membrane stain (Greenspan *et al.*, 1985; Yuan & Heath, 1991; Oparka & Read, 1994). Although visualisation of individual membranes could not be claimed, the presence of a complex network system throughout the apical cytoplasmic regions of rhizoids was made clearly visible (Fig. 30E). In addition, lipid storage droplets were clearly stained in apical chlorocytes (Fig. 30B).

Non-specific staining with DiOC₆ in apical chlorocytes provided further confirmation of the “vesicle or tubule filled” tip form, demonstrating that the network of tubules extended throughout the volume of the apical dome (Fig. 30A).

Indirect evidence for the presence of vacuolar tubules throughout the apices of both apical chlorocytes and rhizoids was obtained with the pH sensitive dye cSNARF-1 which accumulated within the vacuolar system with increasing time after ester-loading. Both the main vacuole and the putative tubular apical vacuolar system were initially unloaded but both appeared to actively accumulate dye with the same time scale. Ratio images of ester loaded cSNARF-1 (Chapter 4; Figs. 36 - 39 and Chapter 5; Fig. 51) revealed that both the apical tubular network and main subapical vacuole were acidic. More detailed Images of cSNARF-1 dye distribution in rhizoids, taken at some time after ester-loading (Chapter 4; Fig. 39B-E and Chapter 6: Fig. 57), suggested that the acidic central vacuole was continuous with acidic tubules that formed a network throughout the apical region (Chapter 4; Fig. 39J).

3.10.2 Endoplasmic reticulum

Endoplasmic reticulum (ER) plays an important part in tip growth; it functions in protein synthesis, vesicle transport and as an intracellular calcium store. Electron microscopy of fungal hyphae (Grove, 1978) and pollen tubes (Pierson & Cresti, 1992) show dense apical accumulations of ER. EM analyses of ferns (Dyer & Cran, 1976; Fraser & Smith, 1974; Cran, 1970; Gantt & Arnott, 1965) also suggest high ER contents in the apical regions, particularly in rhizoids. In the *D. affinis* rhizoid apex the most dense ER accumulation was found by Dyer & Cran (1976) to occur just (10 µm) behind the

extreme tip, parallel to the cell wall, and be several layers deep. The same study showed that the ER in the extreme apex was less developed and did not exhibit any particular orientation relative to the cell wall. In white light grown protonemata of *D. affinis* ER was shown to associate closely with chloroplasts and other organelles including the plasma and nuclear membranes (Cran & Dyer, 1973). Confocal imaging of DiOC₆ has been used to investigate ER in protonemata of the moss *Funaria* (McCauley & Hepler, 1990) as well as other systems (Quader, 1990). This technique was, therefore, used here to investigate ER in fern protonemata cells (see Fig. 31).

Visualisation of ER in rhizoids was not possible due to disruption of structure during dye loading, problems with overloading and non-specific staining.

Fig. 31 shows ER staining by DiOC₆ in chlorocytes. Only the outer layers of cortical ER were visualised. ER could not be seen throughout the general cytoplasm, specifically at the extreme apex. This may reflect the limitations of the technique as well as the nature of the ER itself. It has been suggested that the ER of the extreme apex is less well developed and more disorganised (Yuan & Heath, 1991; Dyer, 1979; Dyer & Cran, 1976). In subapical regions of apical cells (Fig. 31B) and subapical cells (Fig. 31C) the cortical ER formed loose polygonal structures interspersed with flat sheets. In more apical regions in subapical cells and to an even greater extent in apical cells (Fig. 31A) a much tighter polygonal structure was seen. Such ER appeared to extend well into the tip of apical cells, although it could not be clearly imaged amongst the chloroplasts of the nuclear cluster. ER was clearly seen to underlie chloroplasts in both apical and subapical regions. White light-cultured cells displayed a general distribution of ER with a tighter polygonal structure and fewer flat sheets (data not shown).

3.10.3 Mitochondria

Growth requires a significant amount of a cells energy and its metabolic intermediates (as building materials). It is, therefore, unsurprising that the distribution of mitochondria is often polarised relative to the polarity of tip growth. Mitochondria may also have a role in the regulation of pH in the apical regions of tip-growing cells (Sanders & Slayman, 1982). It was additionally expected that the distribution of mitochondria would correlate with the distribution of the cytoplasm. The distribution of mitochondria in has previously been visualised by staining with the potential sensitive dyes DiOC₆ and Rhodamine-123 (Yuan & Heath, 1991; Liu *et al.*, 1987; Matzeke & Matzeke, 1985 and references therein;). Mitochondria appear as brightly staining oval structures roughly 1.0 x 0.5 µm in size. In this study, confocal microscopy of these dyes was used to examine mitochondrial distribution in gametophyte cells (Figs. 32 and 33).

In chlorocytes over-staining was found to be a significant problem, with both DiOC₆ and Rhodamine-123 causing distortion and clumping of mitochondria (data not shown). However, DiOC₆, in general, caused less disruption to mitochondria when used at low concentrations. In contrast, very low concentrations of Rhodamine 123 could be used in rhizoid cells and proved to be

both more specific and less disruptive than DiOC₆ for which a useful loading concentration could not be determined.

In chlorocyte apical cells the distribution of mitochondria, concentrated towards the cell apex, can clearly be seen (Fig. 32A). Mitochondria were present throughout the thickened-apical and peripheral cytoplasm, associated with cytoplasmic strands and amongst the nuclear cluster. The differences between Rhodamine and DiOC₆ staining should be noted - mitochondria deeper within the cell were better detected with the brighter and more bleach resistant Rhodamine.

Mitochondrial distribution was less distinctly polarised to the cell apex than in the apical chlorocyte (Fig. 33). Mitochondria were shown to be associated with the strand like structures (putative cytoplasmic strands) observed in the subapical 10 - 30 μm , however, projected confocal images from different focal depths (Fig. 33) demonstrated that staining for mitochondria was confined to small discrete regions within those strands. These observations of mitochondrial shape and distribution are in good agreement with EM studies (Dyer & Cran, 1976; Fraser & Smith, 1974; Cran, 1970; Gantt & Arnott, 1965).

3.11 Discussion

3.11.1 The fern gametophyte as an experimental system

Gametophytes of the fern *Dryopteris affinis* were selected as the main experimental subject. Initial problems of sensitivity to isolation and handling were largely overcome by the procedures devised (see Chapter 2) and this species was found to be amenable to analysis at the single cell level. Normal growth, development and responses of *D. affinis* gametophytes (in agreement with the work of Dyer (1979) and Dyer & Cran (1976)) were all recorded on the microscope stage under examination conditions.

Apical extension, phototropic re-orientation and "tip-swelling" were all cited in chapter 1 as key targets for the study of: steady-state growth; reorientation of polarity; and transition to non-polarised growth, respectively. The results of the analysis of these events under single cell examination conditions, reported here, has allowed their suitability for further study, and the application of imaging techniques, to be assessed from a more practical view-point. Although only a limited structural analysis was performed it was sufficient for the initial assessment of the experimental system. The main points achieved by this examination were: 1) recognition of the "normal" healthy state in cells; 2) recognition of morphological expression of physiological responses; 3) assessment of cell types and developmental stages for structural features both favourable and detrimental to the application of dye-based imaging methods; 4) provision of a basis for interpreting dye distribution (relevant to Chapter 4).

3.11.2 The study of polarity and tip growth in fern protonemata

For the purpose of examining steady state tip growth, protonemal filaments could be cultured under conditions where growth was predominantly through apical extension. However, even with optimal conditions, recorded rates were relatively slow - see Table 3.3. Whilst other slow growing cell types, namely moss protonema and fucoid zygotes, have been successfully used in studies of cellular polarity (Gibbon & Kropf, 1994; Hahm & Saunders, 1991) such slow growth imposes many experimental limitations. Problems range from the time required for cell culture and gathering data to difficulty in detection and recording the response. This is particularly important when considering experimental manipulations of growth.

Although the apical chlorocyte was shown to exhibit polarised growth under examination, polarity was found to be initially disrupted by the isolation of protonemata as a result of phototropic and possibly geotropic reorientation. Consequently, long "recovery" periods were required to demonstrate continued steady-state apical extension. Phototropic reorientation has been used previously as a "marker" to allow determination of continued growth after an experimental treatment (Murata & Wada, 1989b).

The continued activity of the cell cycle under conditions of apical extension, even at a low rate, (Wada & Furuya, 1970) is an added complication to the study of steady-state apical growth in apical chlorocytes. This includes both cell cycle related structural changes and influences on the growth rate as well as cell cycle associated signal transduction events. The progression of the cell cycle needs to be carefully characterised to assess whether the processes of tip growth can be examined independently. Critically, is there any interaction between the cell cycle and the growth rate? This appears not to be the case for *Funaria* protonemata (Schmiedel & Schnepf, 1980).

In general, the faster growing rhizoid cell, with no chloroplasts or cell cycle problems, provided a much more approachable system for studying polarised growth. However, rhizoid cells have their own potential complications. These include their possible role in the uptake of ions (Miller *et al.*, 1983; Miller, 1980; Smith, 1979) and the uncertainty as to the factors controlling rhizoid polarity; the roles of touch, light and gravity have been only vaguely implicated (Raghavan, 1990). The lack of an obvious physiological stimulus for the modification of growth is an unfortunate limitation. The sensitivity of rhizoids to physical and chemical stress and their ability to regenerate tip structures does provide a range of alternative, non-physiological, manipulations.

3.11.3 Photomorphogenic events and the regulation of polarity

Although changes in the polarity of growth were induced by light treatments it was obvious that photomorphogenesis involved several, possibly independent, responses. Chloroplast movements and changes in the cell cycle were both triggered by the light treatments affecting growth polarity (Yatsuhashi & Wada, 1990; Lino *et al.*, 1988; Wada & Furuya, 1970) events have been examined independently of polarised growth in *Adiantum*, by the use of localised micro-beam irradiation

treatments (e.g. Yatsuhashi & Wada, 1990). It appears that the regulation of these events is to some extent independent of the polarity of growth (Kadota & Wada, 1992b; Yatsuhashi & Wada, 1990; Kadota *et al.*, 1986; Kadota & Furuya, 1977 and 1981). Whether the observed responses in *D. affinis* can be similarly dissected is worth consideration as a means of simplifying the examination of growth polarity. Although the multiple responses are potentially confusing to the study of polarity such orchestration of multiple, concurrent responses is a typical feature of cells. Understanding how this is controlled would be an important advance in our understanding.

In the work here only obvious morphological responses to stimuli were examined. Although this provided information on the ability of cells to respond and the extent of their response it did not indicate the initial underlying events. The long "lag" periods of 3h or more after light-stimulation before a response was observed reflect this. The ability to identify specific, determinant, events in the change of growth polarity at a very early stage would be advantageous, both for detecting whether an individual has responded and narrowing down the time-period over which early stimulus-response events must have occurred. In other species early events such as cytoskeletal restructuring (Kadota & Wada, 1992a; Murata & Wada, 1989b & c) and changes in membrane potential (Racusen *et al.*, 1988; Cooke *et al.*, 1983) have been recorded. Membrane potential measurements in particular would prove useful for monitoring the time-course of response and aid the design of imaging experiments to follow early signalling events.

3.11.4 The application of imaging technology

The use of dye-based measurement and imaging techniques for examining the roles of ions in signalling events was introduced in Chapter 1 and will be further discussed in Chapters 4 and 5. The observations of gametophyte structure and response made here have several implications for the application of such methods.

Averaging methods such as photometry have a potential application for the early examination of the non-steady-state photomorphogenic events. Keeping track of such slow growing cell is unlikely to be a problem, although chloroplast movements may be a nuisance. However, as cytoplasmic redistribution is a key event in the photomorphogenic responses, then ratiometric methods or confocal imaging may be the only way to obtain meaningful data. When examining steady-state phenomena, such as ion-gradients associated with growth, imaging becomes essential. The fact that the relatively complex apical cytoplasmic distribution of gametophyte cells could only be properly appreciated by DIC microscopy or confocal imaging favours the use of the CLSM over conventional fluorescence microscopy for determining cytoplasmic [ion].

The extreme sensitivity of chlorocytes to illumination suggests that difficulties may arise with dye excitation-illumination. This needs to be assessed by careful control experiment, especially for the blue and UV excited dyes. Chloroplast autofluorescence is a common problem with the use of fluorescent dyes (Fricker & White, 1992). Additionally in protonemata, chloroplast movements are

an early event in photomorphogenic responses and may obscure imaging the dye. These problems are considered further in Chapter 4.

The introduction of dyes into cells is considered in Chapter 4 and structural information obtained here, namely: cytoplasmic; vacuolar; and other organelle distributions, is relevant in determining the distribution of intracellular dye.

3.11.5 Further cytological and ultrastructural analysis

There is clearly significant potential for a systematic study of cytological and ultrastructural features associated with the tip growth of *D. affinis* protonemata and rhizoids and the changes associated with the different stages of gametophyte development and photomorphogenic response. A most promising method of further structural analysis would be the application of transition electron microscopy to cryofixed material (Kiss *et al.*, 1995), particularly with respect to identifying the nature of the putative tubular vacuolar system at the apex of rhizoids. In addition, the bright-field microscopy and structural confocal imaging techniques employed in the current work could be extended, in the future, to follow dynamic *in vivo* events. The ER network and cytoskeleton are two areas worth further investigation in this respect.

Changes in ER distribution and structure have been studied in relation to bud formation in *Funaria hygrometrica* (McCauley & Hepler, 1992 and references therein). Buds show a much tighter arrangement of the polygonal network than in the rest of the cell. This is similar to the arrangement seen in protonemal apical filaments. The tight polygonal structure of buds is also similar to the ER structure seen in white light-grown gametophyte cells. The difference observed between ER structure of red and white light grown gametophytes is potentially of interest in relation to polarisation of growth. ER has been implicated in Ca²⁺ homeostasis (Gilroy *et al.*, 1993) as well as having a role in the synthetic and exocytotic activity of cells.

Cytoskeletal organisation is another component of polarity and tip growth which would be relevant to the current study; the regulation of tip growth is likely to be largely dependent upon the regulation of the cytoplasm. Cytoskeletal activity has been shown to be involved in polarity and photomorphogenesis in ferns. Microtubules and actin microfilament involvement has been demonstrated in chloroplast movement (Kadota & Wada, 1989a; 1992b), determination of protonemal apical cell shape (Murata & Wada, 1989b & c; Doonan *et al.*, 1988; Murata *et al.*, 1987) and cell division (Murata & Wada, 1991; 1992). Examination of dynamic cytoskeletal activity could be performed using confocal imaging techniques as employed by Yuan *et al.* (1994).

3.11.6 Tip growth in ferns in relation to other tip-growing cell types

A detailed comparison between the cytology of ferns and other tip-growing cell types is not within the scope of this work, however, certain important points should be noted.

The distribution of the apical cytoplasm in tip-growing cells of *D. affinis* was examined here in some detail. Compared to other tip-growing cells (including: fungal hyphae; pollen-tubes; *Chara* protonemata and rhizoids; and moss protonemata (caulonemata) cells) those of *D. affinis* display a relatively low content of cytoplasm at the apex. Many other cell types also exhibit distinct organisation within the apical cytoplasm, for example: the "clear zone" of pollen tubes (Pierson & Cresti, 1992); the vesicle organising centres of *Chara* rhizoids (Braun & Sievers, 1994; Hodick, 1994) or moss caulonemata (Schmiedel & Schnepf, 1980); and the "Spitzenkörper" of fungi (Lopez-Franco *et al.*, 1995; Grove, 1978). Interestingly, the slow growing moss chloronemata apical cells lack the vesicle organising centre exhibited by the faster growing caulonemata and more closely resemble fern protonemata (Schmiedel & Schnepf, 1980). It is likely that both the content of cytoplasm and the degree of organisation at the apex is strongly correlated with growth rate (see Table 3.6).

Table 3.6: The growth rates of some commonly studied apically extending cell types

Type	Cell type	Extension rate	References
Slow	<i>Pelvetia</i> , rhizoids	< 3 $\mu\text{m/h}$	Gibbon & Kropf, 1994
	<i>Adiantum</i> , apical chlorocytes	10 $\mu\text{m/h}$	Wada <i>et al.</i> , 1982
	" " " "	3.72 $\mu\text{m/h}$	Kadota & Furuya, 1981
	<i>Funaria</i> , chloronemata	4-10 $\mu\text{m/h}$	Schmiedel & Schnepf, 1980
	<i>Funaria</i> , caulonemata	48 $\mu\text{m/h}$	
	<i>Chara</i> rhizoids	100-180 $\mu\text{m/h}$	Bartnick <i>et al.</i> , 1988
Fast	<i>Saprolegnia</i> , vegetative hyphae	0.129 $\mu\text{m/s}$	Lopez-Franco <i>et al.</i> , 1994
	<i>Neurospora</i> , vegetative hyphae	0.201 $\mu\text{m/s}$	
	<i>Tradescantia</i> , pollen-tubes	0.106 $\mu\text{m/s}$	Miller <i>et al.</i> , 1992
	<i>Agapanthus</i> , pollen-tubes	0.27 $\mu\text{m/s}$	Malhó <i>et al.</i> , 1994

The growth rate and degree of apical cytoplasmic organisation may also be significant with respect to the existence of growth-associated tip-focused ion gradients such as described for pollen tubes (Pierson *et al.*, 1994). It is interesting that *D. affinis* also shows a lack of cytoplasmic streaming, another feature associated with the faster growing cell types. The relatively small apical cytoplasmic accumulation of fern protonemal cells, linked to the nucleus by a network of cytoplasmic strands, seems to be closer to the less specialised organisation of general higher plant cells (Prichard, 1994).

Vacuolar organisation is also of interest. In *D. affinis* protonemata the vacuole was seen to take up a considerable proportion of the apical volume, in other tip-growing cell types such as moss caulonemata (Schmiedel & Schnepf, 1980), fungal hyphae (Grove, 1978) and pollen tubes (Pierson *et al.*, 1990; Lancelle & Hepler, 1992) there is no significant vacuolation "separating" the nucleus from the apical cytoplasmic accumulation. In these cell types the appearance of vacuoles at the apex is a sign of stress. It is possible that this reflects the less specialised nature or slower growth rates of apical chlorocytes compared to the other tip-growing cell types which, additionally, have much larger apical accumulations of cytoplasm. Growing fungal hyphae have a complex "dynamic continuum of

pleiomorphic tubules and vacuoles" extending into the apex, although excluded from the extreme tip (Shepherd *et al.*, 1993). A role in transport, with reference to endocytosis, was proposed for this structure. In pollen tubes the main vacuole lies well behind the tip, although smaller, elongate vacuoles extend much further forward (Pierson *et al.*, 1990; Pierson & Cresti, 1992). One possibility for the vacuolation in *D. affinis* chlorocytes compared to the other cell types is that gametophytes must be able support themselves in the air. The apical vacuolar structure of the fern rhizoids again appears to be different from that of the apical chlorocyte. Rhizoids may rely on vacuolar turgor for the mechanical penetration of substrates. Differences between tip-growing cell types may be usefully considered from the point of view of functional specialisation. Understanding the physiology of the relevant systems is, therefore, important. The physiological role of the fern gametophyte is discussed in Dyer (1979).

3.11.7 Conclusions

In light of the findings here it would seem to be sensible to confine the examination of polarity to steady-state tip growth in apical chlorocytes and rhizoids. Phototropic reorientation and apical swelling are arguably the more interesting phenomena to address. However, while these responses can be reasonably reliably reproduced under experimental conditions, a significant number of difficulties remain unresolved and further characterisation of the events involved is required. Phototropic reorientation and apical "swelling" are, therefore, suggested as a future line of investigation, complementing work on: budding in mosses (Mcauley & Hepler, 1990; Quader & Schnepf, 1989); branching in fungi (Hosking *et al.*, 1995); rhizoid outgrowth of furoid zygotes (Kropf, 1992; 1994); and the tropic growth responses of fungi (Gow, 1994) and pollen tubes (Malhó *et al.*, 1994).

Chapter 4

ASSESSMENT OF LOADING METHODS FOR pH AND CALCIUM SENSITIVE DYES

4.1 Introduction

The introduction of dye into cells is one of the major limiting steps in the use of dye-based imaging techniques, often it is the stumbling block that decides whether a particular cell system is suitable or not (e.g. Fricker *et al.*, 1994; Knight *et al.*, 1993a; Read *et al.*, 1992; Miller *et al.*, 1992; Gilroy & Jones, 1992; Kiss *et al.*, 1991; Hahn & Saunders, 1991; Scheuerlein *et al.*, 1991; Russ *et al.*, 1991). A range of methods (Table 4.1) are available for loading dyes into cells. In general these techniques have been developed for loading animal cells (Martinez-Zaguilan & Martinez, 1991 and references therein) and do not always apply well to plant cells. As yet there is no strict format for dye loading so selection of the best method is largely through trial and error. Successful loading depends upon: exact loading conditions; the type of cell; previous handling of cells; and even upon the individual species (Oparka & Read, 1994; Fricker *et al.*, 1994; Read *et al.*, 1992; McCormack & Cobbold, 1991; Moore *et al.*, 1990).

In the work here a range of dyes and loading methods (Materials and Methods, Chapter 2) were tested on gametophyte cells with the aim of determining whether introduction of ion-sensitive dyes was possible and if so the most suitable method. The method of electroporation (Messiaen *et al.*, 1993; Shacklock *et al.*, 1992; Scheuerlein *et al.*, 1991) was not attempted as it was considered potentially too damaging to gametophytes.

The success of dye loading was determined on the basis of the following criteria: 1) that the quantity of dye introduced was sufficient for imaging; 2) the degree of dye localisation to the cell cytoplasm; 3) dye retention in the cytoplasm long enough to provide useful imaging times; 4) that dye remained responsive within the cell (This is dealt with in Chapter 5 in more detail); 5) cells retain normal appearance after loading and imaging and continue normal growth and development during and beyond the time-course of experimentation.

4.2 Microinjection

Microinjection has an advantage over other methods in terms of the flexibility afforded in the introduction of different probes into cells; basically, any dye may be introduced by this method. Two forms of microinjection exist (Oparka & Read, 1994): ionophoretic microinjection, where an applied current is used to drive charged dye molecules down the needle into the cell and pressure injection which relies on applied pressure to drive a volume of liquid into cells. The method is limited mainly by cellular damage upon impalement and difficulty in learning and applying the technique.

A variety of plant cells have been successfully loaded by microinjection, most commonly: *Commelina* guard cells (Gilroy *et al.*, 1991; McAinch *et al.*, 1990), *Tradescantia* stamen hair cells (Hepler *et al.*, 1993; Zhang *et al.*, 1990), leaf trichomes (Oparka *et al.*, 1991b), moss protonemal cells (Read *et al.*, 1992), pollen-tubes (Malhó *et al.*, 1994; Miller *et al.*, 1992), zygotes of marine algae (Gibbon & Kropf, 1994; Berger & Brownlee, 1993) and fungal hyphae (Jackson, 1995; Corrêa & Hoch, 1993; Read *et al.*, 1992). Surprisingly, these plant cell types withstand the procedure well and show only limited effects if sufficient time is allowed for recovery (Callaham & Hepler, 1990). With pollen tubes and fungal hyphae, both of which are fast tip-growing cell types, detailed studies on the effects of ionophoretic microinjection have been made (Malhó *et al.*, 1994; Knight *et al.*, 1993a). Part of the "stress response" upon injection, which involves the temporary cessation of growth, appears to result from the effect of the ionophoretic current on ion channels in the plasma membrane.

With the relatively large diameter of fern protonemal cells microinjection seemed to be a favourable possibility. Attempts were made to inject both apical and subapical chlorocyte cells.

4.2.1 Results of microinjection

Examples of dye loadings achieved by ionophoretic microinjection are shown in Fig. 34. From these images the differences between vacuolar and cytoplasmic injection can be clearly seen. Cytoplasmic loadings exhibited a clear "cell outline" (corresponding to the peripheral cytoplasm), fine cytoplasmic strands, chloroplasts "circled" by dye fluorescence and strong nuclear loading. Similar observations have been made of microinjected *Commelina* guard cells (Gilroy *et al.* 1991). The sequence of events during a loading is shown in Fig. 34B-D. Dye rapidly spread from the site of injection along cytoplasmic strands to the nucleus which quickly became brightly fluorescent. Dye generally spread until the whole cell was "outlined", however, in no case was dye seen to pass between cells - cell end walls show up clearly in the examples shown (Fig. 34E and F). Comparison with an ester-loaded cell (Fig. 34 J) demonstrates the similarities in dye distribution. With increasing time after injection (10 - 30 min.) dye was accumulated into the vacuole from the cytoplasm, severely limiting the useful imaging time.

Vacuolar injections (Fig. 34H) lacked the distinct cell and chloroplast "outlines". In fact, the chloroplasts appeared as dark regions against an even, diffuse, background fluorescence. The loss of turgor can clearly be seen at the site of injection in the corresponding bright-field image (Fig. 34G). Removal of the needle after vacuolar injection usually resulted in collapse of the cell.

4.2.2 Conclusions

Although, in principle, microinjection was successful it proved to have only limited practical application as a routine loading method. The main failings of the method were:

- Poor success rate (< 1 in 10 cytoplasmic loadings).
- Poor recovery rate, conditions of microinjection appeared very stressful to cells.

- Rapid vacuolar sequestration of ionophoretically injected dye free-acids.

Further work is required to optimise this technique. Pressure microinjection, which was only briefly attempted here, deserves more attention than the current study could afford. In particular, injection of dextran-dye conjugates would be important.

4.3 Acid-loading

This technique has found some success with plant cells and tissues (Levina *et al.*, 1995; Kiss *et al.*, 1991; Hahm & Saunders, 1991; Russ *et al.*, 1991; Gilroy & Jones, 1992). It was thought to be of potential here as the normal pH of gametophyte growth medium was low (pH 4.5-5.6). However, no success was achieved with any of the dyes tried (Fig. 35 and Chapter 2; Table 4.2).

4.3.1 Conclusion

This method failed in many respects:

- Requirement for long incubation times, incubation periods up to 6h were tried.
- Rate of cytoplasmic uptake << rate of sequestration into the vacuole.
- Binding of fluorescent dye free-acid to the cell wall (or cuticle).
- Requirement for "washing" steps to remove excess free-acid before imaging.

4.4 Ester-loading

Ester-loading is the easiest method to employ and has been particularly successful in animal cells (Grynkiewicz *et al.*, 1985). Application to plant cells is less favourable, although not entirely without success (Calcium dyes - Kiss *et al.*, 1991; Brownlee *et al.*, 1987; Prof. R.E. Cleland personal communication. pH dyes - Inouye, 1985; Davies *et al.*, 1990; Roos, 1992). The main problem with ester-loading is the tendency for organelle sequestration of dye (Slayman *et al.*, 1994; Gilroy & Jones, 1992; Rathore *et al.*, 1991; Hahm & Saunders, 1991). This problem was examined in the present study with the aid of confocal fluorescence microscopy.

4.4.1 Results of ester-loading

Cell permeant ester-derivatives of calcium sensitive dyes proved to be entirely unsuccessful, even when using newly prepared stock at high concentration (50 μ M) over long periods (up to 6 h). There are several possible explanations for this failure: polar groups on dye molecules are poorly masked; the conformation of dye molecules prevents entry into the cell; or these dyes form a poor substrate for cellular esterases. The explanation is complicated by the varied structures of different calcium dyes, all of which failed to enter the cell (Chapter 2; Table 2.2). For structures see Haugland, (1992).

Table 4.1: Methods for loading ion-sensitive dyes into cells

Method	Dye types	Advantages	Limitations	Reference	Cell type	
Microinjection	ionophoretic	charged dye free-acids	Works for a wide range of dyes. More control over amount/initial localisation of dye. Easier to perform and less physically damaging than pressure injection.	Technically difficult. Electrical damage. Uptake of dye by organelles.	Malhó <i>et al.</i> , 1995 Knight <i>et al.</i> , 1993a Gilroy <i>et al.</i> , 1991 Rathore <i>et al.</i> , 1991 McAinsh <i>et al.</i> , 1990	Pollen-tubes Fungal hyphae Guard cells Pollen tubes Guard cells
	pressure	all dyes including dextran conjugates	Dextran dyes - better dye localisation and intracellular behaviour.	Technically difficult. Physical damage.	Gibbon & Kropf, 1994 Berger & Brownlee, 1993 Corrêa & Hoch, 1993 Miller <i>et al.</i> , 1992 Oparka <i>et al.</i> , 1991	fucoid zygotes fucoid zygotes Fungal hyphae Pollen-tubes Leaf-hairs
Ester-loading	Cell-permeant AM esters	cell permeant dye-esters (in the presence of Pluronic F-127 detergent)	Ease. large numbers of cells loaded simultaneously. Can examine cells during loading.	Limited to certain dyes. Uptake of dye by organelles. Variable cell loadings.	Slayman <i>et al.</i> , 1994 Roos, 1992 Irving <i>et al.</i> , 1992 Hahm & Saunders, 1991 Davis <i>et al.</i> , 1990	Fungal hyphae Cultured cells/protoplasts Guard cells Moss protonemata Fungal hyphae
Acid-loading	at pH 4-5	dye free-acids with suitable pKa and membrane permeability at pH <5	Suitable for some Ca ²⁺ dyes. Less invasive than other methods.	Slow/poor loading. Extracellular dye fluorescence. Organelle uptake of dye. Restricted application.	Levina <i>et al.</i> , 1995 Gilroy & Jones, 1992 Russ <i>et al.</i> , 1991 Hahm & Saunders, 1991	Fungal hypha Protoplasts Algal cells/protoplasts Moss protonemata
Electroporation		unrestricted	Ease. large numbers of cells loaded simultaneously.	Possible cellular damage. Organelle uptake of dye.	Shacklock <i>et al.</i> , 1992 Scheuerlein <i>et al.</i> , 1991 Messiaen <i>et al.</i> , 1993	Protoplasts Fern spores Protoplasts

In complete contrast, all of the pH sensitive probes tried were found to load successfully as their AM-ester forms. The presence of the $-N(CH_2C=OOCH_2OC=OCH_3)_2$ group in all of the calcium dyes used, but not in the pH dyes, should be noted. The degree of loading of the pH dyes could be readily controlled through the concentration of AM-ester applied and the duration of exposure. It was noticed, however, that the degree of loading was generally not uniform for a cell population. Rhizoids tended to load faster than chlorocyte cells. This probably reflects differences in wall structure between the cell types (Raghavan, 1990). Apical chlorocytes tended to load better than subapical cells but showed far greater variation between individuals.

4.5 cSNARF-1 AM ester-loading results

cSNARF-1 AM was found to successfully load into both chlorocyte and rhizoid cells (Figs. 36, 37 and 38). Subsequently, a more detailed analysis and optimisation of cSNARF-1 AM-ester-loading was made to assess its full potential.

4.5.1 Localisation of cSNARF-1 dye

Direct analysis of intracellular cSNARF-1 distribution, by confocal fluorescence imaging and comparison with simultaneously recorded bright-field images (Figs. 36-39), showed clear correlation with: the apical cytoplasmic region; cytoplasmic strands; the nucleus; and large central vacuole of the cell. Further it could be seen that dye was not accumulated into lipid droplets (Fig. 36E and Ei). Association of dye with chloroplasts was more difficult to interpret because of chloroplast associated cytoplasm and autofluorescence from chloroplast pigments. Some chloroplast accumulation of dye did occur, see Fig. 36F. ER uptake of cSNARF-1 could not be conclusively proved, although distribution of cSNARF-1 at the cell periphery (Fig. 36C and G) exhibited a certain similarity to ER specific staining with DiOC₆ (Chapter 3; Fig. 31). Evidence to support ER accumulation comes from carboxy-fluorescein AM ester-loading of onion epidermal cells, which exhibited clear ER accumulation (data not shown). In rhizoid cells, examination of cSNARF-1 distribution (after ester-loading) at high resolution, using a x60 (NA = 1.4) oil immersion objective (Fig. 39H), revealed small (<1µm) areas of brighter fluorescence in the general cytoplasm. These were similar to mitochondria visualised by Rhodamine-123 staining (Chapter 3; Fig. 33).

A plasmolysing treatment of loaded chlorocytes (50 mM sorbitol) showed that the "outline" of fluorescence was not associated with the cell wall but with the protoplast and clearly with cytoplasmic strands (data not shown). However, the examination of plasmolysed cells did not exclude the possible association of cSNARF-1 with membranes (Opitz *et al.*, 1994). In addition, the binding of cSNARF-1 free-acid at the cell wall was observed in some cases, with high or prolonged loading (see Figs. 35 and 39F for examples of "wall loading").

Examination of cSNARF-1 ratio images (Fig. 36H-J, also Chapter 5; Fig. 51 and Chapter 6; Fig. 57) revealed regions of different apparent-pH within the cell which correlated with: the acidic main

vacuole (expected pH 4.8 - 6.0 - Guern *et al.*, 1991); smaller acidic vacuoles and vesicles; the more alkaline cytoplasm (expected pH 7.1 - 7.5 - Guern *et al.*, 1991); and chloroplasts (see also Section 4.8.2). Treatments reported to alter cytoplasmic pH such as azide (which acts through anoxia associated cytoplasmic acidification (Guern *et al.* 1991; Davies *et al.*, 1990)) and NH₃ (which causes alkalisation) (Felle, 1980)) caused rapid changes in intracellular pH in both protonemata and rhizoid cells, as reported by cSNARF-1 (data not shown). The rates and distribution of pH change within the cell suggested a cytoplasmic location of at least some pH responsive dye, although it was clear that the cytoplasmic and vacuolar compartments were affected. Intracellular dye response to pH changes was further demonstrated by the *in situ* calibrations described in Chapter 5.

4.5.2 Vacuolar accumulation of dye

Examination of dye distribution in individual cells over extended periods (Figs. 37C and 39B-E) revealed that dye distribution changed with time. For both chlorocytes and rhizoids most of the cytoplasmic dye was "cleared" within 90 min., providing a useful imaging time of only about 30 min. (see Chapter 5). This was similar to the deterioration, over time, of an initially cytoplasmic microinjection of Calcium Green-1 free-acid (Section 4.1). During continuous ester-loading vacuoles accumulated very high (and probably toxic) dye contents. Vacuolar sequestration has been previously observed for a variety of dyes and cell types (Slayman *et al.*, 1994; Wright & Oparka, 1994; Breeuwer *et al.*, 1994; Oparka *et al.*, 1991a; Steinberg *et al.*, 1987). An active anion transport mechanism has been proposed for this vacuolar sequestration on the basis of work with the anion transport inhibitor probenecid (Oparka *et al.*, 1991a). Vacuolar sequestration in fern protonemata also appeared to be an active process and could be inhibited by probenecid. However, this could not be used as a routine loading treatment as probenecid disrupted cytoplasmic structure and tip growth at effective concentrations (2 - 10 mM). The rate of dye uptake into the vacuole depended upon cell viability and appeared faster with lower initial loading levels. The latter may relate to the health of the cell or to a saturatable rate for the redistribution process.

Only over long time periods (>10 h) did vacuolar fluorescence severely diminish. It was not determined whether this was through dye loss; dilution as a result of growth; or dye inactivation. Evidence of inactive dye was observed in rhizoid cells examined over 10 h after their initial loading. At this stage general dye fluorescence was very low and weakly fluorescent aggregates were seen (Fig. 37G).

4.5.3 Assessment of cell viability

In order to make physiologically relevant statements about intracellular pH, by using fluorescent dye imaging techniques, it had to be demonstrated that the normal processes of the cell were not disrupted (see Oparka & Read, 1994). Methods used to assess viability are described in Chapters 2 and 3. The work described in this section relates specifically to loading and imaging cSNARF-1.

4.5.3.1 Population studies

Initially, population studies were used to determine viability after loading cells with dye. The “swelling” response of the apical chlorocyte in white light was used to determine whether cells were healthy (Table 4.2). Although there was a clear negative on cells as a result of the dye loading procedure interpretation of this was not straightforward. The “population method” proved to be unsatisfactory for several reasons. 1) Differences in the handling procedures used with cell populations and for imaged individuals on the microscope stage. Physical damage, during the washing procedures applied to populations (to remove excess dye), had a significant effect on cell viability. This effect may have been increased with the additional stress of dye loading. 2) Different loading degrees for cells within a population (see Section 4.3.1). 3) Phototoxic effects associated with dye excitation were not properly taken into account using cell populations (Moore *et al.*, 1990). 4) The very variable rates and extents of the “swelling” response. 5) The lack of information about the activity of the cell during the useful imaging time (i.e. before vacuolar sequestration, which was generally significant by ~ 30 min. after loading).

Table 4.2: Chlorocyte viability after cSNARF-1 AM ester-loading: tip-swelling response

Loading [†]	% Swollen*		% evacuated*		Observations
	30 h [‡]	60 h [‡]	30 h [‡]	60 h [‡]	
Unloaded	70.2	92.6	16.7	2.45	Very good swelling D_1/D_2 high. Multiple tip divisions after 60 h.
5 μ M/5 min	65.6	92.3	11.2	6.9	As control for 5 min. but with reduced D_1/D_2 with increased loading time. Cell division and swelling ~ as control values after 60h.
5 μ M/10 min	53.2	80.7	24.6	16.0	
5 μ M/20 min	39.8	65.7	39.0	25.9	
10 μ M/5 min	53.9	77.7	23.6	11.2	Reduced D_1/D_2 throughout with little cell division even after 60 h. Toxic effects apparent at the highest loading level.
10 μ M/10 min	41.6	76.4	37.6	17.4	
10 μ M/20 min	37.6	78.1	42.0	13.5	

[†] Cells were washed (Chapter 2; Section 2.2.7.1) to remove dye.

[‡] Time in continuous white light. White light treatment was begun at the start of the loading. Viability was scored in terms of the white light-induced apical chlorocyte “tip-swelling” response. Swelling should be significant (high D_1/D_2) by 30 h light-treatment (Chapter 3; Section 3.5.1) so only +/- swelling was scored.

* Results were pooled from three concurrent replicates (as discussed in Chapter 3; Section 3.5.1); ~ 3 x 100 protonemata were examined for each loading treatment. The % of unswollen tips (excluding evacuated tips) is not shown.

4.5.3.2 Individual assessment

A better method of analysing cell viability was to follow loaded individuals. Firstly, loading was defined in terms of fluorescence under standard imaging conditions rather than applied loading conditions. Secondly, viability (growth rates in the case of rhizoids) was determined for individual loaded cells and unloaded control cells, again under standard imaging conditions (Table 4.3). Loaded cells were recorded growing at similar rates to unloaded controls. High loadings and repeated laser scanning (Fig. 40) both significantly reduced growth rates. In the case of slight “over-scanning”, the growth rate was able to recover to normal. “Over scanning” of unloaded cells, to the extent examined in Fig. 40, had very little effect on the growth rate of unloaded cells.

Table 4.3: Individual rhizoid cell viability after cSNARF-1 AM ester-loading and confocal imaging

Treatment	Average growth rate [†]	s.d.	n
Unloaded control (minimal imaging [‡])	13.8 $\mu\text{m/h}$	± 1.91	7
Unloaded control (standard imaging [#])	15.8 $\mu\text{m/h}$	± 2.01	4
Standard SNARF loading [§] (standard imaging [#])	14.9 $\mu\text{m/h}$	± 2.38	5
x60 (NA 1.40) oil immersion objective	8.0 $\mu\text{m/h}^*$	± 1.74	6

† - Average growth rate was calculated from time-series images taken at 15 - 20 min. intervals over the 1h period which corresponded to “the window of useful imaging time” for loaded individual cells, Section 4.5.2.

‡ - minimal imaging: Kalman n=2; ND = 3; F2; x40 objective; zoom 4.0 (See Chapter 2).

- Standard imaging: Kalman n=2; ND = 2; F1, (low signal enhance); x40 objective.; zoom 4.0 (See Chapter 2).

§ - Standard loading: cSNARF-1 AM was applied at 2 - 3 μM and cells incubated for 10 - 30 min. Loading was assessed by confocal imaging. Cells were considered to be sufficiently loaded when an image, taken with the standard imaging settings (above), had an average pixel intensity of 100 - 200 for areas corresponding to regions of cytoplasm (See Chapter 5, Figs. 49 and 50).

* - Values were calculated from single 5 - 10 min. time intervals (not averaged as described above in †). Imaging conditions were: Kalman n = 2; ND = 3; F1, (low signal enhance); x60 objective.; zoom 4.0. An unloaded cell imaged under such conditions gave a growth rate of 10.3 $\mu\text{m/h}$.

The time available did not permit viability to be systematically studied in this way with chlorocytes. The main problem encountered was the time required for growth responses (apical swelling and phototropic reorientation). The few cells which were examined demonstrated that continued development was possible under useful imaging conditions, although loading and imaging appeared to delay growth (see Fig. 37C).

4.5.4 Conclusions

External application of cSNARF-1 AM resulted in uptake and de-esterification within gametophyte cells. Dye was not restricted to the cell cytoplasm but probably entered organelles both directly, as the ester form, and by active cellular transport of the dye free-acid. Dye free-acid initially located in the cytoplasm was accumulated within the vacuole with time. Findings were similar for ester-loaded BCECF.

For rhizoid cells, loading and imaging conditions were achieved which allowed the capture of reasonable quality images (see Chapter 5) with minimal stress. However, dye loading levels which did not seriously affect cells were more difficult to determine for chlorocytes. The long term nature of chlorocyte response lead to difficulties in assessing viability during the useful imaging time. The best evidence that development proceeded normally during the useful imaging time (30 - 60 min. after loading) was the fact that rhizoids were able to continue growth under similar imaging conditions.

4.6 Loading pre-treatments

In an attempt to improve the efficiency of ester-loading (particularly for calcium dyes), different treatments of chlorocytes were tried before loading. On the basis that the waxy cuticle present on chlorocytes could interfere with loading (Kadota & Wada, 1989b; Wada & Staehelin, 1981), treatments were based on reducing its formation or removing it. A range of growth conditions designed to reduce cuticle formation were applied, without particular success (Table 4.4). Ease of accessibility of the wall to dye was assessed with Calcofluor (Kadota & Wada, 1989b). Rhizoids and damaged chlorocytes completely stained with Calcofluor without treatment, whereas, intact chlorocytes remained unstained except for the extreme apical wall region of apical chlorocytes. As apical chlorocytes and rhizoids took up AM esters better than the other cell types there does seem to be some correlation between Calcofluor staining and ease of loading.

4.6.1 Protoplasts

Several studies using dye technology have employed protoplasts of higher plant cells (Kiss *et al.*, 1991; Gilroy & Jones, 1992; Shacklock *et al.*, 1992; Messiaen *et al.*, 1993) taking advantage of their better loading properties. Protoplasts have been previously obtained from gametophyte cells (Kadota & Wada, 1989b; Huckaby *et al.*, 1982; Partanen *et al.*, 1980). The failure to obtain protoplasts from *D. affinis* protonemata in this study may have been due to the presence of the cuticle which prevented Calcofluor staining. Although protoplast formation was not thoroughly investigated it could prove to be a useful trick for facilitating pressure microinjection. Protoplasts could be pressure microinjected with dextran dyes then allowed to regenerate cell walls and re-polarise under imaging conditions.

Table 4.4: Loading pre treatments

Pre treatment	Observations with Calcofluor staining
Standard grown protonemata wetted with 0.002% (v/v) Tween-20	Slight, patchy staining of chlorocytes, particularly at the extreme apex. Rhizoid staining. Damaged chlorocytes stained completely.
Growth in standard liquid medium - without Tween-20	as above.
As above; but with 0.01-0.05% (v/v) Tween-20 used for wetting	Increasing Tween-20 concentration causes increasing degrees of "patchy" staining of chlorocytes.
As above but with 0.04% (v/v) Pluronic-127	As above.
As above, but with 0.005% (v/v) Tween-20 during growth	No difference from the standard growth and wetting treatment.
As above, but with 0.01% (v/v) Tween-20 during growth	As above.
Growth on agar-medium, then isolation to liquid medium (0.002% (v/v) Tween-20)	As above.
Protonemata grown fully submerged in liquid medium (no Tween-20)	No staining of chlorocytes at all.

4.7 Different fern species

Three different species of fern gametophyte were examined: *Dryopteris affinis*; *Pteridium aquilinum*; and *Adiantum capillus-veneris*. All three species showed general similarities in loading abilities.

4.8 Practical considerations for dye imaging

As part of the optimisation of the experimental system, the preparation of cells to allow imaging of dye on the CLSM was examined. The two most significant difficulties encountered were: 1) orientating and maintaining cells in position for imaging; and 2) overcoming cellular autofluorescence.

4.8.1 Focal plane maintenance

In order to examine intracellular [ion] within cells it was necessary to image particular focal planes within individual cells over time. Preparation and handling of cells were optimised to facilitate this (refer to Chapter 2). Firstly, culture conditions were designed to promote very straight, even cell growth making it easier to focus on a particular plane within a cell. Secondly, examination chambers were designed to reduce movement of individual cells (Chapter 2; Fig. 8).

4.8.2 Autofluorescence

Problems with autofluorescence were significant for chlorocytes as a result of chloroplast autofluorescence (Fig. 37B; Fricker & White, 1992). Chloroplast autofluorescence was even more severe with gametophytes exposed to white or blue light due to increased chloroplast size and number and their distribution all round the cell periphery. Rhizoids, which lack chloroplasts, had negligible autofluorescence. The autofluorescence of isolated chloroplasts was assessed with the two main excitation lines of the Argon-ion laser used for imaging (488 and 514 nm). The emission peaks at these excitation wavelengths were compared with the emission spectra of the dyes of interest (given in Haugland, 1992). This comparison revealed a general overlap of dye and autofluorescence emissions (in particular, in the ranges 460 - 570 nm and 680 - 780 nm) which could not be completely resolved by the use of selective emission filters. The problem of autofluorescence has previously been tackled at the image processing level by Vandelest *et al.*, (1995). Several different ways to overcome the problem of chloroplast autofluorescence were attempted:

- **Reduced photomultiplier sensitivity** to below the level for autofluorescence detection. This was possible but required toxic levels of dye loading to allow dye fluorescence to be imaged.
- **Mask out regions of autofluorescence** from images. Chloroplast autofluorescence for individuals could be imaged before loading (Fig. 37), however, due to focus shifts and chloroplast movements, the autofluorescence image could not be accurately subtracted from subsequent fluorescence images. Accumulating images until chloroplast autofluorescence reached saturating levels and then thresholding out the high signal was attempted. This method proved to be impractical due to "flare" from chloroplasts, exaggeration of wall autofluorescence and saturation of genuine signal.
- **Confine imaging to the extreme apical cytoplasm** of red grown chlorocyte apical cells (Fig. 37). This method was only applicable to *D. affinis*, red light-grown protonemata where the tip of the apical cell was usually free from chloroplasts. This proved to be the most practical method. Complications arose as a result of chloroplast redistribution during photomorphogenesis (see Chapter 3).

4.9 Discussion

4.9.1 Introduction of fluorescent probes into gametophyte cells

As expected, the introduction of fluorescent probes into gametophyte cells, as with other cell systems, was found to be a major limitation. Despite this, sufficient success was achieved, at least with cSNARF-1 in rhizoid cells, to merit continued study.

As a result of the failure to load calcium sensitive dyes by ionophoretic injection, acid-loading or ester-loading, successful microinjection will be essential for the long term future of fern gametophytes as a system for the investigation of calcium signalling by the application of dye based-imaging technology. Pressure injection represents the best option for further work in this as it opens up the possibility of using dextran dyes, which are reported to have better intracellular properties; in particular, retention in the cytoplasm (Gibbon & Kropf, 1994; Haugland, 1992; Miller *et al.*, 1992).

This would allow much longer "recovery" times between injection and experimentation (Gibbon & Kropf, 1994) and analysis over longer periods. The microinjection of germinating spores and examination of rhizoids after emergence, or microinjection of protoplasts and allowing regeneration, are possible alternatives to injecting gametophyte cells directly.

While not the ideal method for dye introduction, the ease of ester-loading and the large number of cells which may be loaded at one time have proved useful. With the aid of information from the examination of cell structure (Chapter 3), and the use of confocal microscopy the extent of non-cytoplasmic dye distribution with ester-loading has been examined. This has permitted better interpretation of related imaging artefacts (Chapter 5).

The restriction to the use of pH sensitive dyes directed the subsequent research described in this thesis to the examination of the role of pH in gametophyte cells.

4.9.2 Imaging of cSNARF-1

Cells are not completely uniform and different subcellular compartments may differ widely in their ionic contents for example the difference between cytosolic and vacuolar pH. Consequently, knowledge about intracellular distribution of dye - whether or not it has been taken up into organelles with potentially different intracellular ion contents - is an essential requirement for the proper interpretation of results when examining intracellular [ion] by fluorescence methods. Dye distribution into various different subcellular organelles was, therefore, the most significant limitation to the use of cSNARF-1 AM. Specifically, in fern gametophyte cells, ester-loading directly into organelles, such as ER-like structures and possibly mitochondria; and movement of dye free-acid from the cytoplasm to the vacuole were observed. Similar problems have been reported for other dyes, loading methods and cell types (Table 4.1). Further potential problems due to partitioning of dye into membranes is discussed in Chapter 5; Section 5.3.

In non-confocal imaging, where an average fluorescent signal is obtained from the cell, it must be assumed (or proven) that at least the predominant dye signal comes from cytoplasmic dye in order to make statements about cytoplasmic ionic composition (e.g. Gilroy & Jones, 1992) this was clearly not the case with fern gametophyte cells. The use of confocal imaging provides some degree of compensation for the non-specific dye distribution by allowing different dye containing to be identified and taken into account (see Fig. 41). Ratioing further improves the situation by giving a more direct indication of [ion] rather than simply fluorescence intensity (Bright *et al.*, 1987). cSNARF-1 is an emission ratioable dye which can be conveniently examined on the CLSM (Haugland, 1992).

4.9.3 Maintenance of the "normal" state

It should be recognised that imaging involves introducing foreign molecules into a cell and is, therefore, not as "non-invasive" as is often suggested. In addition to the dye itself: solvents added with the dye (DMSO, MeOH, EtOH); products from ester hydrolysis (aldehydes); dye breakdown products and free radicals (as a result of dye excitation), all contribute to cytotoxic effects (Moore *et al.*, 1990). The dye may also directly perturb the ionic composition of the cell acting as an ionic buffer (Thomas & Delaville, 1991) or through involvement in transport mechanisms (for example, vacuolar uptake). In general such problems only become significant at high loading levels - such levels must be determined for each cell type. No absolute measure of the intracellular dye content was made. "Quantification" of dye loading was purely in terms of image fluorescence under defined conditions; this cannot be related directly to *in vitro* dye concentrations due to the effect of "environmental conditions" on dye fluorescence intensity (described in Chapter 5).

The wavelengths of light used for imaging are also important. Certain excitation wavelengths, UV and blue in particular, may cause direct photodamage to cells or act to trigger cellular photoreceptors. This was a major consideration with fern chlorocytes, which are highly sensitive to light, but was probably less significant for rhizoids which were cultured entirely under white light illumination. The instantaneous consequences of laser irradiation were not rigorously examined but would certainly need to be investigated for chlorocyte cells if a study of apical growth in red light-grown protonemata was intended.

As far as possible loading and imaging conditions were reduced to levels at which adverse effects could be considered negligible. The data for the x60 oil immersion objective imaging (Table 4.3) appears to contradict this. However, growth rates were variable and only cells growing at rates of 8 $\mu\text{m}/\text{h}$ or better were used in the analysis of pH. The finding that intracellular dye concentration and dosage of excitation illumination gave the most detrimental effect when combined agreed well with the concept of phototoxic dye effects (Moore *et al.*, 1990). The observation that "over scanning" was better tolerated than "overloading" also fits this theory. cSNARF-1 was imaged with the 514 nm line of an argon-ion laser. This is expected to have fewer effects on the cell than 488 nm which may also be used.

4.9.4 Imaging strategy

The ideal imaging strategy would be to follow individual cells before, during, and after a response or treatment, collecting images at suitable time-intervals. Two major limitations to this were encountered: 1) dye redistribution with time; and 2) the slow rate of morphological expression of response with fern gametophyte cells.

There are two possible ways round the limitation of useful imaging time encountered with cSNARF-1 ester-loading. The first is to extend the useful imaging time. The most obvious solution would be to use pressure microinjected dextran dyes which prevent dye redistribution making long term

imaging a possibility. This was unfortunately limited by the difficulty in applying the pressure injection technique to fern cells. Useful imaging time could not be extended with the ester-loaded dyes, either by continuous loading or reloading at time intervals, because of the deleterious effects of excess dye on cells and saturation of vacuolar signal. A second alternative is to reduce the examination time to fit the available imaging time, this can be achieved in different ways. One possibility is to load and examine populations of individuals at different time points and compare these. The ease of ester-loading made this a practical possibility. However, this type of approach is open to many sources of artefact and error, originating from variation in both the cells and imaging techniques (see Chapter 5), making results difficult to interpret. A second solution would be to restrict examination time to immediately before and immediately after a stimulus and examine and compare these two states. This method is not greatly effective for transient changes or signalling events unless other information is available which can be used to narrow the time-period over which signalling events may be expected (discussed in Chapter 3). Another possibility is to examine only steady-state events, such as steady-state tip growth, and make the assumption that examination at a single time point is representative of that steady-state. This last approach was adopted as the most practical, considering the limitations of both the cell types examined and the techniques employed.

4.9.5 Conclusions

On the basis of the results obtained from examination of the gametophyte system (Chapter 3) and the investigation of dye loading and imaging methods (Chapter 4), the most productive line of further experimentation was judged to be the use of confocal ratio imaging of cSNARF-1 to investigate the role of pH in tip growth. This was in preference to persevering with pressure microinjection to allow the introduction of calcium-sensitive dyes.

Based, in particular, on the work of Gibbon and Kropf, (1994) on fucoid algae and on the work of Racusen *et al.* (1988) in ferns, it is possible that a steady apical cytoplasmic gradient in pH is maintained during steady-state tip growth. Contradictory studies also exist claiming the absence of a pH gradient during tip growth, most notably Herrmann & Felle (1995) in root hairs. It was, therefore, decided to examine this in tip-growing fern gametophyte cells. Rhizoids in particular, presented the opportunity to study steady-state tip growth.

The combination of confocal microscopy and ratio analysis, possible with cSNARF-1 imaging, allows the problems of dye distribution within different organelles, inherent in the ester-loading of cSNARF-1, to be taken into account, therefore, allowing a more convincing analysis of cytoplasmic pH.

Chapter 5

CONFOCAL RATIO-IMAGING OF cSNARF-1: ASSESSMENT OF THE IMAGING METHOD.

5.1 Introduction

In general, the aim of imaging intracellular ion-sensitive dyes is to produce quantitative data about intracellular [ion] and the distribution of ions throughout the cell. Under these circumstances the confocal microscope may be considered to be simply a photon counter with high spatial resolution and the images as arrays of numerical data (Pawley, 1995; Fricker *et al.*, 1994; Kurtz & Emmons, 1993). Subsequent extraction of meaningful numerical data from images is the critical part of image analysis. The quality of captured images directly determines the quality of the data which can be extracted. However, images need to be interpreted carefully; one must be constantly aware of the many artefacts which can corrupt the integrity of image data if not properly taken into account (Oparka & Read, 1994; Fricker *et al.*, 1994; Read *et al.*, 1992; McCormack & Cobbold, 1991; Moore *et al.*, 1990).

The aim of the work described here was to address the problems and artefacts encountered in the ratiometric determination of cytoplasmic pH in gametophyte rhizoids using cSNARF-1. An *in vitro* experimental test system was used to assess imaging procedures. The test system consisted of 25 - 50 μ l volumes of buffer solution at defined pH containing cSNARF-1 free-acid. Dye imaging *in vivo* was also analysed in order to allow *in vitro* findings to be related to the physiological situation and additionally to assess artefacts-specific to imaging biological material.

An understanding of these problems was found to be essential for the correct analysis and interpretation of ratio images and, further, revealed the limitations of the technique and allowed optimisation of imaging procedures.

5.2 Limitations of the dye

Dye limitations may be split into three groups: the physical and chemical properties of the dye; changes in dye performance in the intracellular environment; and the effects of dye on cells. A range of modern dyes are available with properties to suit most physiological applications (Kurtz & Emmons, 1993; Haugland, 1992). Matching the properties of the dye to the experimental situation is largely a matter of selection. It is, therefore, the latter two problems which are of most concern. Characterisation of dye behaviour is complicated as the nature of the intracellular environment is varied between cell types and not fully understood and its effects on dyes are often complex.

Table 5.1: Physical and chemical properties of cSNARF-1

Property	Significance	cSNARF-1	References
Kd	Determines the [ion] range detected.	pKa* 7.5 - 8.15	Haugland, 1992 Owen <i>et al.</i> , 1992 Opitz <i>et al.</i> , 1994
Temperature sensitivity	pKa changes	Slight increase with decreased temperature (25-37 °C).	Opitz <i>et al.</i> , 1994
Ion selectivity	The concentration of ionic species (for example in vitro) can influence dye response	Highly selective for protons.	Seksek <i>et al.</i> , 1991
Spectral properties: excitation/emission	Consequences for: imaging techniques; cell health and behaviour; optical imaging artefacts.	Dual emission ratioable dye. Alternatively: single wavelength or dual excitation ratioable.	Haugland, 1992
Kinetics of photon emission; absorption; saturation; quantum yield.	Determines effective dye brightness and hence the concentration of dye required.	Base form has higher quantum yield/lower absorbance than the acid form. Comparable signal brightness from both forms	Haugland, 1992
Photobleaching / photodamage.	Phototoxic effects. Loss of signal. Appearance of ion insensitive fluorescent species.	Resistant to photobleaching.	(current observation)
Hydrophobicity.	Membrane partitioning. Precipitation. Loading into and retention within cells.	Hydrophobic at low pH (< 6.0).	Opitz <i>et al.</i> , 1994 Levina <i>et al.</i> , 1995

* The K_a (or pK_a) of cSNARF-1 is influenced by environmental conditions. Additionally, the apparent K_a may be influenced by the method used to examine the fluorescence if only part of the emission spectrum is monitored. A shift in the spectral properties of the dye can result in the observed (or apparent) K_a being changed while the true K_a is unaffected.

5.2.1 Physical and chemical properties of cSNARF-1

The key properties for cSNARF-1 dye are listed above in Table 5.1. The emission spectrum of cSNARF-1 free-acid (excitation at 514 nm) is given in Chapter 1; Fig. 4.

5.2.2 The dynamic range of cSNARF-1

The useful range of cSNARF-1 response is dependent upon the K_d ; the intensity of fluorescence emissions of the acid and base forms; the pH range over which the dye is properly responsive; and the method of examining the dye - in this case the Bio-Rad MRC-600 CLSM. Molecular Probes claim a useful pH range of 6.3 - 8.6 for cSNARF dyes (Haugland, 1992). The results of examination of the

response of cSNARF-1 free-acid on the CLSM over the pH range 4 - 9 is given in Fig. 42. This showed that below pH 5.5 (with either citrate or MES/HEPES buffer, or pH 6.5 with Bis-TRIS-propane buffer) precipitation occurred and the dye was no longer properly responsive. At above pH 8.5 the fluorescence of the acid form (Ch-2) was too low to record accurately without saturating fluorescence detection for the alkali form (Ch-1). Approximately linear response was found over the pH range 6.5 - 7.5, roughly in agreement with Opitz *et al.* (1994). This conveniently corresponds to the expected pH range of cytoplasm (Guern *et al.*, 1991). In order to achieve the best dynamic range the Ch-2/Ch-1 ratio was generally set to about 1 for pH 7.0 (Chapter 2; Table 2.5), with pH 6.5 - 7.5 falling within the ratio range 0.25 - 2.25 and pH 6.0 - 8.0 within the range 0 - 3.75. The precipitation of cSNARF-1 at low pH makes the determination of the saturation ratio value (Rmax) impossible. This prevents the calculation of [ion] directly from fluorescence ratio measurements using the formula

$$[\text{ion}] = K_d \cdot (R - R_{\text{min}}) / (R_{\text{max}} - R) \cdot F_{\text{free}} / F_{\text{bound}}$$

(K_d = dissociation constant; R_{max} = fluorescence ratio at saturating [ion]; R_{min} = fluorescence ratio at minimal [ion]; F_{free} = the fluorescence of total dye in the unbound form; F_{bound} = the fluorescence of total dye in the ion bound form; R = the ratio of fluorescence at the two wavelengths at the unknown [ion] - Moore *et al.* (1990).)

The “missing” value of R_{max} may be estimated from extrapolation of calibration data, however, because the relationship between ratio value and pH was approximately linear over the pH range of interest this linear relationship was used to determine pH values from ratio data.

5.3 Changes in cSNARF-1 performance due to environmental conditions

It is now well established that the behaviour of fluorescent dyes is affected by their environment. The most important factors are [ion], hydrophobicity and viscosity (Fricker *et al.*, 1994; Busa, 1992; Moore *et al.*, 1990). Several studies have been performed on cSNARF-1 behaviour by *in vitro* and *in vivo* analysis (Opitz *et al.*, 1994; Blank *et al.*, 1992; Owen *et al.*, 1992; Seksek *et al.*, 1991; Buckler, 1990; 1991; Bassnett, 1990). There is general agreement that cSNARF-1 is influenced to some extent by the intracellular environment, either through direct effect on the K_d or apparent change in K_d through changes in spectral properties. There is less agreement over what the specific cause of the effect is. Suggestions include binding of intracellular components to dye free-acid (Owen *et al.*, 1992; Seksek *et al.*, 1991) and hydrophobic partitioning of the uncharged dye-form into membranes (Opitz *et al.*, 1994).

A complete analysis of cSNARF-1 behaviour was beyond the scope of the current research project. However, a general indication of the possible effect of environmental conditions on the dye, as imaged on the CLSM, was obtained using the “pseudocytosol” buffer solution (Fig. 43) described in Fricker *et al.* (1994). “Pseudocytosol” contained 25% (v/v) ethanol, 60% (w/v) sucrose, MES/HEPES

buffers and a mixture of salts, it was composed on the basis of current knowledge of the composition of cytoplasm. Subsequent tests on components of the “pseudocytosol” identified ethanol and sucrose as the most important influences on cSNARF-1 behaviour, in agreement with Seksek *et al.*, (1991). Ethanol (Fig. 44A.) at concentrations from 10 - 60% (v/v) shifted ratio values towards increasingly lower apparent pH (relative to MES/HEPES buffer alone). The effect was more pronounced with increasing pH (over the range 6 - 8). Increasing ethanol concentration increased fluorescence intensity in both channels with Ch-2 (640 nm) showing greater relative increase than Ch-1 (580 nm). The Ch-2 fluorescence showed a greater than three-fold increase with 60% (v/v) ethanol. Sucrose (Fig. 44B) also had concentration dependent effects. 20 - 60% sucrose (w/v) caused a slight shift in ratio to more alkaline values (relative to MES/HEPES buffer alone). Fluorescence signal intensity was increased by roughly 30% for both emission channels. Ethanol and sucrose were used in the “pseudocytosol” calibration buffer to mimic the hydrophobicity and viscosity of the cytoplasmic environment, respectively (Fricker *et al.*, 1994).

5.4 Intracellular dye response and calibration

The relationship between ratio values from images and actual pH in the *in vitro* test system is shown in Fig. 42. However, from the preceding section it is obvious that such calibrations are prone to misinterpretation when related to the physiological imaging situation (Opitz *et al.*, 1994; Owen *et al.*, 1992; Seksek *et al.*, 1991). *In situ* calibration, by “clamping” intracellular pH at specific values, is a way of bridging some of the differences between *in vitro* and *in vivo* imaging. The difficulty with cSNARF-1 was that, unlike other ratio dyes (e.g. Moore *et al.* (1990)), calibration could not be performed using the equation given in Section 5.2.2. An attempt was, therefore, made to “clamp” the internal pH of cells over the linear range of pH values (pH 6.5 - 7.5 on the basis of *in vitro* calibration) and produce an *in situ* calibration curve relating ratio value to pH.

5.4.1 Ionophore and protonophore methods

A range of ionophore-based *in situ* methods was employed in an attempt to equilibrate intracellular pH with a defined external pH: nigericin (Gehring *et al.*, 1994); nigericin/valinomycin (Seksek *et al.*, 1991); Gramicidin (O’Brodivich *et al.*, 1993); amphotericine (Jelitto, 1995); and DNP (Gibbon & Kropf, 1991; Harold, 1986). In every case significant cellular disruption and loss of fluorescence occurred. Where a change in intracellular pH was achieved it was found to be unstable, non-uniform within the population and not properly reproducible. It is possible that ionophores failed to pass the cell wall effectively - a theory which could be tested by using protoplasts.

5.4.2 Weak acid / weak base calibration methods

Weak acids and bases have been commonly used to manipulate intracellular pH (Gibbon & Kropf, 1994; Kurkdjian & Guern, 1989; Sanders & Slayman, 1982). As a method of calibration, cell

permeant weak acids and bases (propionate, ammonia and trimethylamine) proved more successful in rapidly and reproducibly altering intracellular pH than ionophore methods (see Chapter 2; Section 2.8.2 for the calibration procedures).

Results for intracellular pH “clamping” treatments are summarised in Table 5.2 and a single typical calibration data set is plotted in Fig. 45. Whilst “clamping” treatments were able to adjust intracellular pH, several observations suggested that interpretation of the data was not a simple matter.

A primary difficulty was that the cSNARF-1 ratio was not altered to a stable value, although the initial adjustment ratio and subsequent drift were remarkably consistent for repeat experiments. Change in ratio value over time was likely to be a combined effect of change in actual pH and the effects of deteriorating image quality directly upon ratio value and upon the ability to accurately sample images.

“Clamping” treatments altered ratio values for dye in the cytoplasm, vacuoles and nuclei. With pH 6.0 and 8.0 “clamping” treatments ratios from these different compartments were very similar. Closer to pH 7.0 the vacuole in particular gave slightly higher (apparently more acidic) values than the cytoplasm (Fig. 45). “Clamping” data suggested that there was no significant optical distortions of apparent pH (ratio value) across median optical sections beyond that observed at the extreme periphery ($< 1\mu\text{m}$). The low signal level in vacuoles may have contributed to observed differences in ratio between vacuoles and cytoplasm but different levels of accumulation of the “clamping” agents and different adjustment of pH were also likely factors.

In all cases growth was inhibited at the time of internal pH adjustment and some structural deterioration was observed. Even so, cells were found to be able to survive the “clamping” treatments at pH 6.0 (propionate) and pH 8.0 (NH_3) if returned to normal medium within 15 min. of “clamping” buffer application.

In situ adjustment of ratio value differed from the ratios obtained from *in vitro* calibrations with both simple MES/HEPES buffer and the *in situ* “clamping” buffers. However, because a stable intracellular pH clamp was not achieved, it was not possible to state whether this was due to an effect of the intracellular environment on the pH response of cSNARF-1 or because intracellular pH was never adjusted to the desired value. The apparent over-acidification of cells with propionate buffer at pH 7.0 and over alkalinisation with both ammonia at pH 7.0 and trimethylamine at pH 7.5 (Fig. 45), were consistent with reports of specific (rather than diffusion dependent) accumulation of these compounds (see Guern *et al.*, 1991). Comparison of the calibrations with simple MES/HEPES and “clamping” buffers revealed that, although the ammonium chloride buffer had negligible effects, propionate and trimethylamine both had slight but consistent effects on ratio values (Fig. 44C and D).

5.5 Discussion: The pH response of cSNARF-1 - assessment of the calibration data

Results from *in vitro* calibrations demonstrated that although cSNARF-1 was suitable for examining pH over the physiological range its response could be altered by environmental conditions likely to occur in the intracellular environment. Both the values of ratios and the slope of calibration curves was found to be dependent upon the environment (hydrophobicity and viscosity). This has serious implications for the validity of both absolute pH determination and, more importantly, measurements of changes or differences in pH *in vivo* based on the simple *in vitro* calibration. The fact that the gradient of the cSNARF-1 response to pH could be altered makes the need for a reliable *in situ* calibration more critical if statements are to be made about shallow (< 0.5 pH unit) intracellular pH gradients.

Table 5.2: Summary of the weak acid/weak base *in situ* calibration results*

Buffer	pH	Effect on ratios (apparent pH) [†]	Effect on cells [‡]
sodium propionate	6.0	Alteration in ratios relatively stable and consistent. Ratio value lower than <i>in vitro</i> - even	Very severe disruption.
	6.5	taking into account direct effects of propionate on cSNARF-1 <i>in vitro</i> . Vacuolar and cytoplasmic ratio values very similar.	Cytoplasm dispersed; multiple vacuoles.
	7.0	Alteration in ratios consistent but unstable; drifts to lower values. Ratio values considerably higher than <i>in vitro</i> . Vacuoles still appear more acidic than the cytoplasm.	Little disruption.
trimethylamine	7.5	Ratios very stable and consistent but significantly lower than <i>in vitro</i> - even taking into account direct effects of trimethylamine on cSNARF-1 <i>in vitro</i> . Ratios from cytoplasmic and vacuolar regions indistinguishable.	Cytoplasmic redistribution; large apical vacuoles form.
ammonium chloride	7.0	Ratios consistently very significantly lower than <i>in vitro</i> and very unstable - rapidly increase (apparent decrease in pH _c). Vacuoles still appear more acidic than the cytoplasm.	Little disruption.
	8.0	Variable results, both higher and lower than <i>in vitro</i> . Rapid deterioration in image quality. Ratios very unstable - drift to higher values. Vacuoles indistinguishable from cytoplasmic regions.	Severe disruption; tip evacuation.

* The summary is based on six independent repeat experiments.

† “Expected” ratio values were based on the results of *in vitro* calibration using the appropriate “clamping” buffers (to take account of direct effects on the dye) and simple MES/HEPES *in vitro* calibration.

‡ All treatments immediately arrested growth and no further growth was seen over the duration of experiments (15 - 20 min.).

Previous studies have found differences between *in vitro* and *in situ* calibrations which could not be reproduced by addition of ethanol or proteins or lipids to *in vitro* calibrations. However, confocal imaging was not used and generally cells in cuvettes were analysed using a spectrophotometer. In these studies the effects of optical effects and dye localisation were not fully taken into account. Different studies also failed to completely agree. Although this and the current work raises the question of the suitability of cSNARF-1 as an intracellular pH reporter it does not provide sufficient justification to completely abandon its use until a better reporter becomes available. cSNARF-1 dextran conjugate was found to show similar effects with “pseudocytosol” buffer as cSNARF-1 free-acid (Parton *et al.*, 1996). BCECF was not favoured because it is a dual excitation ratioable dye and could not be used as such with the available CLSM.

Attempts at *in situ* calibration were disappointing. The implication of the results summarised in Table 5.2 is that pH was never effectively clamped by weak acid and base treatments, especially around pH 7.0. The relationship between pH and ratio value, therefore, remains ambiguous. The fact that gametophyte cells could survive “clamping” treatments over the period that data was collected could also be taken to suggest that “clamping” was incomplete. Before giving up the use of weak acids and bases as a means of *in situ* calibration it would be worthwhile exploring further compounds, for example imidazole, procaine and isobutyrate, with more suitable pKa values and better properties with respect to cells. “Clamping” treatments might also be coupled with inhibitors to disable transport and metabolic activities and render the cell more open to pH adjustment. Ultimately *in situ* calibration may require a combination of intracellular pH microelectrode and imaging techniques, either simultaneously or under strictly comparative conditions.

Whilst the *in vitro* calibration does not allow convincing determination of absolute pH values, it does provide an important basis of comparison for *in vivo* data and could be used to relate data to an improved *in situ* calibration at a future time. Simple *in vitro* calibration was performed routinely at the end of each imaging session.

5.6 Quantitative analysis of images

In order to obtain useful quantitative results from imaging intracellular pH sensitive dyes it was important that both the precision of measurement and the spatial resolution limits imposed by the imaging technique were determined. This necessitated statistical analysis of the pixel intensity values obtained from images.

On the basis of the current information on intracellular pH, discussed in Chapter 1, the requirements for useful pH_i determination are a precision of not less than to the nearest 0.1 pH unit and spatial resolution of pH determination of the order of 1 μm². In the work here precision of pH measurement and spatial resolution were examined and optimised, within practical limits, for physiological imaging.

5.6.1 Inherent pixel variation in fluorescence images

Inherent in the process of photon detection and image digitisation is a significant amount of "instrumental" variation and error which imposes fundamental limits on the information which may be obtained from images. An examination of the individual sources of variation and error was not appropriate here; the overall variation in images was of most concern. The main factors contributing to variation are discussed in greater detail elsewhere (Pawley, 1995; Sheppard *et al.*, 1992; Moore *et al.*, 1990).

Examination of test situations *in vitro* with even fields of dye free-acid in strong buffer solutions (25 mM MES/HEPES) revealed the extent of "inherent noise" in fluorescence images (Fig. 46A and Chapter 2; Fig. 17). The fluorescence images collected had a roughly symmetrical - approximately Normal distribution (Fig. 46A). Although a Poisson distribution is expected for photon counting (Pawley, 1995) the distribution approaches Normal for large mean values (Moore *et al.*, 1990). Comparison of direct scanned and Kalman averaged (cumulative filtered) images demonstrated how the random "shot noise" of photon detection could be significantly reduced by averaging the photon detection over time. Kalman averaging 4 x 1.5 s scans (six seconds) significantly reduced the variance of the pixel value distribution as shown in Fig. 46.

5.6.2 Ratioing and image processing errors

The inherent pixel variation in fluorescent images is compounded by the processing steps used to produce a ratio image i.e. the subtraction and division of images. The differences between the distribution of pixel values in fluorescence images and in the corresponding ratio images can be seen in Fig. 46A, B and C. (In Fig. 46B and C the ratio values 0 - 2.5 were scaled to fit 0 - 255 grey levels for display as ratio images.) Pixel variation within ratio images falls into a less even, skewed distribution (compare Fig. 46 A and B). The effect of a median 3x3 filter on ratio pixel value distributions is also shown in Fig. 46B and C; median filtering reduces the degree of skew relative to unfiltered ratios making the distribution approach Normal once more.

The effects of the noise level (signal to noise ratio) in fluorescence images upon the resultant ratio images was examined by testing the effects of different average fluorescence pixel values and of Kalman filtering (cumulative averaging). Clearly, as shown by the effect of Kalman averaging during fluorescence image capture on the ratio in Fig. 46 and the results in Table 5.3, reducing variation in the fluorescence images reduced variation in the ratio image. In Fig. 47 average ratio was plotted against fluorescence image pixel value. In addition to the expected increase in ratio pixel variation with decreasing fluorescence signal, the findings also revealed that average ratio values were also shifted. It was further found that this shift in the mean ratio pixel value observed with low fluorescence pixel values could be corrected by Kalman averaging between 5 and 20 times to improve the "signal to noise ratio" and also by accumulating images or shifting to a higher laser excitation. This proved that the shift in mean ratio pixel value was dependent upon the signal to noise ratio rather

than a property of the dye. The effects of “low signal” were different at different pH values, appearing to be worse at $\text{pH} < 7.0$. This may be due to the higher fluorescence pixel variation from channel 2 (Fig. 46).

The shift in mean ratio pixel value to higher values is only observed when ratio images are sampled directly and does not occur when the ratio is calculated by dividing mean fluorescence intensity values ($\text{Fluorescence mean-2}/\text{Fluorescence mean-1}$) even with very low signal (Table 5.3). When the ratio image is sampled directly the calculated mean ratio value is influenced by the degree to which the ratio pixel distribution is skewed. As the fluorescence image signal to noise ratio decreases then the mean ratio value determined directly from the ratio image shifts to increased values while $F_{\text{mean2}}/F_{\text{mean1}}$ is not altered, although the distribution of mean values determined from sample populations of pixels becomes more noisy. This suggests that ratio values should be determined from division of $\text{Fluorescence mean-2}/\text{Fluorescence mean-1}$ and not by directly sampling from ratio images. This is discussed further in Section 5.6.3.

Table 5.3: Comparison of mean ratio values determined from mean fluorescence intensities and directly from ratio images

Fluorescence image sampling				Ratio image sampling			
Fluo-1 [†] ± s.e.m	Fluo-2 [†] ± s.e.m	Ratio ‡ F2/F1		Ratio image (no median)	± approx. s.e.m*	Ratio image (+ median)	± approx. s.e.m*
Direct image collection - whole image sampled §							
pH 6.5	114.00	152.67	136.58	139.34	\	136.39	\
pH 7.0	130.87	131.80	102.71	104.38	\	102.24	\
pH 7.5	174.10	104.41	61.20	61.62	\	60.47	\
Direct image collection, (low signal: average < 50) - whole image sampled §							
pH 6.5	29.02	39.14	137.60	144.93	\	138.80	\
pH 7.0	36.14	35.62	100.57	108.34	\	100.52	\
pH 7.5	45.15	26.67	60.28	64.18	\	59.39	\
Kalman (n = 3) image collection, (low signal: average < 50) - whole image sampled §							
pH 6.5	28.74	38.04	135.05	139.19	\	135.22	\
pH 7.0	37.79	35.79	96.39	104.63	\	101.75	\
pH 7.5	45.07	26.78	60.59	61.49	\	60.04	\
Direct image collection - 14x14 pixel area sampled							
pH 6.5	114.11 ± 0.83	156.28 ± 1.65	139.69	142.05	± 2.56	141.20	± 0.95
pH 7.0	131.23 ± 1.43	131.80 ± 1.91	102.37	104.58	± 2.02	101.87	± 1.13
pH 7.5	172.90 ± 1.49	105.92 ± 1.80	62.49	62.79	± 1.17	61.65	± 0.44
Kalman n = 3 image collection - 14x14 pixel area sampled							
pH 6.5	109.81 ± 0.81	144.89 ± 1.25	134.58	135.69	± 1.63	132.39	± 0.65
pH 7.0	132.85 ± 0.76	132.28 ± 1.17	101.56	101.46	± 0.77	101.97	± 0.40
pH 7.5	171.49 ± 0.94	102.31 ± 0.95	60.85	60.70	± 0.69	59.64	± 0.28

† s.e.m values were calculated for variation in the mean fluorescence value for 14x14 pixel sample areas.

‡ The ratio of fluorescence values has been re-scaled as ratio image pixel values (ratio values 0 - 2.5 correspond to ratio pixel intensities of 0 - 255) to allow comparison with the ratio values extracted directly from ratio images.

* approximate s.e.m values are given for ratio values on the assumption that the distribution of ratio pixel values approaches Normal - this is more likely with the median filtered images as discussed in Sections 5.6.2 and 5.6.3.

§ The values quoted correspond to population means so s.e.m. values are not appropriate.

5.6.3 Methods of analysis of image variation

Although reduction of variation in fluorescence images at the level of image capture is the best way of dealing with “noise” it ultimately has its limitations. Dealing with variation may then be taken further by the use of sampling methods and statistical analysis. Determination of the variance in the pixel value distribution allows calculation of the certainty with which an individual pixel reports the mean value for the population. By applying the Central Limit Theorem and determining the standard error (s.e.m) this can be extended to the certainty with which a sample mean value reports the mean value for the population. These statistical methods can be applied to the approximately Normally distributed fluorescence value distributions in *in vitro* test images, however, they are a poorer measure of dispersion for the skewed distributions of the ratio images.

Performing statistical analysis on the approximately Normally distributed fluorescence image variation and attempting to relate this to variation in the subsequent ratio image holds considerable attraction, however, this is not a trivial problem (personal communication Professor Tom Leonard - Department of Statistics, University of Edinburgh, JCMB) as simple statistical procedures for combining two distributions do not apply. At the present time no rigorous statistical analysis of ratio images could be found in the literature dealing with imaging methods

The correct statistical approach would be to model the probability density function for the mean ratio according to values derived from the fluorescence image distributions and taking into account the possibility of correlation between corresponding pairs of data in channel 1 and channel 2 images (product moment correlation coefficient). This approach is very complex and, although the subject of continuing research in collaboration with Prof. Tom Leonard and Dr. Bruce Worton (Department of Statistics, University of Edinburgh, JCMB), could not be applied to the data described in this thesis.

A more simplistic approach was adopted with the aim of producing a workable means of dealing with inherent noise in images; a similar approach has been described by Bright *et al.*, (1987). Basically, ratio images were examined directly and analysis of the variation in ratio values was confined to that of pixels within ratio images. Direct analysis of ratio images could be justified on the following basis:

- 1) As shown by the data in Table 5.3, the mean ratio values determined directly from median 3x3 filtered ratio images was roughly equivalent to that calculated from fluorescence intensity mean values for channel 1 and channel 2. The noise dependent shift in mean ratio value (noted in Section 5.6.2) is effectively overcome.
- 2) With Kalman filtering of the fluorescence image and 3x3 median filtering after ratioing the ratio image showed a much less skewed pixel frequency distribution (Fig. 46). On the basis that the distribution of pixel values in these ratio images could then be assumed to approach Normal then standard statistical methods were used and “approximate s.e.m” values calculated as a measure of the accuracy with which the mean ratio value may be determined by sampling.

- 3) By working on ratio images, in which pixels values from the fluorescence image pair were divided on a pixel by pixel basis, the possibility of any spatial correlation in the values of fluorescence image pixel pairs was automatically taken into account.
- 4) In addition to avoiding the use of complicated statistical methods sampling of a single ratio image was easier, especially when using non-uniform sample areas, than sampling corresponding regions in a fluorescence image pair.
- 5) On the basis of s.e.m values determined from variation in ratio pixel values the optimum sample area size (number of pixels sampled) which produced a reliable estimate of the true ratio value (i.e. the average value for the whole image) could be determined. The values of the approximate s.e.m determined from sampling a single area ($s.e.m = s.d. / \sqrt{n}$) corresponded well with the values of approximate s.e.m determined from the deviation in the mean of ratio pixel values of 10 independent sample areas (n pixels each).

The validity of the assumption of an approximately Normal distribution for pixel values in a ratio image was strongly dependent upon the use of defined imaging conditions. The signal to noise ratio in fluorescence images was found to influence the degree of skew in the ratio value distribution of the corresponding ratio image. The signal to noise ratio of fluorescence images was, therefore, kept high by image collection at high average fluorescence intensity. Based upon the *in vitro* test system, “low signal” problems were seen to occur below average fluorescence values of 50 - 75 (Fig. 47); this was taken as the minimum acceptable signal. Kalman filtering was used to further increase the signal to noise ratio of fluorescence images. Standardisation of image collection, such that the average fluorescence pixel intensity of images was always similar, could only be taken so far - at different pH values the fluorescence intensity of the two channels necessarily differed. Variation in ratio, therefore, was itself pH dependent and had to be assessed for different pH values over the pH range of interest. Between pH 6.9 - 7.3 the intensity of both channels could be kept above 50 - 75.

Median filtering of ratio images was used to reduce pixel variation and “correct” for the skewedness in the ratio pixel value distribution. As images were significantly over-sampled (pixel size relative to optical resolution - see Table 5.2 and Section 5.6.2) the 3 x 3 pixel filter used had little effect on genuine spatial resolution.

5.6.4 Estimation of precision and spatial resolution for pH measurement

As described in the previous section, approximate s.e.m. values determined for variation between pixels of ratio images were used to estimate the precision of pH determination in the simple *in vitro* test situation.. The s.e.m values were determined from the deviation in the mean values for multiple small (n = 9 - 196) sample areas (N = 10). Sampling of ratio images was compared over a range of pH values (0.02 pH unit steps over 6.9 - 7.3); the results are shown as graphs in Fig. 48. Double the

approximate s.e.m. (the 95% confidence interval) was used as a measure of the certainty of pH determination i.e. the precision of pH measurement (Table 5.4).

The spatial resolution with which pH could be determined was found to be limited by the area of pixels which had to be sampled to provide a reasonable degree of precision rather than the optical limitations of the imaging system. The relationship between sample area size and precision of pH measurement was examined by taking different sized areas of pixels ($n \times n$ pixels) and comparing the approximate s.e.m, determined from 10 independent sample areas in each case (Fig. 48 and Table 5.4).

Table 5.4: Spatial resolution and precision of pH measurement for cSNARF-1 ratio imaging

Objective	Zoom	Pixel size (μm)	Optical resolution		Sample area		Precision of pH measurement*
			Axial	lateral [‡]	pixels	μm^\dagger	
x40, NA 0.95	3	0.146	1.3 μm	0.55 μm	14x14	1.16x1.16	$\pm 0.02 - 0.06$
	4	0.109	"	"	7x7	0.58x0.58	$\pm 0.04 - 0.10$
x60, NA 1.40	3.5	0.083	0.8 μm	0.4 μm	3x3	0.25x0.25	$\pm 0.07 - 0.17$

‡ Optical resolution was estimated as the FWHM (described in Chapter 2; Section 2.6.3).

† Area calculated for the x60 objective, zoom 3.5.

* precision was estimated on the basis of 2 s.e.m. (determined from the deviation of sample area means). The range in precision is given from the least error bar to the worst, over the range pH 6.9-7.3 (see Fig. 48).

5.7 Application of analysis methods to physiological imaging

The *in vitro* imaging test system represented the "ideal" situation. This entailed caution in attempting to apply the findings of this system to the more complex ratio images of cells. In order to improve the validity of the analysis method both image quality and the methods of sampling images were carefully considered. Image size was increased i.e. pixel size reduced (Table 5.4) to maximise the number of pixels for a given area of the imaged cell. Care was taken at the fluorescence image collection level to ensure physiological image quality was within the limits defined on the basis of the test system. Only images of suitably high average fluorescence signal intensity (>50) were analysed. Despite this, physiological images exhibited a greater range in signal intensity as a result of both uneven dye distribution and regions of varying pH (or apparent pH) distributed irregularly throughout the image (Fig. 49). A further problem was the contribution of zero value pixels to physiological ratio images. Randomly scattered zero pixels in areas of low fluorescence signal and zero pixels at cell boundaries were not discriminated against by the median filtering applied. (Optical problems are dealt with later.) These problems had to be dealt with by the sampling method.

5.7.1 Extraction of numerical data

Several different image sampling procedures were evaluated, some of which are shown in Fig. 50. The aim of the different sampling methods was to provide an estimation of cytoplasmic pH, within the limits of precision and spatial resolution defined on the basis of the *in vitro* test system, but from ratio images of cells. The main difficulties which had to be overcome were: vacuolar contribution; artefactual ratio values (for example at the cell periphery); and operator bias when sampling.

“Boxed sample areas” were applied exactly as with the imaging test system using simple COMOS commands (Fig. 50B). The problem with this method was in positioning areas within an image. A variation of this, “free-drawn areas”, was more versatile and better for avoiding undesirable areas, although more laborious to apply. This method was most commonly used in experimental data extraction.

“Averaged line sampling” was based on the MPL length command (Fig. 50C). Fig. 51A and B provide examples of its use. The major restriction of this method was the difficulty in avoiding undesirable sample areas. It was found to be useful when examining the peripheral cytoplasm (Fig. 50D). Although the MPL command only allowed averaging of n pixels across each pixel of the line the data could be imported into Microsoft Excel (version 7.0) and further averaging along the line performed to obtain the required $n \times n$ sample area (Chapter 6; Fig. 58A and B).

“Thresholding” and “masking procedures” for discriminating against artefacts such as low signal, vacuolar signal and edge effects were employed in an attempt to aid in the placing of sample areas (Figs. 50E and 52). These procedures relied on the selection of regions of high fluorescence signal which generally corresponded to the cytoplasm, at least in the period immediately after loading. “Masking by eye” was favoured in the general analysis of pH performed in Chapter 6. In this procedure areas of high average “cytoplasmic” signal in a combined wavelength fluorescence image were traced onto a transparency then overlaid onto the corresponding ratio image and “free-drawn” sample areas placed according to the tracing. Thresholded images, where low signal and vacuolar signal had been eliminated, could be sampled with a single box to produce an overall average “cytoplasmic” ratio value (Fig. 50E). Such systematic numerical thresholding or masking procedures were not routinely applied to physiological images but would be worth further investigation as a means of simplifying data sampling.

Sampling images of ester-loaded fern rhizoids was particularly difficult. For comparison, an image of a *Neurospora* hypha microinjected with cSNARF-dextran and imaged in the same way as a *Dryopteris* rhizoid is shown in Fig. 53. The apical region of hyphae is highly cytoplasmic (Grove, 1978) and dextran-dyes are excluded from organelles (Miller *et al.*, 1992). In such cases procedures for cytoplasmic pH sampling may be considerably simplified.

5.7.2 Precision of pH measurement and spatial resolution

Estimation of precision of pH measurement and spatial resolution in physiological images was made on the basis of the findings with the *in vitro* test system. The validity of this rests on three key assumptions:

- 1) Image quality in physiological images was comparable to that of the “ideal” test images.
- 2) The relationship between ratio values and pH was the same *in vitro* and *in vivo*.
- 3) Applied sample areas were sufficiently small that, effectively, an even field of pH was sampled.

Attempts to satisfy the first assumption by comparable, systematic fluorescence image capture procedures and by careful ratio image sampling procedures were described in Sections 5.6 and 5.6.1. The second assumption relates to the earlier problem of dye-response *in vitro* and the *in situ* calibration. The method of estimating precision and resolution was strongly dependent upon the linearity and gradient of the relationship between pH and ratio (see Fig. 48). The data obtained on *in vivo* dye response (Section 5.4) was inconclusive, therefore, this assumption stands untested. With respect to the third assumption, the limit of optical resolution was not much better than the dimensions of the sampled areas although it is impossible to guarantee that sample areas did not cover genuine pH differences. This imposed a limitation on the magnitude and spatial distribution of regions of different pH which could be reliably detected.

As the method of analysis was only intended as a rough estimate the effects of the use of different objectives, zoom settings and gain settings on the inherent pixel variation were not examined. The number of pixels sampled (the “sample area” size) was taken as the overall factor determining the “noise” level (variation due to fluorescence pixel intensity already having been taken into account).

The spatial resolution of images was ultimately dependent upon the optical limits. However, when lateral resolution was better than the sample area size (n pixels) this became the limiting factor. For a particular image the spatial resolution was generally limited by the “sample area size multiplied by the pixel size”. Pixel size was related to the objective magnification and electronic zoom (Chapter 2; Table 2.4), by adjusting these parameters spatial resolution (μm) could be optimised for a given pixel area sample size and hence a particular degree of certainty of precision of pH measurement (Table 5.4). The effect, on spatial resolution, of averaging over areas of pixels was thus reduced by “over-sampling” images - choosing a pixel size very much smaller than the optical resolution limit.

For an image taken with: Kalman $n=3$ scanning; a x60 oil (NA 1.4) objective; zoom 3.5; the pixel size was $0.083 \mu\text{m}$. A sample area of 10×10 pixels was equivalent to $10 \times 10 \times 3$ pixels averaged. This gave an estimated spatial resolution of $< 1 \mu\text{m}^2$ (approaching the optical resolution) with a precision of pH measurement of $\pm 0.02 - 0.07$ pH unit (for the range pH 6.9 - 7.5). The calibration data on which this is based is shown in Fig. 45.

5.7.3 Comparison between images

Comparison of data between images, particularly those collected during different imaging sessions, had the complications of both "within-image" pixel variation and "day-to-day" variation in equipment set-up. "Day-to-day" variation was mainly due to positioning of the mirrors for the two fluorescence channels and slight differences in gain and confocal aperture settings. For this reason comparison between images was limited to ratio values of images collected in the same imaging session or calibrated values (estimated pH) where the calibration (Section 5.4.3) took account of "day-to-day" variation.

5.8 Optical artefacts

Optical artefacts not only distort the size, shape and depth of the imaged field sampled but can also influence observed ratios by affecting the two emission wavelengths differently. The problems of refraction and chromatic aberration were reduced by the use of plan apo objectives and ensuring the correct collar settings for coverslip thickness (Pawley, 1995). Optical artefacts were investigated predominantly for physiological imaging where problems are generally more severe as a result of the shape and composition of cells. Only cells resting against the coverslip were imaged and depth of imaging within cells was restricted to less than 10 μm .

5.8.1 "Inner filter" and "shading" effects

"Inner filter" and "shading" effects are where dye emissions are altered by further interaction with dye molecules and excitation and emission intensity is attenuated by the depth of dye through which light must pass (Pawley, 1995; Berger & Brownlee, 1993). This was tested *in vitro* and no significant effects on ratio value were observed for images taken at up to 100 μm into a solution of 200 μM cSNARF-1 free-acid. In rhizoids little effect was seen with section depth.

5.8.2 Fluorescence image misregistration

It was observed that physiological fluorescence images and fluorescent test samples were misregistered in the y axis plane when the two channels were ratioed (Fig. 54). Re-setting the optical mirrors in the scan head and re-alignment of the system did not correct the problem. Similar misregistration was observed for a range of objectives and zoom settings. Misregistration was also even across the imaged field. These findings suggest that the problem was not optical but potentially with the digitisation of the analogue photomultiplier readout or with the ability of the frame-store of the computer to align the image pair. The problem was routinely corrected by shifting one image of the ratio pair laterally by one pixel.

5.8.3 Optical sectioning

The use of confocal optical sectioning introduced further complications to the interpretation of images. Comparison of non-confocal imaging with confocal optical sectioning (Fig. 55) clearly revealed the improvement in spatial resolution achieved. The combination of the complex cytoplasmic and vacuolar distribution throughout the apex of gametophyte cells and the vacuolar sequestration of dye prevented useful interpretation of non-confocal images. However, confocal sectioning was not perfect (section thickness up to $\sim 2\mu\text{m}$) and signal averaging over a volume of cell occurred which was large enough to allow averaging over both cytoplasm and vacuoles. This signal averaging created the impression of a gradual pH gradient through the vacuolated apical region (Fig. 51B). The problem was reduced by examining cells soon after loading when the vacuolar dye content was low and by using high NA oil immersion objectives to produce thin optical sections ($\sim 1\mu\text{m}$).

Further interpretation problems arose, again related to gametophyte cytology, when optical sections were oblique rather than parallel to the long axis of the cell. In a similar way sampling from different depths within the cell caused problems, see Fig. 56. These problems were reduced by selecting cells lying against the coverslip and only sampling to the centre of the cell (up to $7\mu\text{m}$ for a rhizoid). Generally, multiple focus depth ("Z") series (Fig. 56) were collected to allow three dimensional orientation.

The effects of refractive index mismatch along the imaging pathway, which causes apparent signal attenuation and increasing distortion of the optical section position within a specimen with increasing focus depth within a cell (Shotton & White, 1989), were observed when collecting XZ section images of chlorocytes (see Chapter 4; Fig. 41). These were not significant problems in the current study as the depth of sampling was limited and analysis was restricted to two-dimensional imaging.

In theory, refractive index mismatch along the imaging pathway and the differential effects this has on the different wavelengths of light detected can result in optical section misalignment in the Z-plane, this was of more concern. The consequence of this effect is that the light detected to form the two images of the ratio pair is likely to have originated from slightly different optical planes within the cell. This problem should become more significant as the optical section thickness is decreased. Without specific and detailed analysis it is not possible to say to what extent this effects imaging under the conditions used in this study. The only suggestion of it occurring was the anomalous ratio values observed at the cell periphery and regions of the cell which were slightly out of focus. In out-of-focus regions the degree that the two sampled wavelengths are out of focus is likely to differ with the result that there is a greater contribution of fluorescence from one wavelength than the other and hence an anomalous ratio value. The contribution of the low signal to noise ratio and cell wall loading to the effect at the cell periphery should not be forgotten so there is no conclusive proof of a Z-plane misalignment artefact.

5.9 "Biological" artefacts

Several artefacts may occur with the imaging of dye in living cells. Of particular concern was that the handling of cells did not influence their normal behaviour. This included physical damage, anoxia and responses to the excitation or emission wavelengths of light. The possibility that intracellular dye had modified intracellular pH; either directly by buffering; through the loading method; or possibly as a result of vacuolar uptake, was assessed by comparing different loading degrees. Whilst intracellular pH was variable, no systematic correlation between loading and pH, could be found. This may only be properly resolved by independent methods of pH determination in loaded and unloaded cells. Cell viability with loading and imaging was examined in Chapter 4. In general it was assumed that if cells were growing before and after imaging then images represented the "normal" state.

In gametophyte cells the rate of image capture, even with Kalman imaging, was not a significant problem because of the slow rates of growth and absence of cytoplasmic streaming.

5.10 Discussion: image quality and data extraction

The ultimate aim of imaging intracellular ion sensitive dyes may be considered to be achieving absolute measurement of intracellular [ion] with spatial resolution limited only by the imaging optics. In practice this is never achieved, principally because of the limitations imposed on the technique by the examination of biological material. Optimisation of imaging procedures, therefore, represents a compromise between cell viability, image quality and relevance to biological questions (i.e. questions can only be posed within the limits of the technique). This has been examined to determine to what extent meaningful data may be obtained from confocal ratio imaging of cSNARF-1 AM ester-loaded fern rhizoids and to explore the full potential of the technique. The key concepts in imaging analysis of intracellular [ion] are discussed below in relation to the findings of this examination.

5.10.1 Precision of [ion] measurement

Precision is a measure of the smallest differences or changes in estimated [ion] which could be reliably detected. No references where dye based imaging methods were used could be found which claimed a precision value for their technique. Standard deviations, or more commonly standard errors, were quoted on the basis of variation between repeated experimental results which did not take account of the limitations of the technique. This presumably assumes that variation between individual cells was far greater than that in the methods of [ion] determination.

In the current study precision was shown to be mainly limited by the random variation of the imaging system. Precision could be increased by averaging over space (sample areas) or time (Kalman filtering). Determination of precision allows meaningful statements to be made on the basis of individual cells and comparison of data sampled from within individual cells. The extent to which this could be confidently applied was limited here by the failure to achieve a reliable calibration of *in vivo* dye response.

5.10.2 Spatial resolution of [ion] determination

Spatial resolution in the context of [ion] determination relates to the smallest areas over which pH differences could be distinguished. It was found that the spatial resolution limitation imposed by area sampling was generally above that imposed by the optics of the system. The major practical limitation was again the random noise of the system i.e. the number of pixels which had to be sampled to determine [ion] within acceptable confidence limits (Bright *et al.*, 1987). This problem was reduced by “over-sampling”. An alternative approach would have been to select a smaller image size and average over an increased number of consecutive scans. Even so, small differences (< 0.2 pH unit) would be difficult to detect unless they occurred over significant distances (> 3µm), even with the optimum imaging conditions achieved. Optical and edge artefacts also limited the regions of images which could be examined. Cytoplasm within ~0.5µm of the plasma-membrane and tonoplast had to be avoided. Considering the complex apical cytology of rhizoids and their relatively sparse cytoplasm these were considerable restrictions.

The precision of measurement reported for pH microelectrodes is 0.02 pH unit (Guern *et al.*, 1991), this is for very localised readings within the cell. The difficulty with this technique is that to make comparisons of different regions within cells data must either be collected for populations of cells sampled at different sites, or multiple impalements must be performed. Damage to cells upon impalement and the difficulty in taking readings from the growing zone of the extreme tip severely limit the value of microelectrodes. In this respect imaging, despite its poorer precision, has a significant advantage.

5.10.3 Accurate determination of [ion]

Accuracy is defined here as the certainty in absolute [ion] measurement. The degree of accuracy, therefore, depends upon the calibration of the imaging system and its reproducibility. This assumes that any artefacts in pH determination have been taken into account. Accuracy of *in vivo* measurements is, in theory, best determined by verification of *in vivo* calibration with independent techniques such as ion-sensitive microelectrodes. Current attempts at calibration *in situ* were unsuccessful and a reliable method remains elusive. As a result no estimate could be made of the accuracy of pH measurement or the absolute magnitude of differences in pH.

The use of cell permeant buffering compounds was the most promising of the *in situ* calibration methods attempted. To improve this method permeant buffering species with pKa's in the range 5.75 - 8.25 are required. Suitable compounds would be: freely cell permeant; non-metabolised; and have no direct effects on cSNARF-1. Other possible improvements to weak acid / base “clamping” include inhibition of cellular homeostasis with azide. Ionophore methods could be attempted on protoplasts of fern cells. The ideal situation would be the use of an ion-sensitive dye which was not perturbed by the intracellular environment. Some suggestion of this has been made for dextran-conjugated dyes.

However, in “pseudocytosol” buffer 10 kDa dextran cSNARF-1 showed similar changes in fluorescence intensity and ratio as the free-acid.

5.10.4 Reproducibility of [ion] determination

The degree of agreement in [ion] measurement for independent repeats. Reproducibility depended upon "day-to-day" and "cell-to-cell" variation in the imaging system and how well this was taken into account. The reproducibility of the calibration procedure was also a factor - particularly the reading of the pH meter used to test the pH standards. Considerable effort was made at the level of image capture to improve reproducibility by standardising procedures. This provided a common basis for image processing and interpretation and allowed better comparison of data between independent images. To a large extent this overcame the need to perform an *in situ* calibration on every cell examined - which is the best guarantee of comparative results.

5.10.5 Conclusion

In Chapter 4 the direction of investigation into the role of cytoplasmic pH gradients in steady-state tip growth was discussed. Analysis of the steady-state situation by intracellular dye imaging is highly demanding of both numerical and spatial resolution, particularly when this involves making comparisons of different regions from within individual images. In this situation much more care is required to account for artefacts than the examination of changes occurring between sequential images over time where the “before” and “after” images act as internal controls. Critical testing of the limitations of imaging and image analysis procedures allowed those procedures to be optimised (within the biological limitations defined in Chapter 4) with respect to precision, spatial resolution and reproducibility of [ion] determination. Additionally, the limitations of the technique and the implications this has for the interpretation of results have been brought into the open and focused attention on areas of the technique which need to be improved (see Chapter 8). The estimated precision and resolution of imaging achieved here were not unreasonable in relation to existing knowledge on intracellular pH (Gibbon & Kropf, 1991; 1994; Guern *et al.*, 1991; Frelin *et al.*, 1988; Nuccitelli, 1984) and compared well with that obtained with other techniques, in particular microelectrodes (Herrmann & Felle, 1995; Gibbon & Kropf, 1994). The fundamental limitation on the interpretation of data was the inability to make convincing statements about either absolute pH or absolute Δ pH. The *in vitro* calibration allowed an estimate to be made which could then be reassessed in future work.

Chapter 6

THE ROLE OF pH IN THE TIP GROWTH OF RHIZOIDS OF *D. affinis* GAMETOPHYTES

6.1 Introduction

Rhizoids of fern gametophytes elongate by strict apical growth (Takahashi, 1961). Under normal examination conditions, in liquid medium, rhizoids of between 100 and 200 μm in length elongate at 10 - 15 $\mu\text{m}/\text{h}$ (see Chapter 3). In undisturbed cultures growth proceeds at a regular rate along the basal coverslip of the examination chamber. These conditions provide an opportunity to examine the role of pH in steady-state tip growth.

The different ways in which pH or protons could be considered to have a direct role in steady state-tip growth, through either intracellular or extracellular activities, were discussed in Chapter 1. Briefly, two general situations were of interest here:

- 1) A cytoplasmic gradient in pH associated with the polarity of growth (Gibbon & Kropf, 1991; 1994).
- 2) Localised, polarised movements of protons or proton equivalents between the cell and the external medium leading to localised ΔpH at the cell wall or plasma-membrane (Kutschera, 1994; Roos, 1992; Guern *et al.*, 1991; Harold & Caldwell, 1990; Racusen *et al.*, 1988).

While the existence of either of the above states is not conclusive of a causal relationship (Harold & Caldwell, 1990) their investigation is a necessary initial step towards determining whether there is a more specific involvement of pH or protons in tip growth (see Chapter 1; Sections 1.6.4, 1.7; 1.9 and 1.13.6).

The aim of the work in this section was to establish the existence or absence of the above states. The experimental approach was based on simple "observation" of pH in the steady-state and upon manipulations of pH and growth in order to determine their interdependence.

6.2 Examination of intracellular pH

Cytoplasmic pH in growing cells was examined by confocal ratio imaging of AM ester-loaded cSNARF-1 (Fig. 57). The detection of gradients was, necessarily, constrained within the limitations of the imaging technique (as outlined in Chapter 5) to differences in pH of greater than ~ 0.2 unit over distances of greater than $\sim 3 \mu\text{m}$. With the avoidance of regions of "ambiguous" signal this effectively limited examination to the apical cytoplasmic thickening (Zone 1) and selected regions of the subapical and peripheral cytoplasm (Zones 2 and 3), described in Chapter 5; Fig. 50. Numerical analysis was performed, as described in Chapter 5; Section 5.6.1, on defined areas of roughly median optical sections. Only cells which continued growth ($>8 \mu\text{m}/\text{h}$) during imaging were accepted for

analysis. All pH values quoted were determined on the basis of the simple MES/HEPES *in vitro* calibration.

6.2.1 Intracellular pH in growing rhizoids

Results from sampling relatively large areas (> 1000 pixels) according to the Zones described in Chapter 5; Fig. 50, are shown in Table 6.1. On the basis of simple *in vitro* calibration the average cytoplasmic pH was found to be around 7.2 (within ± 0.1) in all cases (n = 15). This value is consistent with that reported for a range of cell types using a variety of methods (Guern *et al.*, 1991).

Table 6.1: Average cytoplasmic pH

Sample region * (distance from tip)	Average cytoplasmic pH of the cell population					
	x60 (NA 0.95) dry objective	s.d. † (n = 6)	s.e.m	x60 (NA 1.4) oil objective	s.d. † (n = 7)	s.e.m
Zone 1 (0 - 3 μm)	7.24	± 0.030	± 0.012	7.16	± 0.018	± 0.007
Zone 2 (3 - 15 μm)	7.19	± 0.024	± 0.009	7.10	± 0.020	± 0.008
Zone 3 (15 - 50 μm)	7.16	± 0.038	± 0.016	7.14	± 0.019	± 0.007

* See Chapter 5; Fig. 50 for a description of the sampling Zones.

† pH_c was determined from pixel areas of > 1000 pixels so the effects of random pixel variation on the variation in pH between different cells was assumed to be negligible. Variation in pH_c values within the cell population (s.d.) was, therefore, determined from the variation between average pH_c values of individual cells.

The results with dry objectives (NA 0.95), providing optical sections of $\sim 2 \mu\text{m}$, and an oil immersion objective (NA 1.4), giving an optical section thickness of $\sim 1 \mu\text{m}$ agreed well. Both suggested the existence of a very slight, but consistent, difference in pH between the apical cytoplasmic "cap" region (Zone 1) and more subapical and peripheral regions of cytoplasm (Zones 2 and 3) for every cell examined. Cytoplasm at the apex, particularly the apical "cap", was consistently slightly more basic than more subapical cytoplasm <0.1 pH unit difference. This was actually below the resolution of the technique. In addition, the validity of such a comparison of different areas was questionable - as argued in Chapter 5 - mainly on the basis of the contribution of vacuolar signal in Zone 2.

A more detailed analysis of the apical 20 - 30 μm of 13 rhizoids was performed with a x60 (NA 1.4) oil immersion objective and typical results are shown in Fig. 58. This data provided further evidence that the observed differences in pH value between the zones were due to vacuolar contribution. The graphs in Fig. 58A clearly show no significant gradient in cytoplasmic pH over the apical 20 μm . Differences in pH were within 0.2 pH unit and varied fairly randomly along the length of the apex. Over the $\sim 3 \mu\text{m}$ thick apical cytoplasmic "cap" (Zone 1) differences in pH of up to ~ 0.1 pH unit were recorded. However in the 13 rhizoids examined, there was no systematic orientation to these

differences from one cell to the next. The three graphs of pH sampled along the length of the apex of growing rhizoids in Fig. 58A show: a drop in pH; a rise in pH and a roughly even pH, respectively over the apical “cap”. An examination was also made of the pH in the peripheral cytoplasm (for the images collected with the x60 oil objective), from the non-growing subapical region ~ 15 μm behind the apex (the tip-most region of Zone 3) to the growing zone at the extreme apex. This also showed that there was no significant gradient in pH for the 7 rhizoids examined (Fig. 58B is a typical example). Areas sampled within the peripheral cytoplasm at between 30 - 50 μm from the tip gave similar pH values (within 0.1 unit) to the apical “cap” (3 rhizoids examined) in agreement with results obtained with the x40 and x60 dry objectives.

Examination was performed on images collected at different focus positions within a single typical rhizoid to determine whether there was a difference in pH between the upper and lower regions of rhizoids. If rhizoids were strongly gravitropic or even negatively phototropic then growth horizontally on the microscope stage could cause a shift in the growing zone to the bottom face of the apex. Results indicate the presence of the slightly higher pH in Zone 1 in all sections (Table 6.2). However, no systematic differences in pH were found with section depth. Similar results were found in all five of the similarly examined rhizoids (x60 plan apo dry NA 0.95 objective).

Table 6.2: Z-series cytoplasmic pH analysis (typical data set)

Section Position	Depth (μm)*	Cytoplasmic pH		
		Zone 1	Zone 2	Zone 3
Bottom	~ 1.5	7.22	7.18	
2	~ 3.5	7.26	7.24	7.19
Central	~ 5.5	7.27	7.21	7.18
4	~ 7.5	7.28	7.23	7.16
Top	~ 9.5	7.24	7.22	7.18

* Depth of focus into the cell estimated from the stepper motor position.

6.3 Intracellular pH and growth

The relationship between intracellular pH and growth was tested by using weak acids and bases to directly alter intracellular pH in rhizoids (Chapter 5; Section 5.4.2). This would be expected to interfere with pH specific events and disturb any existing intracellular pH gradients. Similar treatments have been used in *Pelvetia* zygotes (Gibbon & Kropf, 1994), *Neurospora* hyphae (Sanders & Slayman, 1982), rhizoids of the liverwort *Riccia* (Frachisse *et al.*, 1988) and root hairs (Herrmann & Felle, 1995). Intracellular pH change was recorded by cSNARF-1 ratio imaging and effects on growth were determined from consecutive images and bright-field microscopy.

6.3.1 Effects of intracellular pH manipulation on growth

Application of cell permeant buffers, propionate at pH 6.0 and ammonia at pH 8.0, was observed to shift intracellular pH within three minutes to more acidic and more basic values, respectively in all 15 rhizoids examined for each treatment (see Chapter 5; Fig. 45). Concomitantly with this cytological organisation at the rhizoid apex deteriorated and growth halted. If the internal pH “clamping” media were applied for only 15 min. and then replaced with standard medium then a reasonable proportion of cell recovery was observed within 12 hours; longer treatments resulted in cell death. “Clamping” treatment at pH 7.0 (with NH_3) had the least effects with recovery of growth at the original tip site within only a few hours of medium exchange. Both of the other treatments caused more severe disruption and regeneration of the new apical structure was generally at a subapical site (Fig. 59). With each of the pH treatments similar results were obtained throughout the cell populations examined (>25 cells) in the two experiments performed.

Unfortunately, because of the limitations of the dye-loading, the recovery of internal pH which presumably preceded the resumption of growth could not be examined. One of the few observations of internal pH after exchange of “clamping” buffer (propionate at pH 6.0) for normal medium showed a very rapid return to close to normal pH within about 10 min., significantly before growth was resumed.

6.4 Extracellular pH and tip growth

A range of external pH conditions with different buffer strengths was applied to growing rhizoids to examine the effects of extracellular pH on tip growth. Such treatment would be expected to interfere with the maintenance of extracellular pH profiles and so prevent "acid wall loosening" and interfere with proton coupled transport activities (Gibbon and Kropf, 1991; Gow, 1989; Racusen *et al.*, 1988).

The effect of extracellular buffering (with MES/HEPES) was examined at pH 5.6 (the pH of standard medium), 6.0, 7.0 and 8.0. Population studies in glass flasks were performed over time, between 100 and 150 protonemata were examined at each time point for each treatment (see table 6.3 for treatments). In addition, six individual cells growing in thin-layer chambers were continuously examined under the microscope for each set of conditions, bright field images were collected at intervals to record changes in growth.

Table 6.3: Extracellular pH manipulation media

Medium	pH	[K ⁺] mM	Buffer
Control-standard medium	5.6	1.2	unbuffered
Control-buffered medium	5.6	6.8	25 mM MES/HEPES
Low buffer medium	7.0	5.8	5 mM MES/HEPES
	8.0	~9	
High buffer medium	6.0	12	25 mM MES/HEPES
	7.0	29	
	8.0	45	
High K ⁺ control	6.0	45	25 mM MES/HEPES

6.4.1 Extracellular pH manipulation effects on rhizoids

The effects of altering external pH ranged from no apparent change in structure or growth rate to redistribution of apical cytoplasm and cessation of measurable apical extension. In some affected cells a slight increase in length occurred as a result of a more general apical swelling. Cells generally remained viable; tip structure and growth rate recovered, either after exchange to normal unbuffered medium or spontaneously in the continued presence of buffered conditions. The time-course of tip deterioration and spontaneous recovery for different treatments is shown in (Figs. 60-62). Recovered rhizoids could generally be distinguished from those unaffected by irregularities or kinks behind the tip of recovered cells.

At pH 5.6 and 6.0 up to 25 mM MES/HEPES buffer was found to have virtually no effect on normal appearance and growth rate of rhizoids (Fig. 60). At pH 6.0 (25 mM buffer) some rhizoids exhibited a slight increase in apical diameter but no loss of cytoplasmic structure, this was found to be attributable to the increase in ion content of the medium with increased buffer concentration.

25 mM buffer at pH 7.0 (Fig. 61) caused an effect within about 30 min.; most cells underwent alterations in tip structure, interruption of apical extension and slight apical swelling. Generally within 2 h normal tip structures were regenerated and growth rate recovered to normal. In some cells apical structure was not fully disrupted, especially at 5 mM buffer, and growth rate continued at a reduced rate before full recovery.

The most severe effects were observed with 25 mM buffer at pH 8.0 (Fig. 62). Nearly all rhizoids underwent complete loss of the complex cytoplasmic organisation at the apex with cessation of apical extension within 30 minutes. Tips took on an evacuated appearance with the apical cytoplasm forming a thin peripheral layer. In many cases significant apical swelling occurred. There were occasional examples of spontaneous regeneration of apical structure and recovery of growth after more than 4 h. However, the proportion of recovered tips was still low after 9 h. The effect on cells of weaker buffer strength (5 mM) at pH 8.0 resembled that seen with high buffer strength at pH 7.0.

Controls were performed to determine that the observed effects were not purely a result of variation in ionic strength, $[K^+]$, at different pH (Table 6.3). The effects of 12 mM $[K^+]$ and 45 mM $[K^+]$ with 25 mM MES/HEPES at pH 6.0 were compared. The higher $[K^+]$ was equivalent to that in the 25 mM buffer at pH 8.0 (Table 6.3). Fig. 60 shows the observed tip morphologies. The high $[K^+]$ did not cause the typical structural disruption as seen with pH modification. Cytoplasmic structure was not disrupted, although an increase in the diameter of the continually extending tip was observed. Tip diameter gradually returned to the original size.

Buffer strength, pH and $[K^+]$ all affected rhizoid growth to some extent although not all in the same way. High pH and buffer strength caused severe stress-like response while high $[K^+]$ caused a more subtle alteration of tip growth. Effects were not purely external as the intracellular organisation was disrupted. Rhizoids were able to adapt to even the most harsh treatment, eventually recovering apical structure and growth. Considerable variation occurred in the response of individuals within the population.

Similar responses were observed in both glassware and the plastic thin-layer chambers, demonstrating that the effect was neither a physical damage response nor "chemical" effects as a result of plasticizers leached from the plastic chamber by the buffers.

6.5 Effects of extracellular pH manipulation on intracellular pH

It was considered possible that the extracellular pH conditions which disrupted tip growth in rhizoids also had an effect on intracellular pH, as has been described for other cell types challenged by external pH (Guern *et al.*, 1991; Harold, 1986). Cytoplasmic pH was, therefore, examined in cells after external pH manipulation. Cells were pre-treated with 25 mM buffered MES/HEPES medium (32 mM $[K^+]$) at pH 6.0 and 8.0 for between 20 and 30 minutes. Cells were subsequently ester-loaded with cSNARF-1 AM under the same pH conditions for a further 15 - 20 min. and then imaged on the CLSM. Rhizoids were found to have loaded with dye as normal. The effects of external buffering on growth occurred as previously described and cytological disturbance was very obvious at the time of imaging. However, no difference in average pH_c , significant enough to be detected reliably by the current imaging procedures (> 0.1 pH unit), was found between control and treated cells ($n = 6$ cells examined for each treatment).

As mentioned before (Section 6.3.1), recovery was an important aspect of the response, suggesting an initial effect which was reversible. The experimental procedures used did not allow the determination of whether a rapid, transient intracellular pH change occurred. Intracellular pH was only examined at the time of morphological expression, after the initial disruptive events.

An indication that rhizoids actively resisted the pressure of external pH changes was given by the effect of azide treatment (2 mM sodium azide) under different conditions of external pH. Azide treatment, which disrupts the regulation of intracellular pH (Roncal *et al.*, 1993), caused rapid intracellular acidification of rhizoids. At an external pH of 6.0 (25 mM MES/HEPES buffered)

imaging of cSNARF-1 suggested a fall in pH_c of over 0.5 pH unit (from ~ 7.2 to ~ 6.5 according to *in vitro* calibration) within three minutes in all rhizoids tested ($n = 7$ cells). At external pH 8.0 (25 mM MES/HEPES buffered), however, the acidification observed in the 6 cells examined was much less, only of the order of 0.1 - 0.2 pH unit, even after longer incubation times (greater than 6 minutes). The observation of the reduced pH_c change with azide in the presence of high external pH (pH 8.0) and the fact that a normal healthy cell retains its normal pH_c ($\sim \text{pH } 7.2$) under similar conditions of external buffering suggests a strong influence of the external pH conditions on internal pH - at least at alkaline external pH - which a normal healthy cell is able to actively compensate for. An efficient mechanism for regulating internal pH under variable external pH conditions would explain why external pH treatments were observed to have little effect of pH_c . Such regulatory mechanisms may be an adaptation of the free-living gametophyte to uncertain environmental conditions. Strong regulation of pH_c has previously been recorded in cells of the aquatic liverwort *Riccia* (Frachisse *et al.*, 1988).

6.6 Extracellular pH profiles around cells

Constant localised influx or efflux of protons across the cell membrane should result in localised extracellular modification of pH. Such extracellular "pH profiles" have previously been mapped around tip-growing cells by pH sensitive microelectrodes (see Gow, 1989) and the vibrating pH probe (Herrmann & Felle, 1995). The magnitude of the extracellular pH modification measured varied for different cell types. Differences in pH of -0.5 unit from the bulk medium have been recorded at the apex of fern apical chlorocytes (Racusen *et al.*, 1988). For the oomycetes *Achlya* and *Allomyces* very small pH profiles were detected - less than 0.1 pH unit (De Silva *et al.*, 1992; Gow *et al.*, 1984). In contrast *Neurospora* was reported to acidify the medium around its apex by roughly 1 pH unit (Gow, 1989). Fucoid zygotes acidified the medium by up to 0.1 pH unit behind the tip of the rhizoid (Gibbon & Kropf, 1991). The involvement of localised proton movements between cells and the environment in contributing to endogenous electrical currents has been demonstrated for even more tip-growing cell types using the vibrating probe (Obermeyer *et al.*, 1992; Gow, 1989; Miller *et al.*, 1986).

The pH sensitive dye Bromocresol green has been used to detect the pH profile round *Neurospora* hyphae (Gow, 1989). On this basis ratio imaging of cSNARF-1 free-acid in unbuffered external medium (pH 6.0) was employed in an attempt to visualise such "pH profiles" around growing rhizoids. It was assumed that the cSNARF-1 free-acid concentration (50 - 100 μM) was low enough that buffering by the dye was negligible. Growing cells were examined for over 30 min. in thin-layer chambers.

6.6.1 Absence of a detectable extracellular pH profile

No evidence of modification of the pH in the medium surrounding rhizoid tips was found. The pH of the medium within 2-5 μm of the cell was not measurably different from that of the bulk medium along the apical 30 μm of the 5 cells examined (pH 6.0 according to *in vitro* calibration). This may be due to genuine absence of a measurable gradient. However, it was questionable whether the method was suitable to detect any existing gradient. Examination of the important region within 1 - 2 μm of the cell wall was prevented by binding of dye to the cell wall (see Chapter 4; Section 4.5.1) and difficulty in focusing on the median section at the tip. Rates of dye : proton interaction and diffusion of dye and protons may prevent satisfactory detection of even stable pH gradients in free medium. Imaging cSNARF-1 free-acid using a x4 objective (NA 0.2) was able to detect transient pH gradients over 1000 μm at the interface of diffusing pH 6.0 and 8.0 buffers in 1% (w/v) agar. However, experiments with ferns growing through 1% (w/v) agar also gave negative results. Improved optical sectioning and the use of dextran-conjugated dye may provide the necessary improvements to allow higher magnitude extracellular pH profiles to be examined by imaging. Even so, ΔpH of less than 0.3 are probably below the resolution of imaging. A useful positive test of the method would be to demonstrate the existence of an extracellular gradient with microelectrode techniques.

The possibility of using dye to image pH in the cell wall was also investigated but this too was found to be unsuccessful. Dye free-acid bound to the rhizoid cell wall responded poorly to attempts at calibration with external cell impermeant buffers. It is likely that wall-bound dye was in a fluorescent but pH insensitive state. Ratio values for wall-bound dye suggested that the "acid" form of the dye predominated.

6.7 Discussion

6.7.1 pH, pH gradients and polarised growth

The question of whether pH plays a primary role in polarity and tip growth, i.e. in their regulation, has recently received considerable attention. This mainly followed the work of Gibbon & Kropf (1991; 1994) on *Pelvetia* zygotes. The association of proton movements with polarised events in plants and fungi had been noted some time previously (e.g. Gow, 1989; Racusen *et al.*, 1988; Miller *et al.*, 1986; Weisenseel & Jaffe, 1976). Gibbon & Kropf (1994) demonstrated that the existence of a cytoplasmic pH gradient stretching over $\sim 60 \mu\text{m}$ is associated with rhizoid apical growth in *Pelvetia* rhizoids and proposed a primary role for pH in the maintenance of tip growth. This is similar to the concept of the cytoplasmic Ca^{2+} gradient in pollen tubes (Pierson *et al.*, 1994; Miller *et al.*, 1992; Rathore *et al.*, 1991).

Cytosolic pH gradients have been recently studied *in vitro* by (Al-Baldawi & Abercrombie, 1992). They highlight the balance between the rates of proton movements across cell membranes and proton diffusion through the cytosol. Their findings suggest that cytoplasmic pH gradients are possible but their magnitude and localisation is very dependent upon cytosolic buffer capacity and the mobility of

buffering components within the cytosol. There is also evidence to suggest that pH is able to influence relevant processes such as enzyme activities (Trivedi & Danforth, 1966) and cytoskeletal organisation (Edmonds *et al.*, 1995; Grabski *et al.*, 1994; Kropf, 1994), which in turn could direct polarised vesicle transport and localised fusion. Determining whether such pH gradients were present in fern rhizoids was used as a starting point. The failure to detect a gradient may be interpreted in several ways:

- 1) Was the technique used suitable?
- 2) How do fern rhizoids and *Pelvetia* rhizoids differ?
- 3) Could the location of a physiologically relevant gradient differ in fern rhizoids (Fig. 63)?
- 4) A cytoplasmic pH gradient is not an essential requirement for the maintenance of apical growth?

The limitations of the imaging method were investigated in Chapter 5. The results suggest that the gradient observed by Gibbon & Kropf (1994), of at least 0.3 pH unit over $\sim 40 \mu\text{m}$, could be reliably detected by the current imaging technique. Examination of cytoplasmic pH round the periphery of the rhizoid apex - as far back as the main central vacuole (up to $50 \mu\text{m}$ behind the tip)- failed to reveal any similar gradients. A similar lack of a significant gradient was found within the apical cytoplasm in the region corresponding to the expected growing zone within $\sim 15 \mu\text{m}$ of the tip. The possibility of very localised domains of pH close to membranes has been proposed (Guern *et al.*, 1991) and some preliminary evidence obtained to support their existence (Roos, 1992). This type of pH domain is beyond the limits of reliable resolution by the imaging techniques used. Such “gradients” could, therefore, exist and function in fern rhizoids. However, this is not the situation proposed for the elongating *Pelvetia* rhizoid where the gradient purported to be of relevance to tip growth was spread over $60 \mu\text{m}$. It is interesting to note that the gradient observed in *Pelvetia* only starts from $\sim 10 - 17 \mu\text{m}$ behind the tip. Within the apical $\sim 20 \mu\text{m}$ pH_c may be considered to be relatively even ($\Delta\text{pH}_c < 0.1$ pH unit). However, for a pH gradient to be active in polar organisation at the apex or in directing the activities of apical extension, it should occur over the relevant regions of the cell. While the exact region of expansion in fucoid rhizoids appears not to have been determined, evidence from structural analysis and the localisation of Ca^{2+} gradients (Berger & Brownlee, 1993; Brownlee & Pulsford, 1988) suggests such activity is concentrated in the apical $5 - 10 \mu\text{m}$. This region corresponds to the even pH (7.1 - 7.2) zone in *Pelvetia* rhizoids. It is assumed that this zone actually corresponds to low cytosolic pH and pH further behind the tip (up to 7.55) corresponds to the “resting state” (Dr Daryl Kropf personal communication).

The results in *Pelvetia* and *Dryopteris* rhizoids do show some agreement in that neither have a significant pH_c over their apical $\sim 20 \mu\text{m}$ - the region expected to be the major site of activities associated with tip growth. The major difference lies over the subapical region. This is significant to the validity of the suggestion that a pH gradient may function in regulating the cytoskeleton at the cell apex and the activities of vesicle transport to the tip and fusion with the apical membranes. Although fern and *Pelvetia* rhizoids are of similar size and have similarly slow growth rates (Chapter 3; Table

3.6) the latter does not exhibit the same degree of apical vacuolisation and has a high cytoplasmic content over a much greater distance from the apex (Kropf, 1994; Brawley *et al.*, 1976). Transport of secretory vesicles may occur from greater distances behind the tip - guided by the pH gradient. It is also possible that the gradient observed in *Pelvetia* may not be a primary factor in directing tip growth but is a consequence of the existing polar cytological organisation, for example a result of the distribution of chloroplasts and mitochondrion. This too has received limited attention and requires more detailed structural analysis to clarify the situation.

A gradient in cytosolic pH does not seem to be a feature common to all tip-growing cell types; Herrmann & Felle (1995), using microelectrode techniques, found no significant (> 0.1 unit) pH_c gradient between the cell apex (measurement 10 μm behind the extreme apex) and base (measurement over 200 μm from the extreme apex) in growing *Sinapis alba* root hairs. This suggests that a pH gradient is not a universal feature and hence not of primary importance in polarity and tip growth. In order to clarify this situation two important questions need to be addressed:

- 1) How widespread is the occurrence of cytoplasmic pH gradients in tip-growing cell types?
- 2) What constitutes a physiologically relevant (see Fig 63) ΔpH in terms of both magnitude and localisation?

This requires the examination and comparison of cytoplasmic pH in many different cell types. It also highlights the need to improve both the resolution precision and absolute accuracy of cytoplasmic pH measurement for imaging methods to levels approaching those for pH microelectrodes.

6.7.2 Manipulation of internal pH

The existence of an intracellular pH gradient in tip-growing cells does not prove a primary role for pH in tip growth. A causal relationship must be established, the pH gradient may be a cause or product of polarised growth. Manipulation of intracellular pH using propionic acid, and its resulting effect in reducing both the observed growth and cytoplasmic pH gradient, was taken as proof of a causal relationship by Gibbon & Kropf, (1994). Similar manipulations were used on root hairs by Hermann & Felle (1995). Their conclusion, based on the absence of an intracellular pH gradient, was that any disruption of intracellular pH disturbed cellular activities in general and, therefore, indirectly influenced tip growth. In fern rhizoids intracellular pH manipulation using weak acids and bases inhibited growth, even around pH 7.0. However, the reorganisation and re-initiation of tip growth which followed extracellular pH manipulation and transient internal pH “clamping” treatments, may prove to be of more experimental value if imaging procedures could be improved to allow examinations over prolonged periods.

6.7.3 Manipulation of external pH

Manipulation of external pH proved to be more simple to interpret. Although growth was transiently inhibited it was able to resume and continue under conditions which would prevent localised extracellular modification by the cell. The fact that growth could continue, apparently normally, over a pH range from 6.0 - 8.0 suggests that external pH does not play a key role in polarised growth in fern rhizoids and that “acid wall loosening” is not an essential process in apical extension. The transient disruption to growth may be interpreted in terms of a transient shift in intracellular pH of in membrane potential (Guern *et al.*, 1991). The ability of plant cells to adapt to imposed extracellular pH “stress” by adjustment of their pH regulatory processes is well known (Guern *et al.*, 1991; Harold, 1986). In *Pelvetia*, external pH manipulation was also found to have little effect on growth (Gibbon & Kropf, 1991). Pollen tubes are more sensitive and a distinct pH optimum for growth rate can be determined (Guern *et al.*, 1991) - this may reflect the nature of the growth conditions which pollen tubes normally have to deal with. The more significant effects of external pH on the growth of fungal hyphae has been linked to nutrient uptake (Gow, 1994; De Silva *et al.*, 1992).

6.7.4 Observation versus Manipulation

The reason for manipulation of internal pH is to establish a cause and effect relationship. This technique has been successfully used in the study of the role cytoplasmic Ca^{2+} in polarised growth (Malhó *et al.*, 1994; Pierson *et al.*, 1994). However, this seems to be less appropriate for the study of pH for several reasons. The principal reason is the ubiquitous involvement of protons in all the biochemical activities of the cell. Protons are also intimately associated with the “energetic” processes of cells such as proton coupled transport and energy production by mitochondria. In short, pH is too intimately involved in cellular activities for manipulation experiments to be easily interpreted. However, such “involvement” in cellular processes does not exclude pH as a regulatory mechanism, it would be expected to provide an ideal means of integrating the regulation of many diverse cellular activities. The means used to alter intracellular pH, in particular cell permeant weak acids and bases, are crude and highly delocalised in their effect - influencing pH externally and within the cell in both organelles and the cytosol. The pH in organelles of the exocytotic pathway, an important process in apical growth, has been shown to be important to its function (Seksek *et al.*, 1995; Rost *et al.*, 1995; Klionsky *et al.*, 1992). Intracellular pH manipulations with cell permeant weak acids as employed by Gibbon & Kropf (1994) would, therefore, be expected to influence apical growth independently of any primary organisational role of pH. Another complication of intracellular pH manipulation is the effect it has on significantly increasing intracellular Ca^{2+} levels and on membrane potential (Guern *et al.*, 1991), both of which have been implicated in the regulation of polarity and apical growth (refer to Chapter 1).

Simple observation of growing cells of many different cell types would appear to be the most reliable experimental avenue available. However, there are circumstances where manipulations of

intracellular pH could provide useful information, particularly if the manipulation could be performed in a very localised and controlled manner - for example by intracellular release of caged protons or pH buffers. Treatments which gave positive effects, such as increased growth or bending or branching, would be much easier to interpret than inhibition of cellular activities. The best manipulations would be those which involved physiological stimuli which subsequently lead to a change in intracellular pH which preceded a physiological response. Unfortunately no such trigger is known for fern rhizoids. Interestingly, studies where such a situation has been investigated generally report global, rather than localised, pH changes (Pichon & Desbiez, 1994; Gehring *et al.*, 1994; Irving *et al.*, 1992; Grešić *et al.*, 1991).

6.7.5 Conclusions

Results of the analysis of cytoplasmic pH, by confocal ratio imaging of AM ester-loaded cSNARF-1, demonstrated the lack of a significant (> 0.1 pH unit) cytoplasmic pH gradient within the apical 40 - 50 μm of the apex. This provides evidence that tip growth is not dependent upon an intracellular pH gradient in fern gametophyte rhizoids. Additionally, the ability of rhizoids to grow in buffered medium at different pH (6.0 - 8.0) shows that the external pH does not appear to be critical to tip growth. This argues against the "acid wall loosening" mechanism in extension of the rhizoid tip. However, maintenance of normal intracellular pH was essential for cytological organisation at the apex and continued growth. Whilst the results do not provide conclusive answers, they support the idea that, although pH is inextricably linked with tip growth, it does not play a primary role in polarisation and organisation of the growing tip or in directly regulating growth rate.

Chapter 7

Chapter 7 - SUMMARY

Fern gametophytes have been relatively neglected as an experimental system in more recent times. The work of this thesis has taken a fresh look at this potentially useful model system using the modern techniques of intracellular ion-sensitive dye and confocal ratio imaging to examine the role of intracellular ion concentrations in polarity and tip growth. Such techniques have not previously been employed successfully with fern gametophytes, although some success has been found with moss protonemata (Demkiv *et al.*, 1994; Read *et al.*, 1992; Hahm & Saunders, 1991). The work eventually focused on the role of pH in tip growth and polarity - which over the past ten years has become an area of considerable contention.

While the results obtained may not provide any conclusive answers, an initial groundwork has been laid, providing a good basis for further work. Different avenues have been explored with respect to both the application of imaging technology to and useful biological features of fern gametophytes, focusing on both practical and biological limitations. Certain non-productive lines of investigation have been eliminated and this has outlined the most likely possibilities for the future.

7.1 Fern gametophytes as a model experimental system

The fern gametophyte proved not the easiest experimental system to deal with. Several specific problems were encountered: the extreme sensitivity to physical and chemical damage; slow growth rate; and the slow morphological expression of response being the most important. However, with the techniques and procedures for culture and handling which have been evolved, and sufficient care, gametophytes were able to survive dye loading and confocal imaging. While cells were easy to disturb they proved difficult to completely kill, a feature of interest when considering microinjection of dyes and experimental manipulations.

Analysis of the structure of *D. affinis* gametophyte cells showed some intriguing features of the apical cytological organisation even for fern gametophyte cells, very different from moss protonemata and *Chara* rhizoids. Rhizoids bore some similarity to rhizoids of *Riccia* (Alfano *et al.*, 1993). Such structural differences make an interesting comparison with other tip-growing cell types such as pollen tubes, root hairs and fungal hyphae. The organisation of gametophyte cells bore more similarity to the less specialised polarly expanding cells of higher plant tissues for example, root cells and xylem and phloem initials.

Several interesting features of fern gametophyte biology, relating to polarity and polarised growth, were noted which present interesting possibilities for experimental exploitation.

7.2 cSNARF-1 and ester-loading

In many respects cSNARF-1 AM ester proved to be less than ideal. The questionable intracellular pH response coupled with the problem of dye distribution cast a shadow of doubt on any results

obtained - particularly in light of the difficulties experienced in obtaining adequate calibration. The justification for its use was that some advance could be made into the role of intracellular pH. Care was taken to recognise and limit the disadvantages of the technique so that the best could be made of the data obtained. This will prove advantageous in guiding future work involving potentially more demanding techniques such as microinjection.

7.3 Confocal Microscopy

The use of confocal microscopy could not overcome all of the limitations of intracellular dye distribution and limited useful imaging time which resulted from the use of AM ester-loading but the need to use confocal analysis to obtain useful data was made very obvious. However, confocal ratio imaging alone was insufficient to completely investigate the potential role of pH in tip growth in ferns. The need to combine imaging with electrophysiology techniques (as done by Gibbon & Kropf (1994)) has been recognised, although electrophysiology is seen in a supportive role.

7.4 pH and tip growth

The results of the investigation of intracellular pH and tip growth obtained by confocal ratio imaging of cSNARF-1 find agreement with similar work published for other cell types but disagree with yet others:

- A significant pH gradient was not found to be associated with tip growth.
- Alteration of intracellular pH inhibited tip growth.
- Alteration of external pH did not completely inhibit tip growth, although growth was transiently perturbed.
- Highly buffered external media did not ultimately prevent tip growth.
- Cytoplasmic organisation at the apex correlated with active tip growth. Treatments affecting tip growth disrupted this organisation. Recovery of growth was preceded by the reorganisation of cytoplasm at the apex.

These findings are in accordance with those of Herrmann & Felle (1995) who suggest that, although the maintenance of normal intracellular pH is essential for active tip growth, this is an indirect phenomenon. That is, intracellular pH does not act as a direct regulator of polarity and tip growth but is involved in the mechanics of and is determined as a result of these activities. This is in contrast to intracellular Ca^{2+} where there is more evidence of a purely regulatory role both by direct observation and the ability to influence positive cellular activities specifically by manipulating intracellular Ca^{2+} (e.g. Malhó *et al.*, 1994). That pH does not have specific regulatory activities is by no means conclusive and in the complexities of the intracellular environment, where nothing is truly independent of everything else, pH may be more intimately involved in regulation than is apparent. The extent of the role which pH plays in polarity is still open to question.

Chapter 8

Chapter 8

FURTHER WORK

8.1 Introduction - Areas of further work

During the course of this thesis work has been carried out in the setting up of an experimental system to investigate the role of intracellular ion distributions (Ca^{2+} , H^+) in polarity and tip growth. Whilst research has been extended to the limits of the technical procedures employed (See Chapters 2, 4 and 5) the results have, so far, not provided clear conclusions to the biological questions posed. However, based on the findings of the current study, several key areas may be defined as the basis of any related future work as discussed in the following.

8.2 Technical improvements

In the technology-driven field of imaging it is often technical improvements which are the key to achieving new insights and opening up new possibilities. Potential technical advances covered in Table 8.1 have been split into three areas: 1) dye and loading methods; 2) imaging procedures; and finally, 3) other techniques. The first two areas relate specifically to reducing the problems and limitations of: current dye-loading methods; intracellular dye behaviour; and the other imaging artefacts discussed in Chapters 4 and 5.

The most important single advance to intracellular ion imaging in fern gametophytes would be development of reliable pressure microinjection of dye-dextran conjugates of both pH and Ca^{2+} sensitive dyes (see Table 8.1 references). It is possible that this could be performed on imbibed pre-germination spores or early after germination. Dye could then be imaged at a later time (after 24-48 h) at a more advanced developmental stage (Gibbon & Kropf, 1994). Initial attempts with protonemata and rhizoids suggested that pressure injection, using the pressure probe system, should be possible. Successful application of this method is a fundamental criterion in justifying continued work in fern gametophytes using imaging technology, particularly regarding the roles of Ca^{2+} ions.

Imaging [ion] adjacent to membranes, with lipophilic dyes (Haugland, Bioprobes No. 18, 1993 from Molecular Probes), would introduce an important new dimension. Many important processes occur at membranes: proton flux; regulation of membrane potential; signal detection and transduction by membrane proteins; cytoskeletal interaction with the cell membrane - important in maintenance of tip structure and vesicle traffic (see Chapter 1, Sections: 1.7 - 1.9 and Roos, 1992). Current imaging techniques suffer significantly from artefacts at this biologically relevant site (Chapter 5) preventing meaningful observations.

In order to improve the quality of data recorded from ratio images an attempt to determine the best ways of statistical analysis has been initiated (see Chapter 5; Section 5.6.3). This should not only allow better estimation of precision but also help to define the best way of processing and analysing images and additionally allow more meaningful comparisons of image data.

Table 8.1 Technical improvements

Dyes and loading methods	Advantage	References
Pressure microinjection: SNARF-1 dextran BCECF dextran Calcium green dextran Calcium green-Texas red dextran	Introduction of dye-dextran conjugates: -localisation of dye to the cytosol. -better intracellular dye behaviour. -improved calibration. -longer useful imaging time. -calcium imaging and quantification by ratio analysis using the CLSM.	Gibbon & Kropf, 1994 Berger & Brownlee, 1993 Gilroy & Jones, 1992 Miller <i>et al.</i> , 1992 Oparka <i>et al.</i> , 1991b
Lipophilic pH and calcium dyes: (for example- Fura-C ₁₈)	Free ion concentration determination at membranes (see Pierson <i>et al.</i> , 1995; Roos, 1992)	Haugland (Bioprobes no. 18), 1993
Membrane potential sensitive dyes e.g. Di8 Anepps.	Map differences in membrane potential around cells and assess the effects of experimental treatments.	Haugland, 1992 see also Das <i>et al.</i> , 1993
Low pKa pH dyes: -e.g. cSNARF-6	Analysis of vacuolar pH	Rost <i>et al.</i> , 1995 Seksek <i>et al.</i> , 1995 Haugland, 1992

Imaging procedures

Dual excitation ratio imaging of BCECF	Independent method of pH analysis for comparison with results obtained with cSNARF-1.	Fricker <i>et al.</i> , 1994 Davies <i>et al.</i> , 1990 Bright <i>et al.</i> , 1987
Photomultipliers with increased sensitivity	Lower loading levels. Imaging protocols with Kalman averaging instead of accumulation. Reduced signal to noise problems.	Pawley, 1995
Fast "line scanning" image collection.	Better temporal resolution. Allows increased averaging of scans which provides improved pH precision and spatial resolution.	Pawley, 1995
Photon counting (See Bio-Rad MRC 600 handbook)	Detection of very low signals. Better signal-to-noise ratio than normal scan mode.	Fricker <i>et al.</i> , 1994

Other techniques

Caged probes and flash photolysis	Manipulations of intracellular [ion] with precise localisation and magnitude.	Adams & Tsien, 1993 Kaplan, 1990
Microelectrode measurements: -pH -membrane potential	Independent measure of pH allowing better calibration. Examination of the effects of experimental treatments on membrane potential, possibly in conjunction with imaging changes in intracellular [ion].	Harrmann & Felle, 1995 McAinsh <i>et al.</i> , 1992 Kaplan, 1990 Racusen <i>et al.</i> , 1988

8.3 Further work on the role of pH in tip growth

The technical advances described above would allow improvements in precision and spatial resolution of pH as well as making absolute measurement (calibration) more certain. This would clarify the observations made during the present study about intracellular pH and apical growth.

Technical improvements are, however, insufficient to fully decipher the role of pH in polarity and tip growth. In order to determine the degree of correlation between pH and tip growth one or the other need to be manipulated. A crude initial attempt has been made at this with the current work. However, with improved measurement of pH, examination of pH at membranes, membrane potential measurements and the use of caged probes to modify intracellular pH in a controlled way, such analysis could be taken much further.

There is also the need to incorporate different techniques. Two methods likely to be of particular value are: the use of pH microelectrodes (Felle, 1993), as a collaborative method for measuring pH_c ; and the vibrating probe (Kochian *et al.*, 1992), used to examine extracellular pH profiles. The latter is significant as it fills a deficiency in the current imaging-based techniques by providing information on proton involving events outside cells.

In a continuation of the current work the following questions need to be more fully addressed:

- What is the effect of altering extracellular pH on the rates of proton flux across the membrane, the pH_i adjacent to the membrane and upon membrane potential?
- What is the sequence of events in the recovery of polarised growth after disruption by external pH modification?
- Does complete recovery of pH_c occur before re-establishment of polarised growth after intracellular modification of pH by cell permeant weak acids and bases?
- Does recovery of pH_c proceed in a localised or general fashion?
- Do changes in membrane potential, localised pH at membranes or cytoplasmic pH, occur after treatments which modify polarised growth but preceding morphological expression of response?
- Can the effect of primary stimuli be mimicked by manipulation of pH_c , for example by localised increase in proton concentration within a cell using caged probes?

Cytosolic or cytoplasmic pH has been the major concern of the work here. However, by using dyes sensitive to lower pH an investigation of vacuolar pH could be performed (Rost *et al.*, 1995). The buffering abilities of the vacuole, the effects of extracellular and intracellular pH alteration on the vacuole and differences in pH between the main vacuole and vacuoles distributed throughout the apex are all interesting aspects for examination (Guern *et al.*, 1991).

As was discussed in chapter 7, the fern gametophyte is, in many ways, a less than ideal system, therefore, in any future work an extension to include other cell types would be likely. The other cell types considered in particular, are: *Neurospora crassa* hyphae; *Agapanthus umbellatus* pollen tubes; and *Fucus serratus* zygotes. These cell types all exhibit tip growth but are diverse in their taxonomy, physiology and lifestyle, making them interesting to compare.

8.4 Areas of further interest

Rhizoid growth in ferns does not appear to have been greatly studied in the past (studies have been more commonly performed on rhizoids of *Chara* and *Riccia fluitans* (Leitz *et al.*, 1995; Hodick, 1994; Alfano *et al.*, 1993). As a consequence clear information on the factors which control the rate and orientation of growth in fern rhizoids is lacking, although it is likely that gravity, physical contact and light are all important. Some examination of the effects of medium composition on rhizoid growth has been performed (Sabba & Miller, 1993; Miller *et al.*, 1993; Miller & Wagner, 1987) which revealed the effects of certain ions (K^+ , Ca^{2+}). A systematic examination to determine the most important physiological regulators of rhizoid growth is required (e.g. Sabba *et al.*, 1992).

While structural and ultrastructural examination has been more actively pursued in gametophytes (particularly in *Adiantum*) the complex cytoplasmic and vacuolar distribution in both chlorocytes and rhizoids of *D. affinis* have not been fully investigated in relation to polarised growth. Application of recent cryo-fixation preparation techniques which give improved specimen preservation (Kiss *et al.*, 1995) for scanning electron microscopy, particularly important with rhizoid cells (Dyer & Cran, 1976), would provide better understanding of structure in the apical regions. Examination of cytoskeletal elements, their relationship to the cell wall and interaction with membranes and vesicles, vesicle traffic and ER distribution could all be examined in greater detail. *In vivo* imaging of structural dynamics within cells undergoing response to defined stimuli could be examined in real-time by fluorescence confocal imaging. The most obvious area of interest would be cytoskeletal dynamics examined with the aid of fluorescently tagged antibodies injected into cells (Yuan *et al.*, 1994).

The benefits of having an early indicator of physiological response have been pointed out in previous chapters, as has the possibility of using membrane potential measurement for this purpose. Such measurements have been performed on fern protonema cells (Racusen *et al.*, 1988), and (although not on fern rhizoids) also rhizoids of the liverwort *Riccia* (Felle, 1988). The ability to record membrane potential during confocal imaging would be useful and, although tricky, appears to be possible - Dr. R. Malhó, personal communication.

Membrane potential is itself a potentially important physiological parameter in cellular response and, therefore, worth investigating. As an alternative to microelectrodes, a range of dyes are available for confocal ratio imaging which respond to membrane potential (for example Di8Aneps from Molecular Probes). This type of approach could provide a means of mapping membrane potential around cells during experimental manipulation of polarised growth (Clarke *et al.*, 1995; Das *et al.*, 1993).

The main physiological phenomena considered for investigation during this study have been the effects of illumination on the polarity of the apical chlorocyte and the polarised growth of the primary rhizoid (see Chapters 1 and 3). However, there is a further intriguing system in the determination of secondary rhizoid emergence by exposure of red light-grown protonemata to white light, as described

in Chapter 3 Section 3.8. Nuclear positioning, nuclear and cell division and initiation of polarised growth from a previously non-expanding region of wall all appear to be involved in this process. The response is a long term sequence of events and outgrowth of the new secondary rhizoid occurs 3-4 days after the onset of white light treatment. The actual site of emergence is remarkably predictable and can, in fact, be detected at an early stage by Calcofluor staining of the cell wall. Predictable systems such as this, if they can be well defined (for example see Demkiv & Kardash, 1994), may hold the key to answering the questions of how a complex multitude of events are co-ordinated over time in response to a single defined stimulus - in this case white light.

References

References:

- Abeysekera, R.M. & McCully, M.E. (1993). The epidermal surface of the maize root-tip .1. development in normal roots. *New Phytologist*, **125**, 413-429.
- Adams, S.R. & Tsien, R.Y. (1993). Controlling cell chemistry with caged compounds. *Annual Review of Physiology*, **55**, 755- 784.
- Aeschbacher, R.A., Schiefelbein, J.W. & Benfey, P.N. (1994). The genetic and molecular-basis of root development. *Annual Review of Plant Physiology and Plant Molecular Biology*, **45**, 25-45.
- Akashi, T., Kanbe, T. & Tanaka, K. (1994). The role of the cytoskeleton in the polarised growth of the germ tube in *Candida albicans*. *Microbiology-UK*, **140**, 271-280.
- Al-Baldawi, N.F. & Abercrombie, R.F. (1992). Cytoplasmic hydrogen ion diffusion coefficient. *Biophysical Journal*, **61**, 1470-1479.
- Alfano, F., Russell, A., Gambardella, R. & Duckett, J.G. (1993). The actin cytoskeleton of the liverwort *Riccia fluitans* -effects of cytochalasin-b and aluminium ions on rhizoid tip growth. *Journal of Plant Physiology*, **142**, 569-574.
- Algarra, P., Linder, S. & Thummler, F. (1993). Biochemical-evidence that phytochrome of the moss *Ceratodon purpureus* is a light-regulated protein-kinase. *Febs Letters*, **315**, 69-73.
- Asard, H., Horemans, N., Briggs, W.R. & Caubergs, R.J. (1995). Blue-light perception by endogenous redox components of the plant plasma-membrane. *Photochemistry and Photobiology*, **61**, 518-522.
- Assmann, S.M. (1995). Cyclic-AMP as a 2nd messenger in higher-plants - status and future-prospects. *Plant Physiology*, **108**, 885-889.
- Baluska, F., Barlow, P.W., Hauskrecht, M., Kubica, S., Parker, J.S. & Volkmann, D. (1995). Microtubule arrays in maize root-cells - interplay between the cytoskeleton, nuclear-organisation and postmitotic cellular growth-patterns. *New Phytologist*, **130**, 177-192.
- Bartnicki-Garcia, S., Bartnicki, D.D., Gierz, G., Lopez-Franco, R. & Bracker, C.E. (1995). Evidence that spitzenkörper behaviour determines the shape of a fungal hypha - a test of the hyphoid model. *Experimental Mycology*, **19**, 153-159.
- Bartnik, E. & Sievers, A. (1988). *In-vivo* observations of a spherical aggregate of endoplasmic reticulum and of golgi vesicles in the tip of fast-growing *Chara* rhizoids. *Planta*, **176**, 1-9.
- Bassnett, S. (1990). Intracellular pH regulation in the embryonic chicken lens epithelium. *Journal of Physiology*, **431**, 445-464.
- Benfey, P.N., Linstead, P.J., Roberts, K., Schiefelbein, J.W., Hauser, M.T. & Aeschbacher, R.A. (1993). Root development in *Arabidopsis* - 4 mutants with dramatically altered root morphogenesis. *Development*, **119**, 57-70.

- Barbara, R.L.L., Morris, B.M., Fonseca, H.M.A.C., Reid, B., Gow, N.A.R. & Daft, M.J. (1995). Electrical currents associated with arbuscular mycorrhizal interactions. *New Phytologist*, **129**, 433-438.
- Berger, F. & Brownlee, C. (1993). Ratio confocal imaging of free cytoplasmic calcium gradients in polarising and polarised *Fucus* zygotes. *Zygote*, **1**, 9-15.
- Berger, F. & Brownlee, C. (1994). Photopolarization of the *Fucus* sp zygote by blue-light involves a plasma-membrane redox chain. *Plant Physiology*, **105**, 519-527.
- Berger, F. & Brownlee, C. (1995a). Endogenous releasable cell-wall factors control cell fate during zygotic embryogenesis in the multicellular alga *Fucus*. *Journal of Cellular Biochemistry*, **455**.
- Berger, F. & Brownlee, C. (1995b). Physiology and development of protoplasts obtained from *Fucus* embryos using laser microsurgery. *Protoplasma*, **186**, 63-71.
- Berridge, M.J. (1991). Cytoplasmic calcium oscillations: a two pool model. *Cell Calcium*, **12**, 63-72.
- Bialy, H. (1992). Pathway analysis in plant cells. *Biotechnology*, **10**, 249.
- Bisson, M.A., Kiegle, E., Black, D., Kiyosawa, K. & Gerber, N. (1995). The role of calcium in turgor regulation in *Chara longifolia*. *Plant Cell and Environment*, **18**, 129-137.
- Blank, P.S., Silverman, H.S., Chung, O.Y., Hogue, B.A., Stern, M.D., Hansford, R.G., Lakatta, E.G. & Capogrossi, M.C. (1992). Cytosolic pH measurements in single cardiac monocytes using carboxy-seminaphthorhodafleur-1. *American Journal of Physiology*, **263**, H276-H284.
- Blatt, M.R. (1992). K⁺ channels of stomatal guard-cells - characteristics of the inward rectifier and its control by pH. *Journal of General Physiology*, **99**, 615-644.
- Blatt, M.R. & Armstrong, F. (1993). K⁺ channels of stomatal guard-cells - abscisic-acid-evoked control of the outward rectifier mediated by cytoplasmic pH. *Planta*, **191**, 330-341.
- Blatt, M.R. & Thiel, G. (1994). K⁺ channels of stomatal guard-cells - bimodal control of the K⁺ inward-rectifier evoked by auxin. *Plant Journal*, **5**, 55-68.
- Blatt, M.R., Weisenseel, M.H. & Haupt, W. (1981). A light dependent current associated with chloroplast aggregation in the alga *Vaucheria sessilis*. *Planta*, **152**, 513-526.
- Bliton, C., Lechleiter, J. & Clapham, D.E. (1993). Optical modifications enabling simultaneous confocal imaging with dyes by ultraviolet- and visible-wavelength light. *Journal of Microscopy*, **169**, 15-26.
- Blum, W., Hinsch, K.-D., Schultz, G. & Weiler, E.W. (1988). Identification of GTP-binding proteins in the plasma membrane of higher plants. *Biochemical and Biophysical Research Communications*, **156**(2), 954-959.
- DeBoer, M.J.M. & DeDoes, D. (1990). The relationship between cell division pattern and global shape of young fern gametophytes. I. A model study. *Botanical Gazette*, **151**(4), 423-434.
- Bolsover, S. & Silver, A. (1991). Artefacts in calcium measurement: recognition and remedies. *Trends in Cell Biology*, **1**, 71-74.

- Bouget, F.Y., Gerttula, S. & Quatrano, R.S. (1995). Spatial redistribution of poly(a)(+) RNA during polarisation of the *Fucus* zygote is dependent upon microfilaments. *Developmental Biology*, **171**, 258-261.
- Bowler, C. & Chua, N.H. (1994). Emerging themes of plant signal-transduction. *Plant Cell*, **6**, 1529-1541.
- Bowles, D.J. (1995). Signal-transduction in plants. *Trends in Cell Biology*, **5**, 404-408.
- Braun, M. & Sievers, A. (1994). Role of the microtubule cytoskeleton in gravisensing *Chara* rhizoids. *European Journal of Cell Biology*, **63**, 289-298.
- Brawley, S.H., Wetherbee, R. & Quatrano, R.S. (1976). Fine structural studies of the gametes and embryos of *Fucus vesiculosus*. II. The cytoplasm of the egg and young zygote. *Journal of Cell Science*, **20**, 255-271.
- Breeuwer, P., Drocourt, J.L., Rombouts, F.M. & Abee, T. (1994). Energy-dependent, carrier-mediated extrusion of carboxyfluorescein from *Saccharomyces cerevisiae* allows rapid assessment of cell viability by flow-cytometry. *Applied and Environmental Microbiology*, **60**, 1467-1472.
- Bright, G.R., Fisher, G.W., Rogowska, J. & Taylor, D.L. (1987). Fluorescence ratio imaging microscopy: temporal and spatial measurements of cytoplasmic pH. *Journal of Cell Biology*, **104**, 1019-1033.
- Brownlee, C. (1994). Tansley review No.-70 - signal-transduction during fertilisation in algae and vascular plants. *New Phytologist*, **127**, 399-423.
- Brownlee, C., Pulsford, A.L. (1988). Visualisation of the cytoplasmic Ca²⁺ gradient in *Fucus serratus* rhizoids: correlation with cell ultrastructure and polarity. *Journal of Cell Science*, **91**, 249-256.
- Brownlee, C., Wood, J.W. & Briton, D. (1987). Cytoplasmic free calcium in single cells of centric diatoms. The use of Fura-2. *Protoplasma*, **140**, 118-122.
- Buckler, K.J. & Vaughan-Jones, R.D. (1990). Application of a new pH-sensitive fluoroprobe (carboxySNARF-1) for pH measurements in small, isolated cells. *Plugers Archiv*, **417**, 234-239.
- Buckler, K.J., Vaughan-Jones, R.D., Peers, C., Lagadie-Grossmann, D. & Nye, P.C.G. (1991). Effects of extracellular pH, pCO₂ and HCO₃²⁻ on intracellular pH in isolated type I-cells on the neonatal rat carotid body. *Journal of Physiology*, **444**, 703-721.
- Busa, W.B. (1992). Spectral characterisation of the effect of viscosity on Fura-2 fluorescence - excitation wavelength optimisation abolishes the viscosity artefact. *Cell Calcium*, **13**, 313-319.
- Busa, W.B. & Nuccitelli, R. (1984). Metabolic regulation via intracellular pH. *American Journal of Physiology*, **246**, R409-R438.
- Bush, D.R. (1993). Proton-coupled sugar and amino acid transporters in plants. *Annual Review of Plant Physiology and Molecular Biology*, **44**, 513-542.

- Butor, C., Griffiths, G., Aronson, N.N. & Varki, A. (1995). Colocalization of hydrolytic enzymes with widely disparate pH optima - implications for the regulation of lysosomal pH. *Journal of Cell Science*, **108**, 2213-2219.
- Carpita, N.C. & Gibeaut, D.M. (1993). Structural models of primary cell walls in flowering plants: consistency of molecular structure with the physical properties of the walls during growth. *Plant Journal*, **3**, 1-30.
- Chasan, R. (1994). Pollen - arresting developments. *Plant Cell*, **6**, 1693-1696.
- Chen-Wu, J.L., Zwicker, J., Bowen, A.R. & Robbins, P.W. (1992). Expression of chitin synthase genes during yeast and hyphal growth phases of *Candida albicans*. *Molecular Microbiology*, **6**, 497-502.
- Cheung, W.Y. ed. (1982). Calcium and Cell Function, Vol. II. Academic Press, London.
- Clark, G.B., Turnwals, S., Tirlapur, U.K., Haas, C.J., Mark, C.von der., Roux, S.J. & Scheuerlein, R. (1995). Polar distribution of annexin-like proteins during phytochrome-mediated initiation and growth of rhizoids in the ferns *Dryopteris* and *Anemia*. *Planta*, **197**, 376-384.
- Clarke, R.J., Zouni, A. & Holzwarth, J.F. (1995). Voltage sensitivity of the fluorescent-probe rh421 in a model membrane system. *Biophysical Journal*, **68**, 1406-1415.
- Cooke, T.J. & Lu, B. (1992). The independence of cell-shape and overall form in multicellular algae and land plants - cells do not act as building-blocks for constructing plant organs. *International Journal of Plant Sciences*, **153**, S 7-S 27.
- Cooke, T.J., Hickok, L.G. & Sugai, M. (1995). The fern *Ceratopteris richardii* as a lower plant-model system for studying the genetic-regulation of plant photomorphogenesis. *International Journal of Plant Sciences*, **156**, 367-373.
- Cooke, T.J. & Paolillo, JR. D.J. (1980). The control of the orientation of cell divisions in fern gametophytes. *American Journal of Botany*, **67**(9), 1320-1333.
- Cooke, T.J. & Paolillo, JR., D.J. (1979). The photobiology of fern gametophytes. II. The photocontrol of filamentous growth and its implications for the photocontrol of the transition to two-dimensional growth. *American Journal of Botany*, **66**(4), 376-385.
- Cooke, T.J. & Racusen, R.H. (1982). Cell expansion in the filamentous gametophyte of the fern *Onoclea sensibilis* L. *Planta*, **155**, 449-458.
- Cooke, T.J., Racusen, R.H. & Briggs, W.R. (1983). Initial events in the tip-swelling response of the filamentous gametophyte of *Onoclea sensibilis* L. to blue light. *Planta*, **159**, 300-307.
- Cooke, T.J., Racusen, R.H., Hickok, L.G. & Warne, T.R. (1987). The photocontrol of spore germination in the fern *Ceratopteris richardii*. *Plant and Cell Physiology*, **28**, 753-759.
- Corrêa, A. & Hoch, H.C. (1993). Microinjection of urediospore germings of *Uromyces appendiculatus*. *Experimental Mycology*, **17**, 1-21.
- Corzo, A. & Sanders, D. (1992). Inhibition of calcium uptake in *Neurospora crassa* by lanthanum: a mechanistic study. *Journal of General Microbiology*, **138**, 1791-1795.

- Cote, G.G. & Crain, R.C. (1994). Why do plants have phosphoinositides. *Bioessays*, **16**, 39-46.
- Cran, D.G. (1970). The Fine Structure of Fern Protonemata. Ph.D. Thesis. University of Edinburgh.
- Cran, D.G. (1979). The ultrastructure of fern gametophyte cells. In Dyer, A.F. (ed.). *The Experimental Biology of Ferns*. Academic Press, London, pp 171-212.
- Cran, D.G. & Dyer, A.F. (1973). Membrane continuity and associations in the fern *Dryopteris borrieri*. *Protoplasma*, **76**, 103-108.
- Cyr, R.J. (1994). Microtubules in plant morphogenesis - role of the cortical array. *Annual Review of Cell Biology*, **10**, 153-180.
- Cyr, R.J. & Palevitz, B.A. (1995). Organisation of cortical microtubules in plant-cells. *Current Opinion in Cell Biology*, **7**, 65-71.
- Das, T.K., Periasamy, N. & Krishnamoorthy, G. (1993). Mechanism of response of potential-sensitive dyes studied by time-resolved fluorescence. *Biophysical Journal*, **64**, 1122-1132.
- Davies, J.M., Brownlee, C. & Jennings, D.H. (1990). Measurement of intracellular pH in fungal hyphae using BCECF and digital imaging microscopy. *Journal of Cell Science*, **96**, 731-736.
- Davis, B.D. (1969). The transition from filamentous to two-dimensional growth in fern gametophytes. II. Kinetic studies on *Pteridium aquilinum*. *American Journal of Botany*, **56**(9), 1048-1053.
- Davis, B.D. (1971). The transition from filamentous to two-dimensional growth in fern gametophytes. III. Interaction of cell elongation and cell division. *American Journal of Botany*, **58**(3), 212-217.
- Davis, B.D., Chen, J.C.W. & Philpott, M. (1974). The transition from filamentous to two-dimensional growth in fern gametophytes. IV. Initial events. *American Journal of Botany*, **61**(7), 722-729.
- De Silva, L.R., Youatt, J., Gooday, G.W. & Gow, N.A.R. (1992). Inwardly directed ionic currents of *Allomyces macrogynus* and other water moulds indicate sites of proton-driven nutrient transport but are incidental to tip growth. *Mycological Research*, **96**, 925-931.
- Demkiv, O.T. & Kardash, A.R. (1994). The temporal organisation of the intercalary cells branching and bud formation in the protonemata of *Funaria hygrometrica* cells. *Izvestiya Akademii Nauk Seriya Biologicheskaya*, 411-418.
- Demkiv, O.T., Khorkavtsiv, Y.D. & Kardash, A.R. (1994). Intracellular pH during growth and differentiation of the gametophyte *Funaria-hygrometrica* cells. *Russian Journal of Plant Physiology*, **41**, 84-87.
- Derksen, J. & Emons, A. (1990). Microtubules in tip growth systems. In Heath, I.B. (ed.). *Tip growth in plant and fungal cells*. Academic press, London, pp 147-181.
- Dicker, J.W. & Turian, G. (1990). Calcium deficiencies and apical hyperbranching in wild-type and the "frost" and "spray" morphological mutants of *Neurospora crassa*. *Journal of General Microbiology*, **136**, 1413-1420.
- Dickinson, H. (1994). Self-pollination - simply a social disease. *Nature*, **367**, 517-518.

- Doonan, J.H., Cove, D.J. & Lloyd, C.W. (1988). Microtubules and microfilaments in tip growth: evidence that microtubules impose polarity on protonemal growth in *Physcomitrella patens*. *Journal of Cell Science*, **89**, 533-540.
- Downey, R.J. & Gedeon, C. (1992). Evidence for a H⁺/nitrate symporter in *Aspergillus nidulans*. *Molecular Biology of The Cell*, **3**, A 123
- Downey, R.J. & Gedeon, C.A. (1994). Evidence for a H⁺ nitrate symporter in *Aspergillus nidulans*. *Microbios*, **78**, 35-46.
- Drobak, B.K. (1991). Plant signal perception and transduction - the role of the phosphoinositide system. *Essays in Biochemistry*, **26**, 27-37.
- Drobak, B. K. (1992). The plant phosphoinositide system. *Biochemical Journal*, **288**, 697-712.
- Duckett, C.N. & Gray, J.C. (1995). Illuminating plant development. *Bioessays*, **17**, 101-103.
- Dyer A.F. ed. (1979). *The Experimental Biology of Ferns*. Academic Press, London, pp 171-434.
- Dyer, A.F. & Cran, D.G. (1976). The formation and ultrastructure of rhizoids on protonemata of *Dryopteris borreri* Newm. *Annals of Botany*, **40**, 757-765.
- Dyer, A.F. & King M.A.L. (1979) Cell Division in Fern Protonemata. In Dyer, A.F. (ed.) *The Experimental Biology of Ferns*. Academic Press, London, pp 307-354.
- Edmonds, B.T., Murray, J. & Condeelis, J. (1995). pH regulation of the F-actin binding-properties of *Dictyostelium* elongation-factor 1-alpha. *Journal of Biological Chemistry*, **270**, 15222-15230.
- Edwards, M.E. & Miller, J.H. (1972). Growth regulation by ethylene in fern gametophytes. III. Inhibition of spore germination. *American Journal of Botany*, **59**, 458-465.
- Felle, H. (1988). Cytoplasmic free calcium in *Riccia fluitans* L. and *Zea mays* L.: interaction of Ca²⁺ and pH? *Planta*, **176**, 248-255.
- Felle, H. (1993). Ion-selective microelectrodes - their use and importance in modern plant-cell biology. *Botanica Acta*, **106**, 5-12.
- Felle, H., Tretyn, A. & Wagner, G. (1992). The role of the plasma-membrane Ca²⁺-ATPase in Ca²⁺ homeostasis in *Sinapis alba* root hairs. *Planta*, **188**, 306-313.
- Frachisse, J.M., Johannes, E. & Felle, H. (1988). The use of weak acids as physiological tools: a study of the effects of fatty acids on intracellular pH and electrical plasmalemma properties of *Riccia fluitans* rhizoid cell. *Biochimie et Biophysica Acta*, **938**, 199-210.
- Francis, D. & Halford, N.G. (1995). The plant-cell cycle. *Physiologia Plantarum*, **93**, 365-374.
- Franklin, F.C.H., Lawrence, M.J. & Franklin-Tong, V.E. (1995). Cell and molecular-biology of self-incompatibility in flowering plants. *International Review of Cytology-A Survey of Cell Biology*, **158**, 1-64.
- Franklin-Tong, V.E., Ride, J.P. & Franklin, F.C.H. (1995). Recombinant stigmatic self-incompatibility-(s-) protein elicits a Ca²⁺ transient in pollen of *Papave -rhoeas*. *Plant Journal*, **8**, 299-307.

- Fraser, T.W. & Smith, D.L. (1974). Young gametophytes of the fern *Polypodium vulgare* L. an ultrastructural study. *Protoplasma*, **82**, 19-32.
- Frelin, C., Vigne, P., Ladoux, A. & Lazdunski, M. (1988). The regulation of the intracellular pH in cells from vertebrates. *European Journal of Biochemistry*, **174**, 3-14.
- Fricker, M.D. & White, N.S. (1992). Wavelength considerations in confocal microscopy of botanical specimens. *Journal of Microscopy-Oxford*, **166**, 29-42.
- Fricker, M.D., Tlalka, M., Ermantraut, J., Obermeyer, G., Dewey, M., Gurr, S., Patrick, J. & White, N.S. (1994). Confocal fluorescence ratio imaging of ion activities in plant cells. *Scanning Microscopy* (supplement **8**), 391-405.
- Friesen, W.O., Block, G.D. & Kocker, C.G. (1993). Formal approaches to understanding biological oscillators. *Annual Review of Physiology*, **55**, 661-681.
- Fry, S.C. (1994). Unzipped by expansins. *Current Biology*, **4**, 815-817.
- Furuya, M. (1978). Photocontrol of developmental processes in fern gametophytes. *Botanical Magazine of Tokyo*, Special issue **1**, 219-242.
- Futsaether, C.M., Kjeldstad, B. & Johnsson, A. (1993). Measurement of the intracellular pH of *Propionibacterium acnes* -comparison between the fluorescent-probe BCECF and P-31-NMR spectroscopy. *Canadian Journal of Microbiology*, **39**, 180-186.
- Gabriel, M. & Kopecka, M. (1995). Disruption of the actin cytoskeleton in budding yeast results in formation of an aberrant cell-wall. *Microbiology-UK*, **141**, 891-899.
- Gadd G.M. (1994). Signal Transduction in Fungi. In Gow, N.A.R. & Gadd, G.M. (eds.). *The Growing Fungus*. Chapman & Hall, London, pp 183-201.
- Galway, M.E. & Hardham, A.R. (1986). Microtubule reorganisation, cell wall synthesis and establishment of the axis of elongation in regenerating protoplasts of the alga *Mougeotia*. *Protoplasma*, **135**, 130-143.
- Gantt, E. & Arnott, H.J. (1965). Spore germination and development of the young gametophyte of the Ostrich fern (*Matteuccia struthiopteris*). *American Journal of Botany*, **52**(1), 82-94.
- Garrill, A., Jackson, S.L., Lew, R.R. & Heath, I.B. (1993). Ion channel activity and tip growth - tip-localised stretch-activated channels generate an essential Ca²⁺ gradient in the oomycete *Saprolegnia ferax*. *European Journal of Cell Biology*, **60**, 358-365.
- Garrill, A., Lew, R.R. & Heath, I.B. (1992). Stretch-activated Ca²⁺ and Ca²⁺-activated K⁺ Channels in the hyphal tip plasma membrane of the oomycete *Saprolegnia ferax*. *Journal of Cell Science*, **101**, 721-730.
- Gautier, H., Vavasseur, A., Lasceve, G. & Goudet, A.M. (1992). Redox processes in the blue light response of guard cell protoplasts of *Commelina communis* L. *Plant Physiology*, **98**, 34-38.
- Gehring, C.A., Irving, H.R. & Parish, R.W. (1994). Gibberellic acid induces cytoplasmic acidification in maize coleoptiles. *Planta*, **194**, 532-540.

- Gibbon, B.C. & Kropf, D.L. (1991). pH gradients and cell polarity in *Pelvetia* embryos. *Protoplasma*, **163**, 43-50.
- Gibbon, B.C. & Kropf, D.L. (1994). Cytosolic pH gradients associated with tip growth. *Science*, **263**, 1419-1421.
- Gilissen, L.J.W., Vanstaveren, M.J., Hakkert, J.C., Smulders, M.J.M., Verhoeven, H.A. & Creemersmolenaar, J. (1994). The competence of cells for cell-division and regeneration in tobacco explants depends on cellular location, cell-cycle phase and ploidy level. *Plant Science*, **103**, 81-91.
- Gilman, A.G. (1987). G-proteins: transducers of receptor-generated signals. *Annual Review of Biochemistry*, **56**, 615-649.
- Gilroy, S., Bethke, P.C. & Jones, R.L. (1993). Calcium homeostasis in plants. *Journal of Cell Science*, **106**, 453-462.
- Gilroy, S., Fricker, M.D., Read, N.D. & Trewavas, A.J. (1990). Fluorescence ratio imaging and photometry of calcium in living plant cells. *Micro* **90**, 475-478.
- Gilroy, S., Fricker, M.D., Read, N.D. & Trewavas, A.J. (1991). Role of calcium in signal transduction of *Commelina* guard cells. *The Plant Cell*, **3**, 333-344.
- Gilroy, S. & Jones, R.L. (1992). Gibberellic acid and abscisic acid co-ordinately regulate cytoplasmic calcium and secretory activity in barley aleurone protoplasts. *Proceedings of the National Academy of Science*, **89**, 3591-3595.
- Gilroy, S., Read, N.D. & Trewavas, A.J. (1990). Elevation of cytoplasmic calcium by caged calcium or caged inositol trisphosphate initiates stomatal closure. *Nature*, **346**, 769-771.
- Goldstein, D.J. (1992). Resolution in light-microscopy studied by computer-simulation. *Journal of Microscopy-Oxford*, **166**, 185-197.
- Gooday, G.W. (1995). The dynamics of hyphal growth. *Mycological Research*, **99**, 385-394.
- Goodner, B. & Quatrano, R.S. (1993). *Fucus* embryogenesis - a model to study the establishment of polarity. *Plant Cell*, **5**, 1471-1481.
- Gow, N.A.R. (1989). Circulating ionic currents in micro-organisms. *Advances in Microbial Physiology*, **30**, 89-123.
- Gow, N.A.R. (1994). Growth and guidance of the fungal hypha. *Microbiology-UK*, **140**, 3193-3205.
- Gow, N.A.R. & Gadd, G.M. eds. (1994). *The Growing Fungus*. Chapman & Hall, London.
- Gow, N.A.R., Kropf, D.L. & Harold, F.M. (1984). Growing hyphae of *Achlya bisexualis* generate a longitudinal pH gradient in the surrounding medium. *Journal of General Microbiology*, **130**, 2967-2974.
- Gow, N.A.R., Miller, P.F.P. & Gooday, G.W. (1993). Life at the apex - growth of the hyphal tip. *Journal of Chemical Technology and Biotechnology*, **56**, 217-219.

- Grabski, S., Xie, X.G., Holland, J.F. & Schindler, M. (1994). Lipids trigger changes in the elasticity of the cytoskeleton in plant-cells - a cell optical displacement assay for live cell measurements. *Journal of Cell Biology*, **126**, 713-726.
- Grandin, N. & Charbonneau, M. (1991). Cycling of intracellular free calcium and intracellular pH in *Xenopus* embryos: a possible role in the control of the cell cycle. *Journal of Cell Science*, **99**, 5-11.
- Graziana, A., Bono, J.J. & Ranjeva, R. (1993). Measurements of cytoplasmic calcium by optical fluorescence in plant- systems. *Plant Physiology and Biochemistry*, **31**, 277-281.
- Green, P.B. (1980). Organogenesis - a biophysical view. *Annual Review of Plant Physiology*, **31**, 51-82.
- Green, P.B. (1984). Shifts in plant cell axiality: histogenic influences on cellulose orientation in the succulent, *Graptopetalum*. *Developmental Biology*, **103**, 18-27.
- Greenspan, P., Mayer, E.P. & Fowler, S.D. (1985). Nile red: a selective fluorescent stain for intracellular lipid droplets. *The Journal of Cell Biology*, **11**, 965-973.
- Gresik, M., Kolarova, N., Farkas, V. (1991). Hyperpolarisation and intracellular acidification in *Trichoderma viride* as a response to illumination. *Journal of General Microbiology*, **137**, 2605-2609.
- Grill, R. (1987). Induction of two-dimensional growth by red and green light in the fern *Anemia phyllitidis* L.Sw. *Journal of Plant Physiology*, **131**, 363-371.
- Grill, R. (1990). Red light-mediated two-dimensional growth in gametophytes of the ferns *Adiantum capillus-veneris* L. and *Dryopteris filix-mas* (L) Schott. *Journal of Plant Physiology*, **136**, 765-768.
- Grill, R. & Schraudolf, H. (1993). Phytochrome-mediated mitotic-activity and induction of 2-dimensional growth in gametophytes of *Anemia-phyllitidis* L.Sw. *Journal of Plant Physiology*, **141**, 457-462.
- Grove, S.N. (1978). The cytology of hyphal tip growth. In Smith, J.E., Berry, D.R., Arnold, E. (eds.). *The filamentous fungi, Volume 3 Developmental Mycology*, Wiley, New York, pp 28-50.
- Grynkiewicz, G., Poenie, M. & Tsien, R.Y. (1985). A new generation of Ca²⁺ indicators with greatly improved fluorescence properties. *Journal of Biological Chemistry*, **260**(6), 3440-3450.
- Guern, J.H., Felle, H., Mathieu, Y., Kurkdjian, A. (1991) Regulation of intracellular pH in plant cells. *International Review of Cytology*, **127**, 111-173.
- Guern, J.H., Mathieu, Y., Pean, M., Pasquier, C., Beloeil, J.-C. & Lallemand, J.-Y. (1986). Cytoplasmic pH regulation in *Acer pseudoplatanus* cells. *Plant Physiology*, **82**, 840-845.
- Gustafson, M. & Magnusson, K.E. (1992). A novel principle for quantitation of fast intracellular calcium changes using Fura-2 and a modified image-processing system - applications in studies of neutrophil motility and phagocytosis. *Cell Calcium*, **13**, 473-486.

- Hager A. & Brich, M. (1993). Blue-light-induced phosphorylation of a plasma-membrane protein from phototropically sensitive tips of maize coleoptiles. *Planta*, **189**, 567-576.
- Hahm, S.H. & Saunders, M.J. (1991). Cytokinin increases intracellular Ca^{2+} in *Funaria* detection with Indo-1. *Cell Calcium*, **12**, 675-681.
- Hahn, K., DeBiasio, R. & Taylor, L. (1992). Patterns of elevated free calcium and calmodulin activation in living cells. *Nature*, **359**, 736-738.
- Haley, A., Russell, A.J., Wood, N., Allan, A.C., Knight, M., Campbell, A.K. & Trewavas, A.J. (1995). Effects of mechanical signalling on plant-cell cytosolic calcium. *Proceedings of the National Academy of Sciences of the United States of America*, **92**, 4124-4128.
- Harmon, A.C. & McCurdy, D.W. (1990). Calcium-dependent protein kinase and its possible role in the regulation of the cytoskeleton. In Randall, D.D., Blevins, D.G. (eds.). *Current Topics in Plant Biochemistry and Physiology*, **9**, 119-128.
- Harold, F.M. ed. (1986). *The Vital Force: A Study of Bioenergetics*. Freeman, New York.
- Harold, F.M. & Caldwell, J.H. (1990). Tips and currents: electrobiology of apical growth. In Heath, I.B. (ed.). *Tip growth in plant and fungal cells*. Academic press, San Diego, pp 59-90.
- Haugland, R.P. (1991 & 1993). *Molecular Probes: Bioprobes*, Nos. 13 & 18. Molecular Probes, Inc., Eugene, Oregon.
- Haugland, R.P. (1992). *Molecular Probes: Handbook of Fluorescent Probes and Research Chemicals*. Molecular Probes, Inc., Eugene, Oregon.
- Hayami, J., Kadota, A. & Wada, M. (1992). Intracellular dichroic orientation of the blue light-absorbing pigment and the blue-absorption band of the red-absorbing form of phytochrome responsible for phototropism of the fern *Adiantum protonemata*. *Photochemistry and Photobiology*, **56**, 661-666.
- Heath, I.B. (ed.). (1990). *Tip growth in plant and fungal cells*. Academic press, San Diego.
- Heath, I.B. (1994). The cytoskeleton in hyphal growth, organelle movements, and mitosis. *Mycota*, **1**, 43-65.
- Hedrich, R. & Schroeder, J.I. (1989). The physiology of ion channels and electrogenic pumps in higher plants. *Annual Review of Plant Physiology*, **40**, 539-569.
- Hepler, P.K., Cleary, A.L., Gunning, B.E.S., Wadsworth, P., Wasteneys, G.O. & Zhang, D.H. (1993). Cytoskeletal dynamics in living plant cells. *Cell Biology International*, **17**, 127-142.
- Hepler, P.K. & Wayne, R.O. (1985). Calcium and plant development. *Annual Review of Plant Physiology*, **36**, 397-439.
- Herrmann, A. & Felle, H.H. (1995). Tip growth in root hair-cells of *Sinapis alba* l - significance of internal and external Ca^{2+} and pH. *New Phytologist*, **129**, 523-533.
- Herth, W., Reiss, H. & Hartmann, E. (1990). Role of calcium ions in tip growth of pollen tubes and moss protonema cells. In Heath, I.B. (ed.). *Tip growth in plant and fungal cells*. Academic press, San Diego, pp 91-118.

- Heslop-Harrison, J. (1987). Pollen germination and pollen-tube growth. *International Review of cytology*, **107**, 1-76.
- Hickok, L.G., Warne, T.R. & Fribourg, R.S. (1995). The biology of the fern *Ceratopteris* and its use as a model system. *International Journal of Plant Sciences*, **156**, 332-345.
- Hidaka, H. & Ishikawa, T. (1992). Molecular pharmacology of calmodulin pathways in the cell functions. *Cell Calcium*, **13**, 465-472.
- Hodick, D. (1994). Negative gravitropism in *Chara*-protonemata - a model integrating the opposite gravitropic responses of protonemata and rhizoids. *Planta*, **195**, 43-49.
- Horn, M.A., Meadows, R.P., Apostol, I., Lones, C.R., Gorenstein, D.G., Heinstein, P.F. & Low, P.S. (1992). Effect of elicitation and changes in extracellular pH on the cytoplasmic and vacuolar pH of suspension-cultured soybean cells. *Plant Physiology*, **98**, 680-686.
- Hosking, S.L., Robson, G.D. & Trinci, A.P.J. (1995). Phosphoinositides play a role in hyphal extension and branching in *Neurospora crassa*. *Experimental Mycology*, **19**, 71-80.
- Howland, G.P. & Edwards, M.E. (1979). Photomorphogenesis of Fern Gametophytes. In Dyer, A.F. (ed.). *The Experimental Biology of Ferns*. Academic Press, London, pp 394-435.
- Huckaby, C.S., Bassel, A.R. & Miller, J.H. (1982). Isolation of rhizoid and prothallial protoplasts from gametophytes of the fern, *Onoclea sensibilis*. *Plant Science Letters*, **25**, 203-208.
- Hush, J.M., Wadsworth, P., Callaham, D.A. & Hepler, P.K. (1994). Quantification of microtubule dynamics in living plant-cells using fluorescence redistribution after photobleaching. *Journal of Cell Science*, **107**, 775-784.
- Hyde, G.J. & Heath, I.B. (1995). Ca²⁺-dependent polarisation axis establishment in the tip-growing organism, *Saprolegnia ferax*, by gradients of the ionophore A23187. *European Journal of Cell Biology*, **67**, 356-362.
- Inouye, K. (1985). Measurements of intracellular pH and its relevance to cell differentiation in *Dictyostelium discoideum*. *Journal of Cell Science*, **76**, 235-245.
- Irving, H.R., Gehring, C.A. & Parish, R.W. (1992). Changes in cytosolic pH and calcium of guard cells precede stomatal movements. *Proceedings of the National Academy of Science*, **89**, 1790-1794.
- Ito, M. (1969). Nuclear division in fern protonema. *Embryologia*, **10**(3-4), 273-283.
- Jackson, S.L. (1995). Microinjection of fungal cells: a powerful experimental technique. *Canadian Journal of Botany*, **73** (supplement 1), S435-S443.
- Jackson, S.L. & Heath, I.B. (1993). Roles of calcium-ions in hyphal tip growth. *Microbiological Reviews*, **57**, 367-382.
- Jaffe, L.F. & Nuccitelli, R. (1977). Electrical controls of development. *Annual Review of Biophysics and Bioengineering*, **6**, 445-476.
- Jaffe, L.F., Robinson, K.R. & Nuccitelli, R. (1974). Local cation entry and self-electrophoresis as an intracellular localisation mechanism. *Annual New York Academy of Science*, **238**, 372-389.

- Jelitto, T.C. (1994). Role of external signals and cytosolic pH during the pre-penetration phase of infection by *Magnaporthe grisea*. *Planta*, **194**, 471-477.
- Jelitto, T.C. (1995). Role of external signals in regulating the pre-penetration phase of infection by the rice blast fungus *Magnaporthe grisea*. Ph.D. Thesis, University of Edinburgh.
- Jenkins, G.I. & Cove, D.J. (1983). Phototropism and polarotropism of primary chloronemata of the moss *Physcomitrella patens*: Responses of mutant strains. *Planta*, **159**, 432-438.
- Johnson, C.H., Knight, M.R., Kondo, T., Masson, P., Sedbrook, J., Haley, A. & Trewavas, A. (1995). Circadian oscillations of cytosolic and chloroplastic free calcium in plants. *Science*, **269**, 1863-1865.
- Johri, M.M. & D'Souza, (1988). Auxin regulation of cell differentiation in moss protonema. In Pharis, R.P., Rood, S.P. (eds.). *Plant growth substances*, Springer-Verlag, London, pp 407-418.
- Joos, U., van Aken, J. & Kristen, U. (1994). Microtubules are involved in maintaining the cellular polarity in pollen tubes of *Nicotiana sylvestris*. *Protoplasma*, **179**, 5-15.
- Kadota, A. & Furuya, M. (1977). Apical growth of protonemata in *Adiantum capillus-veneris*. I. Red far-red reversible effect on growth cessation in the dark. *Development Growth and Differentiation*, **19**(4), 357-365.
- Kadota, A. & Furuya, M. (1981). Apical growth of protonemata in *Adiantum capillus-veneris* IV. phytochrome-mediated induction in non-growing cells. *Plant and Cell Physiology*, **22**(4), 629-638.
- Kadota, A., Fushimi, Y. & Wada, M. (1986). Intracellular photoreceptive site for blue light induced cell division in protonema of the fern *Aiantum* - further analysis by polarised light irradiation and centrifugation. *Plant and Cell Physiology*, **27**(6), 989-995.
- Kadota, A. & Wada, M. (1989a). Circular arrangement of cortical F-actin around the subapical region of a tip-growing fern protonemal cell. *Plant Cell Physiology*, **30**(8), 1183-1186.
- Kadota, A. & Wada, M. (1989b). Enzymatic isolation of protoplasts from fern protonemal cells stainable with a fluorescent brightener. *Plant Cell Physiology*, **30**(8), 1107-1113.
- Kadota, A. & Wada, M. (1989c). Photoinduction of circular F-actin on chloroplast in a fern protonemal cell. *Protoplasma*, **151**, 171-174.
- Kadota, A. & Wada, M. (1992a). Reorganisation of the cortical cytoskeleton in tip-growing fern protonemal cells during phytochrome-mediated phototropism and blue light-induced apical swelling. *Protoplasma*, **166**, 35-41.
- Kadota, A. & Wada, M. (1992b). The circular arrangement of cortical microtubules around the subapex of tip-growing fern protonemata is sensitive to cytochalasin-b. *Plant And Cell Physiology*, **33**, 99-102.
- Kagawa, T., Kadota, A. & Wada, M. (1992). The junction between the plasma membrane and the cell wall in fern protonemata cells, as visualised after plasmolysis, and its dependence on arrays of cortical microtubules. *Protoplasma*, **170**, 186-190.

- Kaminskyj, S.G., Garril, A., Heath, I.B. (1992). The relation between turgor and tip growth in *Saprolegnia ferax*: turgor is necessary but not sufficient to explain apical extension rates. *Experimental Mycology*, **16**, 64-75.
- Kaplan, J.H. (1990). Special topic: Caged compounds in cellular physiology. In Kaplan, J.H. (section ed.). Photochemical manipulation of divalent cation levels. *Annual Review of Physiology*, **52**, 897-914.
- Kataoka, H. (1981). Expansion of *Vaucheria* cell apex caused by blue or red light. *Plant and Cell Physiology*, **22**(4), 583-595.
- Kataoka, H. & Weisenseel, M.H. (1988). Blue light promotes ionic current influx at the growing apex of *Vaucheria terrestris*. *Planta*, **173**, 490-499.
- Keating, T.J. & Cork, R.J. (1994). Improved Spatial Resolution in Ratio Images Using Computational Confocal Techniques. In Nuccitelli, R. (ed.). *Methods in Cell Biology*, Vol. 40: A Practical Guide to the Study of Calcium in Living Cells. Academic Press, London, pp 221-241.
- Kiss H.G., Evans, M.L. & Johnson, J.D. (1991). Cytoplasmic calcium levels in protoplasts from the cap and elongation zone of maize roots. *Protoplasma*, **163**, 181-188.
- Kiss, J.Z., Wangcahill, F. & Kiss, H.G. (1995). The ultrastructure of the early development of *Schizaea pusilla* gametophytes. *International Journal of Plant Sciences*, **156**, 131-142.
- Klee, C.B., Crouch, T.H. & Richman, P.G. (1980). Calmodulin. *Annual Review of Biochemistry*, **49**, 489-515.
- Klionsky, D.J., Nelson, H. & Nelson, N. (1992). Compartment acidification is required for efficient sorting of proteins to the vacuole in *Saccharomyces cerevisiae*. *Journal of Biological Chemistry*, **267**, 3416-3422.
- Knight, H., Trewavas, A.J. & Read, N.D. (1993a). Confocal microscopy of living fungal hyphae microinjected with Ca²⁺- sensitive fluorescent dyes. *Mycological Research*, **97**, 1505-1515.
- Knight, M.R., Read, N.D., Campbell, A.K. & Trewavas, A.J. (1993b). Imaging calcium dynamics in living plants using semisynthetic recombinant aequorins. *Journal of Cell Biology*, **121**, 83-90.
- Knox, J.P. (1992). Cell-adhesion, cell-separation and plant morphogenesis. *Plant Journal*, **2**, 137-141.
- Knox, J.P. (1993). Cell-surface glycoproteins and plant morphogenesis. *Journal of Cellular Biochemistry*, **6**.
- Kochian, L.V., Shaff, J.E., Kühtreiber, W.M., Jaffe, L.F. & Lucas, W.J. (1992). Use of an extracellular, ion-selective, vibrating microelectrode system for the quantification of K⁺, H⁺, and Ca²⁺ fluxes in maize roots and maize suspension cells. *Planta*, **188**, 601-610.
- Kranz, E., Vonwiegen, P. & Lorz, H. (1995). Early cytological events after induction of cell-division in egg cells and zygote development following *in-vitro* fertilisation with angiosperm gametes. *Plant Journal*, **8**, 9-23.
- Kropf, D.L. (1992). Establishment and expression of cellular polarity in fucoid zygotes. *Microbiological Reviews*, **56**, 316-339.

- Kropf, D.L. (1994). Cytoskeletal control of cell polarity in a plant zygote. *Developmental Biology*, **165**, 361-371.
- Kropf, D.L., Coffman, H.R., Kloareg, B., Glenn, P. & Allen, V.W. (1993). Cell-wall and rhizoid polarity in *Pelvetia* embryos. *Developmental Biology*, **160**, 303-314.
- Kropf, D.L., Kloareg, B. & Quatrano, R.S. (1988). Cell wall is required for the fixation of the embryonic axis in *Fucus* zygotes. *Science*, **239**, 187-190.
- Kurkdjian, A., Guern, J.H. (1989). Intracellular pH: measurement and importance in cell activity. *Annual Review of Plant Physiology and Molecular Biology*, **40**, 271-303.
- Kurtz, I. & Emmons, C. (1993). Measurement of intracellular pH with a laser scanning confocal microscope. In Taylor, D.L., Wang, Y.-L. (eds.). *Methods in Cell Biology*, volume 30, Academic Press, London, pp 183-193.
- Kuss-Wymer, C.L. & Cyr, R.J. (1992). Tobacco protoplasts differentiate into elongate cells without net microtubule depolymerisation. *Protoplasma*, **168**, 64-72.
- Kutschera, U. (1994). The current status of the acid-growth hypothesis. *New Phytologist*, **126**, 549-569.
- Kwon, Y.H. & Hoch, H.C. (1991). Temporal and spatial dynamics of appressorium formation in *Uromyces appendiculatus*. *Experimental Mycology*, **15**, 116-131.
- Laetsch, W.M. (1967). Ferns. In Wilt, F.W., Wessels, N.K. (eds.). *Methods in developmental Biology*. Crowell, New York, pp 319-328.
- Lamb, J.A., Allen, P.G., Tuan, B.Y. & Janmey, P.A. (1993). Modulation of gelsolin function - activation at low pH overrides Ca^{2+} requirement. *Journal of Biological Chemistry*, **268**, 8999-9004.
- Lancelle, S.A. & Hepler, P.K. (1992). Ultrastructure of freeze-substituted pollen tubes of *Lilium longiflorum*. *Protoplasma*, **167**, 215-230.
- Laurent, M., Johannin, G., Gilbert, N., Lucas, L., Cassio, D., Petit, P.X. & Fleury, A. (1994). Power and limits of laser-scanning confocal microscopy. *Biology of the Cell*, **80**, 229-240.
- Laurent, M., Johannin, G., Leguyader, H. & Fleury, A. (1992). Confocal scanning optical microscopy and 3-dimensional imaging. *Biology of the Cell*, **76**, 113-124.
- Leitz, G., Schnepf, E. & Greulich, K.O. (1995). Micromanipulation of statoliths in gravity-sensing *Chara* rhizoids by optical tweezers. *Planta*, **197**, 278-288.
- Levina, N.N., Lew, R.R. & Heath, I.B. (1994). Cytoskeletal regulation of ion channel distribution in the tip-growing organism *Saprolegnia ferax*. *Journal of Cell Science*, **107**, 127-134.
- Levina, N.N., Lew, R.R., Hyde, G.J. & Heath, I.B. (1995). The roles of Ca^{2+} and plasma membrane ion channels in hyphal tip growth of *Neurospora crassa*. *Journal of Cell Science*, **108**, 3405-3417.
- Lino, M., Nakagawa, Y. & Wada, M. (1988). Blue light-regulation of cell division in *Adiantum* protonemata: an approach with pulse stimulation. *Plant, Cell and Environment*, **11**, 547-554.

- Liu, Z., Bushnell, W.R. & Brambl, R. (1987). Potentiometric cyanine dyes are sensitive probes for mitochondria in intact plant cells. *Plant Physiology*, **84**, 1385-1390.
- Lloyd, C.L. ed. (1991). *The Cytoskeletal Basis of Plant Growth and Form*. Academic Press, London.
- Lloyd, C.W. & Wells, B. (1985). Microtubules are at the tips of root hairs and form helical patterns corresponding to inner wall fibrils. *Journal of Cell Science*, **75**, 225-238.
- Lopez-Franco, R., Bartnicki-Garcia, S. & Bracker, C.E. (1994). Pulsed growth of fungal hyphal tips. *Proceedings of the National Academy of Sciences of the United States of America*, **91**, 12228-12232.
- Lopez-Franco, R., Howard, R.J. & Bracker, C.E. (1995). Satellite spitzkörper in growing hyphal tips. *Protoplasma*, **188**, 85-103.
- Magalhães, B.P., Wayne, R., Humber, R.A., Shields, E.J. & Roberts, D.W. (1991). Calcium-regulated appressorium formation of the entomopathogenic fungus *Zoophthora radiacans*. *Protoplasma*, **160**, 77-88.
- Malhó, R., Feijo, J.A. & Pais, M.S.S. (1992). Effect of electrical fields and external ionic currents on pollen tube orientation. *Sexual Plant Reproduction*, **5**, 57-63.
- Malhó, R., Read, N.D., Pais, M.S. & Trewavas, A.J. (1994). Role of cytosolic-free calcium in the reorientation of pollen tube growth. *Plant Journal*, **5**, 331-341.
- Malhó, R., Read, N.D., Trewavas, A.J. & Pais, M.S. (1995). Calcium-channel activity during pollen tube growth and reorientation. *Plant Cell*, **7**, 1173-1184.
- Martinez-Zaguilan, R. & Martinez, G.M. (1991). Simultaneous measurement of intracellular pH and Ca^{2+} using the fluorescence of SNARF-1 and Fura-1.
- Mathieu, Y., Guern, J.H., Pean, M., Pasquier, C., Beloeil, J.-C. & Lallemand, J.-Y. (1986). Cytoplasmic pH regulation in *Acer pseudoplatanus* cells. *Plant Physiology*, **82**, 846-852.
- Mathieu, Y., Jouanneau, J.P., Thomine, S., Lapous, D. & Guern, J. (1994). Cytosolic protons as secondary messengers in elicitor-induced defence responses. *Biochemical Society Symposium*, 113-130.
- Matzke, M.A. & Matzke, A.J.M. (1986). Visualisation of mitochondria and nuclei in living plant cells by the use of a potential-sensitive fluorescent dye. *Plant, Cell and Environment*, **9**, 73-77.
- Mayerhofer, R., Langridge, W.H.R., Cormier, M.J. & Szalay, A.A. (1995). Expression of recombinant *Renilla* luciferase in transgenic plants results in high levels of light emission. *Plant Journal*, **7**, 1031-1038.
- McAinsh, M.R., Brownlee, C. & Hetherington, A.M. (1990). Abscisic acid-induced elevation of guard cell cytosolic Ca^{2+} precedes stomatal closure. *Nature*, **343**, 186-188.
- McAinsh, M.R., Brownlee, C. & Hetherington, A.M. (1992). Visualising changes in cytosolic-free Ca^{2+} during the response of stomatal guard-cells to abscisic-acid. *Plant Cell*, **4**, 1113-1122.
- McCauley, M.M. & Hepler, P.K. (1992). Cortical ultrastructure of freeze-substituted protonemata of the moss *Funaria hygrometrica*. *Protoplasma*, **169**, 168-178.

- McCauley, M.M. & Hepler, P.K. (1990). Visualisation of the endoplasmic reticulum in living buds and branches of the moss *Funaria hygrometrica* by confocal laser scanning microscopy. *Development*, **109**, 753-764.
- McCormack, J.G. & Cobbold, R.H. (eds.) (1991). Cellular Calcium: A Practical Approach. IRL Press, Oxford.
- Menzel, D. (1994). Cell-differentiation and the cytoskeleton in *Acetabularia*. *New Phytologist*, **128**, 369-393.
- Menzel, D. (1995). *Acetabularia* - a primitive unicellular organism for the study of plant-cell morphogenesis. *Journal of Cellular Biochemistry*, 436.
- Messiaen, J., Read, N.D., Vancutsem, P. & Trewavas, A.J. (1993). Cell-wall oligogalacturonides increase cytosolic free calcium in carrot protoplasts. *Journal of Cell Science*, **104**, 365-371.
- Miller, A.L., Raven, J.A., Sprent, J.I. & Weisenseel, M.H. (1986). Endogenous ion currents traverse growing roots and root hairs of *Trifolium repens*. *Plant, Cell and Environment*, **9**, 79-83.
- Miller, D.D., Callahan, D.A., Gross, D.J. & Hepler, P.K. (1992). Free Ca²⁺ gradient in growing pollen tubes of *Lilium*. *Journal of Cell Science*, **101**, 7-12.
- Miller, J.H. (1968). Fern gametophytes as experimental material. *Botany Reviews*, **38**, 361-440.
- Miller, J.H. (1980). Orientation of the plane of cell division in fern gametophytes: the roles of cell shape and stress. *American Journal of Botany*, **67**(4), 534-542.
- Miller, J.H. & Bassel, A.R. (1980). Effects of caffeine on germination and differentiation in spores of the fern *Onoclea sensibilis*. *Physiologia Plantarum*, **50**, 213-220.
- Miller, J.H. & Greany, R.H. (1976). Rhizoid differentiation in fern spores: experimental manipulation. *Science*, **193**, 687-689.
- Miller, J.H. & Miller, P.M. (1967). Interaction of photomorphogenic pigments in fern gametophytes: phytochrome and a yellow-light-absorbing pigment. *Plant Cell Physiology*, **8**, 765-769
- Miller, J.H. & Stephani, M.C. (1971). Effects of colchicine and light on cell form in fern gametophytes. Implications for a mechanism of light-induced cell elongation. *Physiologia Plantarum*, **24**, 264-271.
- Miller, J.H., Vogelmann, T.C. & Bassel, A.R. (1983). Promotion of fern rhizoid elongation by metal ions and the function of the spore coat as an ion reservoir. *Plant Physiology*, **71**, 828-834.
- Miller, J.H. & Wagner, P.M. (1987). Co-requirement for calcium and potassium in the germination of spores of the fern *Onoclea sensibilis*. *American Journal of Botany*, **74**, 1585-1589.
- Mimura, T. & Kirino, Y. (1984). Changes in cytoplasmic pH measured by ³¹P-NMR in cells of *Nitellopsis obtusa*. *Plant and Cell Physiology*, **25**(5), 813-820.
- Mineyuki, Y. & Furuya, M. (1985). Involvement of microtubules in nuclear positioning during apical growth in *Adiantum protonemata*. *Plant and Cell Physiology*, **26**(4): 627-634.

- Mineyuki, Y., Kataoka, H., Masuda, Y. & Nagai, R. (1995). Dynamic changes in the actin cytoskeleton during the high-fluence rate response of the *Mougeotia* chloroplast. *Protoplasma*, **185**, 222-229.
- Mizuta, S., Kaneko, M., Kimura, S. & Okuda, K. (1994). Experimental studies on the stability of the cortical microtubule cytoskeleton in relation to polarity and cell elongation in the coenocytic green-alga, *Chaetomorpha moniligera*. *Annals of Botany*, **73**, 273-280.
- Mohr, H. (1956). Die Abhaengigkeit des Protonemawachstums und der Protonemapolaritaet bei Farnen von Licht. *Planta*, **47**, 127-58.
- Money, N.P. & Harold, F.M. (1992). Extension growth of the water mold *Achlya* - interplay of turgor and wall strength. *Proceedings of the National Academy of Sciences of the United States of America*, **89**, 4245-4249.
- Money, N.P. & Harold, F.M. (1993). Two water molds can grow without measurable turgor pressure. *Planta*, **190**, 426-430.
- Moore, E.D.W., Becker, P.L., Fogarty, K.E., Williams, D.A. & Fay, F.S. (1990). Ca²⁺ imaging in single living cells: theoretical and practical issues. *Cell Calcium*, **11**, 157-179.
- Morré, D.J. (1990). Transmembrane signal transduction and the control of plant growth. In Randall, D., D., Blevins, D., G. (eds.). *Current Topics in Plant Biochemistry and Physiology*, **9**, 47-65.
- Morse, M.J., Crain, R.C. & Satter, R.L. (1987). Light-stimulated inositol-phospholipid turnover in *Samanea saman* leaf pulvini. *Biochemistry*, **84**, 7075-7078.
- Murashige, T. & Skoog, F. (1962). A revised medium for rapid growth and bio-assays with tobacco tissue cultures. *Physiologia Plantarum*, **15**, 473-497.
- Murata, T., Kadota, A., Hogetsu, T. & Wada, M. (1987). Circular arrangement of cortical microtubules around the subapical part of a tip-growing fern protonema. *Protoplasma*, **141**, 135-138.
- Murata, T. & Wada, M. (1989a). Re-organisation of microtubules during preprophase band development in *Adiantum* protonemata. *Protoplasma*, **151**, 73-80.
- Murata, T. & Wada, M. (1989b). Effects of colchicine and amiprofos-methyl on microfibril arrangement and cell shape in *Adiantum* protonemal cells. *Protoplasma*, **151**, 81-87.
- Murata, T. & Wada, M. (1989c). Organisation of cortical microtubules and microfibril deposition in response to blue-light-induced apical swelling in a tip-growing *Adiantum* protonema cell. *Planta*, **178**, 334-341.
- Murata, T. & Wada, M. (1991). Effects of centrifugation on preprophase band formation in *Adiantum* protonema. *Planta*, **183**, 391-398.
- Murata, T. & Wada, M. (1992). Cell cycle specific disruption of the preprophase band of microtubules in fern protonema: effects of displacement of the endoplasm by centrifugation. *Journal of Cell Science*, **101**, 93-98.

- Nawata, T. (1992). A major role for transcellular Ca^{2+} ion currents in cell elongation in the unicellular green alga *Closterium*. *Plant Cell Physiology*, **33**(7), 881-888.
- Nick, P. & Furuya, M. (1992). Induction and fixation of polarity - early steps in plant morphogenesis. *Development Growth and Differentiation*, **34**, 115-125.
- Nuccitelli, R. ed. (1994). *Methods in Cell Biology*, Vol. 40: A Practical Guide to the Study of Calcium in Living Cells. Academic Press, London.
- O'Brodovich, H., Wang, X., Rafii, C.L.B., Correa, J. & Bear, C. (1993). Novobiocin forms cation-permeable ion channels in rat foetal distal lung epithelium. *American Journal of Physiology*, **264**, C1532-C1537.
- Obermeyer, G., Lutzelschwab, M., Heumann, H.-G. & Weisenseel, M.H. (1992). Immunolocalization of H^+ -ATPases in the plasma membrane of pollen grains and pollen tubes of *Lilium longiflorum*. *Protoplasma*, **171**, 55-63.
- Ootaki, T. & Furuya, M. (1969). Experimentally induced apical dominance in protonema of *Pteris vittata*. *Embryologia*, **10**(3-4), 284-296.
- Oparka, K.J., Murant, E.A., Wright, K.M. & Prior, D.A.M. (1991a). The drug probenecid inhibits the vacuolar accumulation of fluorescent anions in onion epidermal cells. *Journal of Cell Science*, **99**, 557-563.
- Oparka, K.J., Murphy, R., Derrick, P.M., Prior, D.A.M. & Smith, J.A.C. (1991b). Modification of the pressure-probe technique permits controlled intracellular microinjection of fluorescent probes. *Journal of Cell Science*, **98**, 539-544.
- Oparka, K.J. & Read, N.D. (1994). The use of fluorescent probes for studies of living plant cells. In Harris, N. & Oparka, K.J. (eds.). *Plant Cell Biology: A Practical Approach*. IRL Press, Oxford, pp 27-50.
- Opitz, N. Merten, E. & Acker, H. (1994). Evidence for redistribution-associated intracellular pKa shifts of the pH-sensitive fluoroprobe carboxy-SNARF-1. *Pluegers Arch*, **427**, 332-342.
- Owen, C.S., Carango, P., Grammer, S., Bobyock, S. & Leeper, D.B. (1992). pH dependent intracellular quenching of the indicator carboxySNARF-1. *Journal of Fluorescence*, **2**, 75-80.
- Partanen, C.R., Power, J.B. & Cocking, E.C. (1980). Isolation of protoplasts of *Pteridium aquilinum*. *Plant Science letters*, **17**, 333-338.
- Parton, R.M., Fischer, S., Malhó, R., Jelitto, T.C. & Read, N.D. (1996). Pronounced cytoplasmic pH gradients are not a common feature of tip growth in plant and fungal cells. Manuscript in preparation - intended for submission to *Journal of Cell Science*.
- Pawley, J.B. (1995). *Handbook of Confocal Microscopy*. 2nd Edition, Plenum Press, New York.
- Peters, W.S. & Felle, H. (1991). Control of apoplast pH in corn coleoptile segments. I: The endogenous regulation of cell wall pH. *Journal of Plant Physiology*, **137**, 655-661.
- Pichon, O. & Desbiez, M.-O. (1994). Is cytoplasmic pH involved in the regulation of cell cycle in plants. *Physiologia Plantarum*, **92**, 261-265.

- Pierson, E.S. & Cresti, M. (1992). Cytoskeleton and cytoplasmic organisation of pollen and pollen tubes. *International Review of Cytology*, **140**, 73-125.
- Pierson, E.S., Li, Y.Q., Zhang, H.Q., Willemse, M.T.M., Linskens, H.F. & Cresti, M. (1995). Pulsatory growth of pollen tubes - investigation of a possible relationship with the periodic distribution of cell-wall components. *Acta Botanica Neerlandica*, **44**, 121-128.
- Pierson, E.S., Lichtscheidl, I.K. & Derksen, J. (1990). Structure and behaviour of organelles in living pollen tubes of *Lilium longiflorum*. *Journal of Experimental Botany*, **41**(232), 1461-1468.
- Pierson, E.S., Miller, D.D., Callaham, D.A., Shipley, A.M., Rivers, B.A., Cresti, M. & Hepler, P.K. (1994). Pollen tube growth is coupled to the extracellular calcium ion flux and the intracellular calcium gradient; effect of BAPTA-type buffers and hypertonic media. *Plant Cell*, **6**, 1815-1828.
- Pontlezaica, R.F., McNally, J.G. & Pickard, B.G. (1993). Wall-to-membrane linkers in onion epidermis - some hypotheses. *Plant Cell and Environment*, **16**, 111-123.
- Poovaiah, B.W. & Reddy, A.S.N. (1988). The role of calcium in stimulus-response coupling. In Pharis, R.P., Rood, S.P. (eds.). *Plant growth substances*, Springer-Verlag, London, pp 216-229.
- Poovaiah, B.W. & Reddy, A.S.N. (1993). Calcium and signal-transduction in plants. *Critical Reviews in Plant Sciences*, **12**, 185-211.
- Prebble, E.J., Robson, G.D., Denning, D.W. & Robertson, W.R. (1995). Demonstration of an intracellular pH gradient in growing hyphae of *Neurospora crassa*. *Proceedings of the Royal Microscopical Society*, **30**, 33.
- Pritchard, J. (1994). The control of cell expansion in roots. *New Phytologist*, **127**, 3-26.
- Quader, H. (1990). Formation and disintegration of cisternae of the endoplasmic reticulum visualised in live cells by conventional fluorescence and confocal laser scanning microscopy: evidence for the involvement of calcium and the cytoskeleton. *Protoplasma*, **155**, 166-175.
- Quader, H. & Schnepf, E. (1989). Actin filament array during side branch initiation in protonema cells of the moss *Funaria hygrometrica*: an actin organising centre at the plasma membrane. *Protoplasma*, **151**, 167-170.
- Quatrano, R., Shaw, S., Bouget, F.Y., Gerttula, S., Taylor, C., Fowler, J., Brian, L. & Davis, J. (1995a). Role of the cytoskeleton and cell-wall in the establishment of polarity. *Journal of Cellular Biochemistry*, **441**.
- Quatrano, R., Shaw, S., Goodner, B., Bouget, F.Y., Gerttula, S., Taylor, C., Fowler, J. & Davis, J. (1995b). Cell-adhesion and the cytoskeleton in cell polarity. *Journal of Cellular Biochemistry*, **127**.
- Quatrano, R., Wagner, V.T., Goodner, B. & Brian, L. (1993). Establishment of cell polarity in *Fucus*. *Journal of Cellular Biochemistry*, **10**.
- Racusen, R.H. & Cooke, T.J. (1982). Electrical changes in the apical cell of the fern gametophyte during irradiation with photomorphogenetically active light. *Plant Physiology*, **70**, 331-334.

- Racusen, R.H, Ketchum, K.A. & Cook, T.J. (1988). Modifications of electric and ionic gradients preceding the transition from tip growth to isodiametric expansion in the apical cell of the fern gametophyte. *Plant physiology*, **87**, 69-77.
- Raghavan, V. (1990). *Developmental Biology of Fern Gametophytes*. Barlow, P.B., Bray, D., Green, P.B. (series eds.). Cambridge University Press, Cambridge.
- Raghavan, V. (1992). Gene activity during germination of spores of the fern, *Oncoclea sensibilis* - cell-free translation analysis of messenger-RNA of spores and the effect of alpha-amanitin on spore germination. *Journal of Plant Physiology*, **140**, 434-440.
- Raghavan, V. (1993). Chloroplast activities of dark-imbibed and photoinduced spores of the fern *Oncoclea sensibilis*. *Protoplasma*, **175**, 75-84.
- Randall, D.D. & Blevins, D.G. (eds.) (1990). *Current Topics in Plant Biochemistry and Physiology*, **9**.
- Randall, S.K. (1992). Characterisation of vacuolar calcium-binding proteins. *Plant Physiology*, **100**, 859-867.
- Rathore, K.S., Cork, R.J. & Robinson, K.R. (1991). A cytoplasmic gradient of Ca²⁺ is correlated with the growth of lily pollen tubes. *Developmental Biology*, **148**, 62-619.
- Read, N.D., Allan, W.T.G., Knight, H., Knight, M.R., Malhó, R., Russel, A., Shacklock, P.S. & Trewavas, A.J. (1992). Imaging and measurement of cytosolic free calcium in plant and fungal cells. *Journal of Microscopy*, **166**(1), 57-86.
- Read, N.D., Shacklock, P.S., Knight, M.R. & Trewavas, A.J. (1993). Imaging calcium dynamics in living plant-cells and tissues. *Cell Biology International*, **17**, 111-125.
- Reid, R.J. & Smith, F.A. (1988). Measurements of the cytoplasmic pH of *Chara corallina* using double-barrelled pH micro-electrodes. *Journal of Experimental Botany*, **39**(207), 1421-1432.
- Reynolds, T.L. & Corson, G.E. (1979). Apical dominance: The effects of growth regulators on the gametophyte of *Anemia phyllitidis*. *American Journal of Botany*, **66**(10), 1261-1263.
- Roberts, D.M. & Harmon, A.C. (1992). Calcium-modulated proteins - targets of intracellular calcium signals in higher-plants. *Annual Review of Plant Physiology and Plant Molecular Biology*, **43**, 375-414.
- Roncal, T., Ugalde, U.O. & Irastorza, A. (1993). Calcium-induced conidiation in *Penicillium cyclopium* - calcium triggers cytosolic alkalinisation at the hyphal tip. *Journal of Bacteriology*, **175**, 879-886.
- Roos, W. (1992). Confocal pH topography in plant cells-acidic layers in the peripheral cytoplasm and the apoplast. *Botanica Acta*, **105**, 253-259.
- Rost, F.W.D., Shepherd, V.A. & Ashford, A.E. (1995). Estimation of vacuolar pH in actively growing hyphae of the fungus *Pisolithus tinctorius*. *Mycological Research*, **99**, 549-553.
- Roux, S.J., Wayne, R.O. & Datta, N. (1986). Role of calcium ions in phytochrome responses: an update. *Physiologia Plantarum*, **66**, 344-348.

- Rusig, A.M., Leguyader, H. & Ducreux, G. (1994). Dedifferentiation and microtubule reorganisation in the apical cell protoplast of *Sphacelaria* (*Phaeophyceae*). *Protoplasma*, **179**, 83-94.
- Russ, U., Grolig, F. & Wagner, G. (1991). Changes in cytoplasmic free Ca^{2+} in the green alga *Mougeotia scalaris* as monitored with Indo-1, and their effect on the velocity of chloroplast movements. *Planta*, **184**, 105-112.
- Sabba, R.P. & Miller, J.H. (1993). Calcium delays the onset of cell-division and rhizoid elongation in gemmae of the calcifuge fern, *Vittaria graminifolia*. *American Journal of Botany*, **80**, 624-628.
- Sabba, R.P., Hoffman, J.R. & Miller, J.H. (1992). Light-dependent inhibition of cell-division and rhizoid elongation in gemmae of the fern, *Vittaria graminifolia*. *American Journal of Botany*, **79**, 8-13.
- Sachs, T. (1991). Cell polarity and tissue patterning in plants. *Development* (supplement 1), 83-93.
- Sanders, D. & Slayman, C.L. (1982). Control of intracellular pH predominant role of oxidative metabolism, not proton transport, in the eukaryote micro-organism *Neurospora*. *Journal of General Physiology*, **80**, 377-402.
- Sanders, L.C. & Lord, E.M. (1992). A dynamic role for the styler matrix in pollen-tube extension. *International Review of Cytology-A Survey of Cell Biology*, **140**, 297-318.
- Sanders, S.L. & Field, C.M. (1995). Bud-site selection is only skin deep. *Current Biology*, **5**, 1213-1215.
- Saunders, M.J. & Hepler, P.K. (1982). Calcium ionophore A23187 stimulates cytokinin-like mitosis in *Funaria*. *Science*, **217**, 943-945.
- Saunders, M.J. & Hepler, P.K. (1983). Calcium antagonists and calmodulin inhibitors block cytokinin-induced bud formation in *Funaria*. *Developmental Biology*, **99**, 41-49.
- Scheel, D., Hahlbrock, K., Jabs, T., Nennstiel, D., Nurnberger, T. & Sacks, W.R. (1995). Peptide elicitor recognition and signal-transduction in plant defence. *Journal of Cellular Biochemistry*, **472**.
- Scheuerlein, R., Schmidt, K., Poenie, M. & Roux, S.J. (1991). Determination of cytoplasmic calcium concentration in *Dryopteris* spores. *Planta*, **184**, 166-174.
- Scheuerlein, R., Tirlapur, U.K., Roux, S.J. & Poenie, M. (1992). Analysis of intracellular free Ca^{2+} -concentrations with Fura-2 during early gametophyte development in *Dryopteris paleacea*. Unpublished (see Herrmann & Felle, 1995).
- Schiefelbein, J., Galway, M., Masucci, J. & Ford, S. (1993). Pollen-tube and root-hair tip growth is disrupted in a mutant of *Arabidopsis thaliana*. *Plant Physiology*, **103**, 979-985.
- Schiefelbein, J.W., Shipley, A. & Rowse, P. (1992). Calcium influx at the tip of growing root-hair cells of *Arabidopsis thaliana*. *Planta*, **187**, 455-459.
- Schmiedel, G. & Schnepf, E. (1980). Polarity and growth of caulonema tip cells of the moss *Funaria hygrometrica*. *Planta*, **147**, 405-413.
- Schnepf, E. (1986). Cellular polarity. *Annual Review of Plant Physiology*, **37**, 23-47.

- Schumacker K.S. & Sze, H. (1990). Solubalisation and reconstruction of the oat root vacuolar H⁺/Ca²⁺ exchanger. *Plant Physiology*, **92**, 340-345.
- Schmichow, J., Sack, F.D. & Hartmann, E. (1990). Microtubule distribution in gravitropic protonemata of the moss *Ceratodon*. *Protoplasma*, **159**, 60-69.
- Seksek, O., Biwersi, J. & Verkman, A.S. (1995). Direct measurement of *trans*-golgi pH in living cells and regulation by second messengers. *Journal of Biological Chemistry*, **270**, 4967-4970.
- Seksek, O., Henry-Toulmé, N., Sureau, F. & Bolard, J. (1991). SNARF-1 as an intracellular pH indicator in laser microspectrofluorometry: a critical assessment. *Analytical Biochemistry*, **193**, 49-54.
- Shacklock, P.S., Read, N.D. & Trewavas, A.J. (1992). Cytosolic free calcium mediates red light-induced photomorphogenesis. *Nature*, **358**, 753-755.
- Shepherd V.A., Orlovich, D.A. & Ashford, A.E. (1993). A dynamic continuum of pleiomorphic tubules and vacuoles in growing hyphae of a fungus. *Journal of Cell Science*, **104**, 495-507.
- Sheppard, C.J.R., Gu, M. & Roy, M. (1992). Signal-to-noise ratio in confocal microscope systems. *Journal of Microscopy-Oxford*, **168**, 209-218.
- Shotton, D. & White, N. (1989). Confocal scanning microscopy: three-dimensional biological imaging. *Trends in Biological Sciences*, **14**, 435-439.
- Siebke, K., Yin, Z.H., Raghavendra, A.S. & Heber, U. (1992). Vacuolar pH oscillations in mesophyll-cells accompany oscillations of photosynthesis in leaves - interdependence of cellular compartments, and regulation of electron flow in photosynthesis. *Planta*, **186**, 526-531.
- Sievers, A., Kramer-Fischer, M., Braun, M. & Buchen, B. (1991). The polar organisation of the growing *Chara* rhizoid and the transport of statoliths are actin dependent. *Botanica Acta*, **104**, 103-109.
- Silver, A.R., Whitaker, M. & Bolsover, S.R. (1992). Intracellular ion imaging using fluorescent dyes: artefacts and limits to resolution. *Pflugers Arch*, **420**, 595-602.
- Slayman, C.L., Moussatos, V.V. & Webb, W.W. (1994). Endosomal accumulation of pH indicator dyes delivered as acetoxymethyl esters. *Journal of Experimental Biology*, **196**, 419-438.
- Smith, D.L. (1979). Biochemical and physiological aspects of gametophyte differentiation and development. In Dyer, A.F. (ed.). *The Experimental Biology of Ferns*. Academic Press, London, pp 355-392.
- Smith, J.E., Berry, D.R. & Arnold, E. (eds.) (1978). *The filamentous fungi*, Volume 3 *Developmental Mycology*, Wiley, New York.
- Smith, G.A., Hesketh, T.R. & Metcalfe, J.C. (1988). Design and properties of a fluorescent indicator of intracellular free Na⁺ concentration. *Biochemical Journal*, **250**, 227-232.
- Snell, V. & Nurse, P. (1993). Investigations into the control of cell form and polarity: the use of morphological mutants in fission yeast. *Development (supplement)*, 289-299.

- Sodmergen, Chen, G.H., Hu, Z.M., Guo, F.L. & Guan, X.L. (1995). Male gametophyte development in *Plumbago zeylanica*: cytoplasmic localisation and cell determination in the early generative cell. *Protoplasma*, **186**, 79-86.
- Spanswick, R.M. (1981). Electrogenic ion pumps. *Annual Review of Plant Physiology*, **32**, 267-289.
- Steer, M. (1990). Role of actin in tip growth. In Heath, I.B. (ed.). Tip growth in plant and fungal cells. Academic press, London, pp 119-145.
- Steer, M.W. & Steer, J.M. (1989). Tansley review No. 16 pollen tube tip growth. *New Phytologist*, **111**, 323-358.
- Steinberg, T.H., Newman, A.S., Swanson, J.A. & Silverstein, S.C. (1987). Macrophages possess probenecid-inhibitable organic anion transporters that remove fluorescent dyes from the cytoplasmic matrix. *The Journal of Cell Biology*, **105**, 2695-2702.
- Stockwell, C.S. & Miller, J.H. (1974). Regions of cell wall expansion in the protonema of a fern. *American Journal of Botany*, **61**(4), 375-378.
- Sussman, M.R., Schaller, G.E., DeWitt, N. & Harper, J.F. (1990). Regulation of the plasma membrane proton pump. In Randall, D.D., Blevins, D.G. (eds.) (1990). *Current Topics in Plant Biochemistry and physiology*, **9**, 183-189.
- Taiz, L. (1984). Plant cell expansion: regulation of cell wall mechanical properties. *Annual Review of Plant Physiology*, **35**, 585-657.
- Taiz, L. (1994). Expansins - proteins that promote cell-wall loosening in plants. *Proceedings of the National Academy of Sciences of the United States of America*, **91**, 7387-7389.
- Takahashi, C. (1961). The growth of protonemal cells and rhizoids in Bracken. *Cytologia*, **26**, 62-66.
- Takehige, K., Mitsumori, F., Tazawa, M. & Mimuta, T. (1992). Role of cytoplasmic inorganic phosphate in light-induced activation of H⁺-pumps in the plasma membrane and tonoplast of *Chara corallina*. *Planta*, **186**, 466-472.
- Tanaka, I. & Wakabayashi, T. (1992). Organisation of the actin and microtubule cytoskeleton preceding pollen germination - an analysis using cultured pollen protoplasts of *Lilium longiflorum*. *Planta*, **186**, 473-482.
- Taylor, A.R. & Brownlee, C. (1995). Ion channels and signal-transduction in the polarising *Fucus* zygote. *Journal of Cellular Biochemistry*, 466.
- Taylor, J.E., McAinsh, M.R., Montgomery, L., Renwick, K.F., Webb, A.A.R. & Hetherington, A.M. (1994). The use of transgenesis to investigate signal-transduction pathways. *Biochemical Society Transactions*, **22**, 949-952.
- Thimann, K.V., Reese, K. & Nachmias, V.T. (1992). Actin and the elongation of plant cells. *Protoplasma*, **171**, 153-166.
- Thomas, A.P. & Delaville, F. (1991). The use of fluorescent indicators for measurements of cytosolic-free calcium concentrations in cell populations and single cells. In McCormack, J.G., Cobbold, R.H. (eds.). *Cellular Calcium: A Practical Approach*. IRL Press, Oxford, pp 1-39.

- Thorn, E.C. (1993). Plant-regeneration from embryos derived from crosses between *Hordeum vulgare* and *H. bulbosum*. *Hereditas*, **118**, 39-47.
- Tilney, L.G., Cooke, T.J., Connelly, P.S. & Tilney, M.S. (1990). The distribution of plasmodesmata and its relationship to morphogenesis in fern gametophytes. *Development*, **110**, 1209-1221.
- Tiwari, S.C. & Suprenant, K.A. (1994). pH-dependent solubility and assembly of microtubules in bovine brain extracts. *Cell Motility and the Cytoskeleton*, **28**, 69-78.
- Tognoli, L. & Basso, B. (1987). The fusicoccin-stimulated phosphorylation of a 33 kDa polypeptide in cells of *Acer pseudoplatanus* as influenced by extracellular and intracellular pH. *Plant, Cell and Environment*, **10**, 233-239.
- Trevedi, B. & Danforth, W.H. (1966). Effect of pH on the kinetics of frog muscle phosphofructokinase. *The Journal of Physiological Chemistry*, **241**(17), 4110-4114.
- Trewavas, A. & Knight, M. (1994). Mechanical signalling, calcium and plant form. *Plant Molecular Biology*, **26**, 1329-1341.
- Trewavas, A.J. & Gilroy, S. (1991). Signal transduction in plant cells. *Trends in Genetics*, **7**(11/12), 1-5.
- Tsien, R.W. & Tsien, R.Y. (1990). Calcium channels, stores, and oscillations. *Annual Review of Cell Biology*, **6**, 715-760.
- Tsien, R.Y. (1980). New calcium indicators and buffers with high selectivity against magnesium and protons: design, synthesis, and properties of prototype structures. *Biochemistry*, **19**, 2396-2404.
- Tsien, R.Y. & Poenie, M. (1986). Fluorescence ratio imaging: a new window into intracellular ionic signalling. *Trends in Biochemical Sciences*, **11**, 450-455.
- Vandelest, C.H.A., Versteeg, E.M.M., Veerkamp, J.H. & Vankuppevelt, T.H. (1995). Elimination of autofluorescence in immunofluorescence microscopy with digital image-processing. *Journal of Histochemistry and Cytochemistry*, **43**, 727-730.
- Vargas, M.M., Aronson, J.M. & Roberson, R.W. (1993). The cytoplasmic organisation of hyphal tip cells in the fungus *Allomyces macrogynus*. *Protoplasma*, **176**, 43-52.
- Verbelen, J.P., Tao, W.H. & Stickens, D. (1995). Establishment and abolition of polarity in cultured tobacco mesophyll protoplasts. *Journal of Cellular Biochemistry*, **454**.
- Verde, F. Mata, J. & Nurse, P. (1995). Fission yeast cell morphogenesis: identification of new genes and analysis of their role during the cell cycle. *Journal of Cell Biology*, **131**, 1529-1538.
- Verkman, A.S. (1990). Development and biological applications of chloride-sensitive fluorescent indicators. *American Journal of Physiology*, **259**, C375-C388.
- Wacker, I. & Schnepf, E. (1990). Effects of nifedipine, verapamil and diazepam on tip growth in *Funaria hygrometrica*. *Planta*, **180**, 492-501.

- Wada, M. & Furuya, M. (1970). Photocontrol of the orientation of cell division in *Adiantum*. 1. Effects of the dark and red periods in the apical cell of gametophytes. *Development Growth and Differentiation*, **12**(2), 109-117.
- Wada, M. & Kadota, A. (1989). Photomorphogenesis in lower green plants. *Annual Review of Plant Physiology*, **40**, 169-91.
- Wada, M. & Kadota, A. (1992). Photoinduction of formation of circular structures by microfilaments on chloroplasts during intracellular orientation in protonemal cells of the fern *Adiantum capillus-veneris*. *Protoplasma*, **167**, 97-107.
- Wada, M. & Kadota, A., Furuya, M. (1978). Apical growth of protonemata in *Adiantum capillus-veneris* II. Action spectrum for the induction of apical swelling and the intracellular photoreceptive site. *Botanical Magazine of Tokyo*, **91**, 113-120.
- Wada, M., Kadota, A. & Yoshizaki, N. (1995). Phytochrome regulation of tip growth in the apical cell of the fern protonema. *Journal Of Cellular Biochemistry*, **442**.
- Wada, M., Mineyuki, Y. & Furuya, M. (1982). Change in the rate of organelle movement during progression of the cell cycle in *Adiantum* protonemata. *Protoplasma*, **113**, 132-136.
- Wada, M., Mineyuki, Y., Kadota, A. & Furuya, M. (1980). The changes of nuclear position and distribution of circumferentially aligned cortical microtubules during the progression of cell cycle in *Adiantum* protonemata. *Botanical Magazine of Tokyo*, **93**, 237-245.
- Wada, M. & O'Brian, T.P. (1975). Observations on the structure of the protonema of *Adiantum capillus-veneris* L. undergoing cell division following white light irradiation. *Planta*, **126**, 213-227.
- Wada, M. & Staehelin, L.A. (1981). Freeze-fracture observations on the plasma membrane, the cell wall and the cuticle of growing protonemata of *Adiantum capillus-veneris*. *Planta*, **151**, 462-468.
- Wasteneys, G.O., Gunning, B.E.S. & Hepler, P.K. (1993). Microinjection of fluorescent brain tubulin reveals dynamic properties of cortical microtubules in living plant-cells. *Cell Motility and the Cytoskeleton*, **24**, 205-213.
- Wayne, R. & Hepler, P.K. (1984). The role of calcium ions in phytochrome-mediated germination of spores of *Onoclea sensibilis* L. *Planta*, **160**, 12-20.
- Wayne, R. & Hepler, P.K. (1985). Red light stimulates an increase in intracellular calcium in the spores of *Onoclea sensibilis*. *Plant Physiology*, **77**, 8-11.
- Wayne, R., Rice, D. & Hepler, P.K. (1986). Intracellular pH does not change during phytochrome-mediated spore germination in *Onoclea*. *Developmental Biology*, **113**, 97-103.
- Weisenseel, M.H. & Jaffe, L.F. (1976). The major current through Lily pollen tubes enters as K^+ and leaves as H^+ . *Planta*, **133**, 1-7.
- Weiss, J. & Weisenseel, M.H. (1990). Blue light-induced changes in membrane potential and intracellular pH of *Phycomyces* hyphae. *Journal of Plant Physiol*, **136**, 78-85.

- Wiebe, M.G., Robson, G.D. & Trinci, A.P.J. (1992). Evidence for the independent regulation of hyphal extension and branch initiation in *Fusarium graminearum* a-3/5. *Fems Microbiology Letters*, **90**, 179-184.
- Wright, K.M. & Oparka, K.J. (1994). Physicochemical properties alone do not predict the movement and compartmentation of fluorescent xenobiotics. *Journal of Experimental Botany*, **45**(270), 35-44.
- Xu, P., Lloyd, C.W., Staiger, C.J. & Drobak, B.K. (1992). Association of phosphatidylinositol 4-kinase with the plant cytoskeleton. *Plant Cell*, **4**, 941-951.
- Yatsuhashi, H. & Wada, M. (1990). High-fluence rate responses in the light-oriented chloroplast movement in *Adiantum protonemata*. *Plant Science*, **68**, 87-94.
- Yuan S. & Heath, I.B. (1991). A comparison of fluorescent membrane probes in hyphal tips of *Saprolegnia ferax*. *Experimental Mycology*, **15**, 103-115.
- Yuan, M., Shaw, P.J., Warn, R.M. & Lloyd, C.W. (1994). Dynamic reorientation of cortical microtubules, from traverse to longitudinal, in living plant cells. *Proceedings of the National Academy of Science USA*, **91**, 6050-6053.
- Zandomeni, K. & Schopfer, P. (1993). Reorientation of microtubules at the outer epidermal wall of maize coleoptiles by phytochrome, blue-light photoreceptor, and auxin. *Protoplasma*, **173**, 103-112.
- Zhang, D.H., Callaham, D.A. & Hepler, P.K. (1990). Regulation of Anaphase chromosome motion in *Tradescantia* stamen hair cells by calcium and related signalling agents. *The Journal of Cell Biology*, **111**, 171-182.
- Zhu, G.L. & Boyer, J.S. (1992). Enlargement in *Chara* studied with a turgor clamp. *Plant Physiology*, **100**, 2071-2080.